PENTALENE-EMBEDDED ACENES AND THIENOACENES: SYNTHESIS, PROPERTIES AND APPLICATIONS

DAI GAOLE

NATIONAL UNIVERSITY OF SINGAPORE

2014

Pentalene-embedded Acenes and Thienoacenes: Synthesis, Properties and Applications

DAI GAOLE

(*B. Sc. Soochow University*)

A THESIS SUBMITTED

FOR THE DEGREE OF DOCTOR OF PHILOSOPHY

DEPARTMENT OF CHMISTRY

NATIONAL UNIVERSITY OF SINGAPORE

2014

Declaration

I hereby declare that this thesis is my original work and it has been written by me in its entirety, under the supervision of Dr. Chi Chunyan, (in the laboratory S9-05-01C), Chemistry Department, National University of Singapore, between August 2010 and July 2014.

I have duly acknowledged all the sources of information which have been used in the thesis.

This thesis has also not been submitted for any degree in any university previously.

The content of the thesis has been partly published in:

1) **G. Dai**, J. Chang, J. Wu and C* Chi. *J. Mater. Chem.* **2012**, 22, 21201.
2) **G. Dai**, J. Chang, W. Zhang, S. Bai, K.-W. Huang, J. Xu and C. Chi*, *Chem. Commun.*, **2015**, 51, 503-506.
3) **G. Dai**, J. Chang, X. Shi, W. Zhang, B. Zheng, K.-W. Huang and C. Chi*, *Chem. Eur. J.*, **2015**, 21, 2019-2028.

Dai Gaole		
Name	Signature	Date

Acknowledgement

I would like to thank my PhD supervisor Dr. Chi Chunyan for supporting me during the past four years. Dr. Chi is a nice, kind and easygoing professor. She taught me a lot of skills to get my experiments well done. Her guidance, suggestions and tolerance during my PhD study are deeply acknowledged.

I would also like to thank my lab mates: Dr. Qu Hemi, Dr. Shao Jinjun, Dr. Ye Qun, Dr. Tong Chenhua, Mr. Shi Xueliang Dr. Gokulnath Sabapathi and Mr. Arun B. Lakshmi for their advices and help during my PhD study. I also thank the cooperation group members in Dr. Wu Jishan's group for their help and assistance.

I also wish to extend my gratitude to Mr. Chang Jingjing, who did all the device fabrication analysis for my samples. Dr. Huang Kuo-Wei helped with the TD-DFT calculations. Dr. Zhang Wenhua helped with the X-ray crystallographic analysis for my crystal samples. I also wish to thank MOE and NUS for providing me the scholarships to study in Singapore.

Last but not least, I would like to take the opportunity to thank my parents Mr. Dai Guangming and Mrs. Wu Yuehua, for their continuous support during the years. I also thank my wife Mrs. Li Duanxiu for her understanding, tolerance, encouragement and companion all the time. Finally, I would like to thank all my friends.

Dai Gaole (戴高乐)

July 2014

Table of Contents

Publications List

(1) **G. Dai,** J. Chang, J. Wu, C. Chi*, *J. Mater. Chem.*, 2012, 22, 21201.

(2) **G. Dai**, J. Chang, W. Zhang, S. Bai, K.-W. Huang, J. Xu and C. Chi*, *Chem. Commun.*, **2015**, 51, 503-506.

(3) **G. Dai**, J. Chang, X. Shi, W. Zhang, B. Zheng, K.-W. Huang and C. Chi*, *Chem. Eur. J.*, **2015**, 21, 2019-2028.

(4) **G. Dai**, J. Chang, C. Chi*, "Synthesis of Diacenopentalene Diimides for n-Channel Organic Field Effect Transistors" (manuscript in preparation).

(5) **G. Dai**, J. Chang, K.-W. Huang, C. Chi*, "Soluble and Stable *Z*-Shaped Pentaleno-diacenes" (manuscript in preparation).

(6) Q. Ye, J. Chang, K.-W. Huang, **G. Dai**, J. Zhang, Z.-K. Chen, J. Wu, C. Chi*, *Org. Lett.*, 2012, 14, 2786. (Highlighted in *SYNFACTS* 2012, 8, 0846)

(7) Q. Ye, J. Chang, K.-W. Huang, **G. Dai**, C. Chi*, *Org. Biomol. Chem.*, 2013, 11, 6285.

(8) C. Tong, J. Chang, J. M. Tan, **G. Dai**, K.-W. Huang, H. S. O. Chan*, C. Chi*, *Org. Biomol. Chem.*, 2013, 11, 5683.

(9) J. Shao, J. Chang, **G. Dai**, C. Chi*, *J. Polym. Sci., Part A: Polym. Chem.*, 2014, 52, 2454.

(10) Q. Ye, J. Chang, X. Shi, **G. Dai**, W. Zhang, K.-W. Huang, C. Chi*, *Org. Lett.*, 2014, 16,3966.

(11) X. Shi, P. M. Burrezo, S. Lee, W. Zhang, B. Zheng, **G. Dai**, J. Chang, J. T. L. Navarrete, K.-W. Huang*, D. K.*, J. Casado*, C. Chi*, *Chem. Sci.*, 2014, 5, 4490-4503.

Summary

Pentalene as an antiaromatic 4nπ-electron system has attracted many chemists' attention. Pentalene moiety is embedded into the acene or thienoacene framework, and the weak intramolecular donor-acceptor interaction between the antiaromatic pentalene and the annealed aromatic moieties affords their unique electronic properties. In this thesis, pentalene chemistry was developed and a series of novel pentalene-embedded acenes and thienoacenes were designed and synthesized for organic semiconductor materials.

In Chapter 2, we designed and sythesized two soluble and stable dianthraceno-pentalenes, which include fused rings up to eight. The average hole mobility in FET devices is increased from 0.001 to 0.65 $cm^2V^{-1}s^{-1}$ (maximum: 0.86 $cm^2V^{-1}s^{-1}$) through modifying the substituents. Single crystals of both molecules were obtained and used to explain their different FET performances.

In Chapter 3, we incorporated the pentalene unit into the thienoacene framework to provide the bis(benzo(thieno)$_n$)pentalene derivatives (n = 1 - 3). The obtained highly π-extended polycyclic conjugated systems contain a large number of fused rings (up to ten). Their structures, optical and electrochemical properties were studied and their applications in OFETs were also investigated. They exhibit small energy gap, unique electronic absorption and amphoteric redox behavior which are also supported by TD-DFT calculations. All

compounds showed good thermal stability and ordered self-assembly in solid state. The highest hole mobility of 0.036 $cm^2V^{-1}s^{-1}$ was achieved from solution processed FET devices.

In Chapter 4, we introduced dicarboximide group into diacene fused pentalene and obtained the diaceno-pentalene diimide derivatives. Both compounds displayed good solubility and stability. As expected, we got the first n-type semicondutor material based on pentalene unit which showed electron mobility up to 0.06 $cm^2V^{-1}s^{-1}$ by solution processing technique.

In Chapter 5, we designed the Z-shaped pentaleno-diacenes and synthesized the pentaleno-dianthracene and pentaleno-ditetracene successfully. This is a new synthetic method to fuse the pentalene ring onto the zig-zag edges of acenes. The UV-vis absorption spectra showed long wavelength absorption bands due to intramolecular charge transfer character. They have small band gaps around 1.0 eV. DFT calculations suggested that the HOMOs of both molecules are delocalized along the Z-shaped framework while the LUMOs are mainly localized at the central pentalene unit. The single crystal of pentaleno-dianthracene was obtained. It has a planar conformation, and adopted a column-like stacking structure.

In addition, we also investigated the acene contained polymers for organic semiconductors. In Chapter 6, we introduced the naphthalene imide unit into the polythiophene backbone to obtain the planar and imide included building block. Based on the new building block, three alternating conjugated

copolymers were prepared; and achieved stable and high performance p-type polymeric semiconductors. The physical properties and OFET performances of these polymers were investigated in details. The highest average hole mobility up to 0.15 cm^2 V^{-1} s^{-1} was achieved after optimization by solution processes. All the polymers showed relatively good environmental stability after storing in air.

Keywords: pentalene, organic semiconductor, acene, organic field effect transistors, polymer

List of Tables

List of Figures

List of Charts

List of Schemes

List of Abbreviations

AFM	atomic force microscopy
CV	cyclic voltammetry
DCM	dichloromethane
DBP	dibenzopentalene
DIBAL-H	diisobutylaluminium hydride
DMF	dimethylformamide
DSC	differential scanning calorimetry
EA	ethyl acetate
FET	field effect transistor
HAT	hexaazatriphenylene
HATN	hexaazatrinaphthalene
HOMO	highest occupied molecular orbital
LUMO	lowest unoccupied molecular orbital
MALDI-TOF	matrix-assisted laser desorption/ionization - time of flight
m-CPBA	*meta*-chloroperoxybenzoic acid
NBS	*N*-bromosuccinimide
NDI	naphthalene diimide
NIS	*N*-iodosuccinimide
NMR	nuclear magnetic resonance
OFET	organic field effect transistor

OLED	organic light emitting diode
OPV	organic photovoltaic
OTS	octadecyltrichlorosilane
PCC	pyridinium chlorochromate
PDI	perylene diimide
POM	polarizing optical microscopy
rt	room temperature
TBAB	tetra-*n*-butylammonium bromide
TBAF	tetra-*n*-butylammonium fluoride
TD-DFT	time-dependent density functional theory
TFA	trifluoroacetic acid
TIPS	triisopropylsilyl
TGA	thermogravimetric analysis
THF	tetrahydrofuran
UV-Vis	ultraviolet-visible
XRD	X-ray diffraction

Chapter 1: Introduction

1.1 Acene chemistry

Acenes are a family of linearly fused benzene rings (Chart 1.1), which can be named based on the number of benzenes, such as: naphthalene, anthracene, tetracene, pentacene, hexacene, heptacene, octacene, nonacene and so on. Acenes have the intriguing photophysical and electronic properties have been widely investigated during the last two decades,[1] owing to acenes and their derivatives have been applied as organic semiconducting materials.[2] Moreover, many studies results revealed that longer acenes are more valuable because theoretical calculations have predicted the possible formation of interesting diradicals and properties such as ferromagnetism and superconductivity with sufficient length of acenes.[3] However, as the acene goes longer, the longer acenes tend to become more and more unstable, which can be explained by Clar's aromatic sextet rule[4]. The stability issue of higher acene becomes so serious that there are few numbers of longer acene and their derivatives were synthesized and reported up to now. On the other hand, many chemists are attracted to this challenge, to get higher and stable acene derivatives. Several groups (including Wudl,[4] Anthony,[2a,5] Bunz[6] and Chi's[1d,7] groups) are driving the research of acene chemistry and acene based materials for organic electronics. In the following section, representative acenes and their significant derivatives are briefly introduced.

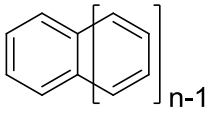

Chart 1.1 General chemical structure of acene.

Naphthalene (n = 2) and anthracene (n = 3) were suggested to exhibit high charge carrier mobilities by using the time of flight method; but only anthracene had field-effect transistor (FET) activity with hole mobility around 0.02 $cm^2V^{-1}S^{-1}$ at a low temperature.[8]

Tetracene (**1-1** in Chart 1.2, n = 4) exhibits a hole mobility of 0.1 $cm^2V^{-1}S^{-1}$ from deposited film and 2.4 $cm^2V^{-1}S^{-1}$ from single crystal.[9] The rubrene(**1-2** in Chart 1.2), 5,6,11,12-tetra-phenyl-tetracene, showed a very good performance of a single crystal transistor owning to its two-dimensional packing. However, the mobility of its thin film was quite low due to the poor planarity which hindered the formation of a crystalline film.[10] To solve the thin film formation issue of rubrene and tuning the molecular packing mode from herringbone to a slipped cofacial array, halogenations of tetracene were utilized to improve hole mobility from 0.1 $cm^2V^{-1}S^{-1}$ to 1.6-1.7 $cm^2V^{-1}S^{-1}$ in thin-film devices (**1-3a** - **1-3c** in Chart 1.2).[11] However, this method can't be used in longer acene effectively, because of the solubility problems of higher acenes.

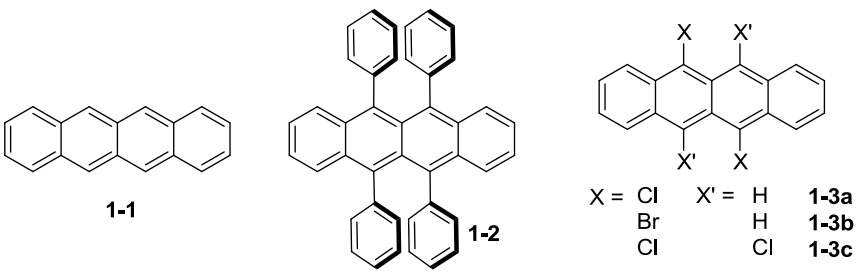

Chart 1.2 Tetracene and its peri-substituted derivatives.

Pentacene **1-4** (Chart 1.3) itself is a good p-type semiconducting material with a high hole mobility up to 5.0 $cm^2V^{-1}S^{-1}$ in the form of polycrystalline film, and even up to 35 $cm^2V^{-1}S^{-1}$ as a single crystal transistor.[12] Thus, pentacene has become a star molecule in both acene chemistry research and new organic electronic devices. A strategy of 6,13-disubstitution by silylethynyl groups has also been successfully applied to prepare pentacene derivatives, which was first studied by Anthony.[13] This approach overcomes the following three problems: solubility, herringbone molecular packing and stability to air and light[9]. Compounds **1-5a** and **1-5b** (Chart 1.3) showed high hole mobilities of 1.8 and 2.5 $cm^2V^{-1}S^{-1}$ respectively, measured from solution-processed thin films.[14]

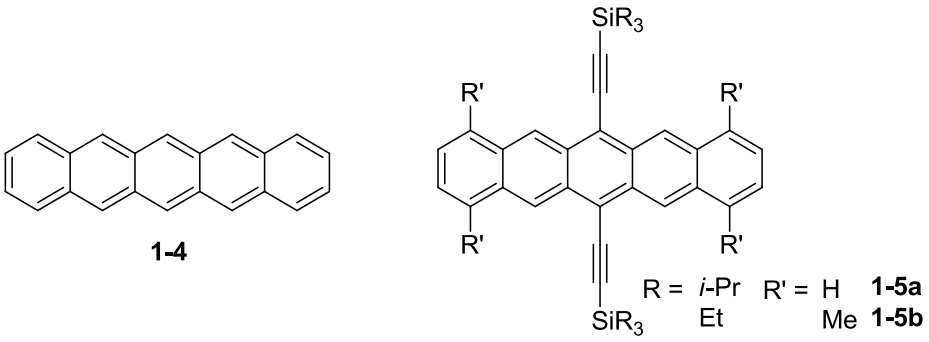

1-4

Chart 1.3 Pentacene and silylethynylated pentacenes.

It is a challenge to synthesize stable longer acenes (n > 5). Since 2005, several exciting milestones have been achieved (see structures in Charts 1.4 and 1.5). The synthetic routes for longer acene frameworks mainly include "center to sides" and "sides to center"; and they are stabilized by different peri-substitutes.

Silylethynylated hexacene **1-6** (n = 6) was first reported by Anthony's

group in 2005.[15] The solution of molecule **1-6** decomposed in a few hours when exposed to air and light but their crystals were quite stable.

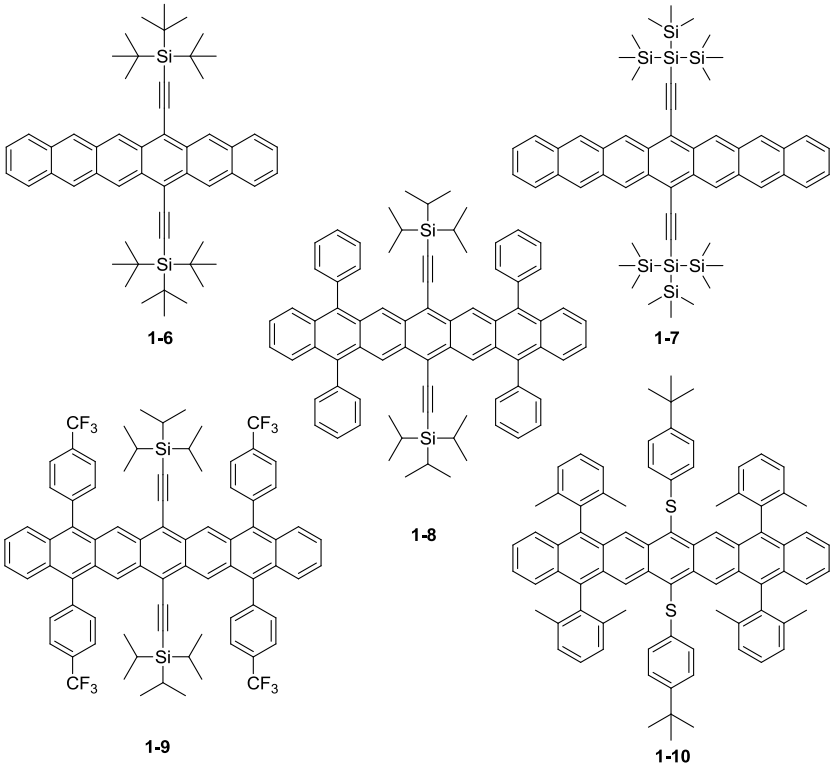

Chart 1.4 Peri-substituted hexacene and heptacenes.

Silylethynylated heptacene **1-7** (n = 7) was first reported together with silylethynylated hexacene **1-6** by Anthony's group in 2005.[15] Three years later, Wudl's group reported a silylethynylated heptacene with additional phenyl groups at the 5,9,14,18-position (**1-8**) to afford a higher stability.[16] Soon after that, Chi's group reported a stable heptacene derivative **1-9** with four electron-withdrawing trifluoromethyl phenyl groups through a different synthetic route,[7b] which is the most stable peri-substituted heptacene reported so far. Miller's group synthesized thioaryl substituted heptacene **1-10**[17] through thioaryl substituents provide resistant to photooxidation.

Thioaryl substituted nonacene **1-11** (Chart **1.5**) was soon developed.[18]

Although, its life time in solution was only two hours, **1**-**11** was the first reported persistent nonacene derivative without single crystal. Anthony's group later reported a series of silylethynylation- and fluorination-stabilized nonacenes **1**-**12** which were characterized by the single crystal X-ray diffraction.[19]

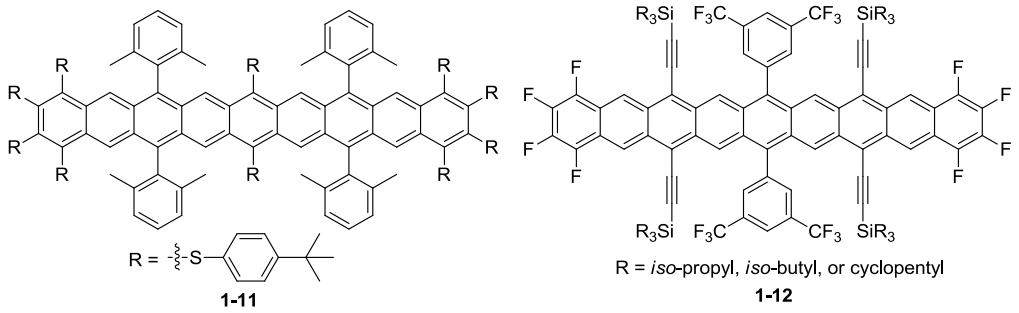

Chart 1.5 Peri-substituted nonacenes.

To summarize, the challenging but rewarding acenes chemistry has been well explored by chemists to stabilize and solubilize these ultra unstable molecules. The synthetic limit of acenes has reached nonacene. Therefore, acene analogues which fused some electron deficient five member rings into acene framework will be another interesting study direction of acene chemistry, such as indenofluorenes[20], rubicenes[21], emeraldicenes[22], Cyclopent[*hi*]aceanthrylenes[23] and dibenzopentalenes[24].

1.2 Overview of the development of pentalene

1.2.1 Background

Pentalene as one of the important antiaromatic systems has attracted many chemists' attention again during several years.[25] The unsubstituted 8π-electron

antiaromatic pentalene (Chart 1.6) is thermally unstable and dimerizes above -196 ^{o}C. In contrast, its dianion has 10π electrons and has considerable aromaticity. The stable pentalene dianion was first synthesized in 1962[26] and the single crystal structure of its dilithium salt was reported in 1991[27]. However, the preparation of pentalene dication has not been reported up to date. In other words, pentalene unit tends to obtain two electrons become dianion. Hence, compare with electron rich framework such as acene, pentalene can be regarded as electron deficient part or electron acceptor. When the pentalene unit fused with aromatic unit (such as acenes), the weak intramolecular donor-acceptor interactions between the antiaromatic pentalene and benzene rings afford corresponding stable dianion and dication species and stabilize both the pentalene and aromatic unit. Therefore, dibenzopentalene (DBP) is a fairly stable compound with a planar structure and 4nπ-electron periphery. Since the first diphenyldibenzopentalene derivative (DBP-Ph) was reported by Brand in 1912,[28] a number of the improved synthetic methods for DBP derivatives have been developed. In the last century, most of organic chemist search the synthetic method of pentalene core and modify by functional group at 5 and 10 positions. Since 2009, several tremendous progresses have been made on synthetic methodologies for accessing dibenzopentalenes. Thus, promoting research on extend the π system and their application for organic electronics. In the following section, representative methodologies of pentalene formation and pentalene

derivatives for organic semiconductors are introduced.

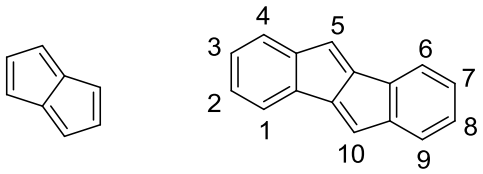

Chart 1.6 Pentalene and dibenzo[*a*,*e*]pentalene

1.2.2 Methodologies of pentalene derivatives

The first synthesis of dibenzopentalenes **1-15a** - **1-15b** was reported by Brand in 1912[28]. The key precursor was diphenylsuccindanedione **1-13**, which was synthesized from diphenylsuccinic acid[29]. Treatment of **1-13** with Grignard reagent phenylmagnesium bromide and *p*-tolylmagnesium bromide provided the corresponding diols **1-14** (Scheme 1.1). Diols **1-14** were reduced by formic acid to provide dibenzopentalenes **1-15a** and **1-15b**. This method could be applied to introduce other aryl or alkyl groups, such as *o*-anisyl [30], *p*-anisyl[30], methyl[31] and ethyl[31] groups.

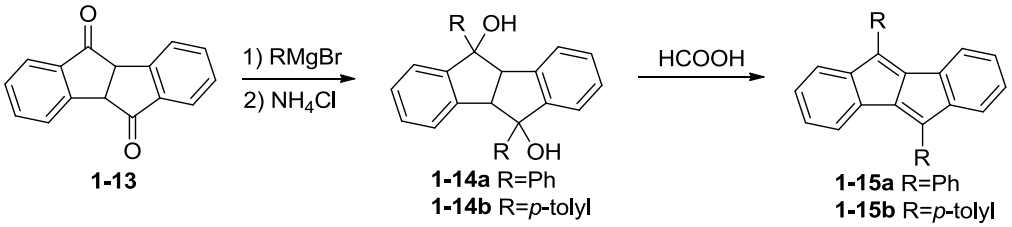

Scheme 1.1 First Studies on the Preparation of Dibenzopentalenes **1-15**

The unsubstituted dibenzopentalene **1-18** was first synthesized also from diphenylsuccindanedione **1-13** in 1952[32]. Diphenylsuccindanedione **1-13**, reacted with phosphorus pentachloride to afford **1-16**[33], and then treated with zinc to provide **1-17**[33b]. Compound **1-17** was treated with bromine and

followed by silver acetate provided the parent dibenzopentalene **1-18** in 59% yield (Scheme 1.2).

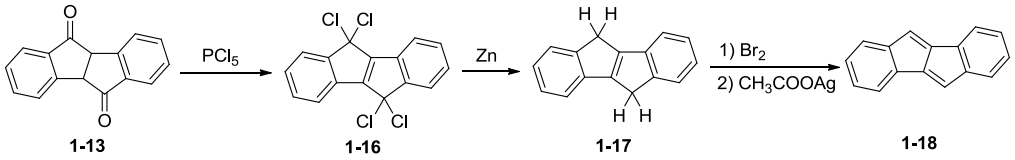

Scheme 1.2 Preparation of the Parent Dibenzopentalene **1-18**

Dibromodibenzopentalene **1-20** was prepared by bromination of tetrahydrodibenzopentalene **1-19** followed by dehydrobromination (Scheme 1.3)[34] in 1963. The thermolysis of dibenzotricyclic tetrabromide **1-21**[35] or by the reaction with sodium iodide also afforded **1-20** (Scheme 1.3)[34]. Above several methods for preparation of dibenzopentalene derivatives are early studies, following decade almost no new methods reported until 1980s.

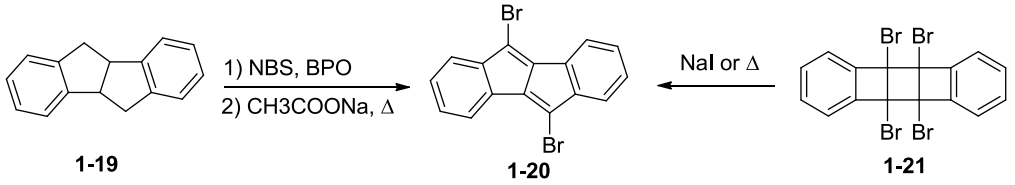

Scheme 1.3 Preparation of the dibromodibenzopentalene **1-20**

Thermolysis, such as heating and the flash vacuum pyrolysis (FVP) technique, is sometimes a very powerful tool for the creation of rigid π-frameworks through somewhat unexpected and complex reaction pathways.

Bis(pentachlorophenyl)acetylene **1-22** was heated at 350 ℃ for 45 min to afford main product perchloro-1,2,3-triphenylnaphtalene (42%) with perchloro-2,3,8-triphenylbenzofulvene **1-23** (31%) and perchlorodibenzopentalene **1-24** (1%) (Scheme 1.4)[36]. Prolonged heating for 2

h revealed an increase of the yield of **1-24** (23%) and a decrease of the yields **1-23** (10%); hence, **1-23** was the intermediate of dibenzopentalene formation.

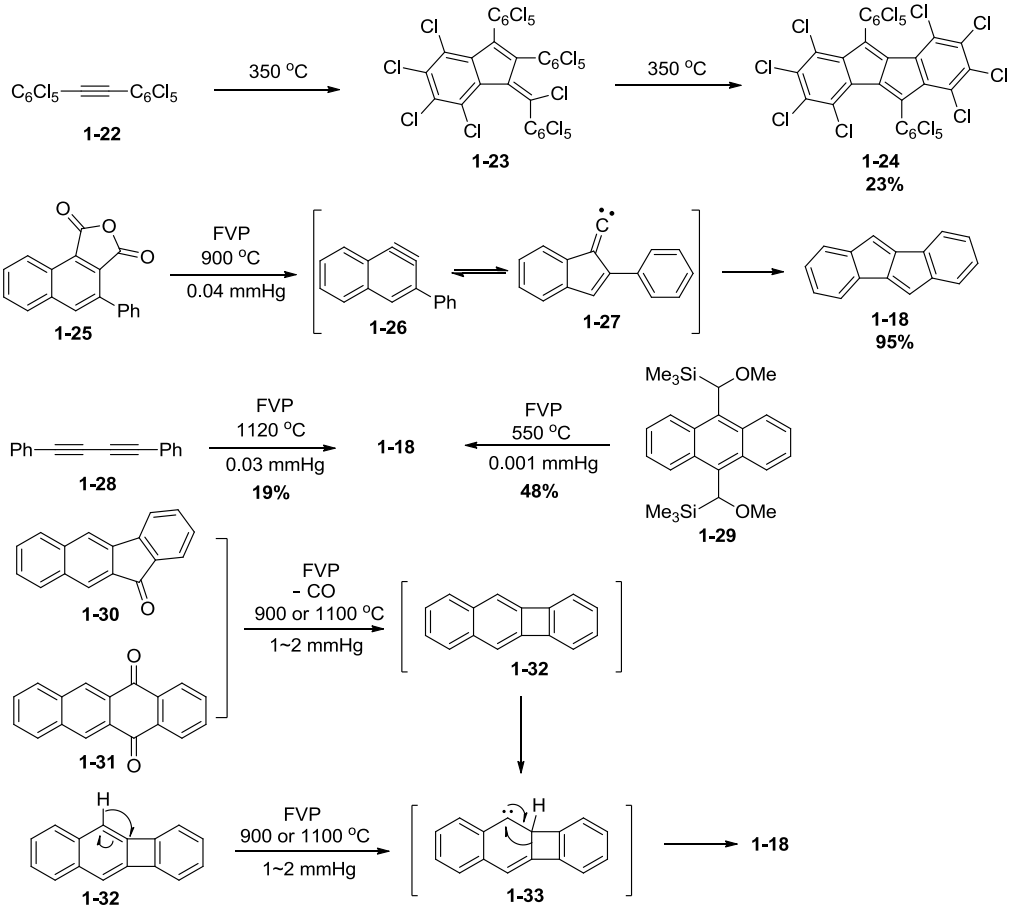

Scheme 1.4 Preparation of the dibenzopentalene derivatives by thermolysis

During the flash vacuum pyrolysis (FVP) studies, several expected or unexpected products include dibenzopentalene unit were reported. Flash vacuum pyrolysis of 3-phenylnaphthalene-1,2-dicarboxylix anhydride **1-25**, diphenylbutadiyne **1-28**, 9,10-bis[(methoxysilyl)methyl]anthracene **1-29** benzo[*b*]fluorenone **1-30**, 5,12-naphthacene quinone **1-31** and Benzo[*b*]biphenylene **1-32** at high temperature and low pressure gave the dibenzopentalene derivatives (conditions and some other details are showed in

Scheme 1.4)[37]. Thermolysis is indeed efficient method for preparation for dibenzopentalene, however the reaction is difficult to be repeated for expand structures or functionalized structures. The special apparatus and strict conditions also limited the application in synthesis work.

Anionic dibenzocyclooctene derivatives are very important intermediates during the skeletal rearrangement reactions to provide the corresponding dibenzopentalenes.

5,6,11,12-Tetrabromodibenzo[*a*,*e*]cyclooctatetraene **1-34** was treated with phenyllithium without electrophiles, 5,10-diphenyldibenzopentalane **1-15a** was obtained (Scheme 1.5)[38]. However, when the compound **1-34** was treated with alkyllithiums followed by an addition of phenyllithium and electrophiles provided dihydrodibenzopentalenes **1-35a - 1-35g**.

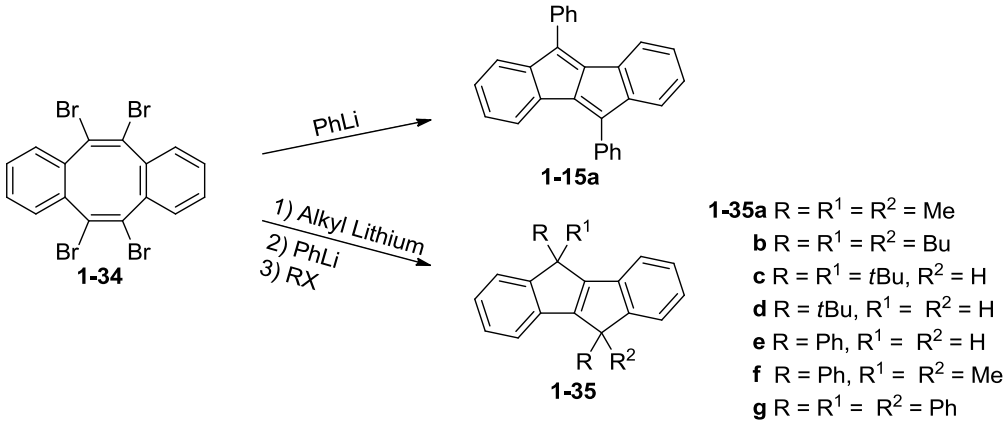

Scheme 1.5 Reactions of 5,6,11,12-Tetrabromodibenzo[*a*,*e*]cyclooctene **1-34** with Lithium Reagents.

A similar method starting from dibenzocyclooctadiyne **1-36** was reported[39]. Dibenzocyclooctadiyne **1-36** reacted with alkyllithiums to provide the corresponding anionic intermediates **1-37**, which underwent isomerization to

anionic dibenzopentalenes **1-38**. The reactions were terminated with electrophiles to afford dibenzopentalenes**1-15c - 1-15n** in very good yields (61-78%) (Scheme 1.6). When anionic dibenzopentalenes **1-38** was treated with iodine, iodine atom can be introduced at 10 position. The iodo-derivatives can be used to introduce an aryl group through Suzuki or Stille coupling reactions and to provide corresponding aryl derivatives **1-15p - 1-15t** (Scheme 1.6).

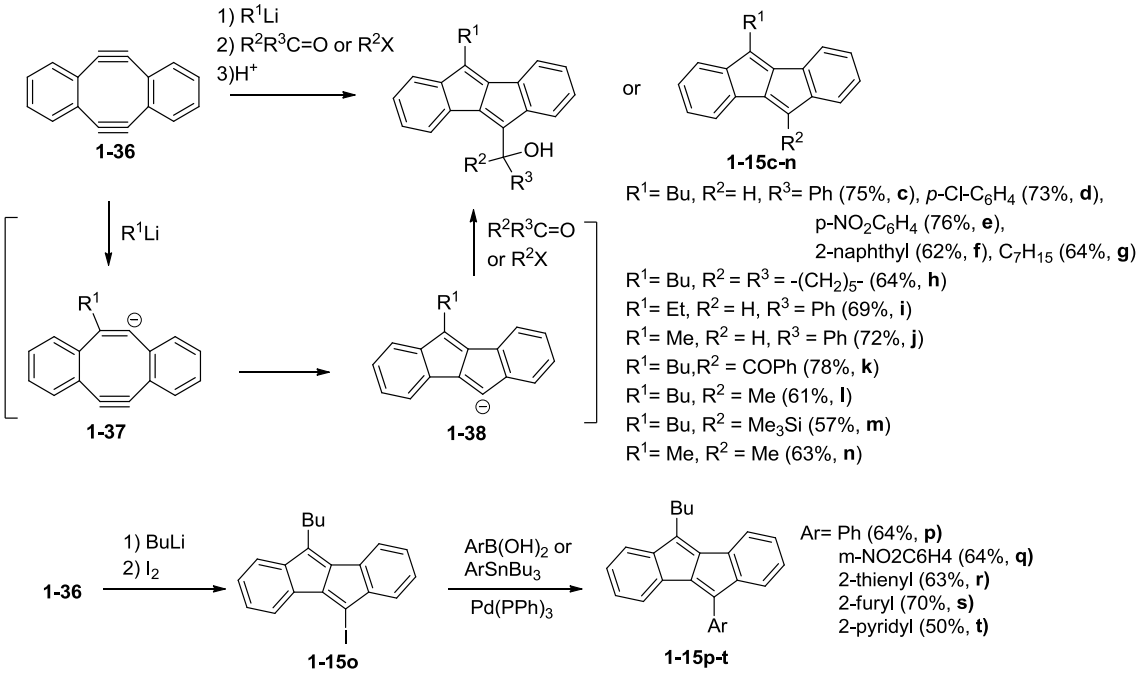

Scheme 1.6 Preparation of Dibenzopentalenes from Dibenzocyclooctadiyne **1-36**

Another similar method also starting from dibenzocyclooctadiyne **1-36** was recently reported[40]. Dibenzocyclooctadiyne **1-36** reacted with iodine or iodine monobromide (IBr) to provide the dihalogo-dibenzopenalene derivatives **1-39** in very good yields (53 and 69%) (Scheme 1.7)[40]. Then the 5 and 10 postion can be used to introduce functionalized groups or aryl groups (**1-40a - 1-40h**). Moreover the iodo atom and bromo atom provide the selectivity for coupling

reactions; hence**1-39b** can introduce the various side groups.

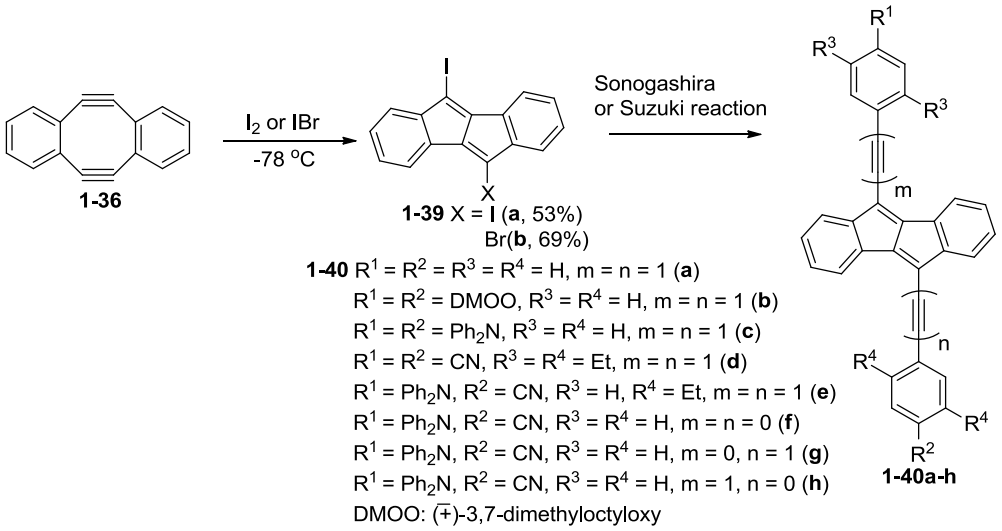

Scheme 1.7 Preparation of Dibenzopentalenes from Dibenzocyclooctadiyne **1-36**.

Another lithium reductive reaction was reported to afford unexpected dibenzopentalene through anionic dibenzocyclooctene intermediate (proposal mechanism in Scheme 1.8)[41]. Phenyl(tri-i-propylsilyl)acetylene **1-41** was treated with lithium providing dilithium dibenzopentalenide **1-44**, which were treated with iodine to afford the corresponding dibenzopentalene **1-15u** in 7% yield.

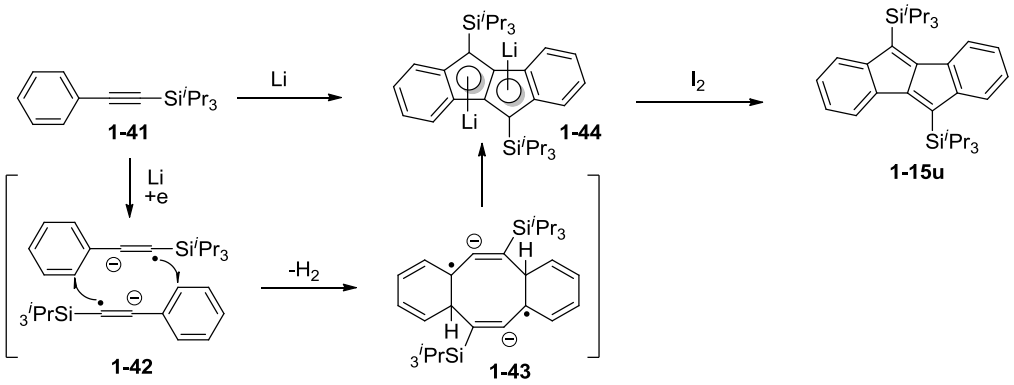

Scheme 1.8 Preparation of Dibenzopentalenes through intermediate Dibenzocyclooctadiene **1-43**

The intramolecular cyclization reactions of *o*-substituted phenylacetylenes are of considerable use for the preparation of benzannulated five-membered

ring compounds[42], such as indenes, indoles, benzofurans and benzothiophenes. A very sophisticated application of this methodology to prepare dibenzopentalene skeletons was reported by Yamaguchi[43]. Reduction of *o,o'*-bis(arylcarbonyl)diphenylacetylenes **1-45** with lithium naphthalenide produced dibenzopentalenes **1-15a**, **b** (8-10% yields) together with 5,10-dihydroxy-5,10-dihydrodibenzopenatanes **1-46** (29-52% yields) (Scheme 1.9). The authors assumed that the over-reduction of the cyclized intermediate **1-47** with the remaining LiNaph produces **1-15** through the elimination of Li_2O. To confirm this possibility, then they carried out the reaction of the isolated trans- **1-46b** with 4 mol amounts of LiNaph, which indeed gave **1-15b** in 49% yield.

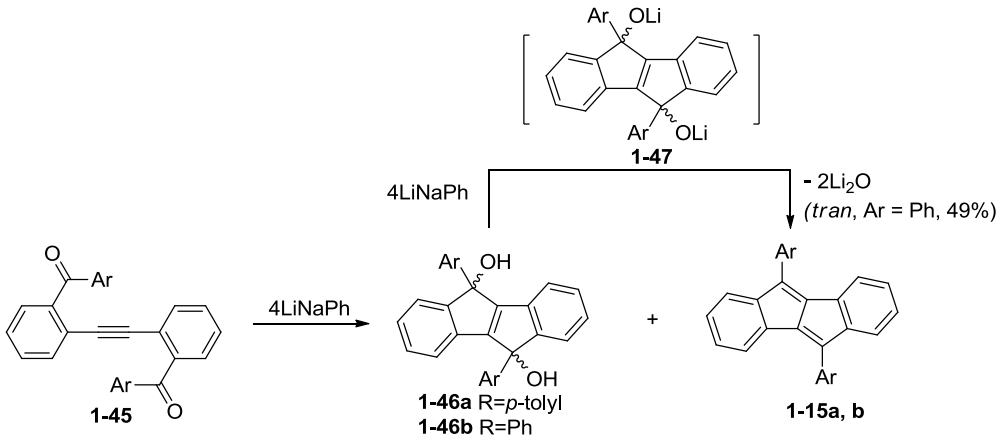

Scheme 1.9 Reductive Cyclization of o,o'-Bis(arylcarbonyl)diphenyl-acetylenes **1-45**

Comparing with above methodologies of dibenzopentalenes formation reaction, catalytic reactions usually possess mild conditions and more widely suitable substrates. Because of these advantages of catalytic reactions, chemists investigate the several catalysts and different kinds of substrates to provide the dibenzopentalenes which include symmetric and unsymmetic

dibenzopentalenes during the last several decades. Almost all the catalytic reactions are occurred between two triple bonds whether in one molecule or in different two molecules. In following section, I will introduce the catalyst present pentalene formation reaction.

In early studies, the key starting compound was 1,2-bis(phenylethynyl)benzene (**1-48a**), treatment of which with $PtCl_4$ in benzene afforded a Pt-complex of dibenzopentalene which is an unstable compound that converted to **1-15v** during purification in 85% yield (Scheme 1.10)[44]. This method was later applied for the preparation of dibenzopentalenes **1-15w - 1-15z** (Scheme 1.10)[45]. A mixture of $H_2PtCl_6 \cdot 6H_2O$ and Aliquat 336® (Aliquat = methyltrioctylammonium chloride) was also used as a catalyst for the preparation of **1-15v** with 80% yield[46]. When the reactions were carried out in the presence of dialkyl acetylenedicarboxylates, the corresponding adducts **1-15aa - 1-15cc** were obtained (25-36% yields) together with **1-15v** (Scheme 1.10)[47].

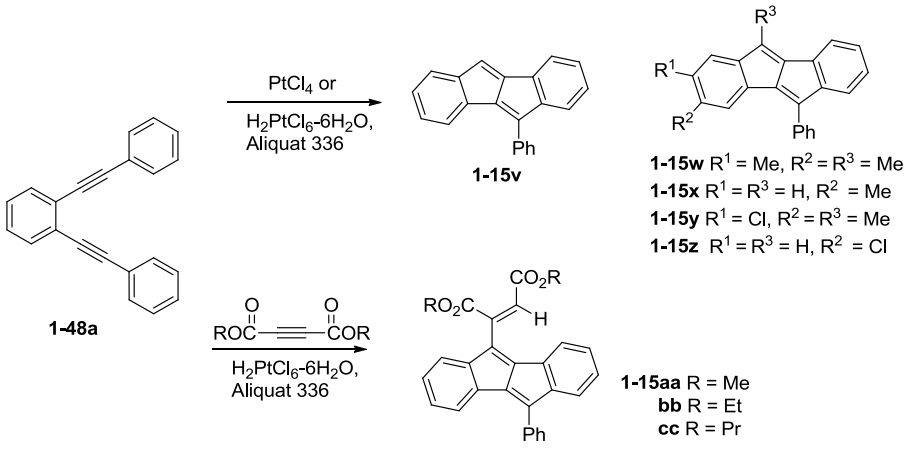

Scheme 1.10 Formation of Dibenzopentalene from 1,2-Bis(phenylethynyl)-benzene (**1-48a**) catalyzed by Platinum complex.

The cyclization reactions of 1,2-bis(phenylethynyl)benzenes to afford dibenzopentalenes were surprisingly catalyzed by tellurium (Scheme 1.11)[44]. Heating of **1-48a** with a catalytic amount of tellurium in pentachloroethane (PCE) under reflux provided dibenzopentalene **1-15dd** in 61% yield through a halogen transfer reaction (Scheme 1.11). When **1-48a** was heated with a catalytic amount of tellurium in tetrabromoethane at 170 ^{o}C, the corresponding bromodibenzopentalene **1-15ii** was obtained in 6% yield (Scheme 1.11)[44]. Treatment of **1-48b** with a catalytic amount of tellurium in PCE under reflux produced a 1:1 mixture of **1-15ee** and **1-15ff** in 79% yield. Likewise, **1-48c** reacted in PCD to afford an 1:1 mixture of **1-15gg** and **1-15hh** in 83% yield.

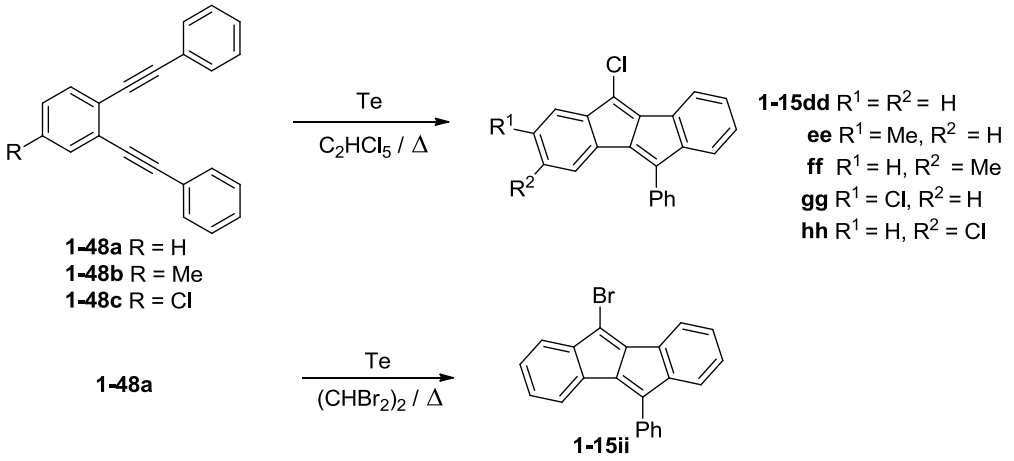

Scheme 1.11 Cyclization of 1,2-Bis(phenylethynyl)benzenes (**1-48**) in the presence of catalytic amount of Tellurium.

Another catalytic synthesis of a dibenzopentalene from 2-halophenylacetylene (**1-49**) was carried out using $Pd(PPh_3)_2Cl_2$ and CuI (Scheme 1.12[48]. Heating of a mixture of 2-iodophenylacetylene **1-49** with $Pd(PhCN)Cl_2$, PPh_3 and CuI in toluene and diisopropylamine at 90 ^{o}C provided dibenzopentalene **1-15jj** in 67% yield (Scheme 1.12). The proposed

mechanism is the dibenzocyclooctadiyne rearrangement reaction which is similar with the above anionic dibenzocyclooctadiene rearrangement reactions. Although this system looks like simpler, no further applications for the synthesis of dibenzopentalenes have been reported.

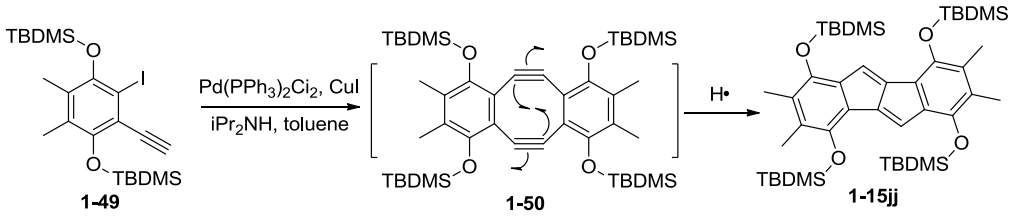

Scheme 1.12 Cyclization of 2-halophenylacetylene through dibenzocyclooctadiyne intermediate.

Two phenylacetylenes, one of which has a halogen atom and the other of which has a Bu_3Sn group were coupled in the presence of CsF, P(*t*Bu)$_3$ and $Pd_2(dba)_3$ to give dibenzopentalenes (Scheme 1.13)[24c]. The coupling reaction of **1-51a** and **1-52a** under the 130-140 ^oC shown in Scheme 1.13 provided dibenzopentalene **1-15a** in 61% yield, however reaction under the 60-70 ^oC only to produce the Stille coupling compound which was heated to 140 ^oC also did not transform to dibenzopentalenes . A crossover coupling reaction of **1-51b** and **1-52a** under the 130-140 ^oC afforded homocoupled products **1-15a** (20% yield) and **1-15ll** (trace), as well as the crossover coupled product **1-15kk** (40% yield), suggesting that the homocoupling reaction of **1-52a** would proceed. Heating of **1-52a** afforded **1-15a** in very high yields with 2 equivalents of hydroquinone, Cs_2CO_3 and CsF in the presence of catalytic amounts of P(*t*Bu)$_3$ and $Pd_2(dba)_3$ in 1,4-dioxane at 135 ℃ (Scheme 1.13). This method could be applied for the preparation of a variety of

dibenzopentalenes (55-72% yields) (Scheme 1.13). The proposed mechanism for the formation of pentalene reveals the palladium cycle and predicts some important intermediates (Scheme 1.14).

One of the most striking features of this catalytic system is that a heteroaromatic analogue of a dibenzopentalene was able to be synthesized, such as dithienopentalenes. Another advantage is that the substrate can be extended or modified by functionalized group which can be utilized to synthesize the longer pentalene derivatives for organic semiconductor materials.

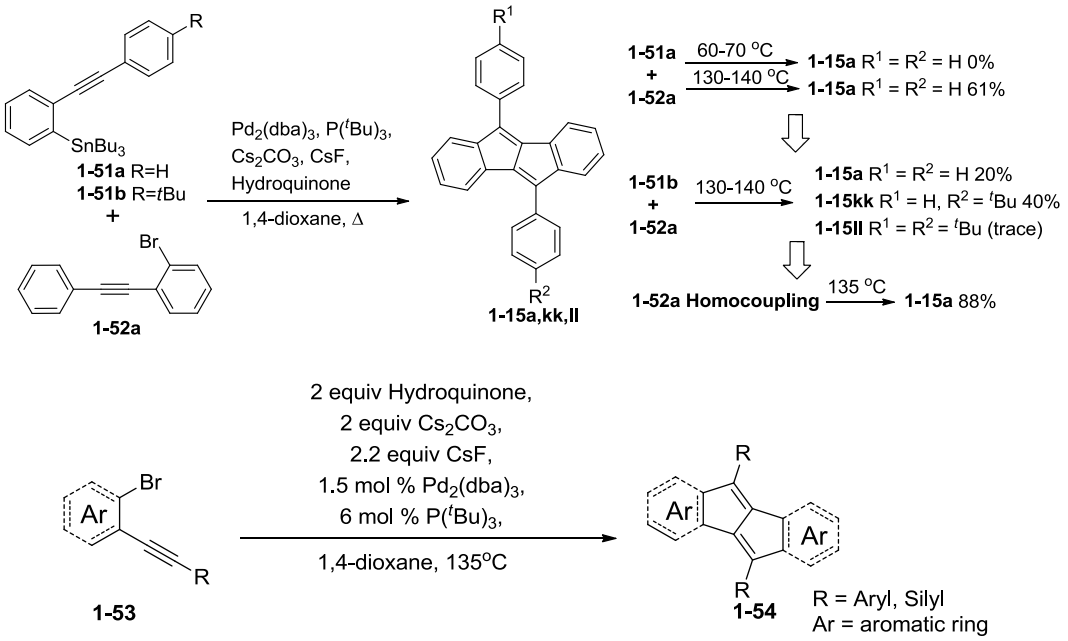

Scheme 1.13 Dibenzopentalene derivatives was synthesized by $Pd_2(dba)_3$

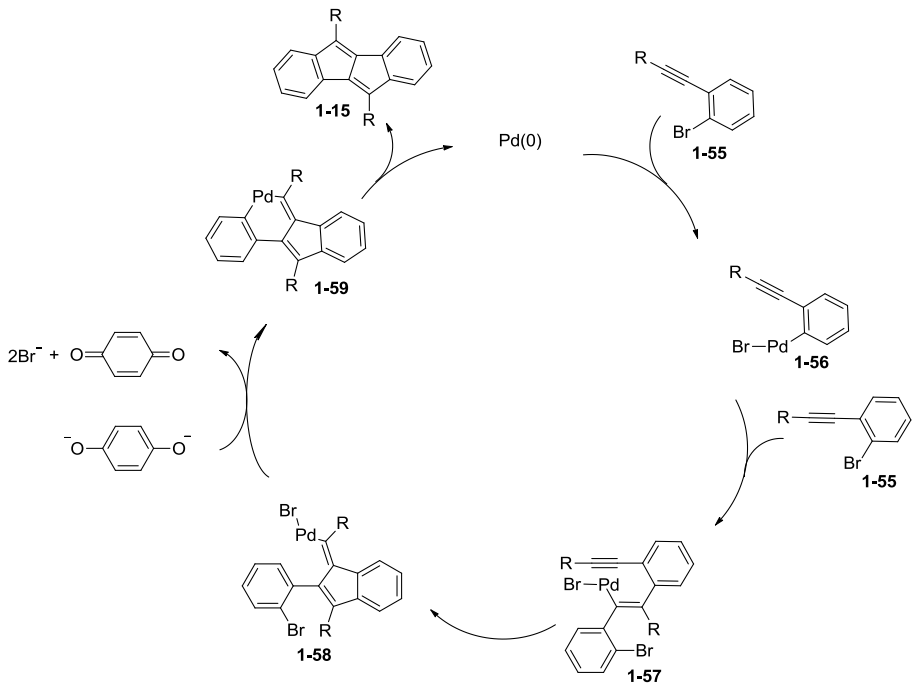

Scheme 1.14 Proposed mechanism for the formation of pentalene by the present of catalyst $Pd_2(dba)_3$.

Almost at the same time another inspired catalytic system, an extremely simple synthesis of dibenzopentalenes from 2-bromoethynylbenzenes was reported[24a]. Treatment of 2-bromoethynylbenzene **1-60a** with an equivalent of $Ni(PPh_3)_2Cl_2$ and 1.5 equivalents of Zn at 80 ℃ produced dibenzopentalene **1-15mm** in 41% yield (Scheme 1.15)[24a]. Reaction of **1-60a** with $Ni(cod)_2$ and PPh_3 at 50 ^oC afforded Ni complex **1-61**, which was transformed into **1-15mm** at 80 ℃ in higher yield which was improved to 83%. This method enabled the synthesis of a variety of dibenzopentalenes (13-24% yields) (Scheme 1.15). It is noted that the electronic nature of substituents on the aromatic rings did not affect the formation of dibenzopentalenes. So this is an important useful method to prepare the dibenzopentalenes bearing various functionalities.

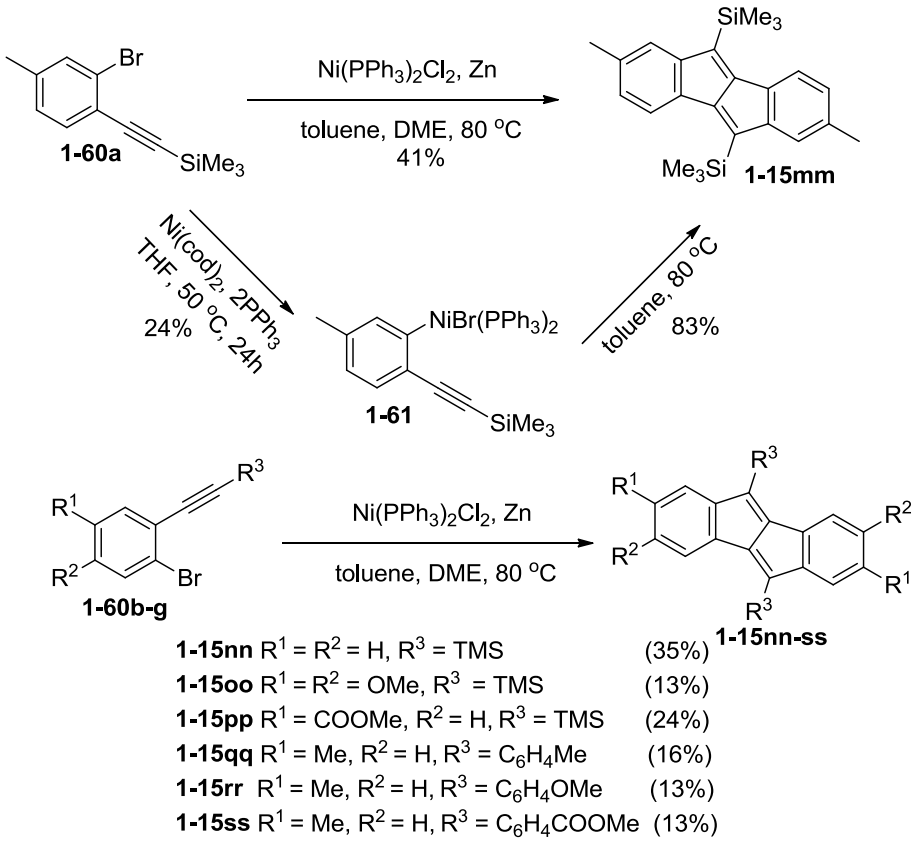

Scheme 1.15 Cyclization of 2-bromoethynylbenzenes (**1-60**) in the presence of one equivalent amount of $Ni(PPh_3)_2Cl_2$ and proposed mechanism for the formation of pentalene and Synthesis of dibenzopentalenes bearing various functionalities

Gold-catalyzed dibenzopentalene synthesis is another new method for unsymmetic dibenzopentalenes which was reported recent years[49]. benzene-1,2-diynes were catalyzed by $IPrAuNTf_2$ in benzene at 80 ^oC to provide the dibenzopentalenes in high yields (54% - 80%) (Scheme 1.16). However, this method has some limitations. Firstly, the R^2 group affects the yield obviously, when the R^2 group was electron-donating group the dibenzopentalene yield was improved, in contrast when the R^2 group was electron-withdrawing group, such as NO_2 or Br, the yield decreased to 0%. Secondly, when the benzene ring which linked with R^2 group was changed to some other group the products maybe not the pentalene derivatives.

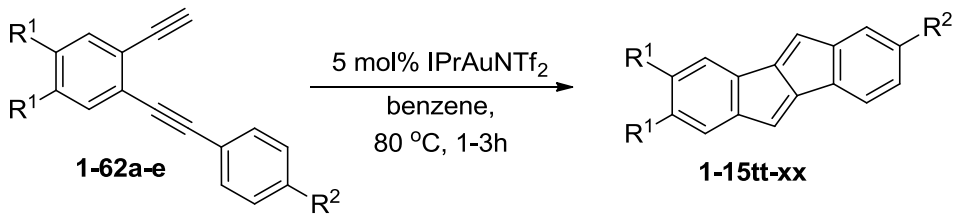

1-15tt R^1 = H, R^2 = H (54%)
1-15uu R^1 = OMe R^2 = H (68%)
1-15vv R^1 = OCH_2O, R^2 = H (62%)
1-15ww R^1 = H, R^2 = C_4H_9 (60%)
1-15xx R^1 = H, R^2 = OMe (80%)

Scheme 1.16 Gold-catalyzed dibenzopentalene synthesis

Recently, another Palladium catalyzed C-H/C-H annulations to synthesize the dibenzopentalenes were reported. Although the mechanism is similar with Scheme 1.14, the strategy is different. Heating of dibenzene-acetylene **1-63** afforded **1-15a** in 52% yields with one equivalent of AgOTf, and *o*-chloranil in the presence of catalytic amounts of $PdCl_2$ in DMAc at 60 ℃ (Scheme 1.17)[50]. The catalytic cycle was investigated by the trapping experiment with methyl acrylate to afford the compound **1-64** which matched with the proposed intermediate. The C–H activation of arylacetylenes holds significant potential to streamline the synthesis of dibenzopentalenes and its derivatives. Such a direct molecular activation/transformation technology not only contributes to the realization of economic synthesis, but also unlocks opportunities for markedly different strategies in synthesis. However the extending of the dibenzopentalene is limited by this method also.

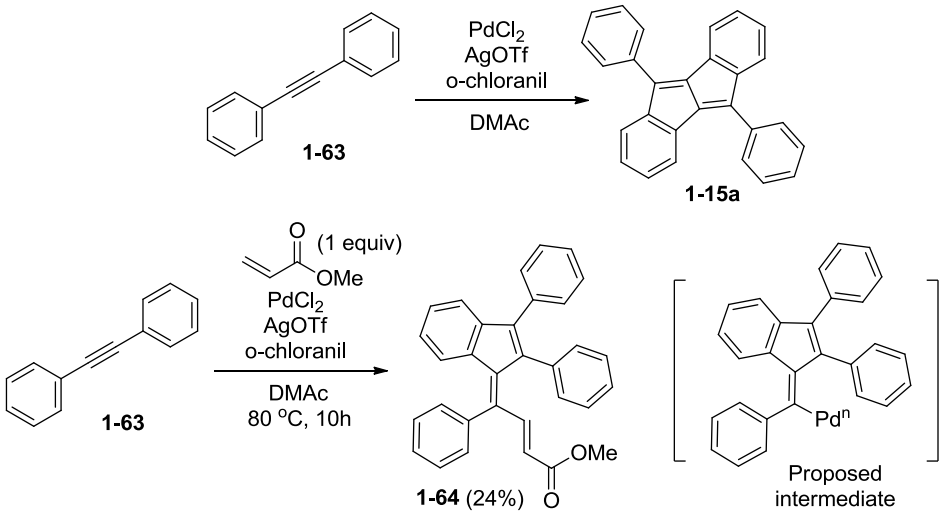

Scheme 1.17 C-H activation route to dibenzopentalenes and trapping experiment with methyl acrylate.

In this C-H activation method, the authors also investigated the effect between the yields of the product and electron-donating or -withdrawing groups at *para* or *meta* positions in the starting material. As shown in Chart 1.7, it can be seen that yields are higher when the key *ortho*-positions match best with the electrophilic reaction sites (**1-15ab** > **1-15ac**; **1-15ae** > **1-15ad**).

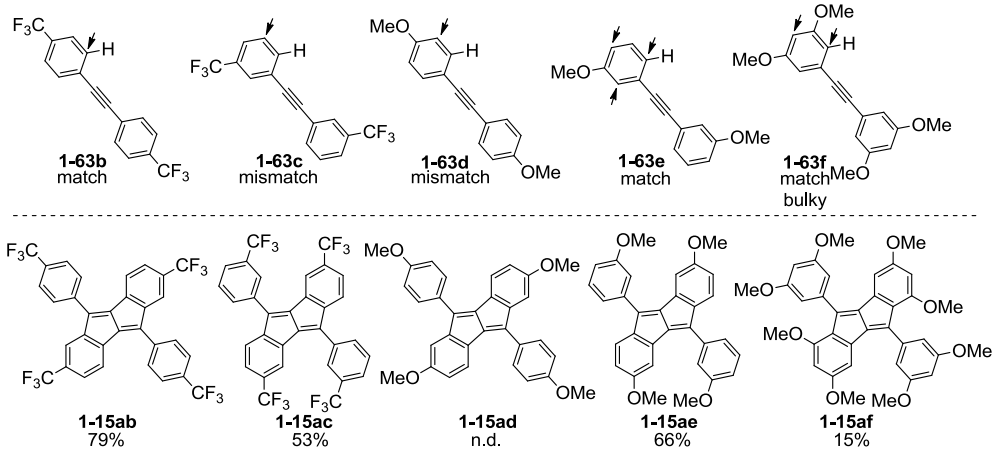

Chart 1.7 Effects of substituent and substitution pattern.

Very recently, a series of *p*-extended pentalenes with fused naphthyl-ring systems in different geometries were reported via a cascade carbopalladation reaction between alkynes and *gem*-dibromoolefins[51]. Heating of

gem-dibromoolefins **1-65a** afforded **1-66b** in 68% yields with one equivalent of znic, two equivalents of K_2CO_3 and 20 equivalents of alkyne in the presence of catalytic amounts of $Pd(PPh_3)_2Cl_2$ in toluene at 100 ℃ (Scheme 1.18). Decreasing the equivalents of diphenylacetylene from 20 to 10, however, yield of **1-66b** also decreased to 48% only, showing the necessity of high excess of the acetylene reagent under these conditions.

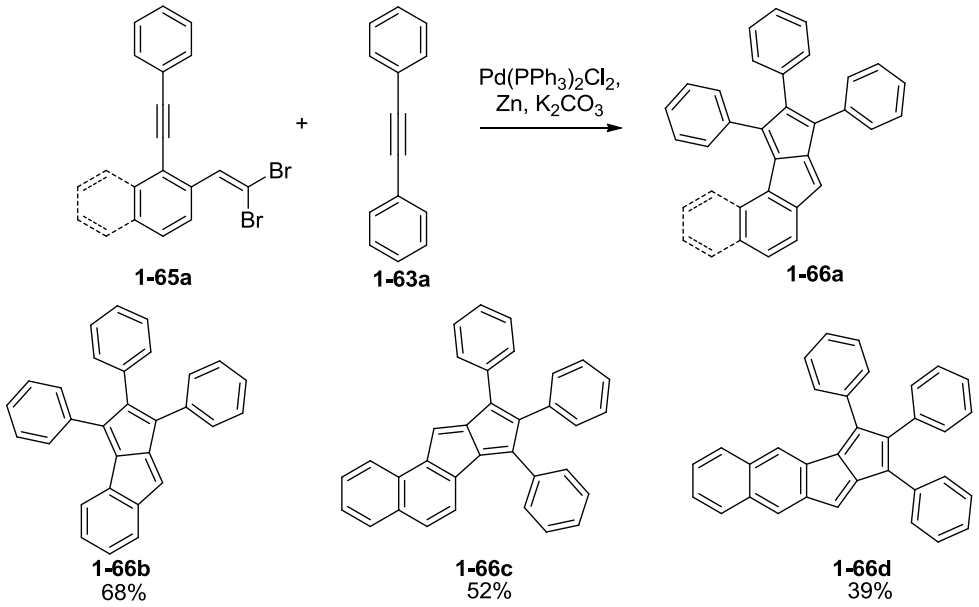

Scheme 1.18 The modol system of carbopalladation reaction between *gem*-dibromoolefins and alkynes leading to monoannelated non-symmetric pentalenes and some products listed.

During the recent years, some interesting methodologies of pentalene formation reactions without catalyst present were reported. The first one, The oxidative cyclization by the $FeCl_3$[52]. The compounds **1-67** and **1-63g** were subjected to standard Heck reaction conditions to afford indene derivative **1-68** in 53% yield. Then oxidative cyclization of **1-68** occurred in the presence of $FeCl_3$ to provide dibenzopentalene **1-15ag** in 38% yield (Scheme 1.19)[52a]. Another same method case was reported by Levi and Tilley,[52b] however the

structures were confirmed without single crystals.

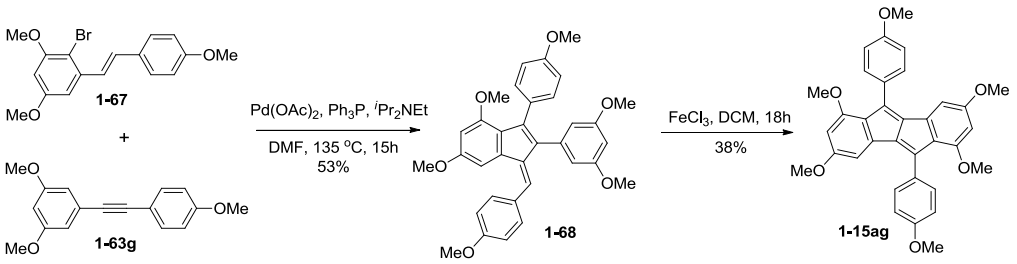

Scheme 1.19 Preparation of dibenzopentalenes through oxidative cyclization by $FeCl_3$.

Another, treatment 1,2-bis(phenylethynyl)-tetrafluorobenzene (**1-48d**) with one equivalent of $B(C_6F_5)_3$ in dichloromethane (-20 ^oC → RT, 2days) gave compound **1-15ah** as a red solid in 58% yield (Scheme 1.20)[53]. The reactions of the bis(phenylethynyl)benzene derivatives **1-48e**, **f** with $B(C_6F_5)_3$ under similar reaction conditions had a slightly more complex outcome which included **1-15ai**, **aj** and **1-15ak**, **al** (Scheme 1.20).

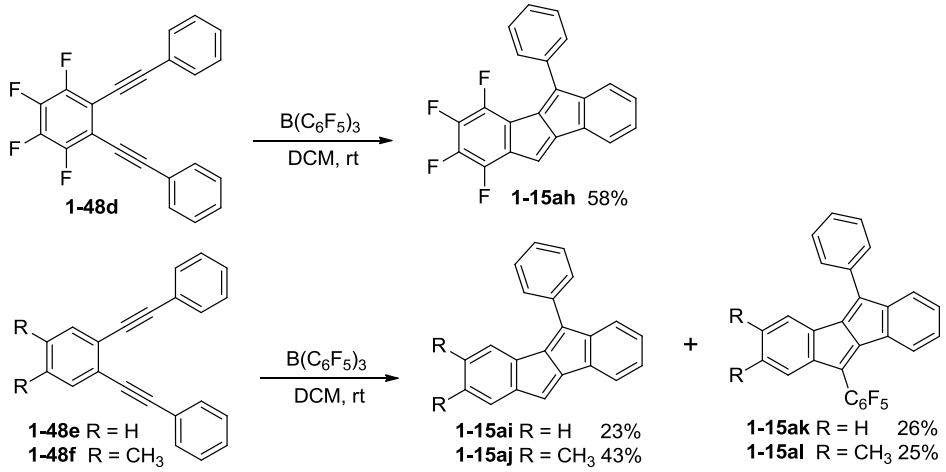

Scheme 1.20 Formation of the unsymmetric dibenzopentalene derivative by $B(C_6F_5)_3$.

1.2.3 Pentalene derivatives for organic electronics

Some fields lie dormant, sometimes for decades, and then is taken up again with new attention – usually because new preparative routes have been discoverd and previous difficultly attainable compounds have become normal

starting materials. As the development of the methodologies of dibenzopentalene derivatives, several mild and widely suitable methods were applied to synthesize the extend or heteroaromatic ring contained diarylpenalene derivatives. Obviously, during the last century the chemists have mostly focused on the methodology of pentalene formation reaction. However, from the viewpoint of materials science, the potential of the pentalene included systems was just explored very recently.[25] The weak intramolecular donor-acceptor interaction between the antiaromatic pentalene and the annealed aromatic moieties afford their unique electronic properties. Further chemical modifications of the aromatic units-fused pentalenes would provide new materials with tunable properties and electronic applications. In 2010, Kawase and Takamiya's groups first reported the extended pentalene derivative, dinaphthopentalene (DNP, Chart 1.8), which was used as organic electronic material firstly with a field effect hole mobility (μ_h) of 0.001 $cm^2V^{-1}s^{-1}$ for vapour deposited thin films.[54] In 2013, Takimiya's group reported the pentalene-based conjugated polymers (PDTDBP2T and *i*PDTDBP2T, Chart 1.8), which showed μ_h higher than 0.1 $cm^2V^{-1}s^{-1}$.[55] In addition, Kawase and Zhu's groups also reported several aromatic unit-fused pentalenes (e.g., *b*-/*c*-DTP and IB1 in Chart 1.8) as potential electronic materials but no device data were reported.[56]

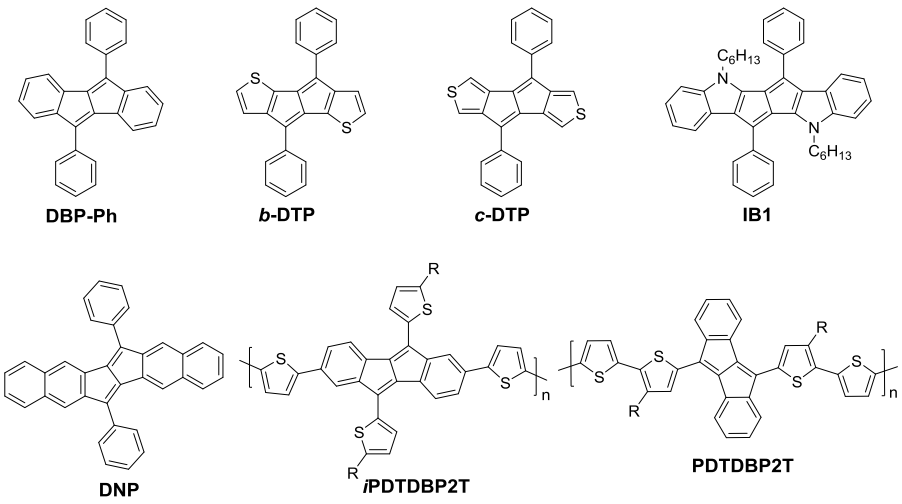

Chart 1.8 Molecular structures of di-aromatic rings fused pentalene derivatives

1.3 Highlights of contributions from this thesis

Recent years have witnessed increased interest in the design and synthesis of cyclic π-conjugated systems incorporated with an antiaromatic unit. Pentalene as an antiaromatic 4nπ-electron system has attracted many chemists' attention. Further chemical modifications of the aromatic units-fused pentalenes would provide new materials with tunable properties and electronic applications. Consequently, pentalene moiety is embedded into the acene or thienoacene framework, the weak intramolecular donor-acceptor interaction between the antiaromatic pentalene and the annealed aromatic moieties afford their unique electronic properties. In this thesis, a series of pentalene-embedded acenes and thienoacenes such as dianthracenopenalenes, bis(benzo(thieno)$_n$)pentalenes (n=1-3), bis(dicarboximide-aceno)pentalenes and di-aceno-fused-penalenes (as Z shape) have been prepared. Their physical properties and applications in organic field effect transistors have been investigated.

In Chapter 2, we designed and sythesized two solube and stable dianthracenopentalene. In these molecules number of fused rings is up to eight. The average hole mobility is increased from 0.001 to 0.65 $cm^2V^{-1}s^{-1}$ (maximum: 0.86 $cm^2V^{-1}s^{-1}$) through the substituents modification. As we know, when the thiophene rings are incorporated into the acene framework, and the obtained thienoacenes usually have excellent performance in organic field effect transistors (OFETs). In Chapter 3, the bis(benzo(thieno)$_n$)pentalene derivatives (n = 1 - 3) have been designed and synthesized. The obtained highly π-extended polycyclic conjugated systems contain a large number of fused rings (up to ten). In Chapter 4, we tried to introduce dicarboximide group into acene fused pentalene and obtain the diaceno-pentalene diimide derivatives. As expected, we got the first n-type organic semicondutor based on pentalene unit. In Chapter 5, we designed and synthesized the penaleno-diacenes. In these molecules different fuse position leads to different molecule orbital distribution and different intramolecular charge transfer model. This thesis mainly illustrates various novel acene fused pentalene derivatives and investigates the properties and device performances of these new materials.

In addition, we also investigated the acene contained polymers for organic semiconductors. In Chapter 6, we introduced the naphthalene imide unit into the polythiophene backbone to achieve stable and high performance p-type polymeric semiconductors. Our strategy is to introduce a new thiophene-fused

naphthalimide unit to the thiophene-based conjugated polymers. Based on this building block, three alternating conjugated copolymers such as **P1** - **P3** were prepared via a Stille coupling polymerization reaction. The optical, electrochemical properties, thermal behavior, and OFET performances of these polymers were investigated in details.

References

[1] (a) Harvey, R. G. *Polycyclic Aromatic Hydrocarbons*, Wiley VCH, New York, **1997**; (b) Anthony, J. E. *Angew. Chem. Int. Ed.* **2008**, 47, 452; (c) Qu, H.; Chi, C. *Curr. Org. Chem.* **2010**, 14, 2070; (d) Bettinger, H. F. *Pure Appl. Chem.* **2010**, 82, 905; (e) Ye, Q.; Chi, C. *Chem. Mater.* **2014**, DOI: 10.1021/cm501536p

[2] (a) Anthony, J. E. *Chem. Rev.* **2006**, 106, 5028; (b) Wu, J. *Curr. Org. Chem.* **2007**, 11, 1220; (c) Wang, C.; Dong, H.; Hu, W. Liu, Y.; Zhu, D. *Chem. Rev.* **2012**, 112, 2208.

[3] (a) Bendikov, M.; Duong, H. M.; Starkey, K.; Houk, K. N.; Carter, E. A.; Wudl, F. *J. Am. Chem. Soc.* **2004**, 126, 7416; (b) Kivelson, S.; Chapman, O. L. *Phys. Rev. B.* **1983**, 28, 7236.

[4] Bendikov, M.; Wudl, F.; Perepichka, D. F. *Chem. Rev.* **2004**, 104, 4891.

[5] Anthony J. E. *Angew. Chem., Int. Ed.* **2008**, 47, 452.

[6] Bunz, H. F. *Chem. Eur. J.* **2009**, 15, 6780.

[7] (a) Qu, H.; Chi, C. *Org. Lett.* **2010**, 12, 3360; (b) Qu, H.; Cui, W.; Li, J.; Shao, J.; Chi, C. *Org. Lett.* **2011**, 13, 924; (c) Chang, J.; Qu, H.; OOI, Z.-E.; Zhang, J.; Chen. Z.; Wu, J.; Chi, C. *J. Mater. Chem. C* **2013**, 1, 456-462.

[8] (a) Warta, W.; Karl, N. *Phys. Rev. B* **1985**, 32, 1172; (b) Karl, N.; Marktanner, J. *Mol. Cryst. Liq. Cryst.* **2001**, 355, 149; (c) Ito, K.; Suzuki, T.; Sakamoto, Y.; Kubota, D.; Inoue, Y.; Sato, F.; Tokito, S. *Angew. Chem., Int. Ed.* **2003**, 42, 1159; (d) Aleshin, A. N.; Lee, J. Y.; Chu, S. W.; Kim, J. S.; Park, Y. W. *Appl. Phys. Lett.* **2004**, 84, 5383.

[9] (a) Gundlach, D. J.; Nichols, J. A.; Zhou, L.; Jackson, T. N. *Appl. Phys. Lett.* **2002**, 80, 2925; (b) Reese, C.; Chung, W.-J.; Ling, M.-M.; Roberts, M.; Bao, Z. *Appl. Phys. Lett.* **2006**, 89, 202108.

[10] (a) Sundar, V. C.; Zaumseil, J.; Podzorov, V.; Menard, E.; Willett, R. L.; Someya,T.; Gershenson,M. E.; Rogers, J. A. *Science* **2004**, 303, 1644; (b) Fong, H. H.; So, S. K.; Sham, W. Y.; Lo, C. F.; Wu, Y. S.; Chen, C. H. *Chem. Phys.* **2004**, 298, 119; (c) Zeis, R.; Besnard, C.; Siegrist, T.; Schlockermann, C.; Chi, X. L.; Kloc, C. *Chem. Mater.* **2006**, 18, 244; (d) Briseno, A. L.; Tseng, R. J.; Ling, M. M.; Talcao, E. H. L.; Yang, Y.; Wudl, F.; Bao, Z. N. *Adv. Mater.* **2006**, 18, 2320; (e) Haas, S.; Stassen, A. F.; Schuck, G.; Pernstich, K. P.; Gundlach, D. J.; Batlogg, B.; Berens, U.; Kirner, H. *J. Phys. Rev. B* **2007**, 76, 115203.

[11] (a) Moon, H.; Zeis, R.; Borkent, E.-J.; Besnard, C.; Lovinger, A. J.; Siegrist, T.; Kloc, C.; Bao, Z. *J. Am. Chem. Soc.* **2004**, 126, 15322; (b) Chi,

X. L.; Li, D. W.; Zhang, H. Q.; Chen, Y. S.; Garcia, V.; Garcia, C.; Siegrist, T. *Org. Electron.* **2008**, 9, 234.

[12] (a) Gundlach, D. J.; Lin, Y. Y.; Jackson, T. N. *IEEE Electron Dev. Lett.* **1997**, 18, 87; (b) Dimitrakopoulos, C. D.; Purushothaman, S.; Kymissis, J.; Callegari, A.; Shaw, J. M. *Science* **1999**, 283, 822; (c) Sirringhaus, H.; Kawase, T.; Friend, R. H.; Shimoda, T.; Inbasekaran, M.; Wu, W.; Woo, E. P. *Science* **2000**, 290, 2123; (d) Klauk, H.; Halik, M.; Zschieschang, U.; Schmid, G.; Radlik, W.; Weber, W. *J. Appl. Phys.* **2002**, 92, 5259; (e) Kelley, T. W.; Boardman, L. D.; Dunbar, T. D.; Muyres, D. V.; Pellerite, M. J.; Smith, T. P. *J. Phys. Chem. B* **2003**, 107, 5877; (f) Knipp, D.; Street, R. A.; Völkel, A.; Ho, J. *J. Appl. Phys.* **2003**, 93, 347; (g) Jurchescu, O. D.; Baas, J.; Palstra, T. T. M. *Appl. Phy. Lett.* **2004**, 84, 3061.

[13] (a) Anthony, J. E.; Eaton, D. L.; Parkin, S. R. *Org. Lett.* **2002**, 4, 15; (b) Sheraw, C. D.; Jackson, T. N.; Eaton, D. L; Anthony, J. E. *Adv. Mater.* **2003**, 15, 2009.

[14] (a) Park, S. K.; Jackson, T. N.; Anthony, J. E.; Mourey, D. A. *Appl. Phys. Lett.* **2007**, 91, 063514; (b) Llorente, G. R.; Dufourg-Madec,M.-B.; Crouch, D. J.; Pritchard, R. G.; Ogier, S.; Yeates, S. G. *Chem. Commun.* **2009**, 3059.

[15] Payne, M. M.; Parkin, S. R.; Anthony, J. E. *J. Am. Chem. Soc.* **2005**, 127, 8028.

[16] Chun, D.; Cheng, Y.; Wudl, F. *Angew. Chem., Int. Ed.* **2008**, 47, 8380.

[17] Kaur, I.; Stein, N. N.; Kopreski, R. P.; Miller, G. P. *J. Am. Chem. Soc.* **2009**, 131, 3424.

[18] Kaur, I.; Jazdzyk, M. N.; Stein, N.; Prusevich, P.; Miller, G. P. *J. Am. Chem. Soc.* **2010**, 132, 1261.

[19] Purushothaman, B.; Bruzek, M.; Parkin, S. R.; Miller, A.-F.; Anthony, J. E. *Angew. Chem., Int. Ed.* **2011**, 50, 7013.

[20] (a) Reisch, H.; Wiesler, U.; Scherf, U.; Tuytuylkov, N. *Macromolecules* **1996**, 29, 8204; (b) Chase, D. T.; Rose, B. D.; McClintock, S. P.; Zakharov, L. N.; Haley, M. M. *Angew. Chem., Int. Ed.* **2011**, 50, 1127; (c) Shimizu, A.; Tobe, Y. *Angew. Chem., Int. Ed.* **2011**, 50, 6906; (d) Chase, D. T.; Fix, A. G.; Rose, B. D.; Weber, C. D.; Nobusue, S.; Stockwell, C. E.; Zakharov, L. N.; Lonergan, M. C.; Haley, M. M. *Angew. Chem., Int. Ed.* **2011**, 50, 11103.

[21] (a) Hseuh, H.-H.; Hsu, M.-Y.; Wu, T.-L.; Liu, R.-S. *J. Org. Chem.* **2009**, 74, 8448; (b) Wood, J. D.; Jellison, J. L.; Finke, A. D.; Wang, L.; Plunkett, K. N. *J. Am. Chem. Soc.* **2012**, 134, 15783; (c) Lee, H.; Zhang, Y.; Zhang, L.; Mirabito, T.; Burnett, E. K.; Trahan, S.; Mohebbi, A. R.; Mannsfeld, S. C. B.; Wudlb, F.; Briseno, A. L. *J. Mater. Chem. C* **2014**, 2, 3361.

[22] (a) Mohebbi, A. R.; Wudl, F. *Chem.- Eur. J.* **2011**, 17, 2642; (b) Mohebbi, A. R.; Yuen, J.; Fan, J.; Munoz, C.; Wang, M. F.; Shirazi, R. S.; Seifter, J.; Wudl, F. *Adv. Mater.* **2011**, 23, 4644.

[23] Lütke Eversloh, C.; Avlasevich, Y.; Li, C.; Müllen, K. *Chem. - Eur. J.* **2011**, 17, 12756.

[24] (a) Saito, M.; Nakamura, M.; Tajima, T. *Chem. - Eur. J.* **2008**, 14, 6062; (b) Kawase, T.; Konishi, A.; Hirao, Y.; Matsumoto, K.; Kurata, H.; Kubo, T. *Chem. - Eur. J.* **2009**, 15, 2653; (c) Levi, Z. U.; Tilley, T. D. *J. Am. Chem. Soc.* **2009**, 131, 2796.

[25] (a) Saito, M. *Symmetry* **2010**, *2*, 950; (b) Hopf, H. *Angew. Chem. Int. Ed.* **2013**, 52, 12224.

[26] (a) Rosenberger, M.; Katz, T. J. *J. Am. Chem. Soc.* **1962**, *84*, 865; (b) Katz, T. J.; Rosenberger, M.; O'Hara, R. K. *J. Am. Chem. Soc.* **1964**, *86*,249.

[27] Stezowski, J. J.; Hoier, H.; Wilhelm, D.; Clark, T.; Schleyer, P. v. R. *J. Chem. Soc. Chem. Commun*. **1985**, 1263.

[28] Brand, K. *Ber. Detsch. Chem. Ges*. **1912**, *45*, 3071.

[29] (a) Mittal, R. S. D.; Sothi, S. C. *Tetrahedron* **1973**, *29*, 1321; (b) Yang, J.; Lakshmikantham, M. V.; Cava, M. P.; Lorcy, D.; Bethelot, J. R. *J. Org. Chem*. **2000**, 65, 6739.

[30] Brand, K.; Hoffmann, F. W. *Ber. Detsch. Chem. Ges*. **1920**, 53, 815.

[31] Brand, K.; Schläger, F. *Ber. Detsch. Chem. Ges*. **1923**, 56, 2541.

[32] Blood, C. T.; Linstead, R. P. *J. Chem. Soc*. **1952**, 2263.

[33] (a) Brand, K.; Müller, O. *Ber. Detsch. Chem. Ges*. **1922**, 55, 601; (b) Wawzonek, S. *J. Am. Chem. Soc*.**1940**, 62, 745.

[34] Cava, M.P.; Pohlke, R.; Mitchell, M. J. *J. Org. Chem.* **1963**, 28, 1861.

[35] Jensen, F. R.; Coleman, W. E. *Tetrahedron Lett.* **1959**, 1, 7.

[36] Ballester, M.; Castañer, J.; Riera, J.; Armet, O. *J. Org. Chem.* **1986**, 51, 1100.

[37] (a) Anderson, M. R.; Brown, R. F. C.; Coulston, K. J.; Eastwood, F. W.; Ward, A. *Aust. J. Chem.* **1990**, 43, 1137; (b) Brown, R. F. C.; Eastwood, F. W.; Wong, N. R. *Tetrahedron Lett.* **1993**, 34, 3607; (c) Preda, D. V.; Scott, L. T. *Org. Lett.* **2000**, 2, 1489; (d) Kendall, J. K.; Shechter, H. *J. Org. Chem*. **2001**, 66, 6643.

[38] Hellwinkel, D.; Hasselbach, H-J.; Lämmerzahl, F. *Angew. Chem. Int. Ed. Engl*. **1984**, 23, 705.

[39] Babu, G.; Orita, A.; Otera, J. *Chem. Lett.* **2008**, 37, 1296.

[40] Xu, F.; Peng, L.; Orita, A.; Otera, J. *Org. Lett.* **2012**, 14, 3970.

[41] Saito, M.; Nakamura, M.; Tajima, T.; Yoshioka, M. *Angew. Chem. Int. Ed*. **2007**, 46, 1504.

[42] Zhang, H.; Karasawa, T.; Tamada, H.; Wakamiya, A.; Yamaguchi, S. *Org. Lett.* **2009**, 11, 3076.

[43] (a) Zeni, G.; Larock, R. C. *Chem. Rev.* **2006**, 106, 4644; (b) Patil, N. P.; Yamamoto, Y. *Chem. Rev.* **2008**, 108, 3395.

[44] (a) Müller, V. E.; Munk, K.; Ziemek, P.; Sauerbier, M. *Liebigs Ann. Chem*. **1968**, 713, 40; (b) Müller, V. E.; Munk, K.; Fritz, H. - G.; Sauerbier, M. *Liebigs Ann. Chem*. **1969**, 723, 76.

[45] Blum, J.; Baidossi, W.; Badrieb, Y.; Hoffman, R. E. *J. Org. Chem.* **1995**,

60, 4738.

[46] Badrieh, Y.; Blum, J.; Amer, I.; Vollhardt, K. P. C. *J. Mol. Catal*. **1991**, 66, 295.

[47] Badrieh, Y.; Greenwald, A.; Schumann, H.; Blum, J. *Chem. Ber*. **1992**, 125, 667.

[48] Chakrabirty, M.; Tessier, C. A.; Youngs, W. J. *J. Org. Chem.* **1999**, 64, 2947.

[49] Hashmi, A. S. K.; Wieteck, M.; Braun,I. Nösel, P.; Jongbloed, L.; Rudolph, M.; Rominger, F. *Adv. Synth. & Catal*. **2012**, 354, 555.

[50] Maekawa, T.; Segawa, Y.; Itami, K. *Chem. Sci*., **2013**, 4, 2369.

[51] London, G.; Rekowski, M. W.; Dumele, O.; Schweizer, W. B.; Gisselbrecht, J.-P.; Boudonb, C.; Diederich, F. *Chem. Sci.* **2014**, 5, 965.

[52] (a) Jeffrey, J. L.; Sarpong, R. *Tetrahedron Lett*. **2009**, 50, 1969; (b) Levi, Z. U.; Tilley, T. D. *J. Am. Chem. Soc.* **2010**, 132, 11012.

[53] Chen, C.; Harhausen, M.; Liedtke, R.; Bussmann, K.; Fukazawa, A.; Yamaguchi, S.; Petersen, J. L.; Daniliuc, C. G.; Fröhlich, R.; Kehr, G.; Erker , G. *Angew. Chem. Int. Ed.* **2013**, 52, 5992.

[54] Kawase, T.; Fujiwara, T.; Kitamura, Ch.; Konishi, A.; Hirao, Y.; Matsumoto, K.; Kurata, H.; Kubo, T.; Shinamura, S.; Mori, H.; Miyazaki, E.; Takimiya, K. *Angew. Chem. Int. Ed.* **2010**, 49, 7728.

[55] M. Nakano, I. Osaka, K. Takimiya, T. Koganezawac, *J. Mater. Chem. C* **2014**, 2, 64.

[56] (a) Konishi, A.; Fujiwara, T.; Ogawa, N.; Hirao, Y.; Matsumoto, K.; Kurata, H.; Kubo, T.; Kitamura, C.; Kawase, T. *Chem. Lett.* **2010**, 39, 300; (b) Yin, X.; Li, Y.; Zhu, Y.; Kan, Y.; Li, Y.; Zhu, D. *Org. Lett.* **2011**, 13, 1520.

Chapter 2: Large π-Extended Dianthraceno-pentalenes: Synthesis, Characterization, and Applications in Organic Field-Effect Transistors

2.1 Introduction

Linear π-extended acene derivatives such as pentacene have been demonstrated to be very good charge transporting materials. Higher mobilities are expected for the even higher order acenes (e.g., hexacene and heptacene), but their intrinsic high reactivity limited their synthesis and material applications.[1] Pentalene, as a 4nπ-electron system, provides corresponding stable dianion and dication species leading to highly amphoteric redox properties. Consequently, pentalene moiety is incorporated into the acene framework, and the acene fused pentalenes are obtained. The weak intramolecular donor-acceptor interaction between the antiaromatic pentalene and the annealed aromatic moieties afford their unique electronic properties. Recently, tremendous progress has been made on synthesis methodologies for acessing pentalene derivatives,[2] thus promoting rearch on their application for organic electronics.[2j,3] Further chemical modifications of the aromatic units-fused pentalenes would provide new materials with tunable properties and electronic applications.

We are particularly interested in incorpating pentalene moiety into the longer acenes in hope of solving the stabilty issue of high acenes. In this chapter, we synthesized two pentalene-centered, eight ring fused system with

phenyl substituents named **DAP1** and **DAP2** (Scheme 2.1). Intersetingly, **DAP2** shows more stable, closer packing mode and much higher hole charge mobility than **DAP1**.

2.2 Results and discussion

2.2.1 Synthesis

The synthesis of compounds **DAP1** and **DAP2** is shown in Scheme 2.1. The 2,3-dibromoanthracene **2-1**,[4] 1-ethynyl-4-nonylbenzene[5] and 1,3-diphenylisobenzofuran **2-3**[6] were prepared by following literature procedures. The Sonogashira coupling reaction between **2-1** and 1-ethynyl-4-nonylbenzene provided the 2-bromo-3-((4-nonylphenyl)-ethynyl)anthracene **2-2** in 35% yield. $Pd_2(dba)_3$ catalyzed dimerization of **2-2** afforded the 7,16-bis(4-nonylphenyl)-[1,2-b:4,5-b']dianthracenopentalene **DAP1** in 16% yield. Diels-Alder addition reaction between 1,3-diphenylisobenzofuran **2-3** and dibromobenzyne which obtained via 1,2,4,5-tetrabromobenzene treated with butyl lithium gave the 2,3-dibromo-9,10-diphenyl-9,10-dihydro-9,10- epoxyanthracene **2-4** in 60% yield. Then dehydration by Znic and Titanium tetrachloride produced the 2,3-dibromo-9,10-diphenylanthracene **2-5** in 80% yield. Similar Sonogashira coupling reaction between 2-5 and 1-ethynyl-4-nonylbenzene formed compound 2-6 in 36% yield. It is followed by $Pd_2(dba)_3$ catalyzed dimerization reaction procedures to give target molecule 7,16-bis(4-nonylphenyl)-5,9,14,18-tetraphenyl-[1,2-b:4,5-b']-dianthracenopent

alene **DAP2** in 15% yield. Similar structures without the alkyl chains showed poor solubility which limited the OFET device test by solution processing and other characterizations. Consequently, we introduced the dialkyl chain to increase the solubility of target molecules. We characterized the molecular structures by NMR, HRMS and X-ray crystallographic analysis.

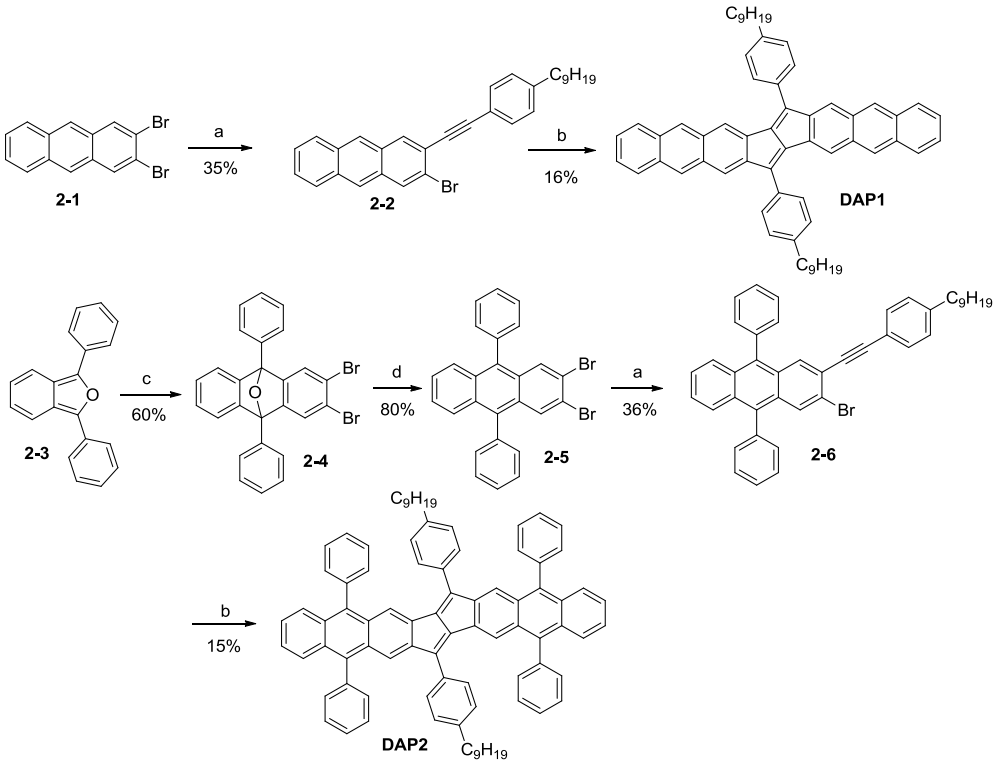

Scheme 2.1 Synthetic route of dianthracenopentalene **DAP1** and **DAP2**. *Reagents and conditions*: (a) 1-ethynyl-4-nonylbenzene, $Pd(PPh_3)_2Cl_2$, CuI, Et_3N/THF, 75 ^oC, overnight; (b) $Pd_2(dba)_3$, $P(2\text{-furyl})_3$, Cs_2CO_3, CsF, hydroquinone, 1,4-dioxane, 135^oC, 36h; (c) 1) 1,2,4,5-tetrabromobenzene, *n*BuLi, toluene, -50 ^oC, 2) RT, overnight; (d) 1) 0-70 ^oC, Zn, $TiCl_4$, THF, reflux 5min, 2) 0-70 ^oC, reflux overnight.

2.2.2 Photophysical properties

The dianthracenopentalene derivatives **DAP1** and **DAP2** have good solubility in common organic solvents. The electronic absorption spectra of **DAP1** and **DAP2** were measured in chloroform solution (Figure 2.1). The

absorption maxima for **DAP1** and **DAP2** in solutions are located at 369 and 379 nm, respectively. A longer-wavelength shoulder with maxima at 556 and 579 nm was observed for **DAP1** and **DAP2**, respectively. The compounds **DAP1** and **DAP2** showed obvious fluorescence (λ_{max} = 578 and 598 nm for **DAP1** and **DAP2** respectively, Figure 2.1) in solution with small Stokes shifts (549-685 cm^{-1}). In thin films, the absorption spectra showed obvious red-shift by 20 and 15 nm for **DAP1** and **DAP2** respectiely, indicating significant intermolecular interactions between the molecules. The fluorescence of thin film can't be observed. The optical HOMO-LUMO gaps can be extracted from onset of absorption edges. They are about 2.14 and 2.05 eV for compounds **DAP1** and **DAP2**, respectively.

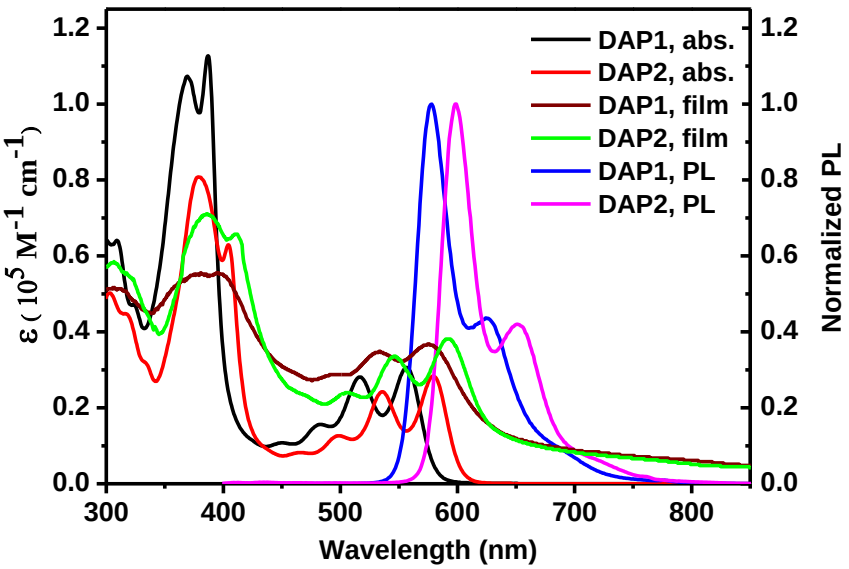

Figure 2.1 (a) UV-vis absorption spectra of **DAP1** and **DAP2** in chloroform (10^{-5} M) , fluorescence spectra of **DAP1** and **DAP2** in chloroform (10^{-6} M) and UV-vis absorption spectra of **DAP1** and **DAP2** in spin-coated thin films

2.2.3 Electrochemical properties

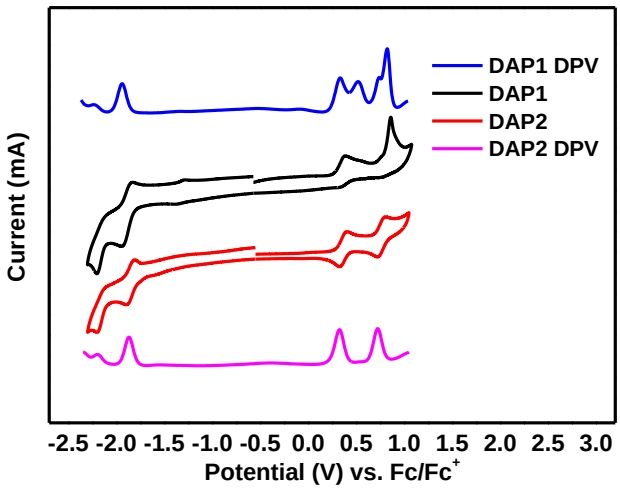

Figure 2.2 Cyclic voltammograms (CV) and differential pulse voltammetry (DPV) of compounds **DAP1** and **DAP2** in dry dichloromethane with 0.1 M Bu_4NPF_6 as the supporting electrolyte, AgCl/Ag as reference electrode, Au as working electrode, Pt wire as counter electrode, and a scan rate at 50 mV s^{-1}.

Cyclic voltommetry (CV) and differential pulse voltammetry (DPV) were used to study the electrochemical properties of compounds **DAP1** and **DAP2** (Figure 2.2). The potential was externally calibrated against the ferrocene/ferrocenium couple. Four irreversible oxidation waves with half-wave potential $E_{1/2}^{ox}$ at 0.33, 0.52, 0.74 and 0.82 V and two reversible reduction waves with half-wave potential $E_{1/2}^{red}$ at -1.94 and -2.24 V were observed for **DAP1**. Compound **DAP2** showed two reversible oxidation waves with $E_{1/2}^{ox}$ at 0.32 and 0.72 V, and two reversible reduction waves with $E_{1/2}^{red}$ at -1.87 and -2.20 V. The HOMO/LUMO energy levels are determined to be -5.08/-2.98 and -5.09/-3.00 for **DAP1** and **DAP2**, respectively. The corresponding electrochemical energy gaps E_g^{EC} are then estimated to be 2.10 eV and 2.09 eV for **DAP1** and **DAP2**. The energy gaps are also in agreement

with the optical energy gaps from the UV-vis absorption spectrum.

The HOMO and LUMO energy levels of **DAP1** and **DAP2** are almost similar, which also correspond with the TD-DFT calculation results. The calculated HOMO and LUMO orbital profiles of **DAP1** and **DAP2** are also similar. Therefore, the additional four phenyl substituents in **DAP2** have no big effect on the HOMO and LUMO energy levels. However, the phenyl groups block the active positions and stabilize the cation of dianthracenopentalene unit which is benefit for hole transfer in OFETs.

Table 2.1 Summary of electrochemical data of compounds **DAP1** and **DAP2**

	$E_{1/2}^{ox}$ (V)	$E_{1/2}^{red}$ (V)	HOMO [eV]	LUMO [eV]	E_g^{EC} [eV]	E_g^{Opt} [eV]
DAP1	**0.33; 0.52; 0.74; 0.82**	**-2.24; -1.94**	**-5.08**	**-2.98**	**2.10**	**2.14**
DAP2	**0.32; 0.72**	**-2.20; -1.87**	**-5.09**	**-3.00**	**2.09**	**2.05**

2.2.4 DFT calculations

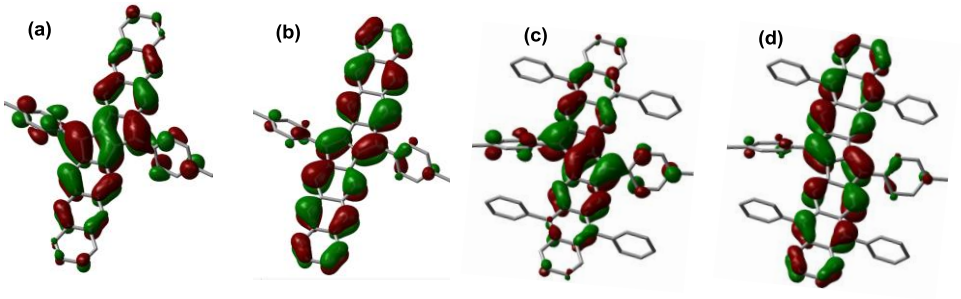

Figure 2.3 TD-DFT(RB3LYP/6-31G*) molecular orbitals of (a) LUMO and (b) HOMO of **DAP1**, (c) LUMO and (d) HOMO of **DAP2**.

Density functional theory (DFT, B3LYP/6-31G*) calculations were conducted to better understand the electronic and optical properties of dianthracenopentalene derivatives. The calculated frontier molecular orbital profiles are shown in Figure 2.3. It was found that the HOMOs of two

molecules are delocalized along the dianthracenopentalene framework while the LUMOs are mainly localized at the central pentalene unit. Time-dependent (TD) DFT calculations predicted that both compounds should show two major absorption bands. The observed strongest absorption band is mainly contributed from the HOMO-2→LUMO+1 transitions (363.6 nm, f = 1.2983 for **DAP1**; 371.5 nm, f = 1.1488 for **DAP2**). The shoulder band around 460-620 nm can be correlated to the HOMO→LUMO transitions (547.3 nm, f = 0.5057 for **DAP1**; 557.3 nm, f = 0.5459 for **DAP2**).

2.2.5 Crystallographic analysis

Single crystals of **DAP1** and **DAP2** suitable for X-ray crystallographic analysis were obtained by slow diffusion of methanol or acetonitrile into a chloroform solution. (CCDC 1008483 for **DAP1** and CCDC 1008484 for **DAP2**) The molecular structures and the packing motif for **DAP1** and **DAP2** are shown in Figure 2.4 and Figure 2.5, respectively. Both compounds have a planar π-skeleton. The two phenyl substituents have a torsion angle of ca. 42^{o} and 45^{o} to the plane of pentalene for **DAP1** and **DAP2**, respectively, which are both smaller than that for dinaphthopentalene (55^{o})[2j].

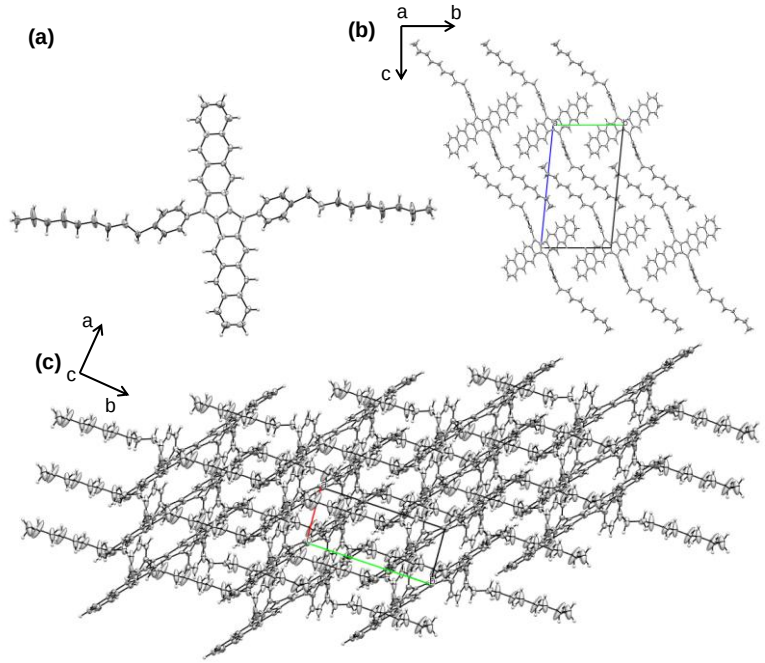

Figure 2.4 (a) Molecular structure of **DAP1**; (b) **DAP1** packing along the a-axis; (c) **DAP1** packing from side view.

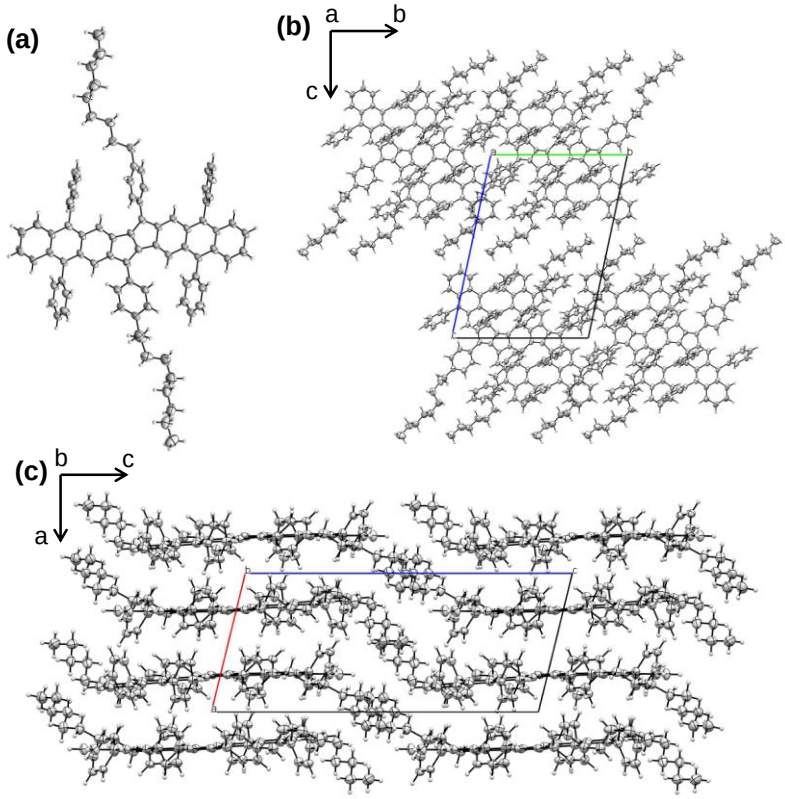

Figure 2.5 (a) Molecular structure of **DAP2**; (b) **DAP2** packing along the a-axis; (c) **DAP2** packing along the b-axis; (d) close contacts between the molecules.

The 3D packing of **DAP1** and **DAP2** both can be figured out in a triclinic unit cell (space group P-1). There are no obvious π-π interactions between the dianthracenopentalene units in **DAP1** and **DAP2**. However, the [C-H···π] interactions (range from 1.835 Å to 2.626 Å) and [π···π] interactions (range from 2.602 Å to 2.995 Å) build a slipped parallel stacking arrangement in the crystal **DAP1** (blue dash line in Figure 2.6 a). In contrast, in **DAP2**, two molecules form dimer via close contacts of [C-H···π] interactions (range from 2.776 Å to 2.836 Å) between the phenyl substituents and dianthracenopentalene units (blue dash line in Figure 2.6 b,c). Moreover, there are also close contacts of [C-H···π] interaction (both 2.899 Å) and [π···π] interaction (both 3.347 Å) between the phenyl substituents of neighbour dimmers. All the different kinds of close contact interactions help the molecules to closely pack into an ordered layer-like structure (red dash line in Figure 2.6 b,c). Compare the two crystals, we can find that the **DAP2** adoping a more tight stacking mode which is benefit for charge transport property. Selected bond lengths of **DAP1** and **DAP2** are shown in Figure 2.7. In both cases, large bond alternation in the pentalene skeleton as well as in the benzene rings was observed.

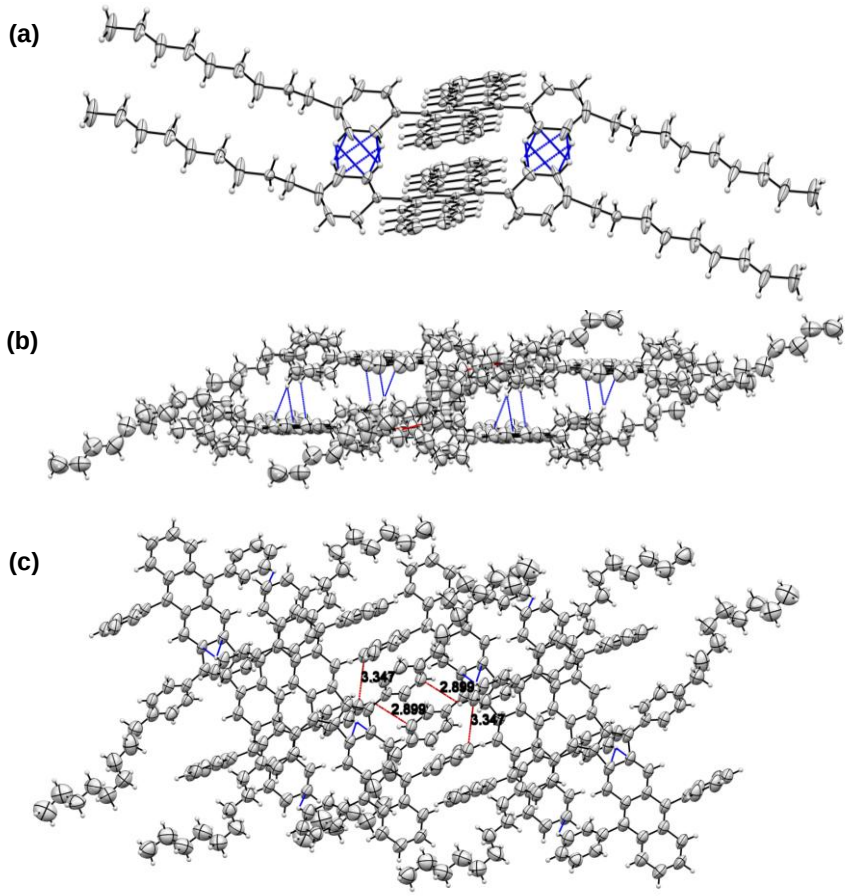

Figure 2.6 (a) Close contacts between the **DAP1** molecules; (b) and (c) close contacts between the **DAP2** molecules.

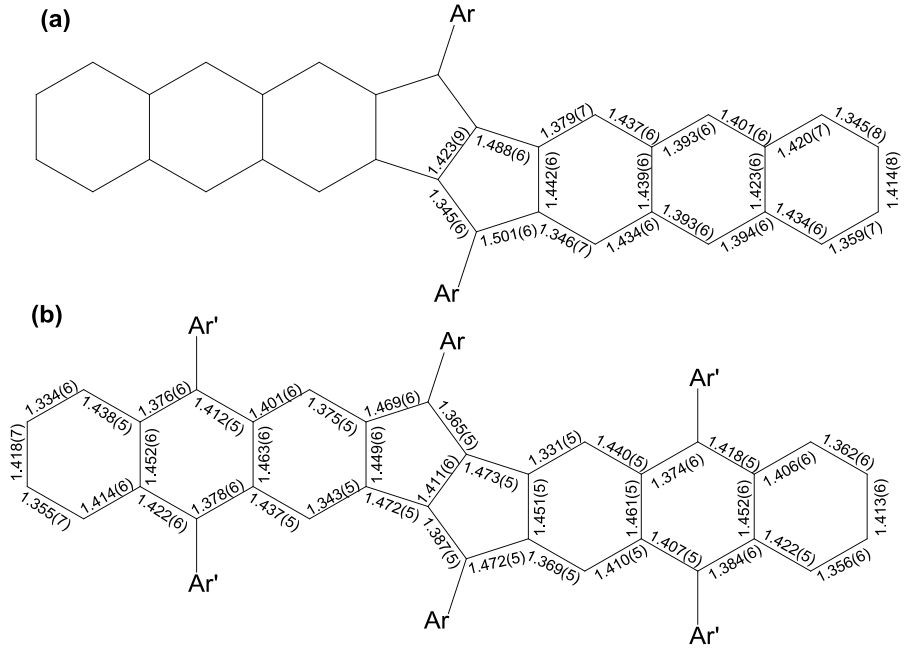

Figure 2.7 Selected bond lengths of **DAP1** and **DAP2** (based on X-ray crystallographic structures).

2.2.6 Thin-film field effect transistors

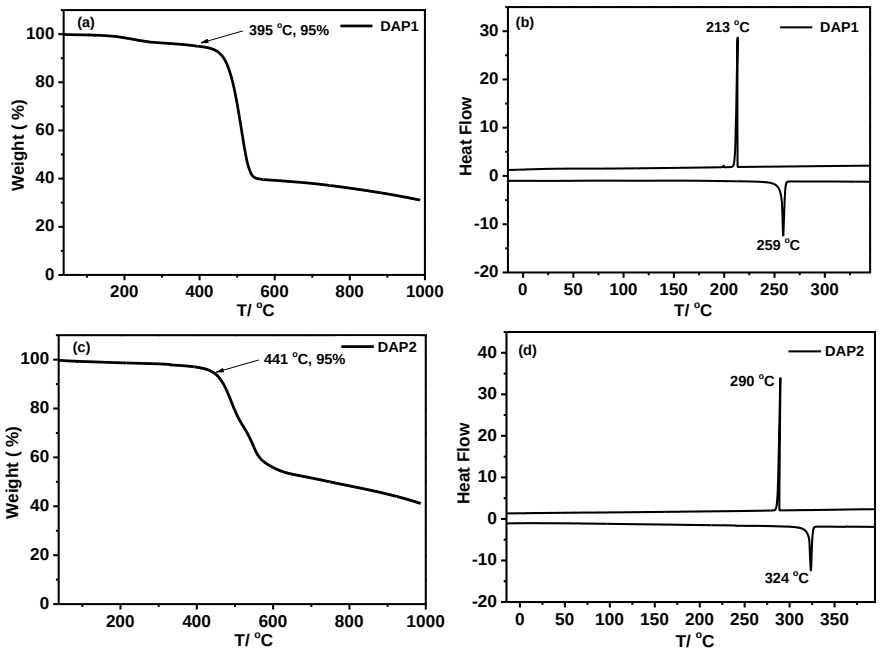

Figure 2.8 Thermogravimetric analysis (TGA) curves of compounds **DAP1** (a) and **DAP2** (c), and differential scanning calorimetry (DSC) curves of compounds **DAP1** (b) and **DAP2** (d) in N_2 at a heating rate of 10 ^oC min^{-1}.

Compounds **DAP1** and **DAP2** showed good thermal stability with decomposition temperatures (T_d, corresponding to a 5% weight loss in thermogravimetric analysis (TGA) curves) at 395 and 441 ^oC, respectively (Figure 2.8 a,c). The melting temperatures of **DAP1** and **DAP2** were observed at 259 ^oC and 324 ^oC, respectively, from differential scanning calorimetry (DSC) curves (Figure 2.8 b,d).

Organic field effect transistors (OFETs) of **DAP1** and **DAP2** were fabricated on n^+-Si/SiO_2 substrates using a bottom-gate top-contact device structure. The SiO_2 dielectric was treated with octadecyltrichlorosilane (ODTS) or hexamethyldisilazane (HMDS), and the thin film was spin-coated from

$CHCl_3$ solution onto the substrates, then thermal annealed at selective temperatures for 20 min. Finally, Au source/drain electrodes (80 nm) were patterned onto the organic layer through a shadow mask to afford the devices. All devices were characterized in N_2 atmosphere. The typical transfer and output curves measured in N_2 are shown in Figure 2.9.

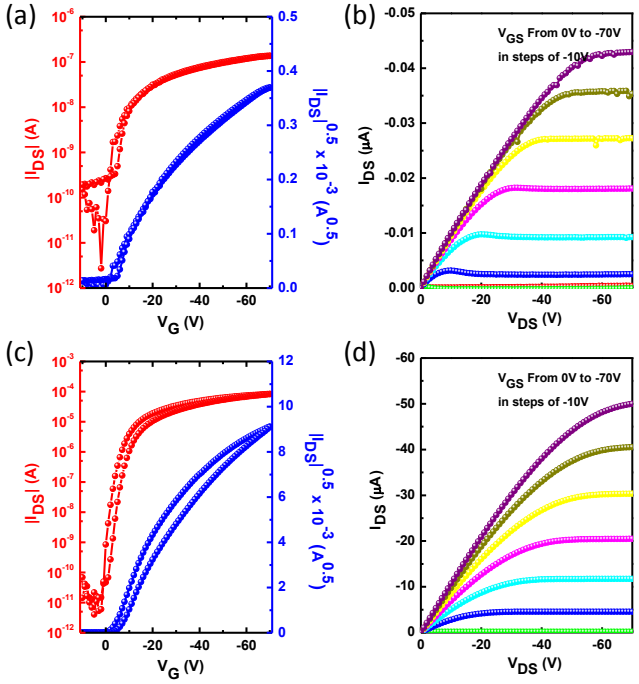

Figure 2.9 Transfer and output characteristics of **DAP1** (a, b) and **DAP2** (c, d) devices with ODTS treatment.

All devices based on **DAP1** and **DAP2** exhibited p-type behavior and exhibited well defined characteristics. The transfer curve revealed an average mobility of 0.001 $cm^2V^{-1}s^{-1}$, threshold voltage of 0 V, and current on/off ratio of 10^4 for **DAP1** (Table 2.2). However, for **DAP2**, the average charge carrier mobility is around 0.65 $cm^2V^{-1}s^{-1}$, and the maximum mobility could reach up to 0.86 $cm^2V^{-1}s^{-1}$ (threshold voltage is 2 V, on/off ratio is 10^5) (Table 2. 2). As far as we know, this value should be among the highest values for solution

processed pentalene based derivatives. The ultra high mobility of **DAP2** compared to **DAP1** could be well explained by the single crystal packing. The **DAP2** adopted a preferable 2-D packing structure with close short contact. However, **DAP1** only exhibited 1-D packing along the a-axis.

Table 2.2 The device characteristics of thin film **DAP1** and **DAP2**.

Compound	Surface treatment	Annealing Temp [^{o}C]	μ[$cm^2V^{-1}s^{-1}$]	V_T [V]	On/off
DAP1	HMDS	As-spun	6.2×10^{-4}	0	1.6×10^{4}
	HMDS	120	2.8×10^{-4}	-2	3.5×10^{4}
	HMDS	150	6.4×10^{-5}	0	1.4×10^{4}
	HMDS	180	2.0×10^{-5}	-5	1.7×10^{4}
	ODTS	As-spun	0.001	0	1.5×10^{4}
	ODTS	120	7.4×10^{-4}	0	1.1×10^{4}
	ODTS	150	1.8×10^{-4}	0	1.7×10^{4}
DAP2	HMDS	As-spun	2.4×10^{-4}	-5	4.2×10^{5}
	HMDS	150	0.012	-13	1.1×10^{6}
	ODTS	As-spun	0.027	-10	8.3×10^{5}
	ODTS	120	0.45	2	7.8×10^{4}
	ODTS	150	0.65(0.86)	2	2.2×10^{5}
	ODTS	180	0.36	0	3.6×10^{4}

Thin film morphology and solid state microstructure were characterized by tapping-mode atomic force microscopy and 2D X-ray diffraction. The thin film exhibited large needle-like crystals for **DAP1** (Figure 2.10) and plate-like crystals for **DAP2** (Figure 2.11). These morphologies are correlated with the single crystal packing motif. The XRD measurements of the thin films on ODTS treated substrates exhibited the primary peak at 2θ = 4.4º and 4.9º,

which corresponds to a d-spacing of 19.97 Å and 18.02 Å for **DAP1** and **DAP2**, respectively (Figure 2.12).

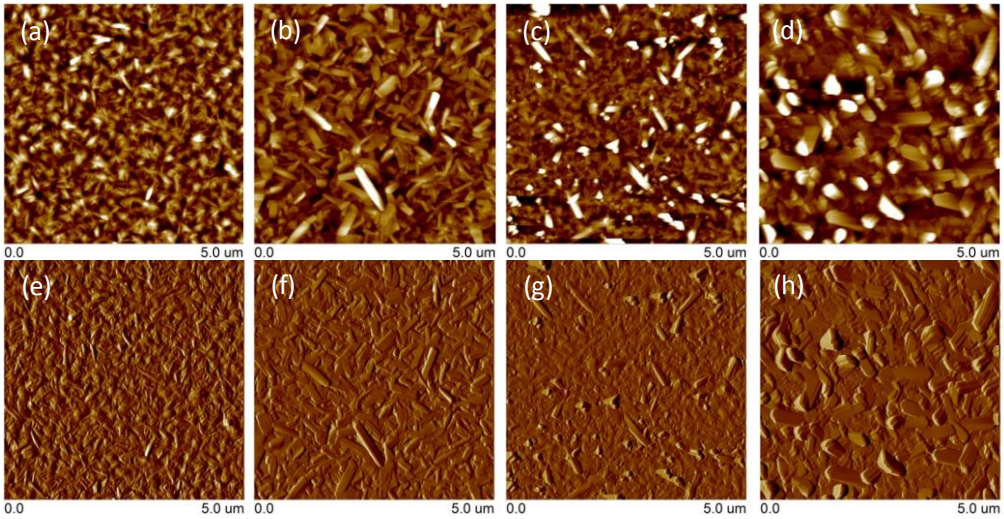

Figure 2.10 The AFM images of the thin film **DAP1** spin coated from $CHCl_3$ solution onto ODTS (a: before annealing; b: annealing at 150 ^oC) and HMDS (c: before annealing; d: annealing at 150 ^oC) treated substrates. (e-h) are the corresponding phase images.

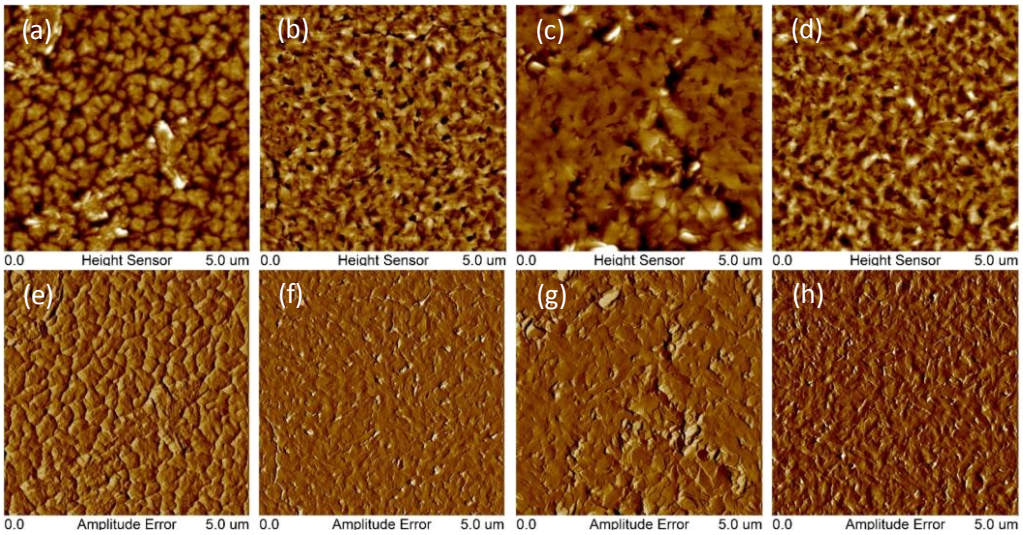

Figure 2.11 The AFM images of thin film **DAP2** spin coated from $CHCl_3$ solution on the ODTS-treated substrates annealing at 120 ^oC (a), 150 ^oC (b), and 180 ^oC (c), and on the HMDS -treated substrates annealing at 150 ^oC (d). (e-h) are the corresponding phase images.

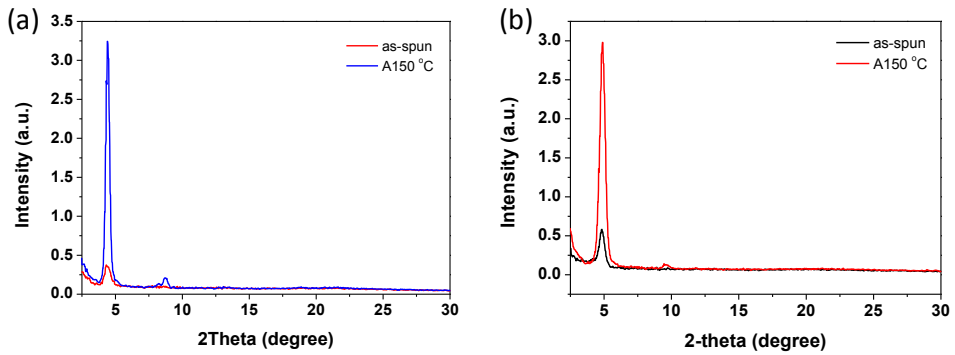

Figure 2.12 XRD patterns of **DAP1** (a) and **DAP2** (b) thin films on ODTS-modified substrates.

A lamellar packing structure was deduced from the diffraction peaks. The more dense layer-like packing structure of **DAP2** in the thin films allows effective charge transport between the source and drain electrodes.

2.3 Summary

In summary, two dianthracenopentalene derivatives **DAP1** and **DAP2** were synthesized, which present longest acene fused penalene derivates reported so far. The DAP2 with six attached phenyl rings adopts a more closed packing structure than DAP1 due to many close contacts existing between molecules. As a result, the average hole charge mobility of **DAP2** up to 0.65 $cm^2V^{-1}s^{-1}$ (maximum: 0.86 $cm^2V^{-1}s^{-1}$) has been achieved by simple solution processing. The finding is very important to design other high performance organic semiconductors for OFETs. More effort will be carried out for the optimization of the FET devices test in future. The synthesis of ambipolar and even n-type pentalene derivatives for organic semiconductor materials will be also conducted.

2.4 Experiment section

2.4.1 General characterization method

^{1}H and ^{13}C NMR spectra were recorded using Advance 500 MHz Bruker spectrometer in $CDCl_3$ with tetramethylsilane (TMS) as the internal standard. The chemical shift was recorded in ppm and the following abbreviations were used to explain the multiplicities: s = singlet, d = doublet, t= triplet, m = multiplet, br = broad. Column chromatography was performed on silica gel 60 (Merck 40-60 nm, 230-400 mesh). EI mass spectra were recorded on Agilent 5975C DIP/MS mass spectrometer. UV-vis absorption and fluorescence spectra were recorded on a Shimadzu UV-1700 spectrophotometer and a RF-5301 fluorometer, respectively. Cyclic voltammetry and differential pulse voltammetry measurements were performed in HPLC grade DCM on a CHI 620C electrochemical analyzer with a three-electrode cell, using 0.1 M Bu_4NPF_6 as supporting electrolyte, AgCl/Ag as reference electrode, gold disk as working electrode, Pt wire as counter electrode, and scan rate at 50 mV s^{-1}. The potential was externally calibrated against the ferrocene/ferrocenium couple. Thermogravimetric analysis (TGA) was carried out on a TA instrument 2960 at a heating rate of 10 ℃ min^{-1} under nitrogen flow. Differential scanning calorimetry (DSC) was performed on a TA instrument 2920 at a heating/cooling rate of 10 ℃ min^{-1} under nitrogen flow. Tapping-mode Atomic Force Microscopy (TM-AFM) was performed on a Nanoscope V microscope (Veeco Inc.). X-ray diffraction (XRD) patterns of

the thin film were measured on a Bruker-AXS D8 DISCOVER with GADDS X-ray diffractometer. Copper Kα line was used as a radiation source with λ = 1.5418 Å

2.4.2 Synthesis

All reagents were purchased from commercial sources without further purification. Anhydrous dichloromethane (DCM) was distilled from CaH_2. 1,4-dioxane, Toluene and THF were distilled from sodium-benzophenone immediately prior to use. 2,3-dibromoanthracene **2-1**, 1,3-diphenylisobenzofuran **2-3** and 1-ethynyl-4-nonylbenzene were prepared by following literature procedures.

Compound **2-2 2-bromo-3-((4-nonylphenyl)ethynyl)anthracene**

A mixture of compound **2-1** (1.80 g, 5.4 mmol), 1-ethynyl-4-nonylbenzene (1.29 g, 5.6 mmol), CuI (31 mg, 3%) and catalyst $Pd(PPh_3)_2Cl_2$ (190 mg, 5%) in anhydrous THF (15 mL) and Et_3N (15 mL) was degassed by three freeze-pupm-thaw cycles. The mixture was stirred at 75 ^oC under argon for overnight. The mixture was extracted with EtOAc (50 mL ×2). The combined organic phase was washed with 10% m/m aqueous HCl solution (50 mL ×2) and brine (50 mL ×1). The organic phase was dried over anhydrous Na_2SO_4 and organic solvent was removed under reduced pressure. The crude product was purified by column chromatography (DCM/Hexane = 1:10) to afford compound **2-2** (0.90 g) in 35% yield. ^1H NMR (500 MHz, $CDCl_3$, ppm): δ = 8.36 (s, 1H), 8.30 (s, 1H), 8.28 (s, 1H), 8.25 (s, 1H), 8.02-7.97 (m, 2H), 7.56

(d, *J* =8.0 Hz, 2H), 7.51-7.48 (m, 2H), 7.20 (d, *J* =8.0 Hz, 2H), 2.64 (t, *J* =7.75 Hz, 2H), 1.65-1.60 (m, 2H), 1.39-1.20 (m, 12H), 0.89 (t, *J* = 6.75 Hz, 3H) ; ^{13}C NMR (125 MHz, $CDCl_3$, ppm): δ = 143.95, 133.18, 132.50, 132.15, 131.65, 131.23, 130.94, 129.74, 128.55, 128.35, 128.17, 126.39, 126.34, 126.05, 125.30, 122.28, 121.34, 120.13, 94.29, 88.06, 35.99, 31.89, 31.27, 29.54, 29.50, 29.32, 29.26, 22.67, 14.11. HRMS (EI): calcd for $C_{31}H_{31}Br$ (M^+), 482.1609; found, 482.1607 (error: -0.40 ppm).

Compound **DAP1**

A reaction flask was charged with monomer **2-2** (0.270g 0.56mmol), hydroquinone (0.125 g, 1.12 mmol), Cs_2CO_3 (0.370 g, 1.12 mmol), CsF (0.187 g, 1.23 mmol), P(2-furyl)$_3$ (30 mg, 0.13 mmol), and $Pd_2(dba)_3$ (30 mg, 0.033 mmol) and then purged with argon. Anhydrous 1,4-dioxane (15 mL) was injected into the reaction mixture and deoxygenated three freeze-pump-thaw cycles. The suspension was immediately heated to135^{o}C. After heating for 24 h the reaction mixture was diluted with $CHCl_3$ (25 mL), filtered through celite, and then concentrated to yield raw solid. After purification via column chromatography (silica gel, DCM/Hexane=1 : 4), the product **2-3** was dissolved in $CHCl_3$, precipitated in methanol: acetone = 3:2 and filtered. This procedure was repeated for 3 times to give the purer product **DPA1** (37 mg) in 16% yield for characterization. ^{1}H NMR (500 MHz, $CDCl_3$, ppm): δ = 8.16 (d, *J* = 6.5 Hz, 4H), 8.11 (s, 2H), 7.89-7.84 (m, 4H), 7.85 (s, 2H), 7.83 (s, 2H), 7.75 (s, 2H), 7.47 (d, *J* = 7.5 Hz, 4H), 7.41-7.37 (m, 4H),

2.81 (t, *J* = 8.0 Hz, 4H), 1.85-1.75 (m, 4H), 1.52-1.30 (m, 24H), 0.92 (t, *J* = 6.75 Hz, 6H); ^{13}C NMR (125 MHz, $CDCl_3$, ppm): δ = 147.21, 144.70, 143.62, 136.11, 132.27, 131.98, 131.95, 131.72, 131.54, 131.30, 128.90, 128.89, 128.14, 128.11, 127.55, 127.15, 125.63, 125.43, 121.72, 120.45, 36.12, 31.97, 31.49, 29.67, 29.63, 29.60, 29.42, 22.73, 14.16. HRMS (EI): calcd for $C_{62}H_{62}$ (M^+), 806.4852; found, 806.4852 (error: 0.11 ppm).

Compound **2-4** **2,3-dibromo-9,10-diphenyl-9,10-dihydro-9,10-epoxyanthracene**

A solution of compound **2-3** (11.10 g, 38.8 mmol) and 1,2,4,5-tetrabromobenzene (16.60 g, 42.0 mmol) in toluene (120 mL) was cooled to -50 ^{o}C, then *n*-butyl lithium (1.6 M, 27 mL) was added dropwise. After addition, the mixture was warmed to room temperature naturally and stirred for overnight. The mixture was extracted with chloroform (80 mL ×2). The combined organic phase was washed with brine (60 mL ×2). The organic phase was dried over anhydrous Na_2SO_4 and organic solvent was removed under reduced pressure. The crude product was purified by column chromatography (CH_2Cl_2/Hexane = 1:4) to afford compound **2-4** (12.05 g) in 58% yield. ^{1}H NMR (500 MHz, $CDCl_3$, ppm): δ = 7.88 (d, *J* = 7.5 Hz, 4H), 7.62 (t, *J* = 7.75 Hz, 4H), 7.56 (s, 2H), 7.52 (t, *J* = 7.25 Hz, 2H), 7.41-7.37 (m, 2H), 7.11-7.07 (m, 2H); ^{13}C NMR (125 MHz, $CDCl_3$, ppm): δ = 151.61, 149.19, 133.95, 128.97, 128.65, 126.49, 126.36, 125.63, 121.77, 120.67, 90.22. HRMS (EI): calcd for $C_{26}H_{16}Br_2O$ (M^+), 503.9547; found, 503.9535 (error:

-2.48 ppm).

Compound **2-5 2,3-dibromo-9,10-diphenylanthracene**

To an ice cold suspension of Zn dust (0.57 g, 8.8 mmol) in THF (10 mL) was carefully added $TiCl_4$ (1.2 mL, 11.0 mmol) under argon, and the reaction mixture was heated to reflux for 5 minutes. Then the mixture was cooled to 0 ^oC and a solution of compound **2-4** (1.02 g, 2 mmol) in THF (10 mL) was added dropwise. After addition, the mixture was reflux overnight. Cooled down the reaction to room temperature and poured into cold 10% m/m aqueous HCl solution (40 mL). The mixture was extracted with chloroform (60 mL ×2). The combined organic phase was washed with brine (50 mL ×2). The organic phase was dried over anhydrous Na_2SO_4 and organic solvent was removed under reduced pressure. The crude product was purified by column chromatography (CH_2Cl_2/Hexane = 1:2) to afford compound **2-5** (0.80 g) in 80% yield. ^1H NMR (500 MHz, $CDCl_3$, ppm): 7.99 (s, 2H), δ = 7.68-7.56 (m, 8H), 7.46-7.43 (m, 4H), 7.38-7.34 (m, 2H); ^{13}C NMR (125 MHz, $CDCl_3$, ppm): δ = 137.81, 136.66, 131.24, 131.15, 130.59, 129.30, 128.68, 128.00, 127.06, 125.91, 121.67. HRMS (EI): calcd for $C_{26}H_{16}Br_2$ (M^+), 485.9619; found, 485.9595 (error: -4.84 ppm).

Compound **2-6 2-bromo-3-((4-nonylphenyl)ethynyl)-9,10-diphenyl-anthracene**

A mixture of compound **2-5** (1.95 g, 4.0 mmol), 1-ethynyl-4-nonylbenzene (1.10 g, 4.8 mmol), CuI (38 mg, 3%) and catalyst $Pd(PPh_3)_2Cl_2$ (140 mg, 5%)

in anhydrous THF (20 mL) and Et_3N (10 mL) was degassed by three freeze-pupm-thaw cycles. The mixture was stirred at 75 ^oC under argon for overnight. The mixture was extracted with Chloroform (60 mL ×2). The combined organic phase was washed with 10% m/m aqueous HCl solution (50 mL ×2) and brine (50 mL ×1). The organic phase was dried over anhydrous Na_2SO_4 and organic solvent was removed under reduced pressure. The crude product was purified by column chromatography (DCM/Hexane = 1:10) to afford compound **2-6** (0.92 g) in 36% yield. ^1H NMR (500 MHz, $CDCl_3$, ppm): δ = 7.97 (s, 1H), 7.94 (s, 1H), 7.69-7.57 (m, 8H), 7.50-7.45 (m, 6H), 7.37-7.33 (m, 2H), 7.15 (d, *J* = 8.0 Hz, 2H), 2.61 (t, *J* = 7.75 Hz, 2H), 1.75-1.65 (m, 2H), 1.35-1.20 (m, 12H), 0.89 (t, *J* = 6.75 Hz, 3H); ^{13}C NMR (125 MHz, $CDCl_3$, ppm): δ = 143.86, 138.08, 138.01, 137.43, 136.36, 132.06, 131.58, 131.28, 131.19, 130.91, 130.48, 129.78, 129.60, 128.64, 128.62, 128.45, 128.18, 127.89, 127.85, 127.18, 127.04, 125.93, 125.64, 121.90, 121.65, 120.02, 94.30, 88.37, 35.94, 31.87, 31.22, 29.52, 29.47, 29.29, 29.21, 22.66, 14.10. HRMS (EI): calcd for $C_{43}H_{39}Br$ (M^+), 634.2235; found, 634.2233 (error: -0.27 ppm).

Compound **DAP2**

A reaction flask was charged with monomer **2-6** (0.53g 0.83mmol), hydroquinone (0.185 g, 1.68 mmol), Cs_2CO_3 (0.547 g, 1.68 mmol), CsF (0.277 g, 1.82 mmol), P(2-furyl)$_3$ (38 mg, 0.16 mmol), and $Pd_2(dba)_3$ (38 mg, 0.04 mmol) and then purged with argon. Anhydrous 1,4-dioxane (18 mL) was injected into the reaction mixture and deoxygenated three freeze-pump-thaw

cycles. The suspension was immediately heated to135^{o}C. After heating for 24 h the reaction mixture was diluted with $CHCl_3$ (25 mL), filtered through celite, and then concentrated to yield raw solid. After purification via column chromatography (silica gel, DCM/Hexane = 1:4), the product was dissolved in $CHCl_3$, precipitated in methanol/acetone = 3:2 and filtered. This procedure was repeated for 3 times to give the purer product **DAP2** (70 mg) in 15% yield for characterization. ^{1}H NMR (500 MHz, $CDCl_3$, ppm): δ = 8.00 (s, 2H),7.65-7.58 (m, 6H), 7.58-7.51 (m, 12H), 7.50-7.44 (m, 6H), 7.42 (d, *J* = 7.5 Hz, 8H), 7.28-7.24 (m, 4H), 6.97 (d, *J* = 8.0 Hz, 4H), 2.66 (t, *J* = 8.0 Hz, 4H), 1.75-1.65 (m, 4H), 1.50-1.20 (m, 24H), 0.96 (t, *J* = 7.0 Hz, 6H); ^{13}C NMR (125 MHz, $CDCl_3$, ppm): δ = 146.03, 144.83, 142.94, 138.99, 138.82, 138.33, 137.93, 135.97, 131.28, 131.16, 131.07, 131.05, 130.63, 130.45, 130.00, 129.44, 128.37, 128.28, 127.38, 127.22, 127.11, 127.06, 125.29, 125.08, 120.77, 119.56, 36.02, 32.00, 31.49, 29.72, 29.61, 29.47, 22.75, 14.16. HR-APCI: calcd for $C_{86}H_{79}$ ($M+H^+$), 1111.6182; found, 1111.6176 (error: -0.54 ppm).

References

[1] (a) Payne, M. M.; Parkin, S. R.; Anthony, J. E. *J. Am. Chem. Soc.* **2005**, 127, 8028; (b) Mondal, R.; Adhikari, R. M.; Shah, B. K.; Neckers, D. C. *Org. Lett.* **2007**, 9, 2505; (c) Zade, S. S.; Bendikov, M. Angew. *Chem. Int. Ed.* **2010**, 49, 4012; (d) Purushothaman, B.; Parkin, S. R.; Anthony, J. E. *Org. Lett.* **2010**, 12, 2060; (e) Watanabe, M.; Chang, Y. J.; Liu, S.-W.;

Chao, T.-H.; Goto, K.; Islam, M. M.; Yuan, C.-H.; Tao, Y.-T.; Shinmyozu, T.; Chow, T. J. *Nat. Chem.* **2012**, 4, 574.

[2] For classic and recent papers on pentalene synthesis, see: (a) Brand, K. *Ber. Deutsch. Chem. Ges.* **1912**, 45, 3071; (b) Lothrop, W. C. *J. Am. Chem. Soc.* **1941**, 63, 1187; (c) Brown, R. F. C.; Choi, N.; Coulston, K. J.; Eastwood, F. W.; Wiersum, U. E.; Jenneskens, L. W. *Tetrahedron Lett.* **1994**, 35, 4405; (d) Chakraborty, M.; Tessier, C. A.; Youngs, W. J. *J. Org. Chem.* **1999**, 64, 2947; (e) Saito, M.; Nakamura, M.; Tajima, T. *Chem. Eur. J.* **2008**, 14, 6062; (f) Kawase, T.; Konishi, A.; Hirao, Y.; Matsumoto, K.; Kurata, H.; Kubo, T. *Chem. Eur. J.* **2009**, 15, 2653; (g) Levi, Z. U.; Tilley, T. D. *J. Am. Chem. Soc.* **2009**, 131, 2796; (h) Zhang, H.; Karasawa, T.; Amada, H.; Wakamiya, A.; Yamaguchi, S. *Org. Lett.* **2009**, 11, 3076; (i) Levi, Z. U.; Tilley, T. D. *J. Am. Chem. Soc.* **2010**, 132, 11012; (j) Kawase, T.; Fujiwara, T.; Kitamura, Ch.; Konishi, A.; Hirao, Y.; Matsumoto, K.; Kurata, H.; Kubo, T.; Shinamura, S.; Mori, H.; Miyazaki, E.; Takimiya, K. *Angew. Chem. Int. Ed.* **2010**, 49, 7728; (k) Rivera-Fuentes, P.; Rekowski, M. v. W.; Schweizer, W. B.; Gisselbrecht, J.-P.; Boudon, C.; Diederich, F. *Org. Lett.* **2012**, 14, 4066; (l) Maekawa, T.; Segawa, Y.; Itami, K. *Chem. Sci.* **2013**, 4, 2369-2373; (m) Li, H.; Wei, B.; Xu, L.; Zhang, W.-X.; Xi, Z. *Angew. Chem. Int. Ed.* **2013**, 52, 10822; (n) Chen, C.; Harhausen, M.; Liedtke, R.; Bussmann, K.; Fukazawa, A.; Yamaguchi, S.; Petersen, J. L.; Daniliuc, C. D.; Fröhlich, R.; Kehr, G.; Erker, G. *Angew. Chem. Int. Ed.* **2013**, 52, 5992;

(o) Zhao, J.; Oniwa, K.; Asao, N.; Yamamoto, Y.; Jin, T. *J. Am. Chem. Soc.* **2013**, 135, 10222.

[3] (a) Konishi, A.; Fujiwara, T.; Ogawa, N.; Hirao, Y.; Matsumoto, K.; Kurata, H.; Kubo, T.; Kitamura, C.; Kawase, T. *Chem. Lett.* **2010**, 39, 300; (b) Yin, X.; Li, Y.; Zhu, Y.; Kan, Y.; Li, Y.; Zhu, D. *Org. Lett.* **2011**, 13, 1520; (c) Hopf, H. *Angew. Chem. Int. Ed.* **2013**, 52, 12224; (d) Nakano, M.; Osaka, I.; Takimiya, K.; Koganezawac, T. *J. Mater. Chem. C* **2014**, 2, 64.

[4] Akula, M. R. *Org. Prep. Proced. Int.* **1990**, 22, 102.

[5] (a) Ongayi, O.; Vicente, M. G. H.; Ghosh, B.; Fronczek, F. R.; Smith, K. M. *Tetrahedron* **2010**, 66, 63; (b) Sista, P.; Nguyen, H.; Murphy, J. W.; Hao, J.; Dei, D. K.; Palaniappan, K.; Servello, J.; Kularatne, R. S.; Gnade, B. E.; Xue, B.; Dastoor, P. C.; Biewer, M. C.; Stefan, M. C. *Macromolecules* **2010**, 43, 8063; (c) Takeuchi, J. A.; Li, L.; Im, W. B. US Patent WO2012142288, 2012.

[6] Benderradji, F.; Nechab, M.; Einhorn, C.; Einhorn,J. *Synlett* **2006**, 13, 2035.

Chapter 3: Thienoacene-fused Pentalenes: Syntheses, Structures, Physical Properties and Applications for Organic Field Effect Transistors

3.1 Introduction

In Chapter 1, we have shown that pentalene as one of the important antiaromatic systems has attracted many chemists' attention. Incorporating antiaromatic pentalene into cyclic π-conjugated systems will make materials with many novel properties. Thiophene rings are incorporated into the acene framework, and the obtained thienoacenes have showed excellent performance in organic field effect transistors (OFETs) as demonstrated by Takamiya *et al.*.[1] Incorporation of the pentalene substructure into the thienoacene framework will be interesting because the anti-aromatic nature of pentalene unit can tune the electronic properties of thienoacenes and at the same time, the donor-acceptor interaction between the thienoacenes and the pentalene can help to stabilize the system. Moreover, the possible sulfur-sulfur and sulfur-hydrogen interactions observed in the thienoacenes could enhance the intermolecular interactions in solid state, which is desirable for OFET applications.

In this chapter, the thienoacenes fused pentalene derivatives **3-1** - **3-3** were designed and synthesized (Figure 3.1). The obtained highly π-extended polycyclic conjugated systems contain a large number of fused rings (up to ten in **3-3**) and were expected to also benefit for intermolecular stacking.

Synthesis of these compounds is challenging and alkyl phenyl substituents are necessary to stabilize and solubilize the target compounds. Their ground-state geometric and electronic structures, optical properties, and electrochemical properties were studied in details both by experiments and theory. Their applications for OFETs were also investigated.

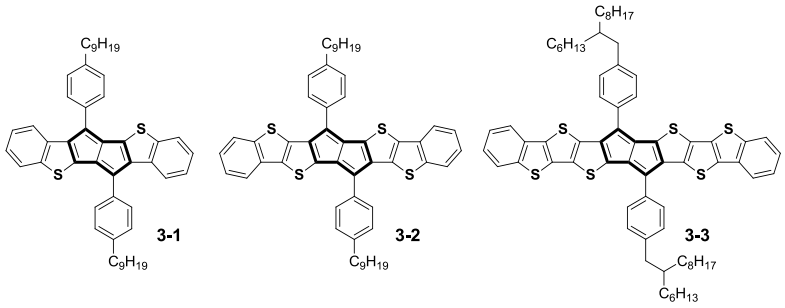

Figure 3.1 Thienoacene-fused pentalene derivatives **3-1 - 3-3**

3.2 Results and discussion

3.2.1 Synthesis

Compounds **3-1 - 3-3** were synthesized from the simplest starting material, e.g. benzo[*b*]thiophene (Scheme 3.1). Bromination of benzo[*b*]thiophene and subsequent iodination of the as-formed 3-bromo-benzo[*b*]thiopehene[2] gave the 2-iodo-3-bromo-benzo[*b*]thiophene **3-4**.[3] The Sonogashira coupling reaction between **3-4** and 1-ethynyl-4-nonylbenzene [4] provided the 3-bromo-2-((4-nonylphenyl)ethynyl) benzo[*b*]thiophene **3-5** in 80% yield. $Ni(PPh_3)_2Cl_2$ catalyzed dimerization of **3-5** afforded the bis(benzo[*b*]thieno)pentalene **3-1** in 15% yield. The synthesis of the target compound **3-2** began with 2-bromo-benzo[*b*]thieno[2,3-*d*]thiophene **3-6** which was obtained from the 3-bromo-benzo[*b*]thiophene according to the literature.[5]

Lithiation of **3-6** by lithium diisopropylamide (LDA) followed by addition of iodine gave the 3-bromo-2-iodo-benzo[*b*]thiophene **3-7** in 75% yield *via* a "halogen dance" reaction. Sonogashira coupling reaction between **3-7** and 1-ethynyl-4-nonylbenzene gave the 3-bromo-2-((4-nonylphenyl)ethynyl) benzo[*b*]thieno[2,3-*d*]thiophene (**3-8**) in 84% yield. Similar $Ni(PPh_3)_2Cl_2$ catalyzed dimerization of **3-8** afforded the bis(benzo(thieno)$_2$)pentalene **3-2** in 18% yield. The synthesis of target compound **3-3** was based on the known 2-bromo-benzo[*d*,*d*′]thieno[3,2-*b*;4,5-*b*′]dithiophene **3-9**.[5c] Halogen dance reaction of compound **3-9** gave the 3-bromo-benzo[*d*,*d*′]thieno[3,2-*b*;4,5-*b*′]dithiophene **3-10** in 90% yield. Iodization of **3-10** with *N*-iodosuccinimide (NIS) in acetic acid/chloroform gave compound **3-11** in 85% yield, and subsequent Sonogashira coupling reaction with 1-ethynyl-4-(pentadecan-7-yl)benzene (**3-13**) gave the 3-bromo-2-((4-(pentadecan-7-yl)phenyl)ethynyl)-benzo[*d*,*d*′]thieno[3,2-*b*;4,5-*b*′]dithiophene **3-12** in 85% yield. Dimerization of **3-12** catalyzed by $Ni(PPh_3)_2Cl_2$ afforded the bis(benzo(thieno)$_3$)pentalene **3-3** in 15% yield. In this case, the long branched alkyl chain (2-hexyldecyl) has to be used as the analogues with shorter chains such as nonyl substituents have shown very poor solubility.

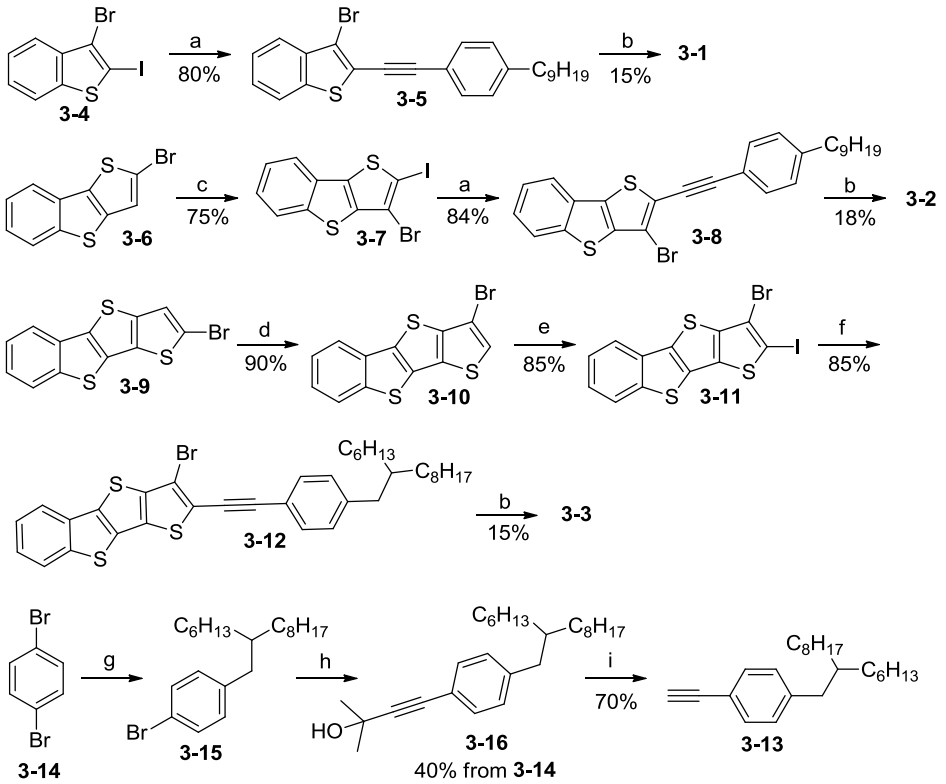

Scheme 3.1. Synthetic route to **3-1** - **3-3**. *Reagents and conditions*: (a) 1-ethynyl-4-nonylbenzene, $Pd(PPh_3)_2Cl_2$, CuI, Et_3N/THF, RT, overnight; (b) $Ni(PPh_3)_2Cl_2$, Zn, toluene, reflux, 24h; (c) 1) LDA, -78 ^oC, 16h, 2) I_2, overnight; (d) LDA, -78 ^oC, 16h, H_2O; (e) NIS, AcOH, $CHCl_3$, RT, 24h; (f) **3-13**, $Pd(PPh_3)_2Cl_2$, CuI, Et_3N/THF, RT, overnight; (g) $Pd(dppf)Cl_2{\cdot}CH_2Cl_2$, THF, 60 ^oC, overnight; (h) 2-methylbut-3-yn-2-ol, $Pd(PPh_3)_2Cl_2$, CuI, Et_3N/THF, 75 ^oC; (i) KOH, toluene, reflux, 3h.

In course of the synthetic work, we faced several problems and need address these challenges. The halogen dance reaction, such as from **3-6** to **3-7**, need long reaction time (> 24 h) and rigid conditions, i.e., anhydrous environment and long-time cryogenic temperature. So, at first, we tried to avoid using the halogen dance reaction and introduced the phenyl acetylene group firstly by Sonogashira coupling reaction between the **3-6** and 1-ethynyl-4-nonylbenzene. However, the subsequent lithiation by LDA followed by quenching with CBr_4 only gave the target compound **3-8** in very low yield (5-10%) and all starting material decomposed. Thus halogen dance

reaction was used although it is time-consuming and requires rigid conditions. From **3-9** to **3-11**, we also tried halogen dance reaction and iodination reaction in one pot, but the reaction stopped at compound **3-10**. Subsequent iodination reaction was optimized by changing the solvent system from chloroform to acetic acid/chloroform mixture. Compound 1-ethynyl-4-nonylbenzene was prepared according to the reported method by reaction of nonylmagnisum bromide with 4-bromobenzaldehyde followed by dehydroxylation.[4] However, similar method was not applicable to the synthesis of **3-13** as the yield of the first step (reaction of Grignard reagent with aldehyde) was less than 5%. So compound **3-13** was prepared by an alternative way (Scheme 3.1). Kumada coupling of 1,4-dibromobenzene (**3-14**) with 2-hexyldecylmagnisium bromide followed by Sonogashira coupling with 2-methylbut-3-yn-2-ol in one pot gave the 4-(4-(2-hexyldecyl)phenyl)-2-methylbut-3-yn-2-ol **3-16** in 40% yield. Then deprotection reaction of **3-16** under basic condition afforded the intermediate alkyne **3-13** in 70% yield.

3.2.2 Photophysical properties

The electronic absorption spectra of **3-1** - **3-3** were measured in chloroform solution (Figure 3.2 and Table 3.1). The absorption maxima for **3-1** - **3-3** in solutions are located at 352, 395 and 422 nm, respectively. With extension of chain length, this absorption band shows obvious red-shift by 43 and 27 nm. A longer-wavelength shoulder with maxima at 495, 512 and 492 nm was observed for **3-1**, **3-2** and **3-3**, respectively. In

addition, a very weak and broad band was clearly observed in the 600-1100 nm region for **3-1**- **3-3** when absorption spectrum was measured at high concentrations (1×10^{-4} M, the insert in Figure 3.2), which could be originated from a low-energy forbidden electronic transition. No fluorescence was observed in the detectable region for all compounds.

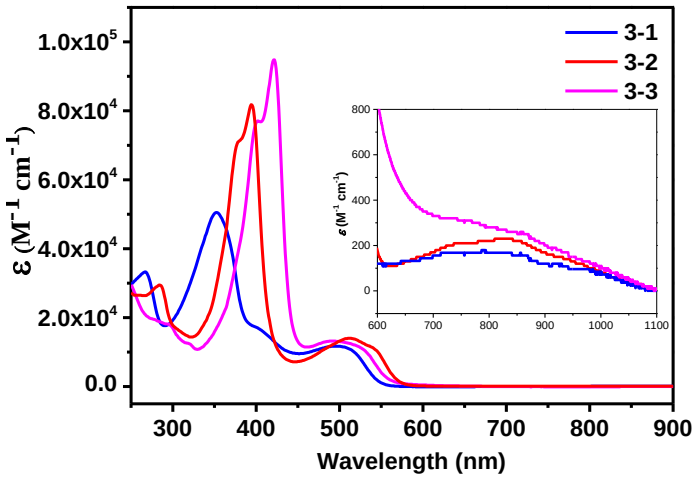

Figure 3.2 UV-vis absorption spectra of **3-1**, **3-2** and **3-3** in chloroform (10^{-5} M); Insert are the magnified absorption spectra at 600-1100 nm.

3.2.3 Electrochemical properties

Cyclic voltommetry (CV) and differential pulse voltammetry (DPV) were used to study the electrochemical properties of compounds **3-1** - **3-3** (Figure 3.3, Table 3.1). The potential was externally calibrated against the ferrocene/ferrocenium couple. Two quasi-reversible oxidation waves with half-wave potential $E_{1/2}^{ox}$ at 0.18 and 0.94 V and two quasi-reversible reduction waves with half-wave potential $E_{1/2}^{red}$ at -1.32 and -2.06 V were observed for **3-1**. Compound **3-2** showed three irreversible oxidation waves with $E_{1/2}^{ox}$ at 0.09, 0.40 and 0.78 V, and two quasi-reversible reduction waves

with $E_{1/2}^{red}$ at -1.28 and -1.95 V. Compound **3-3** exhibited four oxidation waves with $E_{1/2}^{ox}$ at -0.13, 0.07, 0.20 and 0.68 V, and two reduction waves with $E_{1/2}^{red}$ at -1.26 and -1.88 V. The HOMO and LUMO energy levels were calculated using the following equations: HOMO = - [E_{ox}^{onset} + 4.8] eV, LUMO = - [E_{red}^{onset} + 4.8] eV, where E_{ox}^{onset} and E_{red}^{onset} are the onset of the first oxidation and reduction wave, respectively. The HOMO/LUMO energy levels are determined to be -4.93/-3.59, -4.79/-3.62 and -4.61/-3.64 eV for **3-1**, **3-2** and **3-3**, respectively. The corresponding electrochemical energy gaps E_g^{EC} (LUMO-HOMO) are then estimated to be 1.38 eV, 1.15 eV and 0.99 eV for **3-1**- **3-3**. The observed small energy gaps indicated an obvious intramolecular donor-acceptor interaction.

Table 3.1 Summary of optical properties and electrochemical data of compounds **3-1**, **3-2** and **3-3**.

	λ_{max}(abs) [nm]	ε_{max} [$\times 10^4$ M^{-1} cm^{-1}]	$E_{1/2}^{ox}$ (V)	$E_{1/2}^{red}$ (V)	HOMO [eV]	LUMO [eV]	E_g^{EC} [eV]
3-1	352, 495	5.05	0.18, 0.94	-1.32, -2.06	-4.93	-3.59	1.38
3-2	395, 512	8.20	0.09, 0.40, 0.78	-1.28, -1.95	-4.79	-3.62	1.15
3-3	422, 492	9.50	-0.13, 0.07, 0.20, 0.68	-1.26, -1.88	-4.61	-3.64	0.99

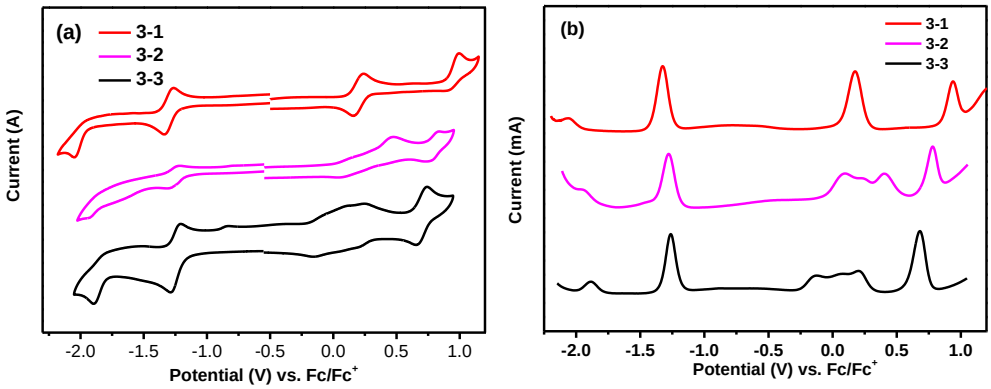

Figure 3.3 (a) Cyclic voltammograms (CV) and (b) Differential pulse voltammetry (DPV) of compounds **3-1** - **3-3** in dry dichloromethane with 0.1 M Bu_4NPF_6 as the supporting electrolyte, AgCl/Ag as reference electrode, Au as working electrode, Pt wire as counter electrode, and a scan rate at 50 mV s^{-1}.

3.2.4 DFT calculations

Density functional theory (DFT, B3LYP/6-31G**) calculations were conducted to better understand the electronic and optical properties of these thienoacene-fused pentalene derivatives. The calculated frontier molecular orbital profiles and energy diagrams are shown in Figure 3.4. It was found that the HOMOs of three molecules are delocalized along the bis(thienoaceno)-pentalene framework while the LUMOs are mainly localized at the central pentalene unit. Time-dependent (TD) DFT calculations predicted that all three compounds should show two major absorption bands. The observed strongest absorption band is mainly attributable to the HOMO→LUMO+1 transitions (352.5 nm, f = 0.7911 for **3-1**; 389.0 nm, f = 1.4591 for **3-2**; 424.3 nm, f = 2.0262 for **3-3** based on DFT calculations). The shoulder band around 500-570 nm can be correlated to the HOMO-1→LUMO

transitions (509.2 nm, f = 0.2319 for **3-1**; 536.5 nm, f = 0.2373 for **3-2**; 536.1 nm, f = 0.1559 for **3-3** based on DFT calculations). The transition of HOMO→LUMO however is symmetry forbidden, which can be correlated to the very weak absorption band in the near infrared region (1089.5, 1078 and 1153.5 nm for **3-1** - **3-3**, respectively, based on DFT calculations).

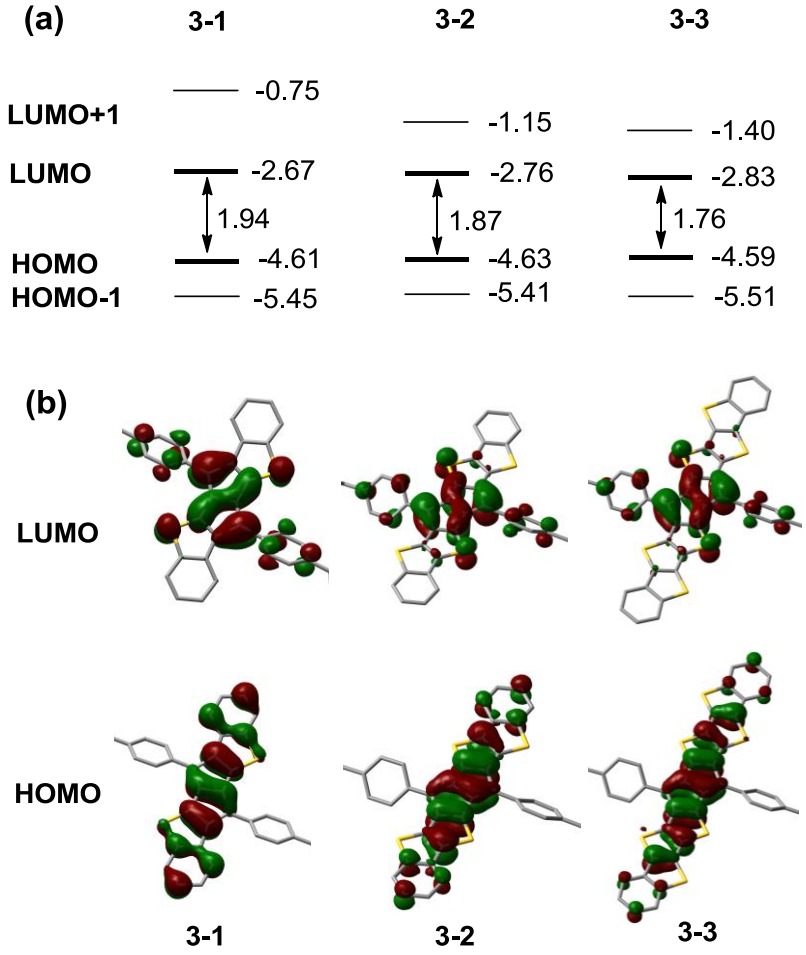

Figure 3.4 (a) Energy diagrams of **3-1** - **3-3** (eV); (b) LUMO and HOMO profiles of **3-1** - **3-3**.

The calculated energy diagrams reveal that with extension of the π-conjugation length from **3-1** - **3-3**, there are slight changes for the HOMO, HOMO-1 and LUMO energy levels, but obvious decrease for the LUMO+1 energy (from -0.75 eV to -1.15 eV and to -1.40 eV), which can well explain

the observed large red-shift of the strongest absorption band and small shift of the shoulder band. The calculated energy gaps slightly decrease with the increase of molecular size, and the trend is in consistence with the determined electrochemical energy gaps.

3.2.5 Crystallographic analysis

Single crystals of **3-1** and **3-2** suitable for X-ray crystallographic analysis were obtained by slow diffusion of methanol or acetonitrile into a chloroform solution.[7] The molecular structures and the packing motif for **3-1** and **3-2** are shown in Figure 3.5 and Figure 3.6, respectively. Both compounds have a planar π-skeleton. The two phenyl substituents have a torsion angle of ca. 37^{o} and 27^{o} to the plane of pentalene for **3-1** and **3-2**, respectively, which are both much smaller than that for dinaphthopentalene (55^{o})[8] due to smaller steric hindrance after incorporation of thiophene rings. DFT calculations predicted that compound **3-3** has a similar geometry. The 3D packing of **3-1** and **3-2** both can be figured out in a monoclinic unit cell (space group P2(1)/n). There is no obvious π-π interactions between the bis(benzothieno)pentalene units in **3-1**. However, close contacts of [C-H⋯π] interaction (2.862 Å) between the outermost benzene rings of the fused pentalene and the phenyl substituents of the neighbouring molecules exist which help the molecules to closely pack into an ordered layer-like structure (Figure 3.5). In **3-2**, continuous π-π interactions (π-π distance ca. 3.60 Å) between the fused pentalene units drive the molecules to pack into a columnar structure along the *b* axis (Figure 3.6).

In addition, in the *ac* plane, additional sulphur-hydrogen bonding (distances: 2.981 Å and 2.941 Å) between the fused pentalene units can be found, which further enhance the ordered molecular packing.

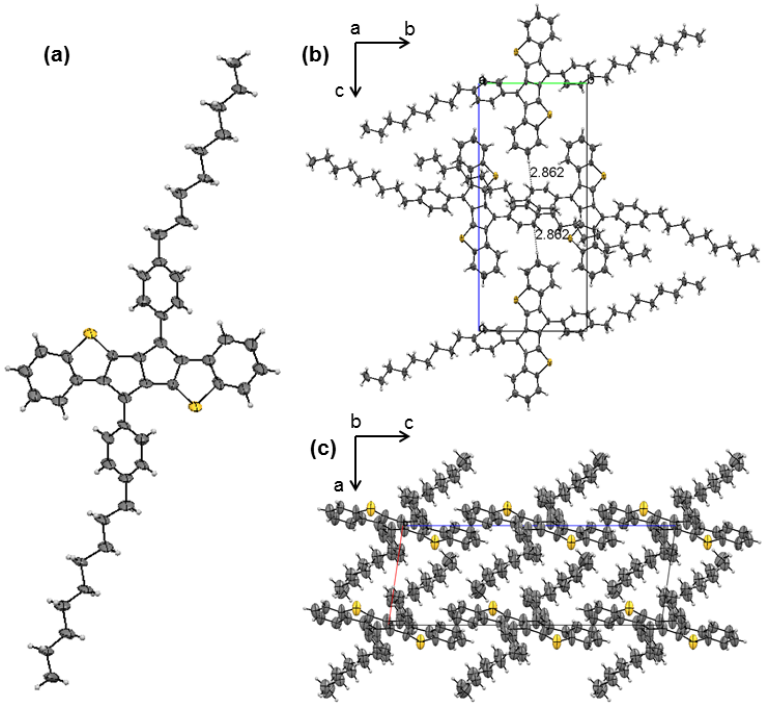

Figure 3.5 (a) ORTEP drawing of **3-1**; (b) packing along the a-axis; (c) packing along the b-axis.

Selected bond lengths of **3-1** - **3-2** and the calculated bond lengths of **3-3** are shown in Figure 3.7. In all cases, large bond alternation in the pentalene skeleton as well as in the outmost benzene rings was observed, as a result of counterbalance between aromatic stabilization of the thienoacene units and destabilization of the pentalene moiety. Nucleus independent chemical shift (NICS) calculations were conducted to understand the aromaticity of each ring (Figure 3.7).[9] It was found that all rings showed small negative $NICS(1)_{zz}$ values with a small aromatic character, again, due to an intramolecular aromatic/antiaromatic interactions.

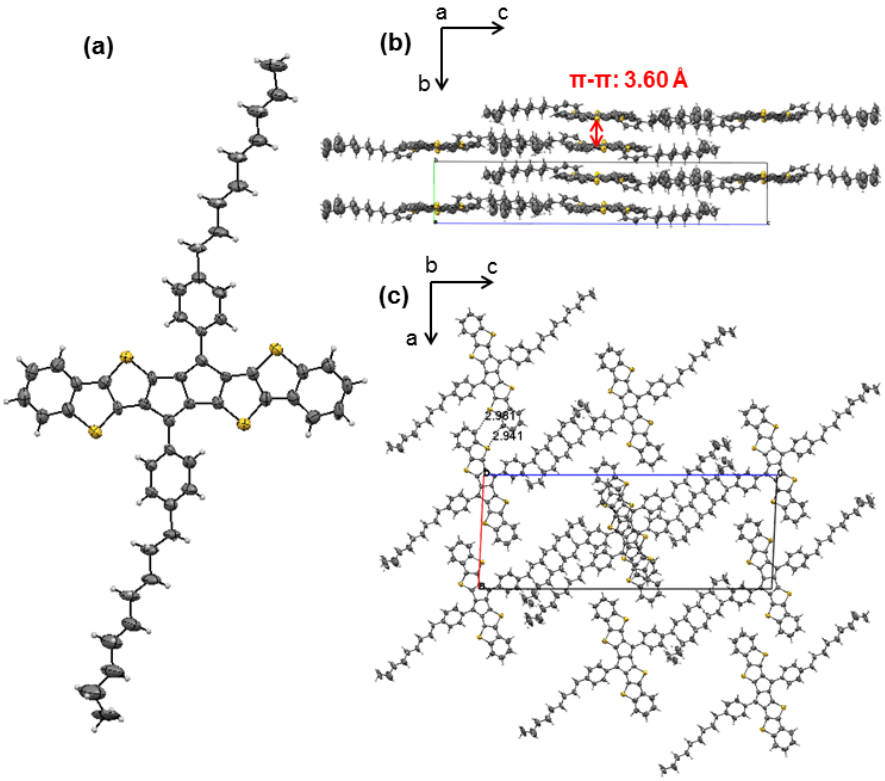

Figure 3.6 (a) ORTEP drawing of **3-2**; (b) packing along the a-axis; (c) packing along the b-axis.

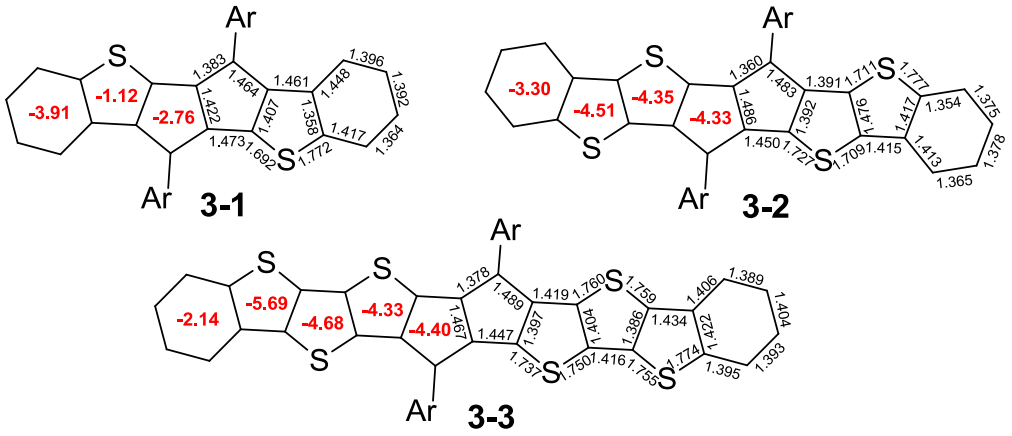

Figure 3.7 Selected bond lengths of **3-1**, **3-2** (based on X-ray crystallographic structures) and **3-3** (based on DFT calculations), and the calculated NICS(1)$_{zz}$ values (in ppm, red numbers in the rings).

3.2.6 Thin-film field effect transistors

Compounds **3-1** - **3-3** showed good thermal stability with decomposition temperatures (T_d, corresponding to a 5% weight loss in thermogravimetric

analysis (TGA) curves) at 375, 380, and 384 ^{o}C, respectively (Figure 3.8). They melt at 178 ^{o}C, 233 ^{o}C and 217 ^{o}C, respectively, from a crystalline phase to isotropic liquid phase based on polarizing optical microscopic measurements. The ordered packing structures of these compounds in solid state provoke us to study their charge transporting properties by field effect transistors.

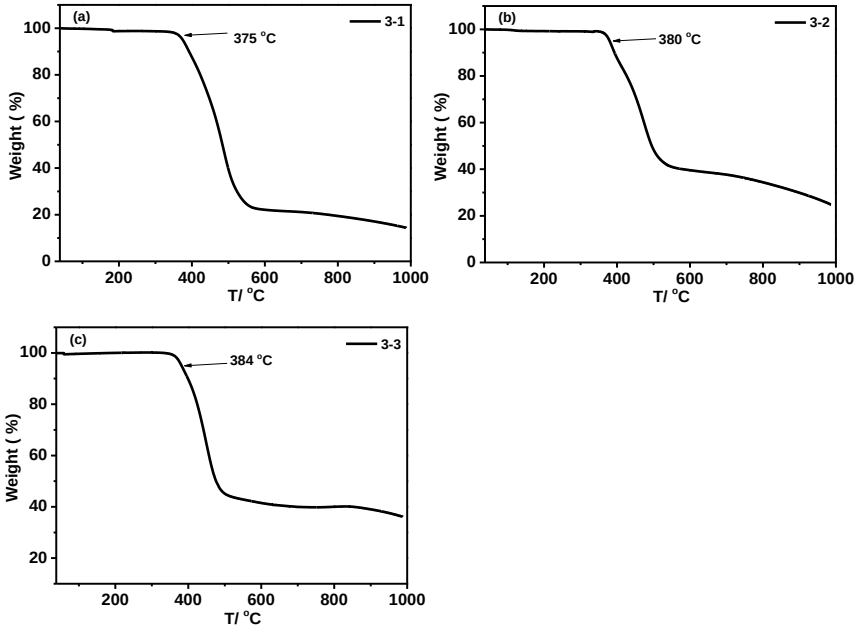

Figure 3.8.Thermogravimetric analysis (TGA) of Compound **3-1 (a)**, **3-2 (b)** and **3-3 (c)** in N_2 at a heating rate of 10 ^{o}C min^{-1}

The thin-film transistors were fabricated in a bottom-gate, top-contact configuration. Thin films of semiconducting materials were deposited by spin coating the $CHCl_3$ solution onto n+-Si wafer with 200 nm of thermally grown SiO_2 as the dielectric layer. The SiO_2 substrate was modified by either octadecyltrichlorosilane (ODTS) or hexamethyldisilazane (HMDS). Compound **3-1** showed strong tendency to aggregate to form small single

crystals on the substrates, and the spin coated device cannot be performed. Therefore, we fabricated the thin film using a slightly modified method reported previously by covering the solution with another ODTS treated substrate to suppress the crystal formation.[10] Uniform thin films of compounds **3-2** - **3-3** were successfully formed by spin coating. Then the thin films were annealed at selected temperatures to enhance the crystallinity. The devices were completed by patterning the Au source/drain electrodes using a shadow mask. The OFET device data for the thin films of **3-1** - **3-3** on different substrates measured under nitrogen are summarized in Table 3.2. All the compounds only showed *p*-type FET behaviour, maybe due to the LUMO orbital (base on TD-DFT calculation) mainly localized on the central pentalene core. The typical transfer and output curves for the **3-1** - **3-3** based OFETs on ODTS modified substrates measured in nitrogen are shown in Figure 3.9. The FET mobility was calculated using the following equation in the saturation regime: $I_D=W/(2L)C_i\mu(V_G-V_T)^2$, where I_D is the drain current, μ is the field-effect mobility, C_i is the capacitance per unit area of the gate dielectric layer (SiO_2, 200 nm, C_i = 17 nF cm^{-2}), and V_G and V_T are gate voltage and threshold voltage, respectively. W and L are channel width and length, respectively. For compound **3-1**, hole mobility of 0.012 $cm^2V^{-1}s^{-1}$ was achieved on ODTS modified substrate, the threshold voltage is around -12 - -15 V, and the current on/off ratio is 10^5 - 10^6. Increasing the conjugation length, compound **3-2** showed much improved hole mobility compared to **3-1**,

with hole mobility of 0.036 $cm^2V^{-1}s^{-1}$ and on/off ratio of 10^4-10^5. However, when increasing the conjugation length to **3-3**, the hole mobility decreased to 1.0 $\times 10^{-3}$ $cm^2V^{-1}s^{-1}$ for the as-spun thin film.

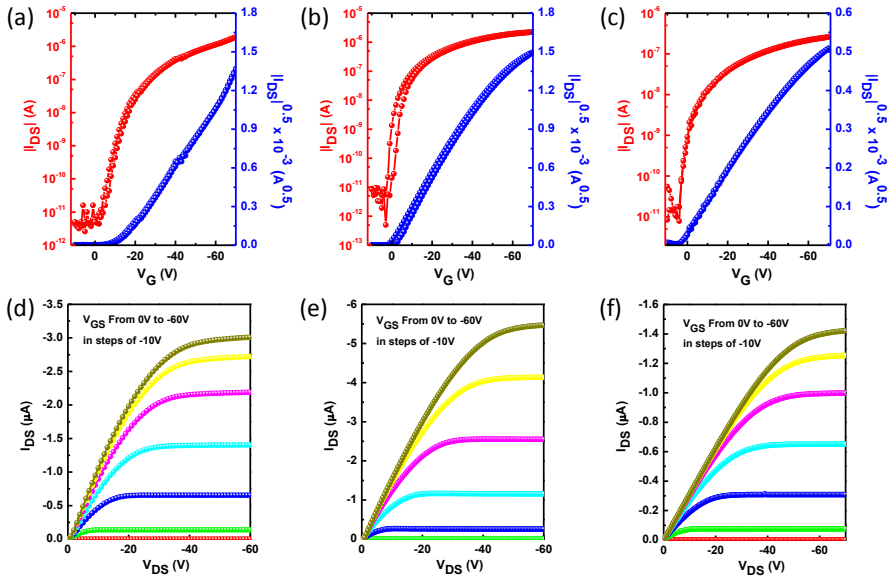

Figure 3.9 Transfer (up) and output (down) characteristics of **3-1** (a, d), **3-2** (b, e), and **3-3** (c, f) devices with ODTS modification.

Table 3.2 OFET characteristics of **3-1** - **3-3** based devices fabricated on Si/SiO_2 substrates with different surface treatments and different annealing temperatures.

	Surface treatment	Annealing Temperature [^oC]	μ [$cm^2V^{-1}s^{-1}$]	V_T [V]	On/off
3-1	ODTS	As-prepared	0.012-0.016	-12±3	10^6
3-2	HMDS	As-spun	5.6×10^{-5}	-4±2	5.8×10^4
		120	8.6×10^{-4}	-3±1	1.7×10^4
		150	4.3×10^{-3}	-2±2	1.4×10^4
	ODTS	As-spun	4.6×10^{-3}	0±3	1.2×10^6
		120	1.0×10^{-2}	6±2	8.2×10^4
		150	3.6×10^{-2}	5±3	1.2×10^4
3-3	HMDS	As-spun	4.0×10^{-5}	0±3	1.8×10^3
		120	6.5×10^{-5}	0±2	3.2×10^3
		150	1.3×10^{-4}	-2±3	6.8×10^3
	ODTS	As-spun	9.4×10^{-4}	3±2	3.3×10^4
		120	1.0×10^{-3}	1±3	4.2×10^4
		150	1.2×10^{-4}	0±4	2.2×10^3

In order to understand the performance difference of **3-1 - 3-3**, their thin films were investigated by atomic force microscope (AFM) and X-ray diffraction (XRD). As shown in Figure 3.10, thin film of **3-1** showed continuous and smooth films with a surface roughness of 1.2 nm, which is different from the spin coated thin film shown in Figure 3.11. This crystalline continuous thin film ensures a good charge transport property. Thin films of **3-2** on HMDS or ODTS modified substrates showed small crystal grains for the as-spun thin film (Figure 3.12). Upon thermal annealing, the crystal grain size was increased to around 1μm in size. Generally, the thin films on HMDS modified substrates exhibited smaller crystal size compared to ODTS treated substrates, which is accordance with the device performance. Compared to thin film **3-2**, thin film of **3-3** showed amorphous morphology on HMDS or ODTS modified substrates after spin coating, and upon thermal ammealing, and plate-like crystals with crystal size over several microns was achieved (Figures 3.10 and 3.13). This is the reason why its charge carrier mobility is enhance after thermal annealing.

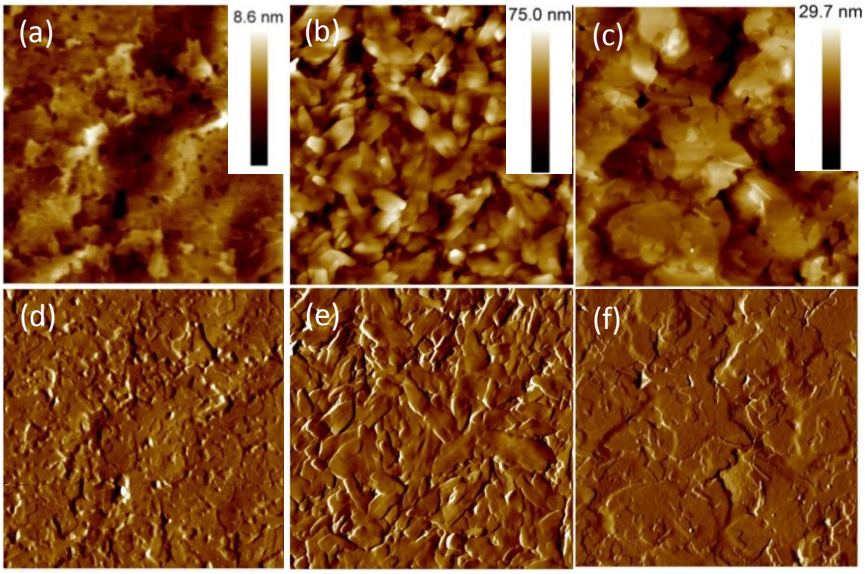

Figure 3.10 AFM images (5μm × 5μm) of thin-films of **3-1** (a, d), **3-2** (b, e) and **3-3** (c, f) on the ODTS treated substrates. The thin films of **3-2** and **3-3** were annealed at 120 ^{o}C.

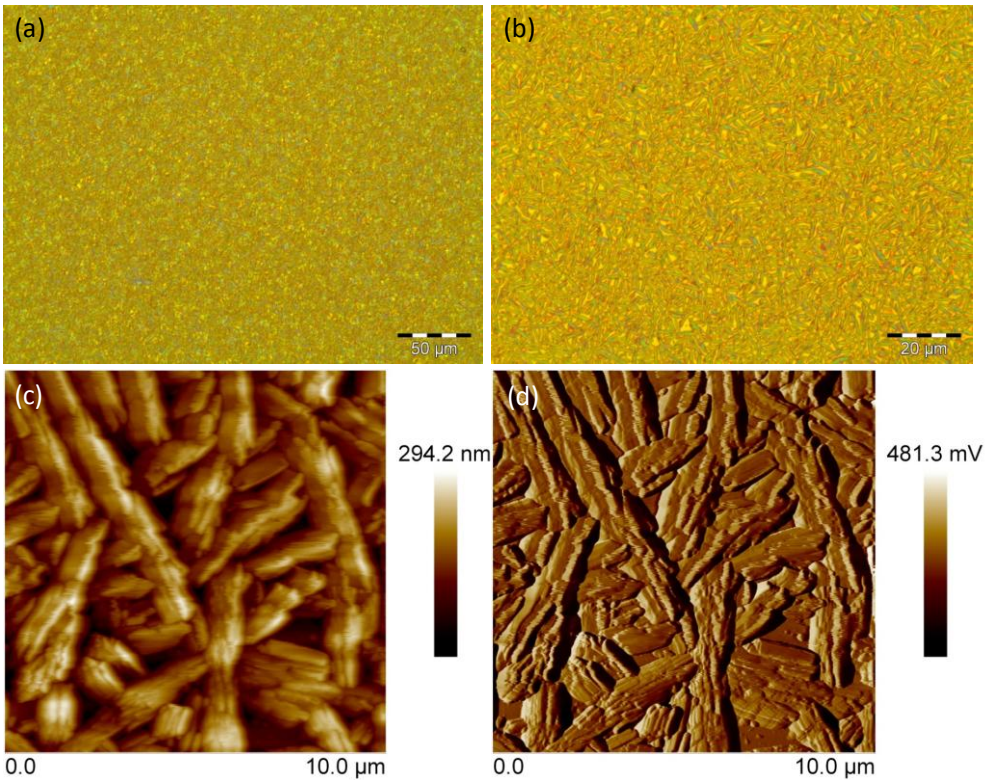

Figure 3.11 The optical microscopy images (a-b) and AFM images (c-d) of the thin film **3-1** spin coated from $CHCl_3$ solution onto ODTS treated substrates.

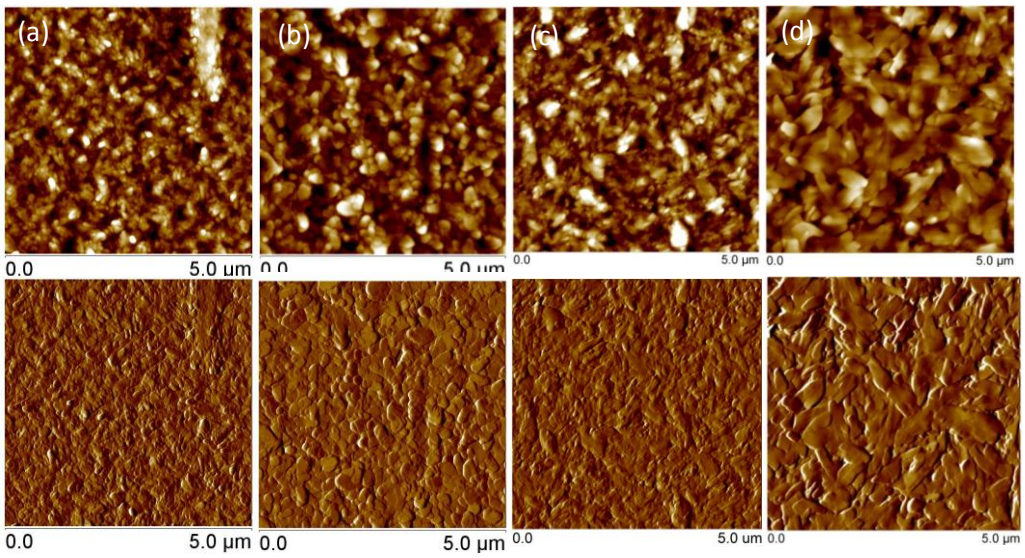

Figure 3.12 AFM images (up: height images; down: amplitude images) (5µm × 5µm) of compound **3-2** based thin-films on the HMDS-treated substrates: (a) without annealing, (b) with annealing at 120 ^{o}C, and on the OTS-treated substrates: (c) without annealing, (d) with annealing at 120 ^{o}C.

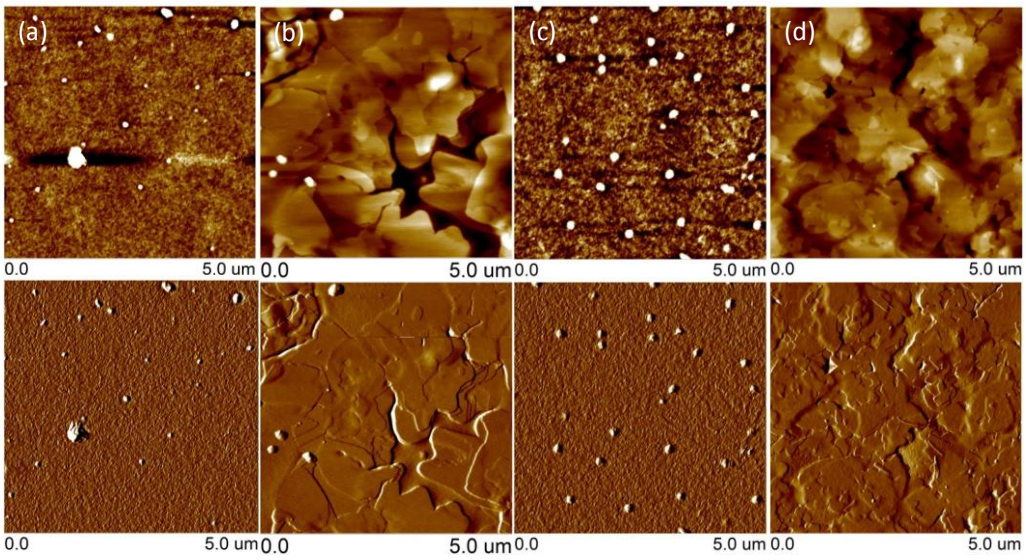

Figure 3.13. AFM images (up: height images; down: amplitude images) (5µm × 5µm) of compound **3-3** based thin-films on the HMDS-treated substrates: (a) without annealing, (b) with annealing at 120 ^{o}C, and on the OTS-treated substrates: (c) without annealing, (d) with annealing at 120 ^{o}C.

XRD diffraction patterns of the thin films showed that all compounds formed crystalline thin films and the intensity of the diffraction peaks was critically related to thermal annealing (Figure 3.14). Especially for thin film of

3-3, XRD spectrum did not show any peaks for the as-spun thin film, which indicates an amorphous nature of the thin film. However, upon thermal annealing at 120 ^{o}C, the XRD showed a strong diffraction peak due to the improved crystallinity, which is consistent with the AFM result. All compounds have a lamellar packing structure on the substrate, with a d_{100} spacing of 19.35 Å for **3-1**, 18.02 Å for **3-2** and 24.02 Å for **3-3**. Compound **3-2** is correlated the distance between molecular d-spacing value than **3-1**, indicating that it has a more dense packing. Compound **3-3** has the largest d-spacing value branched alkyl chains. This is the reason why **3-2** exhibited the highest μ_h, while **3-3** showed lowest μ_h among these molecules.

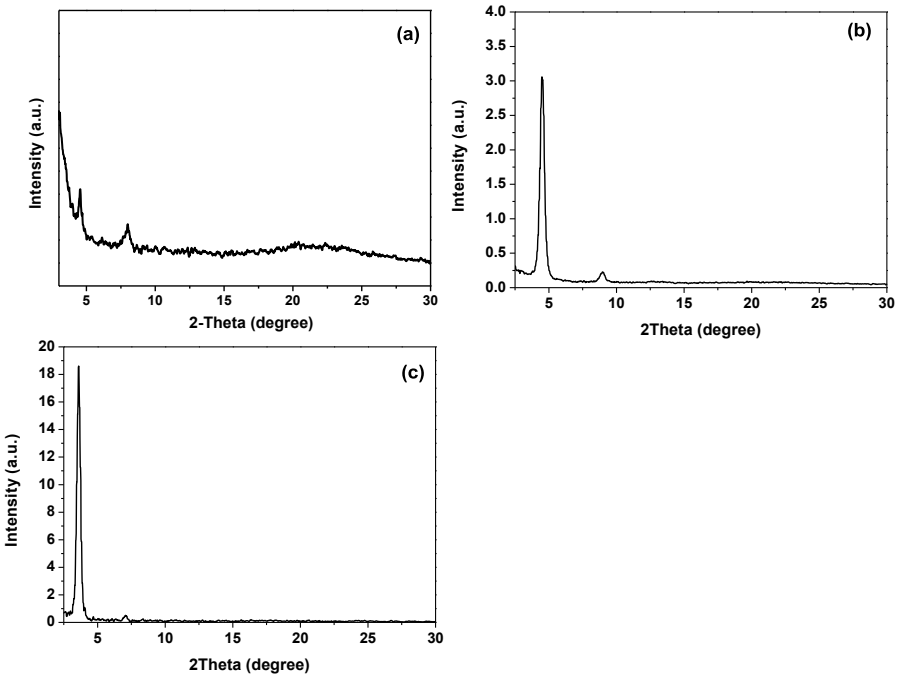

Figure 3.14 XRD patterns of thin films of **3-1** (a), **3-2** (b) and **3-3** (c) on ODTS modified Si/SiO_2 substrates. The thin films of **3-2** and **3-3** were annealed at 120 ^{o}C.

3.3 Summary

In summary, through appropriate design and optimization of the synthetic route, three thienoacene-fused pentalene derivatives with different molecular sizes were synthesized. Their structures, optical properties and electrochemical properties were studied and their applications in OFETs were also investigated. These compounds show unique ground-state geometric and electronic structures due to the intramolecular aromatic/antiaromatic interactions as revealed by X-ray crystallographic analysis. As results, they exhibit small energy gap, unique electronic absorption spectrum and amphoteric redox behavior, which are also supported by DFT calculations. All compounds showed good thermal stability and ordered self-assembly in solid state. The highest hole charge mobility of 0.016, 0.036 and 0.001 $cm^2V^{-1}s^{-1}$ was achieved under optimised conditions for the thin films of **3-1**, **3-2** and **3-3**, respectively, which stands at the higher end of pentalene-based semiconductors.

3.4 Experiment section

3.4.1 General characterization method

^1H and ^{13}C NMR spectra were recorded using Advance 500 MHz Bruker spectrometer in $CDCl_3$ with tetramethylsilane (TMS) as the internal standard. The chemical shift was recorded in ppm and the following abbreviations were used to explain the multiplicities: s = singlet, d = doublet, t= triplet, m = multiplet, br = broad. Column chromatography was performed on silica gel 60 (Merck 40-60 nm, 230-400 mesh). High resolution (HR) EI mass spectra were

recorded on Agilent 5975C DIP/MS mass spectrometer. HR ACPI mass spectra were recorded on a MicrOTOF-QII instrument. MALDI-TOF mass spectra were recorded on a Bruker Autoflex instrument. UV-vis absorption and fluorescence spectra were recorded on a Shimadzu UV-1700 spectrophotometer and a RF-5301 fluorometer, respectively. Cyclic voltammetry and differential pulse voltammetry measurements were performed in HPLC grade chlorobenzene on a CHI 620C electrochemical analyzer with a three-electrode cell, using 0.1 M Bu_4NPF_6 as supporting electrolyte, AgCl/Ag as reference electrode, gold disk as working electrode, Pt wire as counter electrode, and scan rate at 50 mV s^{-1}. The potential was externally calibrated against the ferrocene/ferrocenium couple. TGA measurements were carried out on a TA instrument 2960 at a heating rate of 10 ℃ min^{-1} under nitrogen flow. Tapping-mode AFM measurements were performed on a Nanoscope V microscope (Veeco Inc.). XRD patterns of the thin film were measured on a Bruker-AXS D8 DISCOVER with GADDS X-ray diffractometer. Copper Kα line was used as a radiation source with λ = 1.5418 Å.

3.4.2 Synthesis

All reagents were purchased from commercial sources without further purification. Anhydrous dichloromethane (DCM), *N*, *N*-dimethylformaldehyde (DMF) was distilled from CaH_2. Toluene and THF were distilled from sodium-benzophenone immediately prior to use.

Compound **3-5 3-Bromo-2-((4-nonylphenyl)ethynyl)benzo[b]thiophene**

A mixture of compound **3-4** (1.50 g, 4.4 mmol), 1-ethynyl-4-nonylbenzene (1.21 g, 5.3 mmol), CuI (25 mg, 3%) and $Pd(PPh_3)_2Cl_2$ (155 mg, 5%) in anhydrous THF (12 mL) and Et_3N (12 mL) was degassed by three freeze-pump-thaw cycles. The mixture was stirred at room temperature under argon for overnight. The mixture was extracted with EtOAc (30 mL ×2). The combined organic phase was washed with brine (50 mL ×2) and 10% m/m aqueous HCl solution (50 mL ×1). The organic phase was dried over anhydrous Na_2SO_4 and the organic solvent was removed under reduced pressure. The crude product was purified by column chromatography (EtOAc/hexane = 1:30) to afford compound **3-5** (1.50 g) in 80% yield. ^{1}H NMR (500 MHz, $CDCl_3$, ppm): δ = 7.79 (d, *J* = 8.0 Hz, 1H), 7.75 (d, *J* =7.5 Hz, 1H), 7.52 (d, *J* = 8.0 Hz, 2H), 7.48-7.41 (m, 2H), 7.20 (d, *J* = 8.0 Hz, 2H), 2.63 (t, *J* = 7.75 Hz, 2H), 1.70-1.60 (m, 2H), 1.40-1.25 (m, 12H), 0.89 (t, *J* = 6.5 Hz, 3H). ^{13}C NMR (125 MHz, $CDCl_3$, ppm): δ = 144.50, 138.17, 137.49, 131.68, 128.59, 126.38, 125.44, 123.58, 122.22, 120.66, 119.38, 113.35, 99.53, 81.06, 36.00, 31.88, 31.20, 29.53, 29.47, 29.30, 29.23, 22.66, 14.10. HR MS (EI): calcd for $C_{25}H_{27}BrS$ (M^+), 438.1017; found, 438.1004 (error: -3.06 ppm).

Compound **3-1**

A suspension of compound **3-6** (1.33 g, 3.0 mmol), Zn powder (0.30 g, 4.5 mmol) and $NiCl_2(PPh_3)$ (1.97 g, 3 mmol) in anhydrous toluene (12 mL) was heated at reflux for 24 hours under argon. After the reaction mixture cooling to

room temperature, the reaction mixture was filtered through celite pad and then evaporated under reduced pressure. The crude product was purified by column chromatography (hexane and hexane/CH_2Cl_2 = 10:3) to afford compound **3-1** (0.16 g) in 15% yield.^{1}H NMR (500 MHz, $CDCl_3$, ppm): δ = 7.54 (d, *J* = 7.5 Hz, 4H), 7.47 (d, *J* = 8.0 Hz, 2H), 7.31 (d, *J* = 8.0 Hz, 6H), 7.09 (t, *J* = 7.5 Hz, 2H), 6.99 (t, *J* = 7.5 Hz, 2H), 2.70 (t, *J* = 8.0 Hz, 4H), 1.75-1.65 (m, 4H), 1.45-1.25 (m, 24H), 0.90 (t, *J* = 6.75 Hz, 6H). ^{13}C NMR (125 MHz, $CDCl_3$, ppm): δ = 145.64, 145.37, 143.87, 143.52, 142.28, 141.18, 133.66, 130.60, 128.59, 127.79, 125.18, 123.63, 122.52, 121.30, 36.14, 31.91, 31.24, 29.56, 29.52, 29.45, 29.33, 22.69, 14.11. HR MS (EI): calcd for $C_{50}H_{54}S_2$ (M^+), 718.3667; found, 718.3652 (error: -1.25 ppm).

Compound **3-7 3-Bromo-2-iodobenzo[b]thieno[2,3-d]thiophene**

The 2 M LDA solution (4.4 mL, 8.8 mmol) was slowly added into the solution of compound **3-6** (2.15 g, 8 mmol) in anhydrous THF (25 mL) at -78 ^{o}C. The reaction mixture was stirred for 16 hours at this temperature. Then I_2 (4.1 g, 16 mmol) was added to the reaction mixture at -78 ^{o}C. The mixture was slowly warmed to room temperature and stirred overnight. 3 mL of water was added to quench the reaction and 30 mL of saturated $Na_2S_2O_3$ solution was added to quench the excess I_2. The mixture was extracted with chloroform (50 mL ×2). The combined organic phase was washed with brine (50 mL ×2), dried over anhydrous Na_2SO_4 and the solvent was removed under reduced pressure. The crude product was purified by column chromatography (CH_2Cl_2/hexane = 1:5)

to afford compound **3-7** (2.37 g) in 75% yield. ^{1}H NMR (500 MHz, $CDCl_3$, ppm): δ = 7.86 (d, *J* = 8.0 Hz, 1H), 7.76 (d, *J* = 7.5 Hz, 1H), 7.45-7.37 (m, 2H). ^{13}C NMR (125 MHz, $CDCl_3$, ppm): δ = 141.45, 138.37, 137.88, 132.71, 125.29, 125.09, 124.04, 121.17, 113.25, 78.04. HR MS (EI): calcd for $C_{10}H_4BrIS_2$ (M^+), 395.7962; found, 395.7949 (error: -3.29 ppm).

Compound **3-8** 3-Bromo-2-((4-nonylphenyl)ethynyl)benzo[b]thieno-[2,3-d]thiophene

A mixture of compound **3-7** (2.66 g, 6.7 mmol), 1-ethynyl-4-nonylbenzene (1.69 g, 7.4 mmol), CuI (38 mg, 3%) and $Pd(PPh_3)_2Cl_2$ (236 mg, 5%) in anhydrous THF (15 mL) and Et_3N (30 mL) was degassed by three freeze-pump-thaw cycles. The mixture was stirred at room temperature under argon for overnight. The mixture was extracted with EtOAc (50 mL ×2). The combined organic phase was washed with brine (50 mL ×2) and 10% m/m aqueous HCl solution (50 mL ×1). The organic phase was dried over anhydrous Na_2SO_4 and the solvent was then removed under reduced pressure. The crude product was purified by column chromatography (EtOAc/hexane = 1:30) to afford compound **3-8** (2.80 g) in 84% yield. ^{1}H NMR (500 MHz, $CDCl_3$, ppm): δ = 7.88 (d, *J* = 8.0 Hz, 1H), 7.81 (d, *J* = 7.0 Hz, 1H), 7.51 (d, *J* = 8.0 Hz, 2H), 7.47-7.37 (m, 2H), 7.20 (d, *J* = 8.0 Hz, 2H), 2.63 (t, *J* = 7.5 Hz, 2H), 1.65-1.58 (m, 2H), 1.35-1.20 (m, 12H), 0.88 (t, *J* = 7 Hz, 3H). ^{13}C NMR (125 MHz, $CDCl_3$, ppm): δ = 144.39, 142.25, 139.04, 133.04, 132.85, 131.56, 128.59, 125.39, 125.11, 124.02, 122.37, 121.21, 119.43, 108.96, 98.93, 81.22,

35.99, 31.88, 31.20, 29.69, 29.53, 29.48, 29.30, 29.24, 22.66, 14.10. HR MS (EI): calcd for $C_{27}H_{27}BrS_2$ (M^+), 494.0738; found, 494.0751 (error: 2.70 ppm).

Compound **3-2**

A suspension of compound **3-8** (2.00 g, 4.0 mmol), Zn powder (0.48 g, 7.3 mmol) and $NiCl_2(PPh_3)$ (2.69 g, 4.1 mmol) in anhydrous toluene (40 mL) was heated at reflux for 24 hours under argon. After the reaction mixture cooling to room temperature, the reaction mixture was filtered through celite pad and then evaporated under reduced pressure. The crude product was purified by column chromatography (hexane and hexane/CH_2Cl_2 = 10:3) to afford compound **3-2** (0.30 g) in 18% yield. ^{1}H NMR (500 MHz, $CDCl_3$, ppm): δ = 7.63 (d, *J* = 8.0 Hz, 2H), 7.58 (d, *J* = 8.0 Hz, 4H), 7.51 (d, *J* = 8.0 Hz, 2H), 7.30 (d, *J* = 8.0 Hz, 4H), 7.26 (t, *J* = 7.5 Hz, 2H), 7.17 (t, *J* = 7.5 Hz, 2H), 2.69 (t, *J* = 8.0 Hz, 4H), 1.75-1.68 (m, 4H), 1.41-1.21 (m, 24H), 0.92 (t, *J* = 7.0 Hz, 6H). ^{13}C NMR (125 MHz, $CDCl_3$, ppm): δ = 145.51, 144.41, 141.71, 141.22, 141.16, 140.06, 136.33, 132.96, 132.82, 130.37, 128.98, 127.48, 124.83, 123.92, 123.46, 119.59, 36.21, 31.96, 31.11, 29.60, 29.55, 29.51, 29.35, 22.69, 14.01. MALDI-TOF MS (HR): calcd for $C_{54}H_{54}S_4$ (M^+), 830.3108; found, 830.3073 (error: -2.09 ppm).

Compound **3-10 3-Bromo-benzo[d,d′]thieno[3,2-b;4,5-b′]dithiophene**

The 2 M LDA solution (3.4 mL, 6.8 mmol) was slowly added into the solution of compound **3-9** (2.01 g, 6.2 mmol) in anhydrous THF (80 mL) at -78 ^{o}C. The reaction mixture was stirred for 16 hours at this temperature. Then 3 mL of

water was added to quench the reaction at -78 ^{o}C. After the mixture warmed to room temperature, the mixture was extracted with chloroform (80 mL ×2). The combined organic phase was washed with brine (60 mL ×2), dried over anhydrous Na_2SO_4 and the solvent was removed under reduced pressure. The crude product was purified by column chromatography (CH_2Cl_2/hexane = 1:5) to afford compound **3-10** (1.81 g) in 90% yield. ^{1}H NMR (500 MHz, $CDCl_3$, ppm): δ = 7.88 (d, *J* = 8 Hz, 1H), 7.84 (d, *J* = 8.0 Hz, 1H), 7.45 (t, *J* = 7.25 Hz, 1H), 7.38 (t, *J* = 7.5 Hz, 1H), 7.31 (s, 1H). Compared to compound **9**, the characteristic ^{1}H NMR peak shifts from δ = 7.34 to δ = 7.31. ^{13}C NMR (125 MHz, $CDCl_3$, ppm): δ = 142.52, 141.46, 136.79, 133.29, 131.15, 129.99, 125.14, 124.98, 123.98, 123.45, 120.87, 103.70. HR MS (EI): calcd for $C_{10}H_4BrIS_2$ (M^+), 323.8737; found, 323.8728 (error: -2.78 ppm).

Compound **3-11 3-Bromo-2-iodo-benzo[d,d′]thieno[3,2-b;4,5-b′]-dithiophene**

After compound **3-10** (2.04 g, 6.3 mmol) was dissolved into 60 mL of $CHCl_3$, 60 mL of acetic acid was added to the solution. Then *N*-iodosuccinimide (NIS) (2.85 g, 12.6 mmol) was added at 0 ^{o}C. The mixture was warmed to room temperature and stirred overnight under argon. The mixture was extracted with chloroform (100 mL ×2). The combined organic phase was washed with brine (80 mL ×2), dried over anhydrous Na_2SO_4 and the solvent was removed under reduced pressure. The crude product was purified by column chromatography (CH_2Cl_2/hexane = 1:3) to afford compound **3-11** (2.41 g) in 85% yield. ^{1}H

NMR (500 MHz, $CDCl_3$, ppm): δ = 7.87 (d, *J* = 8.5 Hz, 1H), 7.84 (d, *J* = 7.5 Hz, 1H), 7.46 (t, *J* = 7.5 Hz, 1H), 7.39 (t, *J* = 7.5 Hz, 1H). ^{13}C NMR (125 MHz, $CDCl_3$, ppm): δ = 141.44, 141.30, 136.33, 134.92, 133.00, 129.83, 125.26, 125.24, 123.99, 120.99, 113.40. HR MS (EI): calcd for $C_{12}H_4BrIS_3$ (M^+), 449.7703; found, 449.7702 (error: -0.21 ppm).

Compound **3-12** **3-Bromo-2-((4-(pentadecan-7-yl)phenyl)ethynyl)-benzo[d,d′]thieno[3,2-b;4,5-b′]dithiophene**

A mixture of compound **3-11** (1.20 g, 2.7 mmol), 1-ethynyl-4-(pentadecan-7-yl)benzene **3-13** (0.96 g, 2.9 mmol), CuI (15 mg, 3%) and $Pd(PPh_3)_2Cl_2$ (50 mg, 5%) in anhydrous THF (30 mL) and Et_3N (15 mL) was degassed by three freeze-pump-thaw cycles. The mixture was stirred at room temperature under argon for overnight. The mixture was extracted with EtOAc (60 mL ×2). The combined organic phase was washed with brine (50 mL ×2) and 10% m/m aqueous HCl solution (50 mL ×1), was dried over anhydrous Na_2SO_4 and the solvent was removed under reduced pressure. The crude product was purified by column chromatography (EtOAc/hexane = 1:30) to afford compound **3-12** (1.47 g) in 85% yield. ^1H NMR (500 MHz, $CDCl_3$, ppm): δ = 7.89 (d, *J* = 7.5 Hz, 1H), 7.85 (d, *J* = 8.0 Hz, 1H), 7.51 (d, *J* = 8.0 Hz, 2H), 7.46 (t, *J* = 7.75 Hz, 1H), 7.42-7.38 (m, 1H), 7.16 (d, *J* = 8.5 Hz, 2H), 2.55 (d, *J* = 7.0 Hz, 2H), 1.65-1.58 (m, 1H), 1.30-1.15 (m, 24H), 0.92-0.85 (m, 6H).^{13}C NMR (125 MHz, $CDCl_3$, ppm): δ = 143.52, 141.99, 141.66, 137.52, 133.11, 131.42, 130.03, 129.98, 129.37, 125.25, 124.02, 121.49, 121.00,

119.32, 109.15, 99.17, 81.20, 40.67, 39.66, 33.20, 33.17, 31.90, 31.88, 29.96, 29.65, 29.60, 29.32, 26.55, 22.68, 14.11, 14.09. HR MS (EI): calcd for $C_{36}H_{41}BrS_3$ (M^+), 648.1554; found, 648.1550 (error: -0.63 ppm).

Compound **3-3**

A suspension of compound **3-12** (0.98 g, 1.5 mmol), Zn powder (0.18 g, 2.7 mmol) and $NiCl_2(PPh_3)$ (1.03 g, 1.6 mmol) in anhydrous toluene (15 mL) was heated at reflux for 24 hours under argon. After the reaction mixture cooling to room temperature, the reaction mixture was filtered through celite pad and then evaporated under reduced pressure. The crude product was purified by column chromatography (hexane and hexane/CH_2Cl_2 = 10:3) to afford compound **3-3** (0.13 g) in 15% yield. ^{1}H NMR (500 MHz, $CDCl_3$, ppm): δ = 7.50 (d, *J* = 8.0 Hz, 2H), 7.47-7.42 (m, 6H), 7.17-7.11 (m, 6H), 7.00 (t, *J* = 7.25 Hz, 2H), 2.60 (d, *J* = 7.0 Hz, 4H), 1.80-1.70 (m, 2H), 1.50-1.22 (m, 48H), 0.95-0.80 (m, 12H); ^{13}C NMR (125 MHz, $CDCl_3$, ppm): δ = 144.77, 144.01, 141.90, 140.91, 139.76, 138.93, 135.85, 134.92, 133.00, 132.86, 130.14, 129.67, 129.50, 127.45, 124.44, 123.60, 123.18, 119.63, 40.90, 39.68, 33.43, 33.37, 31.98, 31.96, 30.14, 29.78, 29.73, 29.44, 26.68, 26.58, 22.78, 22.74, 14.22, 14.15. HR-APCI: calcd for $C_{72}H_{83}S_6$ ($M+H^+$), 1139.4819; found, 1139.4814 (error: -0.44 ppm).

Compound **3-16 4-(4-(2-Hexyldecyl)phenyl)-2-methylbut-3-yn-2-ol**

The Grignard reagent (2-hexyldecyl)magnesium bromide (25 mL, 1 M, 25 mmol) was dropwise to the mixture of 1,4-dibromobenzene **3-14** (5.00 g , 21

mmol) and catalyst Pd(dppf)Cl_2 CH_2Cl_2 (0.69 g, 4%) in 50 mL of anhydrous THF at 0 ^oC. Then the mixture was heated to reflux and stirred under argon at this temperature for overnight. After the reaction mixture was cooled down, 2-methylbut-3-yn-2-ol (5.30g, 63 mmol), Pd$(PPh_3)_2Cl_2$ (0.59 g, 4%), CuI (80 mg, 2%) and anhydrous Et_3N (25 mL) were added into the mixture. After de-oxygen by vacuum, the mixture was heated to 70 ^oC and stirred under argon at this temperature for overnight. After cooling down to room temperature, the mixture was extracted with EtOAc (80 mL ×2). The combined organic phase was washed with brine (60 mL ×2) and 10% m/m aqueous HCl solution (60 mL ×1), dried over anhydrous Na_2SO_4 and the solvent was removed under reduced pressure. The crude product was purified by column chromatography (EtOAc/Hexane = 1:10) to afford compound **3-16** (3.2 g) in 40% yield. ^1H NMR (500 MHz, $CDCl_3$, ppm): δ = 7.32 (d, *J* = 8.0 Hz, 2H), 7.07 (d, *J* = 8.0 Hz, 2H), 2.50 (d, *J* = 7.0 Hz, 2H), 2.06 (s, 1H), 1.70-1.60 (m, 7H), 1.30-1.10 (m, 24H), 0.90-0.82 (m, 6H). ^{13}C NMR (125 MHz, $CDCl_3$, ppm): δ = 142.44, 131.37, 129.12, 119.71, 93.11, 82.31, 65.63, 40.48, 39.61, 33.14, 33.11, 31.88, 31.86, 31.53, 29.94, 29.63, 29.57, 29.30, 26.51, 22.66, 22.65, 14.10, 14.07. HR MS (EI): calcd for $C_{27}H_{44}O$ (M^+), 384.3392; found, 384.3375 (error: -4.42 ppm).

Compound **3-13 1-Ethynyl-4-(2-hexyldecyl)benzene**

A suspension of compound **3-16** (3.00 g, 7.8 mmol) and KOH powder (0.80 g, 14.3 mmol) in anhydrous toluene (15 mL) was heated at reflux for 3 hours

under argon. After the reaction was cooled down to room temperature, the mixture was extracted with EtOAc (50 mL ×2). The combined organic phase was washed with brine (50 mL ×2), dried over anhydrous Na_2SO_4 and the solvent was removed. The crude product was purified by column chromatography (Hexane) to afford compound **3-13** (1.80 g) in 70% yield. ^{1}H NMR (500 MHz, $CDCl_3$, ppm): δ = 7.40 (d, *J* = 8.0 Hz, 2H), 7.09 (d, *J* = 8.0 Hz, 2H), 3.03 (s, 1H), 2.52 (d, *J* = 7.0 Hz, 2H), 1.66-1.58 (m, 1H), 1.35-1.20 (m, 24H), 0.95-0.85 (m, 6H). ^{13}C NMR (125 MHz, $CDCl_3$, ppm): δ = 143.05, 131.87, 129.17, 119.11, 83.93, 76.42, 40.53, 39.59, 33.14, 33.11, 31.89, 31.86, 29.95, 29.63, 29.58, 29.31, 26.52, 26.51, 22.67, 14.10, 14.08. HR MS (EI): calcd for $C_{24}H_{38}$ (M^+), 326.2974; found, 326.2969 (error: -1.51 ppm).

Reference

[1] (a) Takimiya, K.; Ebata, H.; Sakamoto, K.; Izawa, T.; Otsubo, T.; Kunugi, Y. *J. Am. Chem. Soc.* **2006**, 128, 12604; (b) Yamamoto, T.; Takimiya, K. *J. Am. Chem. Soc.* **2007**, 129, 2224; (c) Zschieschang, U.; Ante, F.; Yamamoto, T.; Takimiya, K.; Kuwabara, H.; Ikeda, M.; Sekitani, T.; Someya, T.; Kern, K.; Klauk, H. *Adv. Mater.* **2010**, 22, 982; (d) Niimi, K.; Shinamura, S.; Osaka, I.; Miyazaki, E.; Takimiya, K. *J. Am. Chem. Soc.* **2011**, 133, 8732; (e) Sokolov, A. N.; Atahan-Evrenk, S.; Mondal, R.; Akkerman, H. B.; Sánchez-Carrera, R. S.; Granados-Focil, S.; Schrier, J.; Mannsfeld, S. C. B.; Zoombelt, A. P.; Bao, Z.; Aspuru-Guzik, A. *Nat.*

Commun. **2011**, 2, 437; (f) McCarthy, M. A.; Liu, B.; Donoghue, E. P.; Kravchenko, I.; Kim, D. Y.; So, F.; Rinzler, A. G. *Science* **2011**, 332, 570; (g) Zschieschang, U.; Kang, M. J.; Takimiya, K.; Sekitani, T.; Someya, T.; Canzler, T. W.; Werner, A.; Blochwitz-Nimothd, J.; Klauk, H. *J. Mater. Chem.* **2012**, 22, 4273; (h) Xie, W.; Willa, K.; Wu, Y.; Häusermann, R.; Takimiya, K.; Batlogg, B.; Frisbie, C. D. *Adv. Mater.* **2013**, 25, 3478; (i) Mori, T.; Nishimura, T.; Yamamoto, T.; Doi, I.; Miyazaki, E.; Osaka, I.; Takimiya, K. *J. Am. Chem. Soc.* **2013**, 135, 13900.

[2] (a) Yamamoto, T.; Ogawa, S.; Sato, R. *Tetrahedron Lett.* **2004**, 45, 7943; (b) Chabert, J. F. D.; Joucla, L.; David, E.; Lemaire, M. *Tetrahedron* **2004**, 60, 3221.

[3] Kienle, M.; Unsinn, A.; Knochel, P. *Angew. Chem. Int. Ed.* **2010**, 49, 4751.

[4] (a) Ongayi, O.; Vicente, M. G. H.; Ghosh, B.; Fronczek, F. R.; Smith, K. M. *Tetrahedron* **2010**, 66, 63; (b) Sista, P.; Nguyen, H.; Murphy, J. W.; Hao, J.; Dei, D. K.; Palaniappan, K.; Servello, J.; Kularatne, R. S.; Gnade, B. E.; Xue, B.; Dastoor, P. C.; Biewer, M. C.; Stefan, M. C. *Macromolecules* **2010**, 43, 8063; (c) Takeuchi, J. A.; Li, L.; Im, W. B. *Patent* **2012**, WO2012142288.

[5] (a) Björk, M.; Grivas, S. *J. Heterocyclic Chem.* **2006**, 43, 101; (b) Lyaskovskyy, V.; Fröhlich, R.; Würthwein, E.-U. *Synthesis* **2007**, 14, 2135; (c) Tian, H.; Han, Y.; Bao, C.; Yan, D.; Geng, Y.; Wang, F. *Chem. Commun.* **2012**, 48, 3557.

[6] (a) Schnürch, M.; Spina, M.; Khan, A. F.; Mihovilovic, M. D.; Stanetty, P. *Chem. Soc. Rev.* **2007**, 36, 1046; (b) Souza, M. V. N. d. *Curr. Org. Chem.* **2007**, *11*, 637.

[7] (a) Crystallographic data for **3-1**: $C_{50}H_{54}S_2$. M_w: 719.05; Monoclinic; space group P2(1)/c; a = 8.4962(8) Å, b = 10.0547(6) Å, c = 23.1703(17) Å, α = 90°, β = 98.262(7)°, γ = 90°; V = 1958.8(3) Å^3; Z = 2; ρ_{calcd} = 1.219 Mg/m^3; R_1 =0.1915, wR_2 = 0.3919 (I > 2σ(I)); R_1 = 0.3724, wR_2 = 0.4773 (all data); b) Crystallographic data for **3-2**: $C_{54}H_{54}S_4$. M_w: 831.21; Monoclinic; space group P2(1)/n; a = 15.3716(3) Å, b = 7.3070(2) Å, c = 39.5565(7) Å, α = 90°, β = 92.696(2)°, γ = 90°; V = 4438.08(17) Å^3; Z = 4; ρ_{calcd} = 1.244 Mg/m^3; R_1 = 0.0985, wR_2 = 0.1933 (I > 2σ(I)); R_1 = 0.2498, wR_2 = 0.2397 (all data). CCDC 1003816 (**3-1**) and CCDC 1003817 (**3-2**) contain the supplementary crystallographic data.

[8] Kawase, T.; Fujiwara, T.; Kitamura, C.; Konishi, A.; Hirao, Y.; Matsumoto, K.; Kurata, H.; Kubo, T.; Shinamura, S.; Mori, H.; Miyazaki, E.; Takimiya, K. *Angew. Chem. Int. Ed.* **2010**, 49, 7728.

[9] Fallah-Bagher-Shaidaei, H.; Wannere, C. S.; Corminboeuf, C.; Puchta, R.; Schleyer, P. v. R. *Org. Lett.* **2006**, 8, 863.

[10] Chang, J.; Shao, J.; Zhang, J.; Wu, J.; Chi, C. *RSC Adv.* **2013**, 3, 6775.

Chapter 4: Synthesis of Diacenopentalene Diimides for n-Channel Organic Field Effect Transistors

4.1 Introduction

In Chapter 1, we have known that several pentalene derivatives have been reported. However, all those materials show p-type FET behavior. Up to now, n-type or ambipolar pentalene derivatives haven't been seen in reported literatures. Dicarboximide group possess highly-electron deficient property and hence it has been widely used to design n-type or ambipolar semiconductor materials such as naphthalene diimides[1], perylene diimides[2] and pentacene diimides[3].

In this chapter, we introduce electron-withdrawing imide groups into pentalene derivatives successfully, N-alkylated dibenzopentalene diimide (**DBPDI**) and N-alkylated dinaphthopentalene diimide (**DNPDI)** as shown in Scheme 4.1 were designed as n-type semiconductors for OFETs. The physical properties and OFET device performance were studied.

4.2 Results and discussion

4.2.1 Synthesis

The synthetic routes of compounds **DBPDI** and **DNPDI** are shown in Scheme 4.1. Initially, the raw material o-xylene was selectively brominated at 4 and 5 position by bromine to give 4,5-dibromo-*o*-xylene**.** Then two methyl

groups of this compound were oxidized by potassium permanganate to give dibromophthalic acid **4-1**.[4] Subsequently, the activated aryl chloride was formed by treating **4-1** with thionyl chloride, and then attacked by alkylated amine to provide key precursor **4-2** in 37% yield**.** In the following step, compound **4-2** reacted with phenyl acetylene through Sonogashira cross-coupling reaction to give unilateral intermediate **4-3** in 34% yield. Eventually, the target molecule **DBPDI** was synthesized through palladium catalyzed pentalene formation reaction in 10% yield.

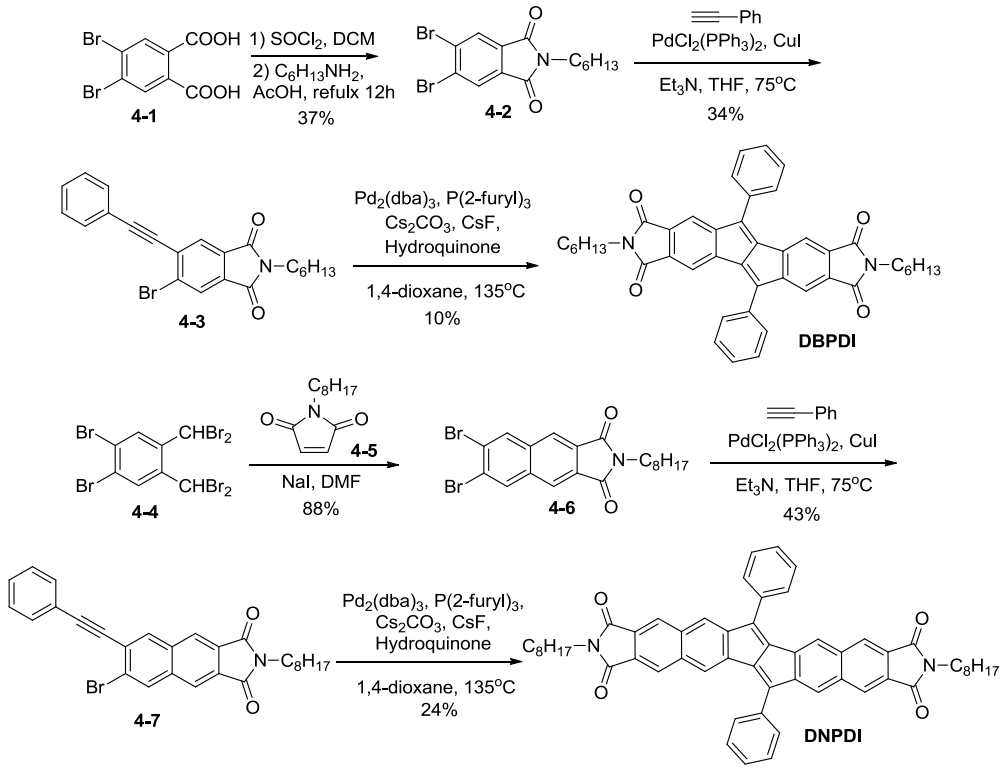

Scheme 4.1 Synthetic routes of **DBPDI** and **DNPDI**.

DNPDI was prepared by starting from 1,2-dibromo-4,5-bis(dibromomethyl)-benzene **4-4**[5] and 1-octyl-1H-pyrrole-2,5-dione **4-5** [6]. Compounds **4-4** and **4-5** underwent Diels-Alder addition reaction to obtain precursor **4-6** in 88% yield. It was followed by Sonogashira cross-coupling reaction between **4-6** and

phenylacetylene to give **4-7** in 43% yield, and then dimerization of **4-7** by using palladium catalyst produced **DNPDI** in 24% yield**.**

4.2.2 Photophysical properties

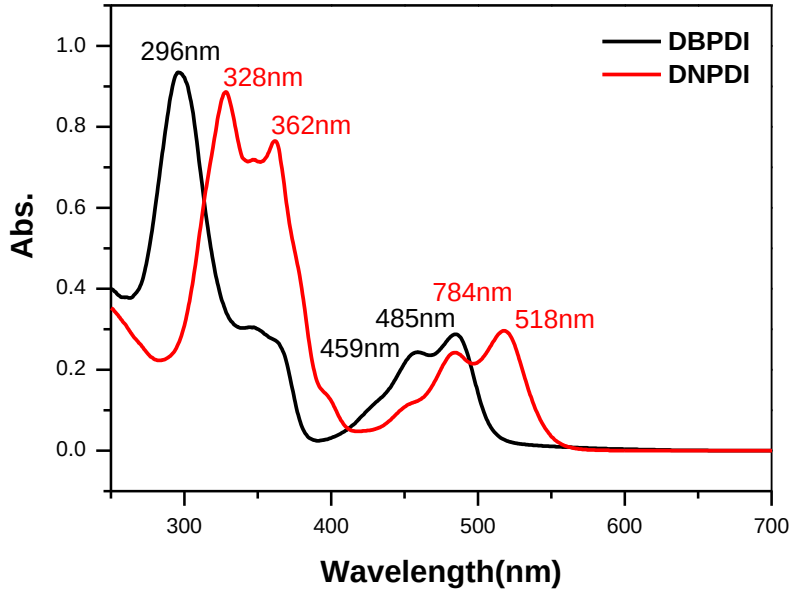

Figure 4.1 UV-vis absorption spectra of **DBPDI** and **DNPDI** in chloroform (10^{-5} M).

The UV-vis absorption spectra of **DBPDI** and **DNPDI** were measured in chloroform solution. The spectra are shown in Figure 4.1 and the relevant data are summarized in Table 4.1. Broad absorption bands located in the visible region were observed for the solutions of them. The maximum absorption wavelengths of **DBPDI** and **DNPDI** in chloroform solutions are located at 296 and 328 nm. The molar absorption coefficient is 93500 and 88600 M^{-1} cm^{-1} respectively. The optical energy band gap (E_g^{Opt}) of 2.42 and 2.25 eV can be calculated based on the lowest energy of absorption edge in solution (Table 4.1). Compared to **DBPDI**, the

absorption maximum of **DNPDI** in solution is red-shifted 32 nm. This may be due to its more planar conformation and longer efficient π-conjugation length.

Table 4.1 Summary of photophysical properties and electrochemical data of **DBPDI** and **DNPDI**

	λ_{max}(abs)[nm] in solution	logε_{max} [$M^{-1}cm^{-1}$]	$E_{1/2}^{ox}$ (V)	$E_{1/2}^{red}$ (V)	HOMO [eV]	LUMO [eV]	E_g^{Opt} [eV][a]
DBPDI	296	4.97	1.36	-1.46; -1.11	-5.84	-3.76	2.42
DNPDI	328	4.95	1.03	-1.71; -1.47	-5.72	-3.45	2.25

4.2.3 Electrochemical properties

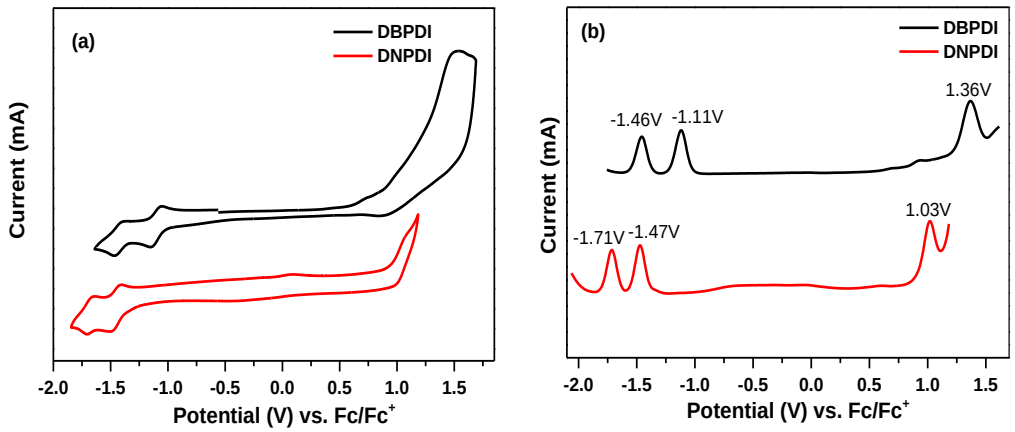

Figure 4.2 (a) Cyclic voltammograms (CV) and (b) Differential pulse voltammetry (DPV) of **DBPDI** and **DNPDI** in chlorobenzene with 0.1 M Bu_4NPF_6 as the supporting electrolyte, AgCl/Ag as reference electrode, Au as working electrode, Pt wire as counter electrode, and a scan rate at 50 mV s^{-1}.

Cyclic voltommetry (CV) and differential pulse voltammetry (DPV) were used to study the electrochemical properties of target molecules **DBPDI** and **DNPDI** (Figure 4.2, Table 4.1). The potential was externally calibrated against the ferrocene/ferrocenium couple. The target molecule **DBPDI** show one reversible oxidation with half-wave potent $E_{1/2}^{ox}$ of 1.36 V and two reversible

reduction wave with half-wave potential $E_{1/2}^{red}$ at -1.46 and -1.11 V. While one reversible oxidation waves with $E_{1/2}^{ox}$ at 1.03V, and two reversible reduction waves with $E_{1/2}^{red}$ at -1.71 and -1.47 V were observed for molecule **DNPDI**. The HOMO and LUMO energy levels were calculated using the following equations: HOMO = - [E_{ox}^{onset} + 4.8] eV, LUMO = - [E_{red}^{onset} + 4.8] eV where E_{ox}^{onset} and E_{red}^{onset} are the onset of the first oxidation and reduction wave, respectively. The HOMO/LUMO energy levels are calculated to be -5.84/-3.76, and -5.72/-3.45 eV for **DBPDI** and **DNPDI**, respectively. The corresponding electrochemical energy gaps E_g^{EC} (LUMO-HOMO) are estimated to be 2.08 and 2.27 for **DBPDI** and **DNPDI**, which are close to the optical band gaps E_g^{opt}.

4.2.4 Thermal properties

The thermal stability is one of the key requirements for the practical applications of organic electronic materials. Compounds **DBPDI** and **DNPDI** showed good thermal stability with decomposition temperatures (T_d, corresponding to a 5% weight loss in thermogravimetric analysis (TGA) curves) at 419 and 460 ^oC, respectively (Figure 4.3 a,c). The melting points of **DBPDI** and **DNPDI** were observed at 337 ^oC and 369 ^oC, respectively, from differential scanning calorimetry (DSC) curves (Figure 4.3 b,d).

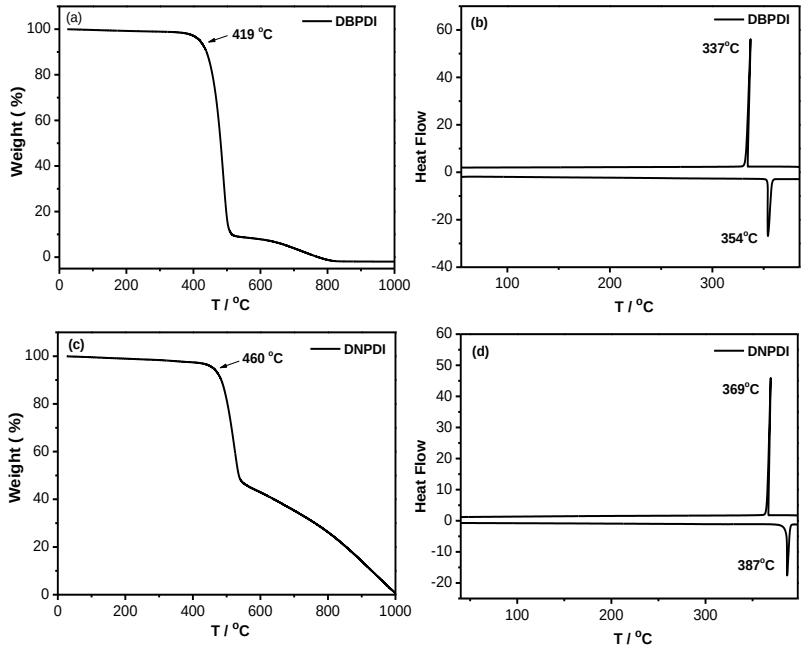

Figure 4.3 Thermogravimetric analysis (TGA) of compounds **DBPDI** (a) and **DNPDI** (c); Differential scanning calorimetry (DSC) of compounds **DBPDI** (b) and **DNPDI** (d) in N_2 at a heating rate of 10 $^oC\ min^{-1}$

4.2.5 Thin-film field effect transistors

To probe the charge transport properties of compounds **DBPDI** and **DNPDI**, we have fabricated the field effect transistors (FETs) for both compounds **DBPDI** and **DNPDI** by solution processing method. The bottom-gate top-contact FETs were fabricated on p+-Si/SiO_2 substrates by spin coating 1wt% chloroform ($CHCl_3$) solutions onto octyltrichlorosilane (OTS) or hexamethyldisilazane (HMDS) treated substrates. The thin films were then annealed at selected temperatures for 20 min in N_2. Au source/drain electrodes (80 nm) were patterned on the organic layer through a shadow mask to afford the devices. The typical transfer and output curves measured in N_2 are shown in Figure 4.4. The OFET device data for the thin films of **DBPDI** and **DNPDI** on different substrates measured under nitrogen are summarized in Table 4.2.

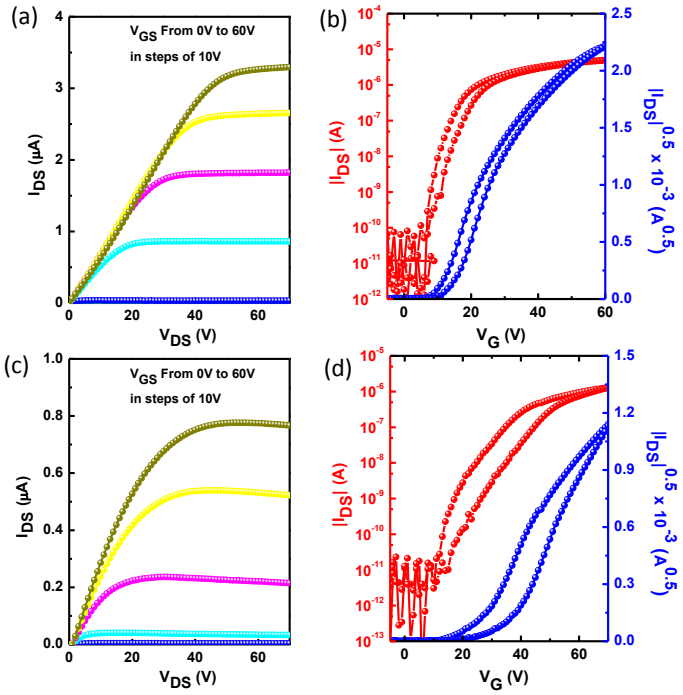

Figure 4.4 Output and transfer characteristics of the thin films **DBPDI** (a, b) and **DNPDI** (c, d) spin coated on OTS modified substrates.

Table 4.2 OFET characteristics of **DBPDI** and **DNPDI** based devices fabricated on Si/SiO_2 substrates with different surface treatments and different annealing temperatures.

	Surface treatment	**Annealing Temp**	**μ[$cm^2V^{-1}s^{-1}$]**	**V_T [V]**	**On/off**
DBPDI	HMDS	XA	0.003	2-4	9.6×10^5
	HMDS	A120	0.0046	2-4	7.8×10^5
	OTS-C8	XA	0.05	7-10	2.6×10^6
	OTS-C8	A120	0.06	5-8	2.9×10^6
DNPDI	HMDS	XA	4.7×10^{-3}	28-30	3.2×10^6
	HMDS	A120	8.6×10^{-3}(0.011)	24-26	2.0×10^6
	HMDS	A160	6.8×10^{-3}	23-25	2.1×10^5
	OTS-C8	XA	0.025	16-18	1.7×10^6
	OTS-C8	A120	0.034	15-17	1.1×10^6

Both compounds showed n-type FET behavior. For compound **DBPDI**, the devices revealed an average electron mobility of 0.0046 $cm^2V^{-1}s^{-1}$ (I_{on}/I_{off} =

10^6) and 0.06 $cm^2V^{-1}s^{-1}$ (I_{on}/I_{off} = 10^6) for HMDS and OTS treated substrates, respectively. The device based on **DNPDI** displayed an average saturation mobility of 0.011 $cm^2V^{-1}s^{-1}$ (I_{on}/I_{off} = 10^6) and 0.034 $cm^2V^{-1}s^{-1}$ (I_{on}/I_{off} = 10^6) for HMDS and OTS treated substrates, respectively. As far as we know, this series compounds should be first kinds of n-type pentalene based derivatives.

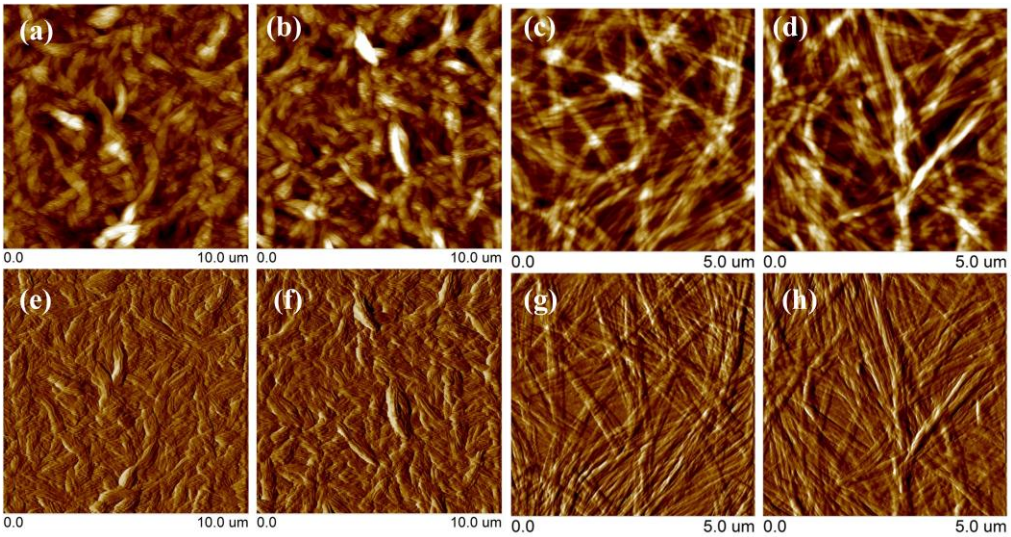

Figure 4.5 The AFM images of the thin film spin coated from $CHCl_3$ solution onto OTS: **DIDBP** (a: before annealing; b: annealing at 120 ^oC) and **DIDNP** (c: before annealing; d: annealing at 120 ^oC); (e-h) are the corresponding phase images.

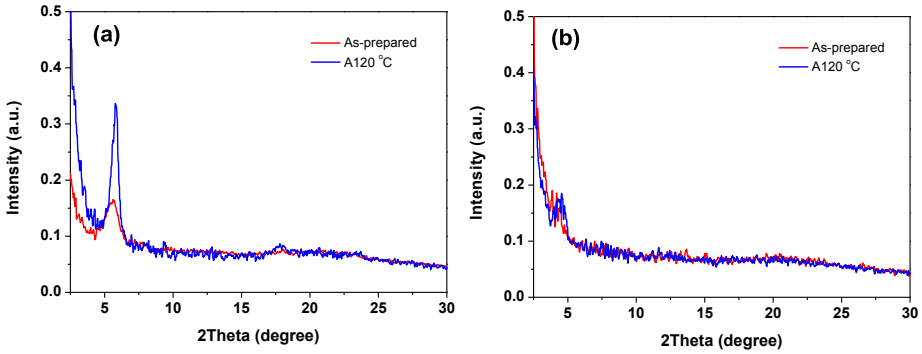

Figure 4.6 XRD patterns of DIDBP (a) and DIDNP (b) thin films on OTS-modified substrates.

Thin film morphology and solid state microstructure were characterized by tapping-mode atomic force microscopy and 2D X-ray diffraction. The thin film exhibited plate-like crystals for **DIDBP** and large needle-like crystals for

DIDNP (Figure 4.5). The XRD measurements of the thin films on OTS treated substrates exhibited the primary peak at $2\theta = 5.8^{o}$ and 4.5^{o}, which corresponds to a d-spacing of 15.2 Å and 19.6 Å for **DIDBP** and **DIDNP**, respectively (Figure 4.6). A lamellar packing structure was deduced from the diffraction peaks. The more dense layer-like packing structure of **DIDBP** in the thin films allows effective charge transport between the source and drain electrodes.

4.3 Summary

In this chapter, two new *N, N*'-dihexyl-dibenzopentalene dicarboximide (**DBPDI**) and *N, N*'-dioctyl-dibenzopentalene dicarboximide (**DNPDI**) have been successfully synthesized as new π-conjugated organic semiconducting materials for organic field effect transistors (OFETs). Both of them are soluble in organic solvent and show good thermal stability. The thin film transistor test indicated that the molecules **DBPDI** and **DNPDI** are both n-type semiconductors. The **DBPDI** displayed the average electron mobility up to 0.06 $cm^2V^{-1}s^{-1}$ and I_{on}/I_{off} ratio of 1.0×10^6 without optimization, which is the first n-type organic semiconductor based on pentalene unit. More effort will be carried out for the optimization of the OFET devices in future.

4.4 Experiment section

4.4.1 General characterization method

All reagents were purchased from commercial sources and used without further purification. ^1H and ^{13}C NMR spectra were recorded using an Advance

500 MHz Bruker spectrometer in $CDCl_3$ with tetramethylsilane (TMS) as the internal standard. The chemical shift was recorded in ppm and the following abbreviations are used to explain the multiplicities: s = singlet, d = doublet, t = triplet, m = multiplet, br = broad. Column chromatography was performed on silica gel 60 (Merck 40–60 nm, 230–400 mesh). EI mass spectra were recorded on an Agilent 5975 C DIP/MS mass spectrometer. UV-vis absorption was recorded on a Shimadzu UV-1700 spectrophotometer. Cyclic voltammetry and differential pulse voltammetry measurements were performed in HPLC grade chlorobenzene on a CHI 620C electrochemical analyzer with a three-electrode cell, using 0.1 M Bu_4NPF_6 as the supporting electrolyte, AgCl/Ag as the reference electrode, a gold disk as the working electrode, Pt wire as the counter electrode, and at a scan rate of 50 mV s^{-1}. The potential was externally calibrated against the ferrocene/ferrocenium couple. Differential scanning calorimetry (DSC) was performed on a TA instrument 2920 at a heating/cooling rate of 10^{o}C min^{-1} under nitrogen flow. Anhydrous dichloromethane (DCM) and N,N-dimethylformaldehyde (DMF) were distilled from CaH_2. Anhydrous acetic acid was distilled form acetic anhydride. THF were distilled from sodium benzophenone immediately prior to use.

4.4.2 Synthesis

All reagents were purchased from commercial sources without further purification. Anhydrous dichloromethane (DCM), *N, N*-dimethylformaldehyde (DMF) was distilled from CaH_2. Toluene and THF were distilled from

sodium-benzophenone immediately prior to use.

Compound **4-2 5,6-dibromo-2-hexylisoindoline-1,3-dione**

A mixture of **4-1** (4.0 g, 12.35 mmol) and thionyl chloride (6 mL) in 30 mL dry dichloromethane was stirred overnight at reflux temperature under argon atmosphere. After removing excessive thionyl chloride and solvent, the yellowish solid was directly dissolved in 30 mL dry acetic acid and engaged in next reaction. The hexyl amine (1.3 g, 13.58 mmol) was slowly added and the mixture was heated to 135^{o}C overnight under argon. The mixture was cooled to room temperature and extracted with EtAc (50 mL ×2). The combined organic phase was washed with brine (100 mL ×2) and saturated $NaHCO_3$ (100 mL) and dried over anhydrous Na_2SO_4. The organic solvent was removed under reduced pressure and the residue was purified by column chromatography (silica gel, DCM/Hexane= 1:5) to afford compound **4-2** (1.75 g) in 37% yield. ^{1}HNMR (500MZ, $CDCl_3$, ppm) δ = 8.07 (s, 2H), 3.66 (t, *J* = 7.0 Hz, 2H), 1.33-1.25 (m, 8H), 0.87 (t, *J* = 7.0 Hz, 3H). ^{13}C NMR ($CDCl_3$, 125 MHz): δ = 166.47, 131.87, 131.23, 128.33, 38.52, 31.28, 28.37, 26.46, 22.47, 13.95. HR MS (EI): calcd for $C_{14}H_{15}Br_2NO_2$ (M^+), 386.9470; found, 386.9458 (error: -3.10 ppm).

Compound **4-3 5-bromo-2-hexyl-6-(phenylethynyl)isoindoline-1,3-dione**

A suspension of $Pd(PPh_3)_2Cl_2$ (135 mg, 5 mol%), CuI (36 mg, 5 mol%) and **4-2** (1.50 g, 3.88 mmol) were purged with argon. Dissolving the mixture with 20 mL of tetrahydrofuran (THF) and 20 mL of triethylamine (Et_3N), the

phenyl acetylene (0.435 g, 4.26 mmol) was slowly added to solution then the mixture was stirred at 75^{o}C overnight. After cooling down to room temperature, the mixture was poured into EtOAc (100 mL) and washed with 10% hydrochloride solution (60 mL × 2). The organic layer was dried on Na_2SO_4 and concentrated under vacuum. Finally, the residue was purified by column chromatography (silica gel, DCM/Hexane = 1:10) to give compound **4-3** (530 mg) in 34% yield. ^{1}HNMR (500MZ, $CDCl_3$, ppm) δ = 8.07 (s, 1H), 7.97 (s, 1H), 7.62-7.60 (m, 2H), 7.45-7.38 (m, 3H), 3.67 (t, *J* = 7.0 Hz, 2H), 1.34-1.29 (m, 8H), 0.88 (t, *J* = 7.0 Hz, 3H). ^{13}C NMR ($CDCl_3$, 125 MHz): δ = 167.15, 166.69, 131.96, 131.63, 131.29, 131.07, 130.82, 129.57, 128.56, 127.34, 127.26, 121.92, 98.70, 87.20, 38.45, 31.31, 28.44, 26.49, 22.49, 13.97. HR MS (EI): calcd for $C_{22}H_{20}BrNO_2$ (M^+), 409.0677; found, 409.0669 (error: -1.96 ppm).

Compound **DBPDI**

A reaction flask was charged with hydroquinone (0.113 g, 1.20 mmol), Cs_2CO_3 (0.334 g, 1.02 mmol), CsF (0.171 g, 1.13 mmol), P(2-furyl)$_3$ (15 mg, 0.08 mmol), and $Pd_2(dba)_3$ (15 mg, 0.02 mmol) and purged with argon. A solution of **4-3** (0.200 g, 0.50 mmol) in 1,4-dioxane (15 mL) was injected into the catalyst mixture with a syringe. The suspension was immediately heated to 135^{o}C. After heating for 24 h the reaction mixture was diluted with $CHCl_3$ (25 mL), filtered through celite, and then concentrated to yield raw solid. After purification via column chromatography (silica gel, DCM/Hexane = 1:4), the

product was dissolved in $CHCl_3$, precipitated in methanol/acetone = 3:2 and filtered. This procedure was repeated for 3 times to give the purer product **DBPDI** (12 mg) in 10% yield for characterization. ^{1}HNMR (500MZ, $CDCl_3$, ppm) δ = 7.64-7.57 (m, 10H), 7.56 (s, 2H), 7.49 (s, 2H), 3.61 (t, *J* = 7.0 Hz, 4H), 1.29-1.25 (m, 16H), 0.86 (t, *J* = 7.0 Hz, 6H). ^{13}C NMR ($CDCl_3$, 125 MHz): δ = 168.17, 168.05, 154.70, 143.98, 143.44, 140.43, 132.51, 132.45, 131.77, 130.42, 129.47, 128.31, 117.70, 116.41, 38.11, 31.34, 28.50, 26.46, 22.48, 13.98. HR MS (EI): calcd for $C_{44}H_{40}N_2O_4$ (M^+), 660.2988; found, 660.2994 (error: 0.91 ppm).

Compound **4-6 6,7-dibromo-2-octyl-1H-benzo[f]isoindole-1,3(2H)-dione**

NaI (1.55 g, 10.5 mmol) was added with stirring to a solution of **4-4** (1.20 g, 2.1 mmol) and N-octylmaleimide **4-5** (0.50 g, 2.39 mmol) in N,N-dimethylacetamide (20 mL). The mixture was heated at 80^{o}C for 12h. The product was collected from the dark solution by filtration, and washed with water and boiling dioxane to provide compound **4-6** (0.85 g) in 88%yield. ^{1}HNMR (500MZ, $CDCl_3$, ppm) δ = 8.33 (s, 2H), 8.20 (s, 2H), 3.74 (t, *J* = 7.0 Hz, 2H), 1.72-1.69 (m, 2H), 1.37-1.25 (m, 10H), 0.87 (t, *J* = 7.0 Hz, 3H). ^{13}C NMR ($CDCl_3$, 125 MHz): δ=167.37, 134.79, 134.18, 129.12, 126.15, 123.27, 38.55, 31.75, 29.13, 28.48, 26.90, 22.60, 14.04. HR MS (EI): calcd for $C_{20}H_{21}Br_2NO_2$ (M^+), 464.9939; found, 464.9951 (error: 2.58 ppm).

Compound **4-7 6-bromo-2-octyl-7-(phenylethynyl)-1H-benzo[f]isoindole-1,3(2H)-dione**

A suspension of $Pd(PPh_3)_2Cl_2$ (65 mg, 5 mol%), CuI (15 mg, 5 mol%) and **4**-**6** (850 mg , 1.8 mmol) were purged with argon. Dissolving the mixture with 15 mL tetrahydrofuran (THF) and 15 mL triethylamine (Et_3N), the phenyl acetylene (180 mg, 1.8 mmol) was slowly added to solution then the mixture was stirred at 75^oC overnight. After cooling down to room temperature, the mixture was poured into EtOAc (100 mL) and extracted with diluted hydrochloride (60 mL ×3). The organic layer was dried on Na_2SO_4 and concentrated under vacuum. Finally, the residue was purified by column chromatography (silica gel, DCM/Hexane = 1:10) to give compound **4**-**7** (380 mg) in 43% yield. ^{1}HNMR (500MZ, $CDCl_3$, ppm) δ = 8.31 (s, 1H), 8.25 (s, 1H), 8.23 (s, 1H), 8.20 (s, 1H), 7.65-7.63 (m, 2H), 7.42-7.40 (m, 3H), 3.74 (t, *J* = 7.0 Hz, 2H), 1.72-1.68 (m, 2H), 1.35-1.26 (m, 10H), 0.88 (t, *J* = 7.0 Hz, 3H). ^{13}C NMR ($CDCl_3$, 125 MHz): δ = 167.58, 167.49, 135.25, 134.28, 133.78, 133.12, 131.88, 129.24, 129.22, 128.82, 128.52, 126.37, 125.95, 123.94, 123.19, 122.30, 96.38, 87.42, 38.49, 31.75, 29.14, 28.50, 26.91, 22.60, 14.05. HR MS (EI): calcd for $C_{28}H_{26}BrNO_2$ (M^+), 487.1147; found, 487.1136 (error: -2.26 ppm).

Compound **DNPDI**

A reaction flask was charged with hydroquinone (0.172 g, 1.83 mmol), Cs_2CO_3 (0.508 g, 1.55 mmol), CsF (0.260 g, 1.72 mmol), P(2-furyl)$_3$ (23 mg, 0.12 mmol), and $Pd_2(dba)_3$ (23 mg, 0.026 mmol) and purged with argon. A solution of **4**-**7** (0.372 g, 0.76 mmol) in 1,4-dioxane (20 mL) was injected into

the catalyst mixture with a syringe. The suspension was immediately heated to 135^{o}C. After heating for 24 h the reaction mixture was diluted with toluene (50 mL), filtered through celite, and then concentrated under the vacuum to yield raw solid. After purification via column chromatography (silica gel, DCM/Hexane = 1:4), the product was dissolved in $CHCl_3$, precipitated in methanol/acetone = 3:2 and filtered. This procedure was repeated for 3 times to give the purer product **DNPDI** (75 mg) in 24% yield for characterization. ^{1}HNMR (500MZ, $CDCl_3$, ppm) δ=8.07 (s, 2H), 8.03 (s, 2H), 7.95 (s, 2H), 7.82 (d, *J* = 7.0 Hz, 4H), 7.72 (s, 2H), 7.69 (t, *J* = 7.0 Hz, 4H), 7.63 (t, *J* = 7.0 Hz, 2H), 3.70 (t, *J* = 7.0 Hz, 4H), 1.73-1.68 (m, 4H), 1.48-1.25 (m, 20H), 0.89 (t, *J* = 7.0 Hz, 6H). ^{13}C NMR ($CDCl_3$, 125 MHz): δ = 167.85, 150.29, 144.83, 139.78, 136.67, 136.01, 134.77, 133.19, 129.80, 129.34, 129.03, 128.72, 124.86, 124.70, 123.45, 123.33, 38.41, 31.80, 29.17, 29.15, 28.58, 27.00, 22.59, 13.93. HR MS (EI): calcd for $C_{56}H_{52}N_2O_4$ (M^+), 816.3927; found, 816.3908 (error: -2.33 ppm).

Reference

[1] Shukla, D.; Nelson, S. F.; Freeman, D. C.; Rajeswaran, M.; Ahearn, W. G.; Meyer, D. M.; Carey, J. T. *Chem. Mater.* **2008**, 20, 7486.

[2] Chesterfield, R. J.; Mckeen, J. C.; Newman, C. R.; Ewbank, P. C.; Filho, S.; Bre, J.; Miller, L. L.; Mann, K. R.; Frisbie, C. D. *J. Phys. Chem. B* **2004**, 108, 19281.

[3] Chang, J.; Qu, H.; Ooi, Z.-E.; Zhang, J.; Chen, Z.; Wu, J.; Chi, C. *J. Mater. Chem. C* **2013**, 1, 456.

[4] Dai, G.; Chang, J.; Wu, J.; Chi, C. *J. Mater. Chem.* **2012**, 22, 21201.

[5] Usta, H.; Kim, C.; Wang, Z.; Lu, S.; Huang, H.; Facchetti, A.; Marks, T. J. *J. Mater. Chem.* **2012**, 22, 4459.

[6] Uchoa, A. F.; Oliveira, K. T. De; Baptista, M. S.; Bortoluzzi, A. J.; Iamamoto, Y.; Serra, O. A. J. Org. Chem. **2011**, 76, 8824.

Chapter 5: Soluble and Stable Z-Shaped Pentaleno-diacenes

5.1 Introduction

In Chapter 1, we have known that chemists have developed several useful methodologies for pentalene ring formation, and several uncomplicated pentalene derivatives have been reported for organic electronic materials. In chapters 2 - 4, we have also synthesized some p-type and n-type pentalene containing molecules for OFET applications. In above three chapters, all the target molecules are linear structures, e.g. pentalene ring internally fused with one end of acenes or thienoacenes. Dibenzopentalenes, as a series of classical internally fused systems, show promise for functionalization and posses good stability and relatively low band gaps due to weak intramolecular charge transfer character.[1] However, previous studies of the electron acceptor behavior of cyclopenta-fused polycyclic aromatic hydrocarbons (CP-PAHs) have shown that externally fused CP-PAHs (five membered rings fused on zig-zag edges of PAH) are often more capable electron acceptors than their internally fused counterparts[2], such as rubicenes and indenofluorenes. Therefore, it is great interest for us to prepare pentaleno-diacenes with pentalene unit fused on the zig-zag edges of acenes, which may show lower band gap due to the enhanced intramolecular charge transfer character. Up to now, the synthetic method for pentalene ring which is externally fused acenes has not been reported. In this chapter, we designed suitable dibenzopentalenes

as the starting materials to build up the expected pentaleno-diacenes. Their synthesis, characterization and properties have been studied.

5.2 Results and discussion

5.2.1 Synthesis

The synthesis of pentaleno-dianthracene derivatives **5-1** is outlined in Scheme 5.1. The methyl 2-((2-bromophenyl)ethynyl)benzoate **5-7**,[3] methyl 3-(((trifluoromethyl)sulfonyl)oxy)-2-naphthoate **5-13**[4] and 2,3-dibromo-9,10-dihydro-9,10-epoxyanthracene **5-22**[5] were prepared by reported literature procedures. The Sonogashira coupling reaction between compound **5-4** and 2-methylbut-3-yn-2-ol provided the compound **5-5** in 66% yield. It is followed by deprotrction with KOH to give compound **5-6** in 65% yield. The Sonogashira reaction between compound **5-6** and methyl 2-iodobenzoate gave the monomer **5-7** in 95% yield. Then $Pd_2(dba)_3$ catalyzed dimerization reaction of **5-7** provided the dibenzopentalene **5-8** in 8% yield. The di-ester **5-8** was hydrolyzed by LiOH to form diacid **5-9** in 90% yield. Thionyl chloride was used to treat **5-9** to give acyl chloride, it followed by intramolecular Friedel–Crafts reaction to obtain the di-ketone **5-10** in 30% yield. Lithium reagent of triisopropylsilyl acetylene was used to attack the di-ketone **5-10** to provide the di-ol, which was treated with $SnCl_2$ to obtain the target molecule **5-1** in 38% yield.

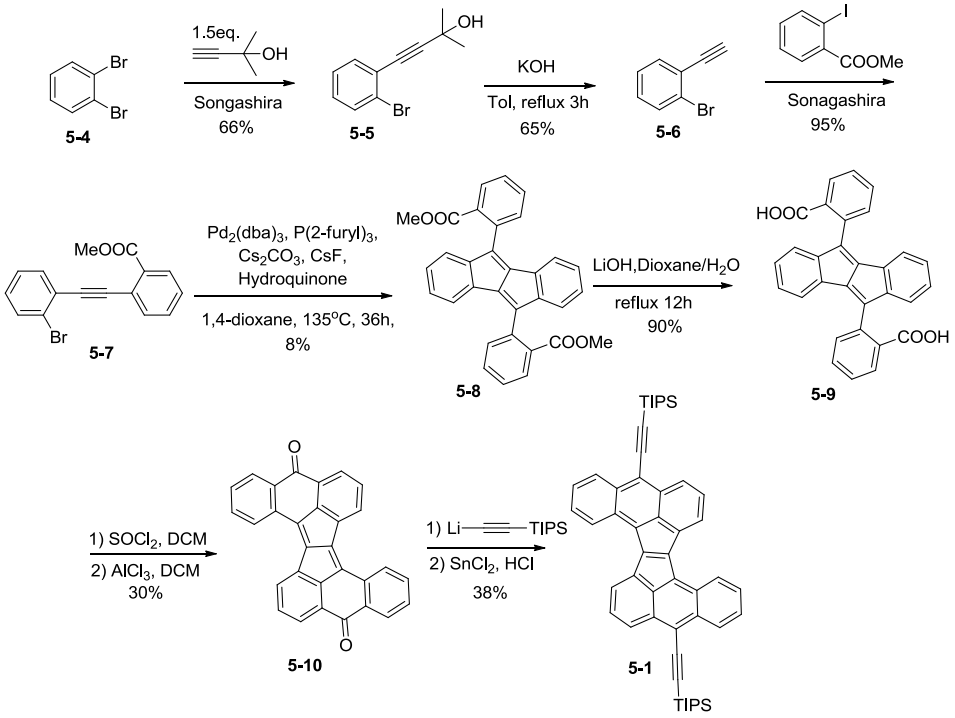

Scheme 5.1 Synthetic route of pentaleno-dianthracene **5-1**

The synthesis of pentaleno-ditetracene derivatives **5-2** is outlined in Scheme 5.2. Esterification of compound **5-11** and subsequent introduction the trifluoromethanesulfonate (OTf) group provided the compound **5-13** in total 72% yield. The Sonogashira reaction between compound **5-6** and compound **5-13** gave the **5-14** in 95% yield. Then similar $Pd_2(dba)_3$ catalyzed dimerization reaction was conducted to form the dibenzopentalene **5-15** in 15% yield. It was followed by similar hydrolysis by LiOH and intramolecular Friedel–Crafts reaction to give di-ketone **5-17** in 95% and 30% yield, respectively. Lithium reagent was used to attack the di-ketone **5-17** to provide the di-ol, which was treated with $SnCl_2$ to obtain the target molecule **5-2a** in 20% yield and **5-2b** in 60% yield. Compound **5-2a** has poor solubility in

common organic solvents, so ethynyl triisobutylsilane was introduced to improve the solubility of pentaleno-ditetracene. In the following part, the characterization and physical property studies will be mainly focused on compound **5-2b**.

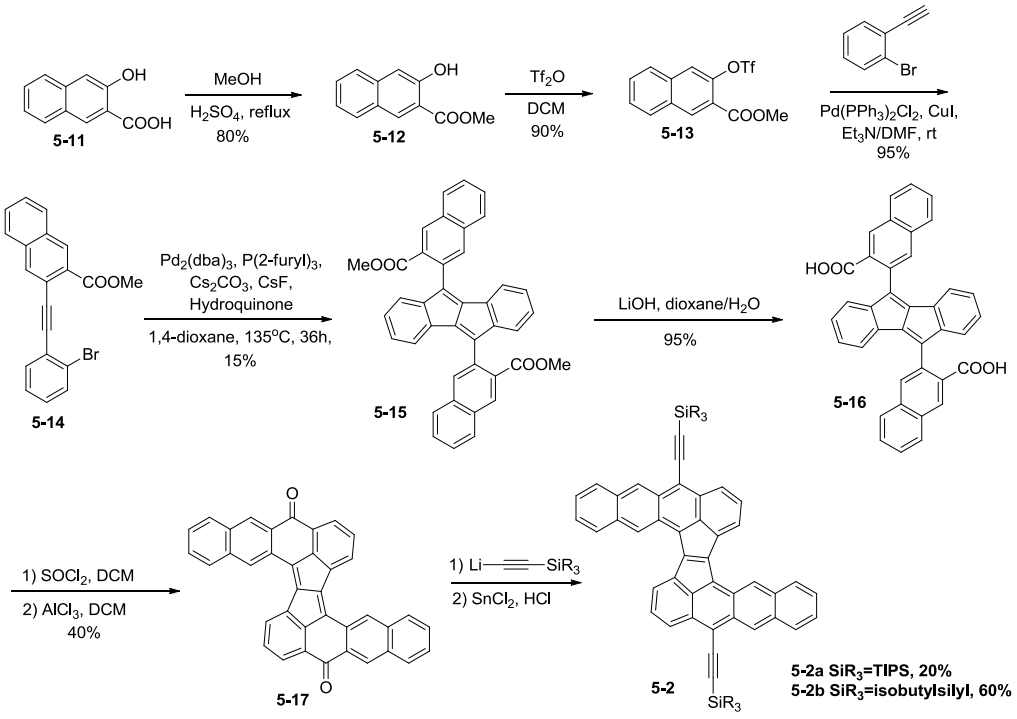

Scheme 5.2 Synthetic route of pentaleno-ditetracene **5-2**

The synthesis of pentaleno-dipentacene derivatives **5-3** is outlined in Scheme 5.3. 1-methoxy-1,3-dihydroisobenzofuran **5-21** was prepared from compound **5-18** by esterification, followed by aldolization, reduction by $LiAlH_4$ and rearrangement reactions in 77% total yield. It was then treated with *n*-butyl lithium to give the isobenzofuran, which underwent Diels-Alder addition with the in-situ generated dibromobenzyne from 1,2,4,5-tetrabromobenzene to give the compound **5-22** in 25% yield. The Sonogashira reaction between compound **5-22** and triisopropylsilyl acetylene

gave the compound **5-23** in 40% yield. Treatment of **5-23** with zinc and titanium tetrachloride produced compound **5-24** in 70% yield. Subsequent reaction with *n*-butyl lithium and quenched with ethyl cyanoformate gave the compound **5-25** in 65% yield. Removed of triisopropylsilyl (TIPS) group in **5-25** was conducted by using tetra-*n*-butylammonium fluoride (TBAF) to give **5-26** in 85% yield. The Sonogashira reaction between compound **5-2****6** and 2-bromo-iodobenzene formed **5-27** in 85% yield. Similar $Pd_2(dba)_3$ catalyzed dimerization of **5-27** was done to provide the dibenzopentalene **5-28** in 10% yield. It was followed hydrolysis with NaOH and intramolecular Friedel–Crafts reaction to give di-ketone **5-30** in 90% and 80% yield, respectively. Subsequent reaction between **5-30** and lithium reagent and Grignard reagent did not produce the expected di-ol, but some complicated products. The reaction conditions and synthetic routes need to be modified, and the synthesis of pentaleno-dipentacene is still underway in our lab.

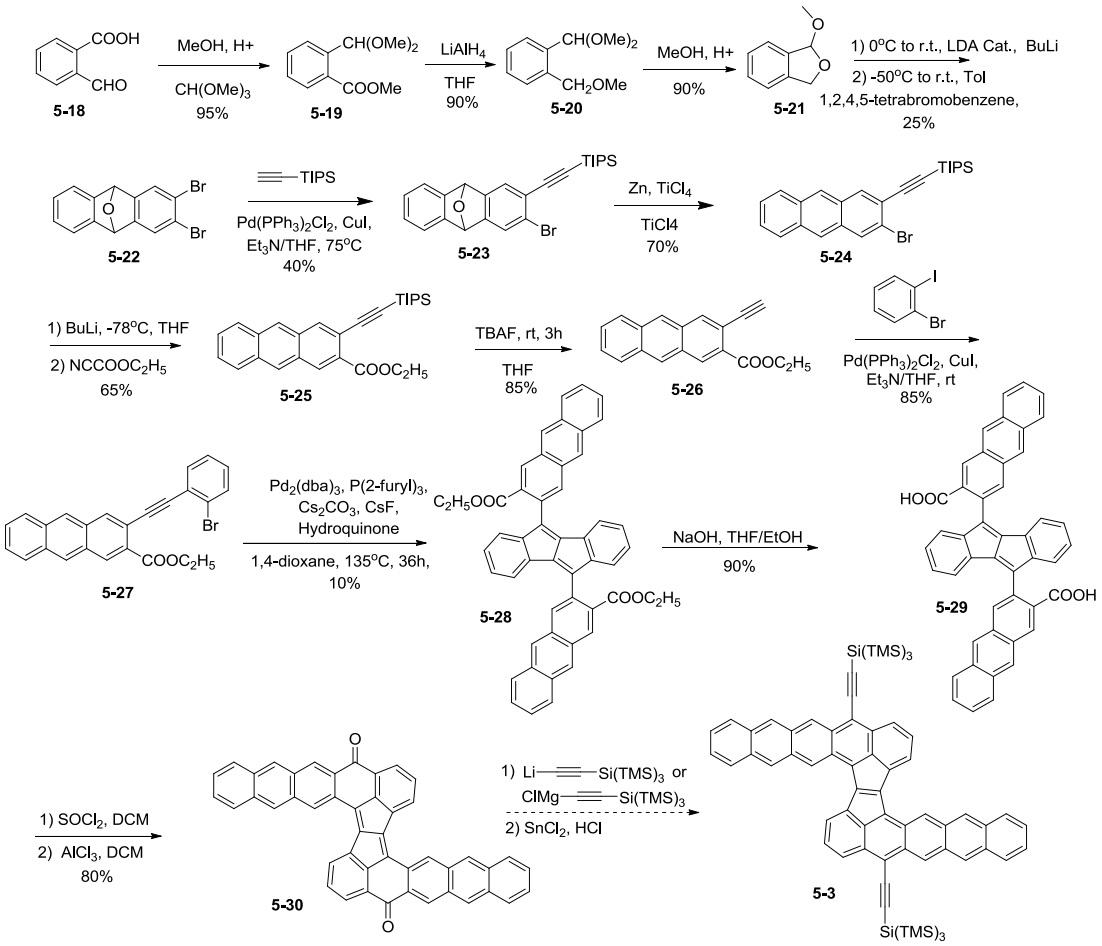

Scheme 5.3 Synthetic route of pentaleno-dipentacene **5-3**

5.2.2 Photophysical properties

The UV-vis absorption spectra of **5-1** and **5-2b** were measured in chloroform solution (Figure 5.1). The absorption maxima for **5-1** and **5-2** in solutions are located at 252 and 285 nm, respectively. With extension of acene length, this absorption band shows obvious red-shift by 32 nm. A longer-wavelength shoulder with maxima at 567 and 665 nm was observed for **5-1** and **5-2b**, respectively. In addition, a broad band in range of 600-850 nm for **5-1** and 700-1050 nm for **5-2** was seen clearly, which is due to intramolecular charge transfer character. The wavelength of absorption maximum is red shift about 200nm. The optic energy band gaps

derived from the onset of absorption edge are 1.09 and 0.94 eV for compound **5-1** and **5-2b**, respectively. No fluorescence was observed in the detectable region for all compounds.

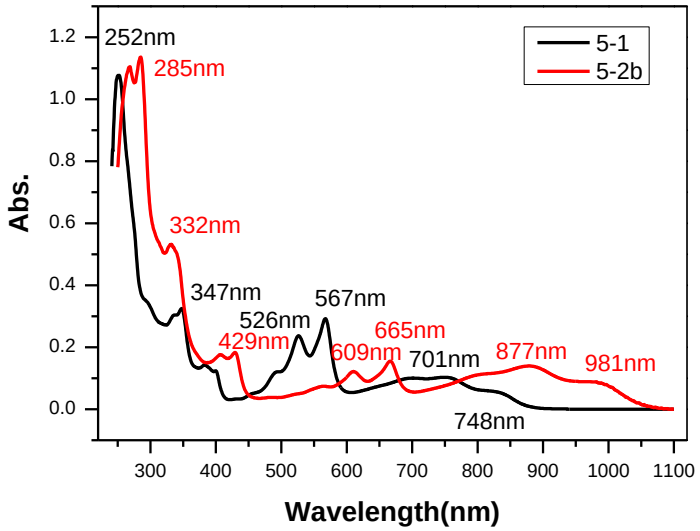

Figure 5.1 UV-vis absorption spectra of **5-1** and **5-2b** in chloroform (10^{-5} M)

5.2.3 Electrochemical properties

Cyclic voltommetry (CV) and differential pulse voltammetry (DPV) were used to study the electrochemical properties of compounds **5-1** - **5-2b** (Figure 5.2, Table 5.1). The potential was externally calibrated against the ferrocene/ferrocenium couple. Three quasi-reversible oxidation waves with half-wave potential $E_{1/2}^{ox}$ at 0.22, 0.44 and 1.00 V and two reversible reduction waves with half-wave potential $E_{1/2}^{red}$ at -1.27 and -1.78 V were observed for **5-1**. Compound **5-2b** showed three quasi-reversible oxidation waves with $E_{1/2}^{ox}$ at 0.01, 0.29 and 0.67 V, and two reversible reduction waves with $E_{1/2}^{red}$ at -1.13 and -1.61 V. The HOMO and LUMO energy levels were calculated using the following equations: HOMO = - [E_{ox}^{onset} + 4.8] eV,

LUMO = - [E_{red}^{onset} + 4.8] eV, where E_{ox}^{onset} and E_{red}^{onset} are the onset of the first oxidation and reduction wave, respectively. The HOMO/LUMO energy levels are determined to be -4.95/-3.62 and -4.69/-3.75 eV for **5-1**and **5-2**, respectively. The corresponding electrochemical energy gaps E_g^{EC} (LUMO-HOMO) are then estimated to be 1.33 eV and 0.94 eV for **5-1**and **5-2**. They are consistent with their optical energy band gaps.

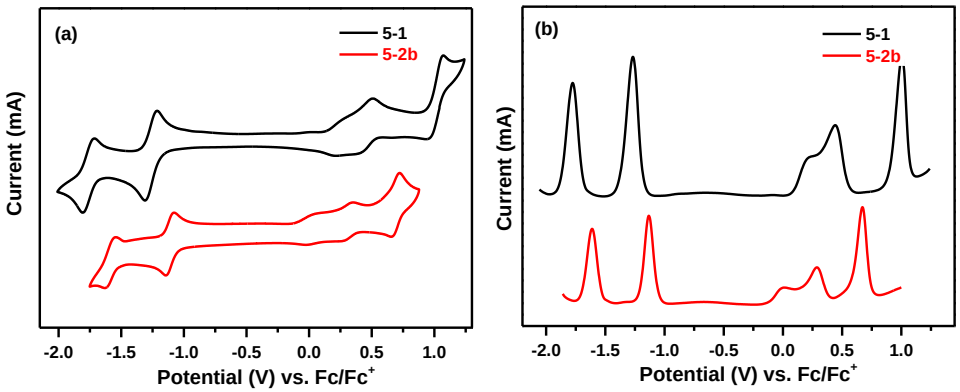

Figure 5.2 (a) Cyclic voltammograms (CV) and (b) differential pulse voltammetry (DPV) of compounds **5-1** and **5-2b** in dry dichloromethane with 0.1 M Bu_4NPF_6 as the supporting electrolyte, AgCl/Ag as reference electrode, Au as working electrode, Pt wire as counter electrode, and a scan rate at 50 mV s^{-1}

Table 5.1 Summary of electrochemical data of compounds **5-1** and **5-2b**

	$E_{1/2}^{ox}$ (V)	$E_{1/2}^{red}$ (V)	HOMO [eV]	LUMO [eV]	E_g^{EC} [eV]	E_g^{Opt} [eV]
5-1	0.22, 0.44, 1.00	-1.27, -1.78	-4.95	-3.62	1.33	1.09
5-2b	0.01, 0.29, 0.67	-1.13, -1.61	-4.69	-3.75	0.94	0.94

5.2.4 DFT calculations

Density functional theory (DFT, B3LYP/6-31G*) calculations were conducted to better understand the electronic and optical properties of these Z-shaped pentaleno-diacenes. The calculated frontier molecular orbital profiles are shown in Figure 5.3.

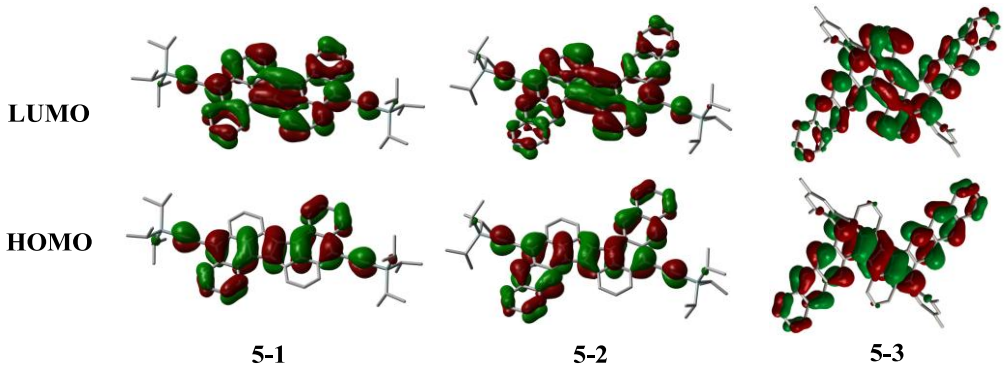

Figure 5.3 LUMO and HOMO profiles of **5-1**- **5-3**.

It was found that the HOMOs of both molecules are delocalized along the Z type framework while the LUMOs are mainly localized at the central pentalene unit. Time-dependent (TD) DFT calculations predicted that both two compounds should show three major absorption bands. The observed strongest absorption band is mainly contributed by HOMO→LUMO+5 transition of **5-1** (282.0 nm, *f* = 0.3952) and HOMO→LUMO+6 transition of **5-2** (309.7 nm, *f* = 0.3563). Their shoulder band around 500-600 nm for **5-1** and 600-700 nm for **5-2** can be correlated to the HOMO-1→LUMO transition (567.8 nm, *f* = 0.4741 for **5-1** based on DFT calculations) and HOMO-2→LUMO transition (655.7 nm, *f* = 0.2354 for **5-2** based on DFT calculations), respectively. Their longest broad band can be correlated to the transition of HOMO→LUMO (816.5 nm, *f* = 0.2354 for **5-1**; 1009.7 nm, *f* = 0.3197 for **5-2** based on DFT calculations).

5.2.5 Crystallographic analysis

Single crystals of **5-1** and **5-2b** suitable for X-ray crystallographic analysis were obtained by slow diffusion of methanol or acetonitrile into a THF

solution.[6] (CCDC 1055934 for **5-1** and CCDC 1055935 for **5-2b**) The molecular structures and the packing motif for **5-1** is shown in Figure 5.4. The 3D packing of **5-1** can be figured out in a monoclinic unit cell (space group P-1). There is no obvious π-π interactions between the pentaleno-dianthracene units. **5-1** adopts a column-like stacking structure (Figure 5.4 (b)), and in each column the molecules are packed in an alternating orthogonal arrangement. The molecular structures and the packing motif for **5-2b** is shown in Figure 5.5. The 3D packing of **5-2b** can be figured out in a triclinic unit cell (space group P-1). Compound **5-2b** exhibits very unique 1D slip-stack (D-A) column formation.

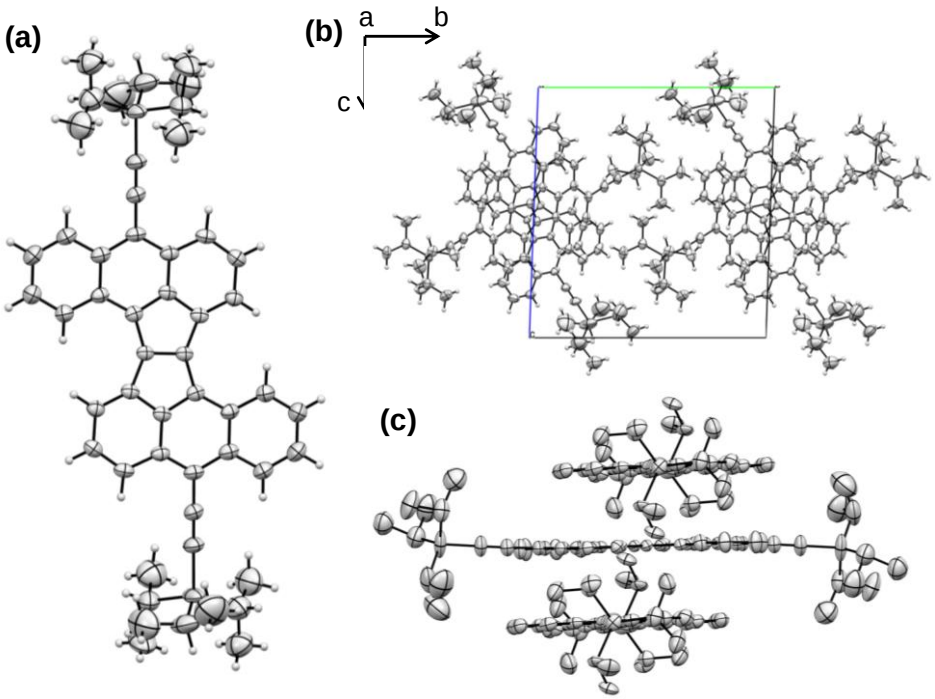

Figure 5.4 (a) ORTEP drawing of **5-1**; (b) packing along the a-axis; (c) packing column side view.

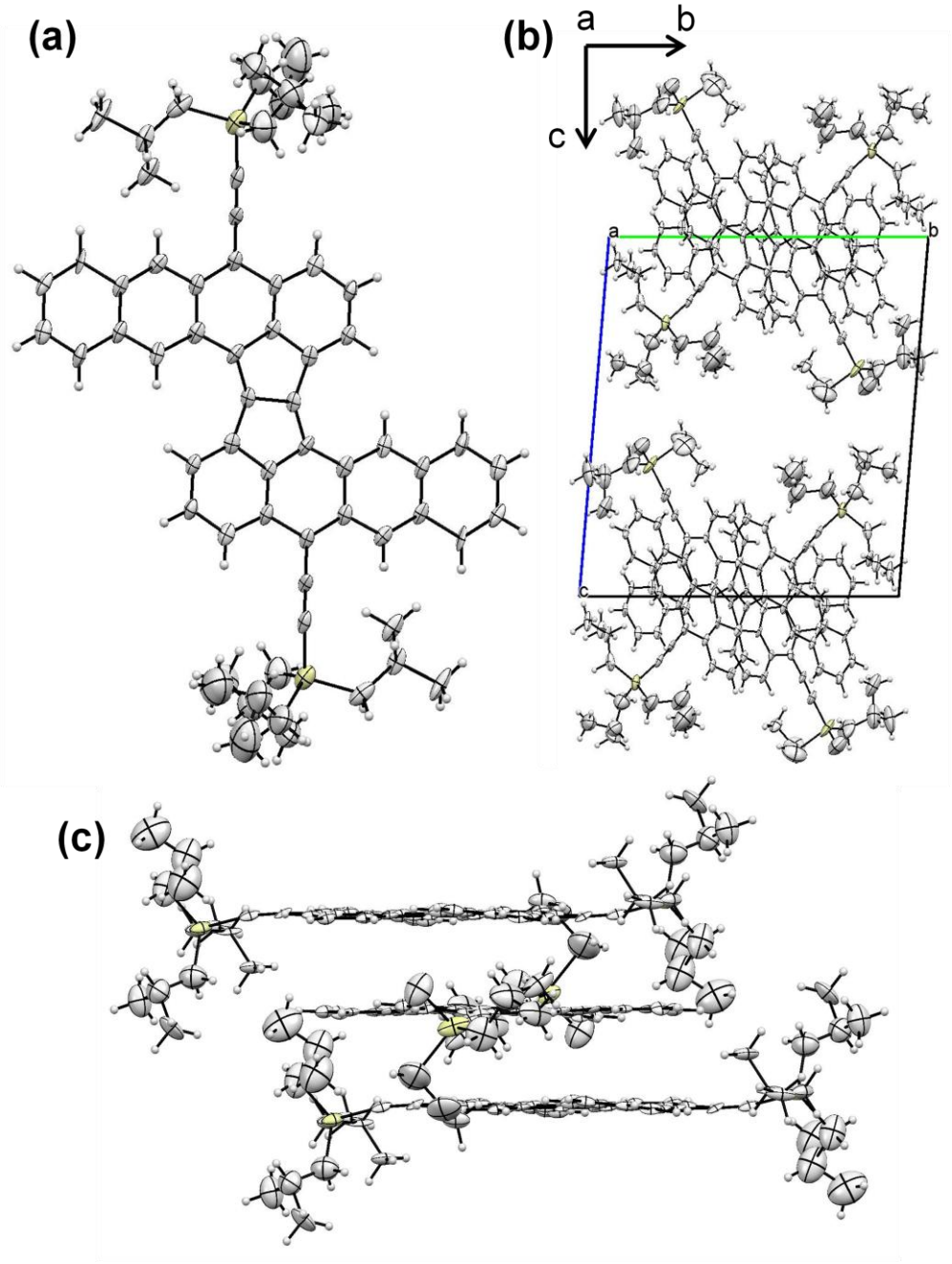

Figure 5.5 (a) ORTEP drawing of **5-2b**; (b) packing along the a-axis; (c) packing column side view

5.3 Summary and outlook

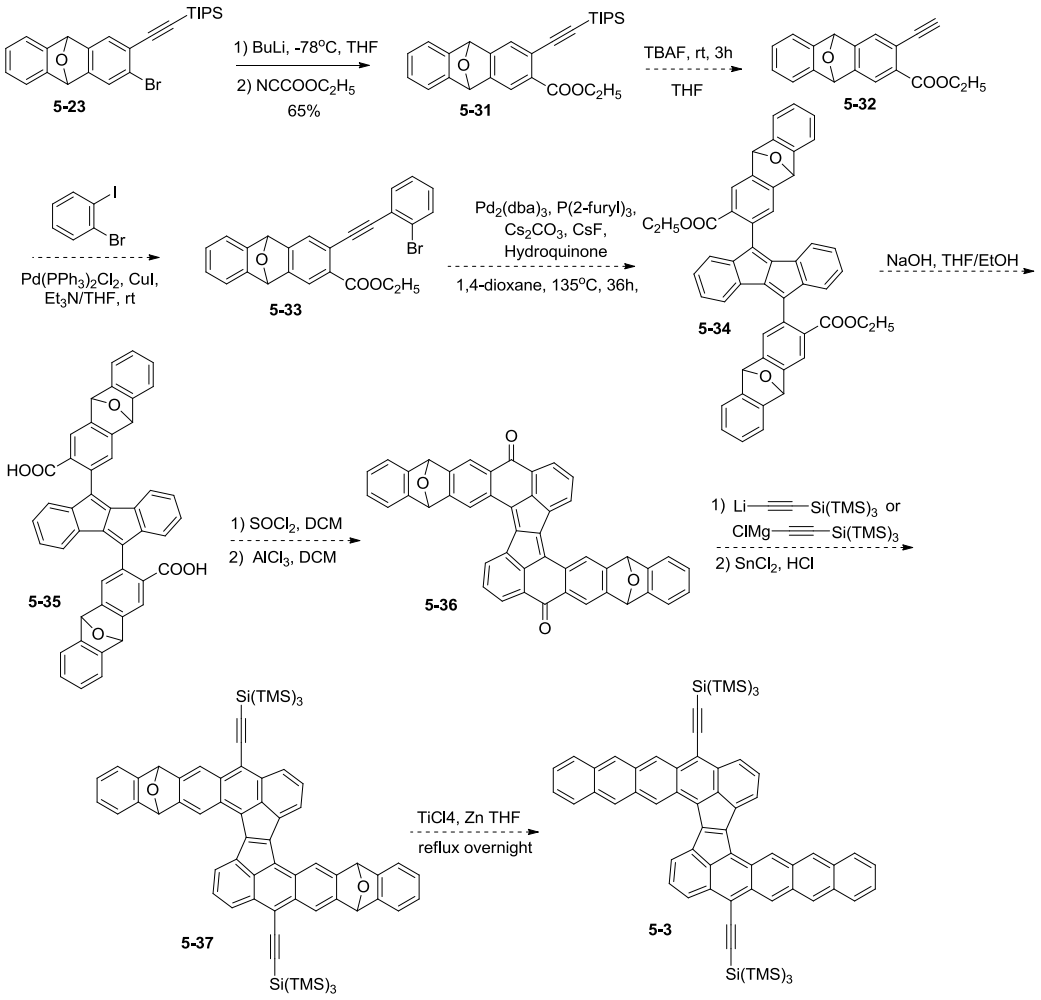

Scheme 5.4 Proposal synthetic route of pentaleno-dipentacene **5-3**

In this chapter, we designed and synthesized the pentaleno-dianthracene **5-1** and pentaleno-ditetracene **5-2** successfully. The UV-vis absorption spectra showed long wavelength absorption bands due to intramolecular charge transfer character. They have small band gaps around 1.0 eV. TD-DFT calculations suggested that the HOMOs of both molecules are delocalized along the Z-shaped framework while the LUMOs are mainly localized at the central pentalene unit. The single crystal of **5-1** was obtained. It has a planar conformation, and adopted a column-like stacking structure.

The Synthetic route for pentaleno-dipentacene will be modified. As shown in Scheme 5.4, the oxygen atoms will be removed after preparation of diketone **5-36**. Compound **5-36** can be considered as a modified **5-10**, which can react with lithium reagent or Grignard reagent to form diol **5-37**. As a result, the reaction from **5-36** to **5-37** may be successful. In the final step, the oxygen atoms will be removed by using zinc and $TiCl_4$ to get target products. The physical properties and applications of these pentaleno-diacenes will be studied in the near future.

5.4 Experiment section

5.4.1 General characterization method

^{1}H and ^{13}C NMR spectra were recorded using Advance 500 MHz Bruker spectrometer in $CDCl_3$ with tetramethylsilane (TMS) as the internal standard. The chemical shift was recorded in ppm and the following abbreviations were used to explain the multiplicities: s = singlet, d = doublet, t = triplet, m = multiplet, br = broad. Column chromatography was performed on silica gel 60 (Merck 40-60 nm, 230-400 mesh). EI mass spectra were recorded on Agilent 5975C DIP/MS mass spectrometer. UV-vis absorption and fluorescence spectra were recorded on a Shimadzu UV-1700 spectrophotometer and a RF-5301 fluorometer, respectively. Cyclic voltammetry and differential pulse voltammetry measurements were performed in HPLC grade chlorobenzene on a CHI 620C electrochemical analyzer with a three-electrode cell, using 0.1 M Bu_4NPF_6 as supporting electrolyte, AgCl/Ag as reference electrode, gold disk

as working electrode, Pt wire as counter electrode, and scan rate at 50 mV s^{-1}. The potential was externally calibrated against the ferrocene/ferrocenium couple. Thermogravimetric analysis (TGA) was carried out on a TA instrument 2960 at a heating rate of 10 ℃ min^{-1} under nitrogen flow. Differential scanning calorimetry (DSC) was performed on a TA instrument 2920 at a heating/cooling rate of 10 ℃ min^{-1} under nitrogen flow. GPC were performed on a Waters 410 differential refractometer with two columns connected in series with a THF (the mobile phase) flowing rate of 0.3 mL min^{-1}. Tapping-mode Atomic Force Microscopy (TM-AFM) was performed on a Nanoscope V microscope (Veeco Inc.). X-ray diffraction (XRD) patterns of the thin film were measured on a Bruker-AXS D8 DISCOVER with GADDS X-ray diffractometer. Copper Kα line was used as a radiation source with λ = 1.5418 Å

5.4.2 Synthesis

All reagents were purchased from commercial sources without further purification. Anhydrous dichloromethane (DCM), *N*, *N*-dimethylformaldehyde (DMF) was distilled from CaH_2. Toluene and THF were distilled from sodium-benzophenone immediately prior to use. The methyl 2-((2-bromophenyl)ethynyl)benzoate **5-7**[3], methyl 3-((2-bromophenyl)-ethynyl)-2-naphthoate **5-14**[4] and 2,3-dibromo-9,10-dihydro-9,10-epoxyanthracene **5-22**[5] were prepared by following literature procedures.

Compound **5-5 4-(2-bromophenyl)-2-methylbut-3-yn-2-ol**

A mixture of compound **5-4** (20.0 g, 85.5 mmol), 2-methylbut-3-yn-2-ol (10.79 g, 128.3 mmol), CuI (0.244 g, 1.5%) and catalyst $Pd(PPh_3)_2Cl_2$ (0.912 mg, 1.5%) in anhydrous THF (50 mL) and Et_3N (50 mL) was degassed by three freeze-pupm-thaw cycles. The mixture was stirred at 75 ^oC under argon for overnight. The mixture was extracted with EtOAc (100 mL ×2). The combined organic phase was washed with 10% m/m aqueous HCl solution (80 mL ×2) and brine (80 mL ×1). The organic phase was dried over anhydrous Na_2SO_4 and organic solvent was removed under reduced pressure. The crude product was purified by column chromatography (EtAc /Hexane = 10:1) to afford compound **5-5** (13.60 g) in 66% yield. ^1H NMR (500 MHz, $CDCl_3$, ppm): δ = 7.57 (dd, *J* = 1.25, 8.2 Hz, 1H), 7.44 (dd, *J* = 1.25, 7.55 Hz, 1H), 7.24 (m, 1H), 7.15 (m, 1H), 2.17 (s, 1H), 1.65 (s, 6H); ^{13}C NMR (125 MHz, $CDCl_3$, ppm): δ =133.19, 132.34, 129.42, 126.94, 125.71, 124.78, 98.42, 80.89, 65.74, 31.29. MS (EI): calcd for $C_{11}H_{11}BrO$ (M^+), 238.00; found, 238.2.

Compound **5-6 1-bromo-2-ethynylbenzene**

Compound **5-5** (13.6 g, 56.8 mmol) was taken in dry toluene (100 mL) under argon atmosphere. Powdered potassium hydroxide (5.8 g, 103.4 mmol) was added to the reaction mixture. The reaction mixture was refluxed for 12 h under argon. The reaction mixture was cooled to room temperature and filtered off the solid residue. The filtrate was evaporated and residue purified over flash column chromatography (Hexane) to afford compound **5-6** (6.69 g)

in 65% yield. ^{1}H NMR (500 MHz, $CDCl_3$, ppm): δ = 7.59 (d, *J* = 8.15 Hz, 1H), 7.53 (dd, *J* =1.9, 7.6 Hz, 1H), 7.27 (t, *J* = 7.25 Hz, 1H), 7.21 (m, 1H), 3.38 (s, 1H); ^{13}C NMR (125 MHz, $CDCl_3$, ppm): δ =134.10, 132.46, 129.99, 127.01, 125.57, 124.29, 81.89, 81.78. MS (EI): calcd for C_8H_5Br (M^+), 179.96; found, 180.10.

Compound **5-7 methyl 2-((2-bromophenyl)ethynyl)benzoate**

A mixture of compound **5-6** (4.36 g, 24 mmol), methyl 2-iodobenzoate (6.2 g, 24 mmol), CuI (0.137 g, 3%) and catalyst $Pd(PPh_3)_2Cl_2$ (0.674 g, 4%) in anhydrous THF (40 mL) and Et_3N (20 mL) was degassed by three freeze-pupm-thaw cycles. The mixture was stirred at 75 ^{o}C under argon for overnight. The mixture was extracted with EtOAc (60 mL ×2). The combined organic phase was washed with 10% m/m aqueous HCl solution (50 mL ×2) and brine (50 mL ×1). The organic phase was dried over anhydrous Na_2SO_4 and organic solvent was removed under reduced pressure. The crude product was purified by column chromatography (EtAc/Hexane = 1:10) to afford compound **5-7** (7.08 g) in 95% yield. ^{1}H NMR (500 MHz, $CDCl_3$, ppm): δ = 7.55 (dd, *J* = 1.25, 7.55 Hz, 1H), 7.73 (m, 1H), 7.62 (m, 1H), 7.52 (m, 1H), 7.41 (m, 1H), 7.31 (m, 1H), 7.20 (m, 1H), 3.97 (s, 3H); ^{13}C NMR (125 MHz, $CDCl_3$, ppm): δ =166.68, 134.35, 133.67, 132.45, 131.83, 131,71, 130.48, 129.63, 128.29, 127.05, 125.51, 125.49, 123.30, 92.73, 92.58, 52.31. MS (EI): calcd for $C_{16}H_{11}BrO_2$ (M^+), 313.99; found, 313.80.

Compound **5-8 dimethyl 2,2'-(indeno[2,1-a]indene-5,10-diyl)dibenzoate**

A reaction flask was charged with monomer **5-7**(7.30 g 23 mmol), hydroquinone (5.09 g, 46 mmol), Cs_2CO_3 (15.05 g, 46 mmol), CsF (7.72 g, 51 mmol), P(2-furyl)$_3$ (0.64 g, 2.8 mmol), and $Pd_2(dba)_3$ (0.63 g, 0.7 mmol) and then purged with argon. Anhydrous 1,4-dioxane (100 mL) was injected into the reaction mixture and deoxygenated three freeze-pump-thaw cycles. The suspension was immediately heated to135^oC. After heating for 24 h the reaction mixture was diluted with $CHCl_3$ (25 mL), filtered through celite, and then concentrated to yield raw solid. After purification via column chromatography (silica gel, DCM/Hexane = 1:4), the product was dissolved in $CHCl_3$, precipitated in methanol and filtered to give the purer product **5-8** (435 mg) in 8% yield for characterization. ^{1}H NMR (500 MHz, $CDCl_3$, ppm): δ = 8.07 (d, *J* = 7.6 Hz, 2H), 7.67-7,59 (m, 4H), 7.55-7.50 (m, 2H), 6.85-6.79 (m, 4H), 6.79-6.73 (m, 2H), 6.61-6.56 (m, 2H), 3.68 (s, 3H), 3.66 (s, 3H) ; ^{13}C NMR (125 MHz, $CDCl_3$, ppm): δ = 167.92, 167.75, 150.63, 150.58, 143.35, 140.23, 140.12, 134.66, 134.50, 134.15, 132.23, 132.18, 130.85, 130.82, 130.77, 130.62, 130.44, 130.05, 128.55, 128.53, 127.83, 127.80, 126.98, 126.91, 121.86, 121.83, 121.34, 121.29, 52.31, 52.20. HRMS (EI): calcd for $C_{32}H_{22}O_4$ (M^+), 470.1518; found, 470.1519 (error: 0.23 ppm).

Compound **5-9 2,2'-(indeno[2,1-a]indene-5,10-diyl)dibenzoic acid**

A suspension of compound **5-8** (1.18 g, 2.5 mmol) and LiOH (1.20 g, 50 mmol) in dioxane (30 mL) and water (33 mL) was heated to reflux for overnight under argon. After mixture cooled to room temperature and the

reaction mixture was poured into water. The concentration HCl was added into the water mixture and the di-acid compound **5-9** precipitated out. Then filtered and washed the solid by water and dichloromethane to obtain the compound **5-9** (0.99 g) in 90% yield. The compound **5-9** can't dissolve into common organic solvent so we did the following step directly without NMR characterization. HRMS (MALDI-TOF): calcd for $C_{30}H_{18}O_4$ (M^+), 442.1205; found, 442.1192 (error: -2.94 ppm).

Compound **5-10 aceanthryleno[2,1-a]aceanthrylene-5,13-dione**

To a suspension of acid **5-9** (1.51 g, 4.7 mmol) in anhydrous dichloromethane (35 mL) was added the thionyl chloride (2 mL, 19.8 mmol). The mixture was heated to 60 ^oC for overnight under argon, and then cooled to room temperature. The solvent and excess thionyl chloride was removed in vacuum. The anhydrous dichloromethane (20 mL) and $AlCl_3$ (30 mL) were added in ice bath and the mixture was warmed to room temperature naturally. After stirring for overnight under argon, the 10% m/m aqueous HCl solution (20 mL) was added to quench the reaction. Then the solid was filtered and washed by the solvents (10% m/m HCl, methanol, acetone, dichloromethane, THF) to give the di-ketone compound **5-10** (0.42 g) in 30% yield. The compound **5-9** can't dissolve into common organic solvent so we did the following step directly without NMR characterization. HRMS (EI): calcd for $C_{30}H_{14}O_2$ (M^+), 406.0994; found, 406.0975 (error: -4.68 ppm).

Compound **5-1 5,13-bis((triisopropylsilyl)ethynyl)aceanthryleno-**

[2,1-a]aceanthrylene

To a dried 50 ml round bottle flask was added Triisopropylsilyl acetylene (370 mg, 2 mmol) and anhydrous THF (20 mL).Then butyl lithium (1.6 M, mL) was added dropwise via syringe in ice bath. The mixture was stirred for 2 hours at room temperature. Then 50 mg (0.05 mmol) of the di-ketone **5-10** was added to the solution and the mixture was stirrred for 12 hours at room temperature in the dark. The reaction was quenched by H_2O (1 ml) and then the $SnCl_2$ (g) was added. The reaction mixture was stirred at room temperature for 12 hours under argon. The mixture was extracted with dichloromethane (60 mL ×2). The combined organic phase was washed with 10% m/m aqueous HCl solution (50 mL ×2) and brine (50 mL ×1). The organic phase was dried over anhydrous Na_2SO_4 and organic solvent was removed under reduced pressure. The crude product was purified by column chromatography (DCM/Hexane = 4:1) to afford compound **5-1** (0.92 g) in 38% yield. ^{1}H NMR (500 MHz, $CDCl_3$, ppm): δ = 8.54 (d, *J* = 7.75 Hz, 2H), 8.11 (d, *J* = 8.5 Hz, 2H), 8.04 (d, *J* = 7.5 Hz, 2H), 7.70 (d, *J* = 6.5 Hz, 2H), 7.46 (m, 4H), 7.35 (t, *J* = 7.5 Hz), 1.65-1.55 (br, 42H); ^{13}C NMR (125 MHz, $CDCl_3$, ppm): δ = 143.45, 135.13, 133.57, 131.84, 130.69, 128.85, 128.45, 127.78, 127.67, 127.36, 127.03, 126.87, 126.11, 125.92, 119.77, 104.70, 104.00, 19.00, 11.65. HRMS (APCI): calcd for $C_{52}H_{57}Si_2$ ($M+H^+$), 737.3993; found, 737.4009 (error: 2.17 ppm).

Compound **5-12 methyl 3-hydroxy-2-naphthoate**

To a solution of compound 11 (18.80g, 100 mmol) in methanol (100 mL) was added con. H_2SO_4 (2 mL). After reflux overnight, the reaction mixture cooled to room temperature. The mixture was extracted with EtOAc (80 mL ×2). The combined organic phase was washed brine (60 mL ×2). The organic phase was dried over anhydrous Na_2SO_4 and organic solvent was removed under reduced pressure. The crude product was purified by column chromatography (EtAc/Hexane = 10:1) to afford compound **5-12** (16.18 g) in 80% yield. ^{1}H NMR (500 MHz, $CDCl_3$, ppm): δ = 10.43 (s, 1H), 8.49 (s, 1H), 7.80 (d, *J* = 8.15 Hz, 1H), 7.69 (d, *J* = 8.8 Hz, 1H), 7.52-7.46 (m, 1H), 7.34-7.28 (m, 2H), 4.03 (s, 3H); ^{13}C NMR (125 MHz, $CDCl_3$, ppm): δ = 170.28, 156.28, 137.91, 132.43, 129.20, 127.03, 126.30, 123.93, 114.18, 111.67, 52.55. MS (EI): calcd for $C_{12}H_{10}O_3$ (M^+), 202.06 found, 202.20.

Compound **5-13 methyl 3-(((trifluoromethyl)sulfonyl)oxy)-2-naphthoate**

To a solution of compound **5-12** (15.46 g, 76.6 mmol) in 150 mL of dry dichloromethane was cooled to 0 ^{o}C. Dry pyridine (12.7 mL) and trifluoromethanesulfonic anhydride (15.5 mL, 92.2 mmol) were then added sequentially to the stirred solution. After the addition, the reaction mixture was warmed up to room temperature and stirred for 5 h until the phenol was fully consumed (monitored by TLC). The mixture was extracted with EtOAc (80 mL ×2). The combined organic phase was washed brine (60 mL ×2). The organic phase was dried over anhydrous Na_2SO_4 and organic solvent was

removed under reduced pressure. The crude product was purified by column chromatography (EtAc/Hexane = 10:1) to afford compound **5-13** (23.03 g) in 90% yield. ^{1}H NMR (500 MHz, $CDCl_3$, ppm): δ = 8.66 (s, 1H), 7.99 (d, *J* = 8.2 Hz, 1H), 7.89 (d, *J* = 8.2 Hz, 1H), 7.75 (s, 1H), 7.69 (t, *J* = 7.55 Hz, 1H), 7.64 (t, *J* = 7.6 Hz, 1H), 4.02 (s, 3H); ^{13}C NMR (125 MHz, $CDCl_3$, ppm): δ = 164.41, 144.77, 134.98, 134.86, 131.39, 129.78, 129.13, 128.09, 127.73, 121.99, 121.04, 52.70. MS (EI): calcd for $C_{13}H_9F_3O_5S$ (M^+), 334.01 found, 334.10.

Compound **5-14 methyl 3-((2-bromophenyl)ethynyl)-2-naphthoate**

A mixture of compound **5-6** (3.98 g, 22 mmol), compound **5-13** (6.69 g, 20 mmol), CuI (0.114 g, 3%) and catalyst $Pd(PPh_3)_2Cl_2$ (0.561 g, 4%) in anhydrous THF (40 mL) and DMF (40 mL) was degassed by three freeze-pupm-thaw cycles. The mixture was stirred at room temperature under argon for overnight. The mixture was extracted with EtOAc (60 mL ×2). The combined organic phase was washed with brine (50 mL ×2) and 10% m/m aqueous HCl solution (50 mL ×1). The organic phase was dried over anhydrous Na_2SO_4 and organic solvent was removed under reduced pressure. The crude product was purified by column chromatography (EtAc/Hexane = 1:10) to afford compound **5-14** (7.08 g) in 95% yield. ^{1}H NMR (500 MHz, $CDCl_3$, ppm): δ = 8.54 (s, 1H), 8.23 (s, 1H), 7.68-7.53 (m, 4H), 7.32 (td, *J* = 1.0, 7.5 Hz, 1H), 7.20 (td, *J* = 1.5, 7.5 Hz, 1H), 4.02 (s, 3H); ^{13}C NMR (125 MHz, $CDCl_3$, ppm): δ = 166.77, 134.65, 134.26, 133.66, 132.44, 131.98,

131.83, 129.48, 128.97, 128.77, 128.43, 127.61, 127.48, 127.05, 125.70, 125.42, 119.05, 93.01, 91.61, 52.40. HRMS (EI): calcd for $C_{20}H_{13}BrO_2$ (M^+), 364.0099; found, 364.0099 (error: -0.01 ppm).

Compound **5-15 dimethyl 3,3'-(indeno[2,1-a]indene-5,10-diyl)-bis(2-naphthoate)**

A reaction flask was charged with monomer **5-14** (3.65 g 10 mmol), hydroquinone (2.26 g, 20 mmol), Cs_2CO_3 (6.68 g, 20 mmol), CsF (3.42 g, 22 mmol), P(2-furyl)$_3$ (0.18 g, 0.8 mmol), and $Pd_2(dba)_3$ (0.25 g, 0.3 mmol) and then purged with argon. Anhydrous 1,4-dioxane (50 mL) was injected into the reaction mixture and deoxygenated three freeze-pump-thaw cycles. The suspension was immediately heated to135^{o}C. After heating for 24 h the reaction mixture was diluted with $CHCl_3$ (20 mL), filtered through celite, and then concentrated to yield raw solid. After purification via column chromatography (silica gel, DCM/Hexane = 1:4), the product was dissolved in $CHCl_3$, precipitated in methanol and filtered to give the purer product **5-15** (460 mg) in 15% yield for characterization. ^{1}H NMR (500 MHz, $CDCl_3$, ppm): δ = 8.65 (s, 2H), 8.17 (s, 1H), 8.12 (s, 1H), 8.03 (d, *J* = 8.0 Hz, 2H), 7.93 (dd, *J* = 3.0, 8.0 Hz, 2H), 7.69-7,60 (m, 4H), 6.90 (dd, *J* = 3.0, 7.5 Hz, 2H), 6.84-6.79 (m, 2H), 6.84-6.79 (m, 2H),6.78-6.73 (m, 2H), 6.68-6.63 (m, 2H), 3.78 (s, 3H), 3.73 (s, 3H) ; ^{13}C NMR (125 MHz, $CDCl_3$, ppm): δ = 167.94, 167.74, 151.02, 150.93, 143.45, 143.39, 140.36, 140.28, 134.79, 134.73, 134.42, 134.38, 132.32, 132.30, 132.25, 132.19, 130.76, 130.65, 129.95,

129.57, 129.02, 128.99, 128.64, 128.62, 128.53, 128.29, 127.92, 127.90, 127.79, 127.74, 127.34, 127.00, 126.92, 121.83, 121.79, 121.41, 121.36, 52.46, 52.33. HRMS (EI): calcd for $C_{32}H_{22}O_4$ (M^+), 470.1518; found, 470.1536 (error: 0.85 ppm).

Compound **5-16 3,3'-(indeno[2,1-a]indene-5,10-diyl)bis(2-naphthoic acid)**

A suspension of compound **5-15** (1.21 g, 2.1 mmol) and LiOH (1.0 g, 42 mmol) in dioxane (30 mL) and water (33 mL) was heated to reflux for overnight under argon. After mixture cooled to room temperature and the reaction mixture was poured into water. The concentration HCl was added into the water mixture and the di-acid compound **5-16** precipitated out. Then filtered and washed the solid by water and dichloromethane to obtain the compound **5-16** (1.04 g) in 90% yield. The compound **5-16** can't dissolve into common organic solvent so we did the following step directly without NMR characterization. HRMS (MALDI-TOF): calcd for $C_{38}H_{22}O_4$ (M^+), 542.1518; found, 542.1495 (error: -4.24 ppm).

Compound **5-17 pentaleno[1,2,3-de:4,5,6-d'e']ditetracene-1,11-dione**

To a suspension of acid **5-16** (0.27 g, 0.5 mmol) in anhydrous dichloromethane (20 mL) was added the thionyl chloride (1.5 mL). The mixture was heated to 60 ^oC for overnight under argon, and then cooled to room temperature. The solvent and excess thionyl chloride was removed in vacuum. The anhydrous dichloromethane (20 mL) and $AlCl_3$ (0.28 g, 2 mmol) were added in ice bath and the mixture was warmed to room temperature

naturally. After stirring for overnight under argon, the 10% m/m aqueous HCl solution (20 mL) was added to quench the reaction. Then the solid was filtered and washed by the solvents (10% m/m HCl, methanol, acetone, dichloromethane, THF) to give the di-ketone compound **5-17** (0.10 g) in 40% yield. The compound **17** can't dissolve into common organic solvent so we did the following step directly without NMR characterization. HRMS (MALDI-TOF): calcd for $C_{38}H_{18}O_2$ (M^+), 506.1307; found, 506.1287 (error: -3.98 ppm).

Compound **5-2a** **1,11-bis((triisopropylsilyl)ethynyl)pentaleno-[1,2,3-de:4,5,6-d'e']ditetracene**

To a dried 50 ml round bottle flask was added triisopropylsilyl acetylene (760 mg, 4 mmol) and anhydrous THF (30 mL).Then butyl lithium (1.6 M, 2.2 mL) was added dropwise via syringe in ice bath. The mixture was stirred for 2 hours at room temperature. Then 150 mg (0.3 mmol) of the di-ketone **5-17** was added to the solution and the mixture was stirrred for 12 hours at room temperature in the dark. The reaction was quenched by H_2O (1 ml) and then the $SnCl_2$ (g) was added. The reaction mixture was stirred at room temperature for 12 hours under argon. The mixture was extracted with dichloromethane (60 mL ×2). The combined organic phase was washed with10% m/m aqueous HCl solution (50 mL ×2) and brine (50 mL ×1). The organic phase was dried over anhydrous Na_2SO_4 and organic solvent was removed under reduced pressure. The crude product was purified by column chromatography

(DCM/Hexane = 4:1) to afford compound **5-2a** (50 mg) in 20% yield. ^{1}H NMR (500 MHz, D_8-THF, ppm): δ = 9.55 (s, 2H), 9.48 (s, 2H), 8.88 (d, *J* = 6.5 Hz, 2H), 8.62 (d, *J* = 8.5 Hz, 2H), 8.41 (d, *J* = 8.5 Hz, 2H), 8.14 (d, *J* = 8.5 Hz, 2H), 7.98 (t, *J* = 7.75 Hz, 2H), 7.70 (t, *J* = 7.25 Hz, 2H), 7.65 (t, *J* = 7.5 Hz, 2H), 1.62-1.58 (m, 42H). HRMS (MALDI-TOF): calcd for $C_{52}H_{56}Si_2$ (M^+), 736.3921; found, 736.3897 (error: -3.26 ppm).

Compound **5-2b** **1,11-bis((triisopropylsilyl)ethynyl)pentaleno-[1,2,3-de:4,5,6-d'e']ditetracene**

To a dried 50 ml round bottle flask was added ethynyl triisobutylsilane (250 mg, 1.1 mmol) and anhydrous THF (20 mL).Then butyl lithium (1.6 M, 0.6 mL) was added dropwise via syringe in ice bath. The mixture was stirred for 2 hours at room temperature. Then 40 mg (0.8 mmol) of the di-ketone **5-17** was added to the solution and the mixture was stirrred for 12 hours at room temperature in the dark. The reaction was quenched by H_2O (1 ml) and then the $SnCl_2$ (g) was added. The reaction mixture was stirred at room temperature for 12 hours under argon. The mixture was extracted with dichloromethane (60 mL ×2). The combined organic phase was washed with 10% m/m aqueous HCl solution (50 mL ×2) and brine (50 mL ×1). The organic phase was dried over anhydrous Na_2SO_4 and organic solvent was removed under reduced pressure. The crude product was purified by column chromatography (DCM/Hexane = 4:1) to afford compound **5-2b** (45 mg) in 60% yield. ^{1}H NMR (500 MHz, D_8-THF, ppm): δ = 9.25 (s, 2H), 8.81 (s, 2H), 8.38 (d, *J* =

8.5 Hz, 2H), 8.22 (br, 2H), 7.99 (d, *J* = 7.5 Hz, 2H), 7.91 (d, *J* = 8.0 Hz, 2H), 7.66 (t, *J* = 7.25 Hz, 2H), 7.56-7.48 (m, 4H), 2.50-2.44 (m, 6H), 1.47-1.44 (br, 36H), 1.28-1.23 (br, 12H). HRMS (MALDI-TOF): calcd for $C_{66}H_{72}Si_2$ (M^+), 920.5173; found, 920.5186 (error: 1.41 ppm).

Compound **5-19 methyl 2-(dimethoxymethyl)benzoate**

To a suspension of 2-carboxybenzaldehyde (15.5 g, 100 mmol), trimethyl orthoformate (51 mL, 470 mmol) and Dowex 50W-X8 resin (7.7 g) in dry methanol (150 mL). The reaction mixture was refluxed with stirring for 15 h under argon. The mixture was cooled and filtered and the solvent removed on a rotary evaporator. The residue, an oil, was purified by flash column chromatography (EtAc/Hexane = 1:5) to afford compound **5-19** (20.6 g) in 95% yield. ^{1}H NMR (500 MHz, $CDCl_3$, ppm): δ = 7.78 (dd, *J* = 1.3, 8.2 Hz, 1H), 7.73 (d, *J* = 8.2 Hz, 1H), 7.50 (td, *J* = 1.25, 7.55 Hz, 1H), 7.37 (td, *J* = 1.25, 7.55 Hz, 1H), 3.90 (s, 3H), 3.37 (s, 6H); ^{13}C NMR (125 MHz, $CDCl_3$, ppm): δ = 168.25, 138.74, 131.38, 130.20, 129.76, 128.20, 126.91, 100.89, 53.96, 52.07. MS (EI): calcd for $C_{11}H_{14}O_4$ (M^+), 210.09 found, 210.20.

Compound **5-20 1-(dimethoxymethyl)-2-(methoxymethyl)benzene**

To a suspension of $LiAlH_4$ (4.9 g, 128 mmol) in anhydrous THF (60 mL) was added dropwise the solution of compound **5-19** in anhydrous THF (60 mL) at room temperature. The mixture was stirred at room temperature for 12 h. After hydrolysis with water and dilution with ether, the decanted ether solution was dried by Na_2S0_4 and organic solvent was removed under reduced pressure.

The crude product was purified by column chromatography (EtAc/Hexane = 1:8) to afford compound **5-20** (16.4 g) in 90% yield. ^{1}H NMR (500 MHz, $CDCl_3$, ppm): δ = 7.51 (dd, *J* = 1.9, 7.55 Hz, 1H), 7.38 (dd, *J* = 1.9, 7.55 Hz, 1H), 7.36-7.30 (m, 2H), 5.50 (s, 1H), 4.70 (d, *J* = 6.3 Hz, 1H), 3.36 (s, 6H), 3.16 (t, *J* = 6.0 Hz, 1H); ^{13}C NMR (125 MHz, $CDCl_3$, ppm): δ = 138.98, 135.63, 130.00, 129.09, 127.50, 127.43, 103.30, 63.27, 53.50. MS (EI): calcd for $C_{11}H_{16}O_3$ (M^+), 196.11 found, 196.10.

Compound **5-21** 1-methoxy-1,3-dihydroisobenzofuran

To a suspension of compound **5-20** (16.0 g, 88 mmol) and Dowex 50W-X8 resin (8.5 g) in dry methanol (150 mL) was stirring for 12 h under argon. The reaction mixture filtered and the solvent removed on a rotary evaporator. The residue, an oil, was purified by column chromatography (EtAc/Hexane = 1:10) to afford compound **5-21** (11.8 g) in 90% yield. ^{1}H NMR (500 MHz, $CDCl_3$, ppm): δ = 7.40 (d, *J* = 6.9 Hz, 1H), 7.39-7.30 (m, 2H), 7.27 (d, *J* = 8.2 Hz, 1H), 6.19 (d, *J* = 2.5 Hz, 1H), 5.22 (d, *J* = 12.6 Hz, 1H), 5.05 (d, *J* = 13.25 Hz, 1H), 3.44 (s, 3H); ^{13}C NMR (125 MHz, $CDCl_3$, ppm): δ = 139.94, 137.31, 129.18, 127.65, 122.94, 121.00, 107.58, 72.33, 54.20. MS (EI): calcd for $C_9H_{10}O_2$ (M^+), 150.07 found, 150.20.

Compound **5-22 2,3-dibromo-9,10-dihydro-9,10-epoxyanthracene**

To a solution of compound **5-21** (8.55 g, 56 mmol) in toluene (110 mL), diisopropylamine (0.4 mL, 2.8 mmol) was added, and then butyl lithium (1.6 M, 36 mL) was added dropwise at ice bath. The mixture was stirred at room

temperature for 3 hours. Then 1,2,4,5-tetrabromobenzene (22.3 g, 56 mmol) was added, and the mixture was cooled to -50 ^{o}C and butyl lithium (1.6 M, 36 mL) was added over 30 minutes. After addition, the mixture warmed to room temperature and stirred for overnight. The mixture was extracted with chloroform (80 mL ×2). The combined organic phase was washed with brine (60 mL ×3). The organic phase was dried over anhydrous Na_2SO_4 and organic solvent was removed under reduced pressure. The crude product was purified by column chromatography (CH_2Cl_2/Hexane = 1:5) to afford compound **5-22** (4.9 g) in 25% yield. ^{1}H NMR (500 MHz, $CDCl_3$, ppm): δ = 7.56 (s, 2H), 7.33 (dd, *J* = 3.15, 5.05 Hz, 2H), 7.06 (dd, *J* = 3.15, 5.0 Hz, 2H), 6.02 (s, 2H); ^{13}C NMR (125 MHz, $CDCl_3$, ppm): δ = 149.25, 146.87, 126.54, 125.68, 121.61, 120.73, 82.03. MS (EI): calcd for $C_{14}H_8Br_2O$ (M^+), 349.89; found, 349.90.

Compound **5-23 ((3-bromo-9,10-dihydro-9,10-epoxyanthracen-2-yl)-ethynyl)triisopropylsilane**

A mixture of compound **5-22** (2.0 g, 5.7 mmol), triisopropylsilyl acetylene (1.1 g, 6.2 mmol), CuI (32 mg, 3%) and catalyst $Pd(PPh_3)_2Cl_2$ (206 mg, 5%) in anhydrous THF (20 mL) and Et_3N (20 mL) was degassed by three freeze-pupm-thaw cycles. The mixture was stirred at 75 ^{o}C under argon for overnight. The mixture was extracted with EtOAc (50 mL ×2). The combined organic phase was washed with brine (50 mL ×2) and 10% m/m aqueous HCl solution (50 mL ×1). The organic phase was dried over anhydrous Na_2SO_4 and organic solvent was removed under reduced pressure. The crude product was

purified by column chromatography (DCM/Hexane = 10:1) to afford compound **5-23** (1.0 g) in 40% yield. ^{1}H NMR (500 MHz, $CDCl_3$, ppm): δ = 7.52 (s, 1H), 7.44 (s, 1H), 7.32 (dd, *J* = 3.5, 5.5 Hz, 2H), 7.04 (dd, *J* = 3.0, 5.5 Hz, 2H), 6.02 (s, 2H), 1.13-1.11 (br, 21H); ^{13}C NMR (125 MHz, $CDCl_3$, ppm): δ = 149.80, 147.12, 147.11, 146.82, 126.47, 126.41, 125.23, 124.64, 123.48, 122.69, 120.69, 120.61, 105.03, 95.92, 82.12, 18.64, 11.26. HRMS (EI): calcd for $C_{25}H_{29}BrOSi$ (M^+), 452.1171; found, 452.1167 (error: -0.83 ppm).

Compound **5-24 ((3-bromoanthracen-2-yl)ethynyl)triisopropylsilane**

To an ice cold suspension of Zn dust (1.7 g, 26 mmol) in THF (20 mL) was carefully added $TiCl_4$ (3.6 mL, 32 mmol) under argon, and the reaction mixture was heated to reflux for 5 minutes. Then the mixture was cooled to 0 ^{o}C and a solution of compound **5-23** (2.7 g, 6 mmol) in THF (20 mL) was added dropwise. After addition, the mixture was reflux overnight. Cooled down the reaction to room temperature and poured into cold 10% m/m aqueous HCl solution (40 mL). The mixture was extracted with chloroform (60 mL ×2). The combined organic phase was washed with brine (50 mL ×2) and 10% m/m aqueous HCl solution (50 mL ×1). The organic phase was dried over anhydrous Na_2SO_4 and organic solvent was removed under reduced pressure. The crude product was purified by column chromatography (CH_2Cl_2/Hexane = 1:3) to afford compound **5-24** (1.8 g) in 70% yield. ^{1}H NMR (500 MHz, $CDCl_3$, ppm): δ = 8.33 (s, 1H), 8.26 (s, 1H), 8.23 (s, 1H), 8.21 (s, 1H), 7.97 (dd, *J* = 3.0, 6.5 Hz, 2H), 7.49 (dd, *J* = 3.0, 6.5 Hz, 2H),

1.22-1.20 (br, 21H); ^{13}C NMR (125 MHz, $CDCl_3$, ppm): δ = 134.19, 132.51, 132.06, 131.23, 130.84, 129.54, 128.36, 128.14, 126.36, 126.00, 125.22, 122.24, 121.14, 105.26, 96.20, 18.73, 11.40. HRMS (EI): calcd for $C_{25}H_{29}BrSi$ (M^+), 436.1222; found, 436.1221 (error: -0.21 ppm).

Compound **5-25 ethyl 3-((triisopropylsilyl)ethynyl)-anthracene-2-carboxylate**

To a solution of compound **5-24** (0.22 g, 0.5 mmol) in anhydrous THF (20 mL), *n*-BuLi (1.6 M in hexane, 0.35 mL) was slowly added at -78 ^{o}C under argon. The reaction mixture was stirred for 1 h. Ethyl cyanoformate (55 mg, 0.55 mmol) was added by syringe at -78 ^{o}C. The reaction was slowly warmed to room temperature and stirred overnight. The reaction was quenched by water at 0 ^{o}C. The mixture was extracted with dichloromethane (50 mL ×2). The combined organic phase was washed with brine (50 mL ×2) and 10% m/m aqueous HCl solution (50 mL ×1). The organic phase was dried over anhydrous Na_2SO_4 and organic solvent was removed under reduced pressure. The crude product was purified by column chromatography (EtAc/Hexane = 1:10) to afford compound **5-25** (0.14 g) in 65% yield. ^{1}H NMR (500 MHz, $CDCl_3$, ppm): δ = 8.58 (s, 1H), 8.47 (s, 1H), 8.38 (s, 1H), 8.28 (s, 1H), 8.02-7.98 (m, 2H), 7.54-7.47 (m, 2H), 4.47 (q, *J* = 7.0 Hz, 2H), 1.46 (t, *J* = 7.25 Hz, 3H), 1.21-1.19 (br, 21H); ^{13}C NMR (125 MHz, $CDCl_3$, ppm): δ = 166.60, 135.79, 133.18, 132.46, 132.04, 131.29, 129.33, 128.99, 128.44, 128.34, 128.04, 126.64, 126.22, 125.97, 118.31, 105.72, 95.03, 61.28, 18.74,

14.40, 11.46. HRMS (EI): calcd for $C_{28}H_{34}O_2Si$ (M^+), 430.2328; found, 430.2330 (error: 0.55 ppm).

Compound **5- 26 ethyl 3-ethynylanthracene-2-carboxylate**

To a solution of compound **5-25** (1.55 g, 3.6 mmol) in anhydrous THF (50 mL), TBAF (1 M in THF, 4.2 mL) was slowly added at 0 ^oC under argon. The reaction mixture was stirred for 1 h. at room temperature. The mixture was extracted with dichloromethane (50 mL ×2). The combined organic phase was washed with brine (50 mL ×2) and 10% m/m aqueous HCl solution (50 mL ×1). The organic phase was dried over anhydrous Na_2SO_4 and organic solvent was removed under reduced pressure. The crude product was purified by column chromatography (EtAc/Hexane = 1:10) to afford compound **5-26** (0.84 g) in 85% yield. ^1H NMR (500 MHz, $CDCl_3$, ppm): δ = 8.69 (s, 1H), 8.50 (s, 1H), 8.38 (s, 1H), 8.31 (s, 1H), 8.04-7.99 (m, 2H), 7.56-7.49 (m, 2H), 4.48 (q, *J* = 7.5 Hz, 2H), 3.41 (s, 1H), 1.48 (t, *J* = 7.0 Hz, 3H); ^{13}C NMR (125 MHz, $CDCl_3$, ppm): δ = 166.17, 136.22, 133.31, 132.86, 132.61, 131.18, 129.37, 128.46, 128.36, 128.31, 127.96, 126.86, 126.42, 126.13, 117.18, 82.69, 80.94, 61.41, 14.29. HRMS (EI): calcd for $C_{19}H_{14}O_2$ (M^+), 274.0994; found, 274.0982 (error: -4.17 ppm).

Compound **5-27 ethyl 3-((2-bromophenyl)ethynyl)-anthracene-2-carboxylate**

A mixture of compound **5-26** (1.07 g, 3.9 mmol), 2-bromo-iodobenzene (1.16 g, 4 mmol), CuI (23 mg, 3%) and catalyst $Pd(PPh_3)_2Cl_2$ (0.14 g, 5%) in

anhydrous THF (20 mL) and Et_3N (20 mL) was degassed by three freeze-pupm-thaw cycles. The mixture was stirred at 75 ^oC under argon for overnight. The mixture was extracted with EtOAc (60 mL ×2). The combined organic phase was washed with brine (50 mL ×2) and 10% m/m aqueous HCl solution (50 mL ×1). The organic phase was dried over anhydrous Na_2SO_4 and organic solvent was removed under reduced pressure. The crude product was purified by column chromatography (EtAc/Hexane = 1:10) to afford compound **5-27** (1.10 g) in 80% yield. ^1H NMR (500 MHz, $CDCl_3$, ppm): δ = 8.72 (s, 1H), 8.51 (s, 1H), 8.42 (s, 1H), 8.40 (s, 1H), 8.02 (d, *J* = 6.5 Hz, 2H), 7.69-7.63 (m, 2H), 7.56-7.50 (m, 2H), 7.33 (td, *J* = 0.5, 7.5 Hz, 1H), 7.20 (td, *J* = 1.5, 7.75 Hz, 1H), 4.51 (q, *J* = 7.5 Hz, 2H), 1.47 (t, *J* = 7.0 Hz, 3H); ^{13}C NMR (125 MHz, $CDCl_3$, ppm): δ = 166.34, 135.32, 133.50, 133.33, 132.93, 132.55, 132.44, 131.36, 129.39, 128.47, 128.37, 128.31, 127.91, 127.05, 126.80, 126.35, 126.23, 125.80, 125.51, 117.90, 93.43, 91.61, 61.38, 14.42. HRMS (EI): calcd for $C_{25}H_{17}BrO_2$ (M^+), 428.0412; found, 428.0406 (error: -1.44 ppm).

Compound **5-28 diethyl 3,3'-(indeno[2,1-a]indene-5,10-diyl)-bis(anthracene-2-carboxylate)**

A reaction flask was charged with monomer **5-27** (0.50 g 1.2 mmol), hydroquinone (0.27 g, 2.4 mmol), Cs_2CO_3 (0.80 g, 2.4 mmol), CsF (0.41 g, 2.6 mmol), P(2-furyl)$_3$ (36 mg, 0.14 mmol), and $Pd_2(dba)_3$ (36 mg, 0.04 mmol) and then purged with argon. Anhydrous 1,4-dioxane (20 mL) was injected into

the reaction mixture and deoxygenated three freeze-pump-thaw cycles. The suspension was immediately heated to135^{o}C. After heating for 24 h the reaction mixture was diluted with $CHCl_3$ (10 mL), filtered through celite, and then concentrated to yield raw solid. After purification via column chromatography (silica gel, DCM/Hexane= 1:3), the product was dissolved in $CHCl_3$, precipitated in methanol and filtered to give the purer product **5-28** (42 mg) in 10% yield for characterization. ^{1}H NMR (500 MHz, $CDCl_3$, ppm): δ = 8.87 (d, *J* = 3.0 Hz, 2H), 8.65 (s, 2H), 8.50 (s, 2H), 8.30 (d, *J* = 14.5 Hz, 2H), 8.08 (dd, *J* = 9.5, 16.0 Hz, 4H), 7.59-7,54 (m, 4H), 7.00 (dd, *J* = 7.0, 24.5 Hz, 2H), 6.88-6.83 (m, 2H), 6.80-6.73 (m, 4H), 4.31-4.18 (m, 4H), 1.26 (t, *J* = 7.0 Hz, 3H), 1.10 (t, *J* = 7.0 Hz, 3H); ^{13}C NMR (125 MHz, $CDCl_3$, ppm): δ = 167.62, 167.50, 151.29, 151.20, 143.24, 143.06, 140.90, 140.61, 134.55, 134.53, 133.55, 133.40, 133.29, 132.46, 131.88, 131.86, 130.01, 129.67, 129.60, 128.53, 128.35, 128.27, 127.78, 127.69, 126.99, 126.96, 126.78, 126.55, 126.24, 121.84, 121.65, 121.59, 61.49, 29.68, 13.76, 13.52. HRMS (EI): calcd for $C_{50}H_{34}O_4$ (M^+), 698.2457; found, 698.2453 (error: -0.56 ppm).

Compound **5-29** **3,3'-(indeno[2,1-a]indene-5,10-diyl)bis-(anthracene-2-carboxylic acid)**

A suspension of compound **5-28** (75 mg, 0.1 mmol) and NaOH (0.3 g, 8 mmol) in ethanol (16 mL) and THF (8 mL) was heated to reflux for overnight under argon. After mixture cooled to room temperature and the reaction mixture was poured into water. The concentration HCl was added into the

water mixture and the di-acid compound **5-29** precipitated out. Then filtered and washed the solid by water and dichloromethane to obtain the compound **5-29** (62 mg) in 90% yield. The compound **5-29** can't dissolve into common organic solvent so we did the following step directly without NMR characterization. HRMS (MALDI-TOF): calcd for $C_{46}H_{26}O_4$ (M^+), 642.1831; found, 642.1844 (error: 2.02 ppm).

Compound **5-30 pentaleno[1,2,3-de:4,5,6-d'e']dipentacene-1,13-dione**

To a suspension of acid **5-29** (60 mg, 0.1 mmol) in anhydrous dichloromethane (15 mL) was added the thionyl chloride (1.0 mL). The mixture was heated to 60 ^oC for overnight under argon, and then cooled to room temperature. The solvent and excess thionyl chloride was removed in vacuum. The anhydrous dichloromethane (15 mL) and $AlCl_3$ (80 mg, 0.6 mmol) were added in ice bath and the mixture was warmed to room temperature naturally. After stirring for overnight under argon, the 10% m/m aqueous HCl solution (20 mL) was added to quench the reaction. Then the solid was filtered and washed by the solvents (10% HCl, methanol, acetone, dichloromethane, THF) to give the di-ketone compound **5-30** (45 mg) in 80% yield. The compound **5-30** can't dissolve into common organic solvent so we did the following step directly without NMR characterization. HRMS (MALDI-TOF): calcd for $C_{46}H_{22}O_2$ (M^+), 606.1620; found, 606.1644 (error: 3.96 ppm).

Reference

[1] Wood, J. D.; Jellison, J. L.; Finke, A. D.; Wang, L.; Plunkett, K. N. *J. Am. Chem. Soc.* **2012**, 134, 15783.

[2] Koper, C.; Sarobe, M.; Jenneskens, L. W. *Phys. Chem. Chem. Phys.* **2004**, 6, 319.

[3] (a) Li, Zhen; Hong, Jianquan; Weng, Linhong; Zhou, Xigeng *Tetrahedron* **2012**, 68, 1552; (b) Bowden, Keith; Ghadir, Khalaf D. F. *J. Chem. Soc., Perkin Trans. 2* **1990**, 8, 1333.

[4] (a) Mori, K.; Kawasaki, T.; Akiyama, T. *Org. Lett.*, **2012**, 14, 1436; (b) Huang, Z.; Liu, Z.; Zhou, J. S. *J. Am. Chem. Soc.* **2011**, 133, 15882.

[5] Akula, M. R. *Org. Prep. Proced. Int.* **1990**, 22, 102.

[6] Crystallographic data for **5-1**: C_{52} H_{56} $Si_{2.}$ M_w: 737.15; Triclinic; space group P-1; a = 8.0423(3) Å, b = 16.3291(7) Å, c = 16.9633(7) Å, α = 90.551(3)^o, β = 96.422(3)^o, γ = 102.865(3)^o; V = 2156.76(15) Å^3; Z = 2; ρ_{calcd} = 1.135 Mg/m^3; R_1 =0.0593, wR_2 = 0.1547 (I > 2σ(I)); R_1 = 0.0796, wR_2 = 0.1728 (all data).

Chapter 6: Dithieno-naphthalimide Based Copolymers for Air-stable Field Effect Transistors: Synthesis, Characterization and Device Performance

6.1 Introduction

In chapters 2 – 5, aceno-fused-pentalene derivatives were synthesized and their properties and application were studied. In Chapter 4, we introduced the dicarboxylic imide group to aceno-fused pentalenes, which showed n-type FET behavior with mobilities up to 0.06 $cm^2V^{-1}s^{-1}$. In this chapter, we designed and synthesized a new building block with dicarboximide group for solution-processable polymeric semiconductors. Solution-processable organic semiconductors are attractive for their potential applications in low-cost electronics and their compatibility with plastic substrates, which is essential for fabrication of large-area and flexible devices by printing.[1] Compared with small molecule based organic semiconductors, polymeric semiconductors typically exhibit minimal grain boundaries (film uniformity) and excellent film-forming properties.[2] Since the sulfur-sulfur interaction between the thiophene rings enhances the interchain π-π stacking, polythiophenes become an important class of conjugated polymers that form some of the most environmentally and thermally stable materials.[3] The regioregular poly(3-hexylthiophene) (P3HT) is the benchmark among the polymeric electronic materials. To improve the stability of P3HT based devices which can be oxidized by oxygen, some structural modifications have been achieved

through introducing electron-withdrawing group into the polythiophene backbone. So far, several new polymers which contain thiophene backbone and electron-withdrawing group (e.g. imide group) have been designed and synthesized.[4] For example, Marks's group reported di-thiophene-imide-based polymeric semiconductors which exhibited high device performance in organic field effect transistors (OFETs).[4a, 4b] Dithienophthalimide based conjugated polymers for organic solar cells were also reported by Zhan's group.[4c]

In this chapter, we use an alternative approach by introducing the imide group into the polythiophene backbone to achieve stable and high performance p-type polymeric semiconductors. Our strategy is to introduce a new thiophene-fused naphthalimide unit (**6-4**) to the thiophene-based conjugated polymers (Scheme 6.1). The larger size conjugated building block compared to the previous reported ones is supposed to enhance intermolecular π-orbital interactions between the polymer chains and the electron-withdrawing imide group is expected to improve the stability of the polymers. Based on this building block, three alternating conjugated copolymers such as **P1** - **P3** were prepared via a Stille coupling polymerization reaction (Scheme 6.2). The optical, electrochemical properties, thermal behavior, and OFET performance of these performances were investigated in details.

6.2 Results and discussion

6.2.1 Synthesis

The synthetic routes to the monomer and polymers are outlined in Scheme 6.1 and Scheme 6.2. Bromination of the *o*-xylene and subsequent oxidation of the as-formed 1,2-dibromo-4,5-xylene gave the 4,5-dibromophthalic acid **6-1**[5]. Compound **6-1** was treated with $SOCl_2$ to give the corresponding acyl chloride. After removing the excess of $SOCl_2$, the acyl chloride reacted with 2-decyltetradecan-1-amine ($C_{24}H_{49}NH_2$) in acetic acid under reflux for 12h to afford the imide **6-2**[6] in 40% yield. Stille coupling reaction between the imide **6-2** and the tin reagent of thiophene gave the 4,5-di(thiophen-3-yl) phthathlic imide **6-3** in 90% yield. Intramolecular oxidative cyclization[7] of **6-3** by $FeCl_3$ afforded the ring-fused product **6-4** in 60% yield. It is worth noting that only the α-α coupling between the two thiophene rings took place under carefully controlled condition. The monomer **6-5** was obtained in 85% yield by bromination of **6-4** with Br_2 in $CHCl_3$. Homopolymerization of **6-5** under Yamamoto coupling condition mediated by $Ni(COD)_2$ gave an insoluble polymer. Thus dibromo-monomer **6-5** was used to prepare copolymers by reacting with (4,4'-didodecyl-[2,2'-bithiophene]-5,5'-diyl)bis-(trimethylstannane) (**6-6**)[8], (4,8-bis(dodecyloxy)benzo[1,2-b:4,5-b']-dithiophene-2,6-diyl)bis(trimethylstannane) (**6-7**)[9] and (3,6-didodecylthieno[3,2-b]thiophene-2,5-diyl) bis(trimethylstannane) (**6-8**)[10] through Stille coupling reaction to give the polymers **P1**, **P2**, and **P3**,

respectively. The three new polymers have good solubility in common organic solvents such as THF, $CHCl_3$ and chlorobenzene. The structures of these polymers were characterized by ^1H NMR spectra and elemental analysis. Their molecule weight (M_n) and polydisperisty index (PDI) were determined by gel permeation chromatography (GPC) measurements by using THF as solvent and polystyrene (PS) as standard. The M_n (PDI) are 23,586 (2.0), 28,862 (2.06) and 9,739 (1.45) for P1, P2 and P3, respectively. Maybe the steric hindrance of alkyl chain of thienothiophene unit caused the polymerization reaction slowly and low Mn of **P3**.

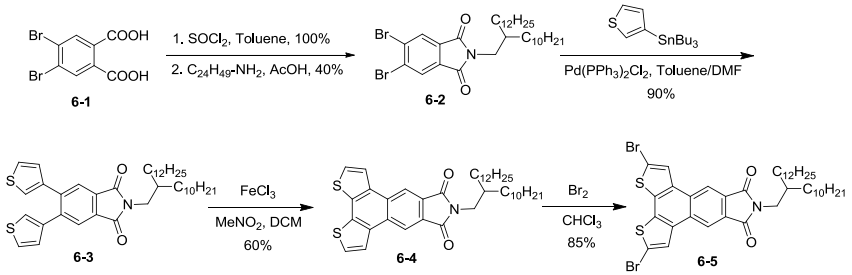

Scheme 6.1 Synthesis of the monomer **6-5.**

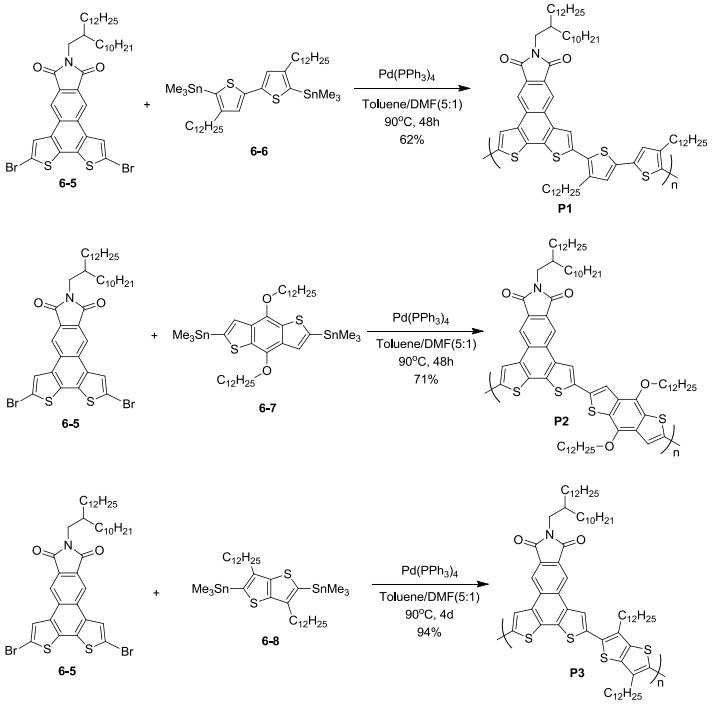

Scheme 6.2 Synthesis of polymers **P1** - **P3**.

6.2.2 Photophysical properties

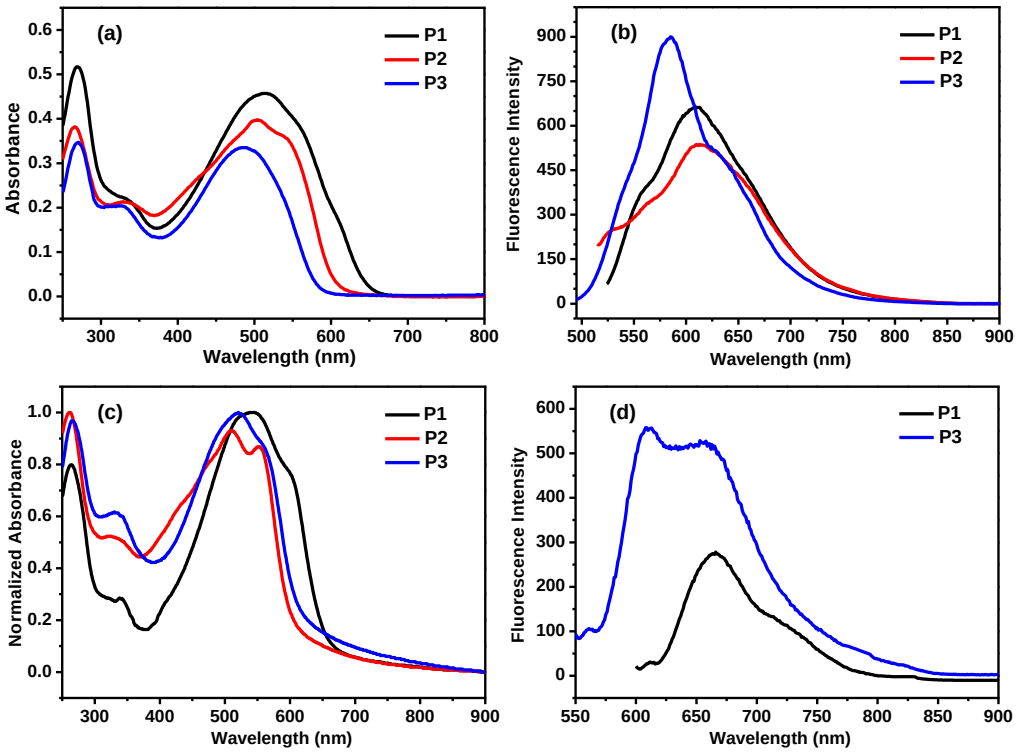

Figure 6.1 (a) UV-vis absorption spectra of **P1**, **P2** and **P3** in chloroform (10^{-5} M). (b) Photoluminescence spectra of **P1**, **P2** and **P3** in chloroform (10^{-6} M). (c) UV-vis absorption spectra of **P1**, **P2** and **P3** in spin-coated thin films. (d) Photoluminescence spectra of **P1** and **P3** in spin-coated thin films.

The UV-vis absorption and photoluminescence (PL) spectra of **P1** - **P3** were measured in chloroform solution and spin-coated thin films. The spectra are shown in Figure 6.1 and the relevant data are summarized in Table 6.1. Broad absorption bands located in the visible region were observed for the solutions and thin films of **P1** - **P3** (Figure 6.1). The absorption maxima for **P1** - **P3** in solutions are located at 514, 504 and 485 nm, respectively. In thin films, the absorption spectra showed obvious red-shift by 28, 6 and 35 nm for **P1**, **P2** and **P3**, respectiely, indicating significant intermolecular interactions between the polymer chains. Compared to **P2** and **P3**, the absorption maximum of **P1**

in solution is red-shifted 10 and 29 nm, respectively. This may be due to its more planar conformation and efficient π-conjugation. The corresponding optical energy gaps were estimated to be 1.92, 2.04 and 2.13 eV for **P1**, **P2** and **P3**, respectively, from the lowest-energy absorption edge of the absorption spectra in solution (Table 6.1). The copolymers **P1** - **P3** have weak fluorescence both in solution and in film with large Stokes shifts (3035-3525 cm^{-1}) due to significant intramolecular donor-acceptor interaction.

Table 6.1. Summary of photophysical properties data of polymers **P1** - **P3**.

	λ_{max}(abs) [nm] in solution	logε_{max} [M^{-1} cm^{-1}]	λ_{max}(em) [nm] in solution	λ_{max}(abs) [nm] in thin film	λ_{max}(em) [nm] in thin film	E_g^{Opt} [eV][a]
P1	514	4.59	609	542	666	1.92
P2	504	3.98	612	510	-	2.04
P3	485	3.35	585	520	608	2.13

[a]Optical band gap estimated from the red edge of the longest wavelength absorption in solution.

6.2.3 Electrochemical properties

Cyclic voltammetry (CV) and differential pulse voltammetry (DPV) were used to study the electrochemical properties of polymers **P1** - **P3** (Figure 6.2, Table 6.2). The potential was externally calibrated against the ferrocene/ferrocenium couple. One quasi-reversible oxidation with half-wave potential $E_{1/2}^{ox}$ at 0.42 V and one irreversible reduction wave with half-wave potential $E_{1/2}^{red}$ at -2.14 V were observed for **P1**. Polymer **P2** showed three irreversible oxidation with $E_{1/2}^{ox}$ at 0.45, 0.75 and 1.06 V, and two quasi-reversible reduction waves with $E_{1/2}^{red}$ at -2.14 and -2.30 V. Polymer **P3** exhibited one reversible oxidation with $E_{1/2}^{ox}$ at 0.44 V, and two

quasi-reversible reduction waves with $E_{1/2}^{red}$ at -2.07 and -2.23 V. The HOMO and LUMO energy levels were calculated using the following equations: [11] HOMO = - [E_{ox}^{onset} + 4.8] eV, LUMO = - [E_{red}^{onset} + 4.8] eV where E_{ox}^{onset} and E_{red}^{onset} are the onset of the first oxidation and reduction wave, respectively. The HOMO/LUMO energy levels are determined to be -4.93/-2.76, -5.07/-2.74, and -5.16/-2.81 eV for **P1**, **P2** and **P3**, respectively.. The corresponding electrochemical energy gaps E_g^{EC} (LUMO-HOMO) are estimated to be 2.17, 2.33 and 2.35 eV for **P1** - **P3**, which are larger than the optical bandgaps E_g^{opt}, and similar trend was observed for the bithiophoimide[4a] and dithienophthalimide[4c] homopolymers and copolymers.

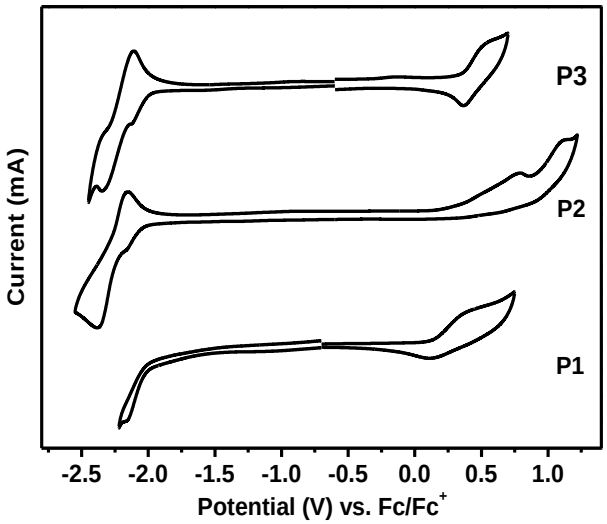

Figure 6.2 Cyclic voltammograms of polymers **P1** - **P3** in chlorobenzene with 0.1 M Bu_4NPF_6 as the supporting electrolyte, AgCl/Ag as reference electrode, Au as working electrode, Pt wire as counter electrode, and a scan rate at 50 mV s^{-1}.

Table 6.2 Summary of electrochemical properties data of polymers **P1** - **P3**.

	$E_{1/2}^{ox}$ (V)	$E_{1/2}^{red}$ (V)	HOMO [eV]	LUMO [eV]	E_g^{EC} [eV]
P1	0.42	-2.14	-4.93	-2.76	2.17
P2	0.45, 0.75, 1.06	-2.14, -2.30,	-5.07	-2.74	2.33
P3	0.44	-2.07, -2.23	-5.16	-2.81	2.35

6.2.4 Thermal properties

The thermal stability is one of the key requirements for the practical applications of organic electronic materials. The thermal stability of the polymers **P1 - P3** was examined by thermogravimetric analysis (TGA) in N_2 at a heating rate of 10 ^oC min^{-1}, and all the compounds have high thermal stability, with decomposition temperatures (T_d, corresponding to a 5% weight loss) at 367, 334, and 430 ^oC for **P1**, **P2** and **P3**, respectively (Figure 6.3a). These results confirm that the copolymers are thermally stable. The glass transition temperatures of **P1** and **P3** were observed at 213 ^oC and 313 ^oC, respectively, from differential scanning calorimetry (DSC) curves. However no obvious glass transition or melting point was observed under 300 ^oC for **P2**. The polymers **P1** and **P3** entered a nematic liquid crystalline phase above glass transition temperature, which can be judged by the typical schlieren texture under a polarizing optical microscope (Figure 6.3b, c).

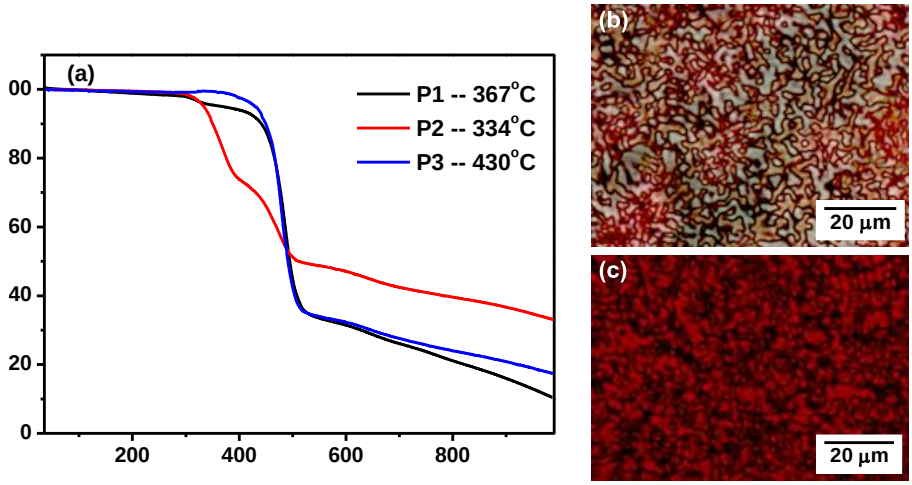

Figure 6.3 (a) Thermogravimetric analysis (TGA) of copolymer **P1 (a)**, **P2 (b)** and **P3 (c)** in N_2 at a heating rate of 10 ^oC min^{-1}; (b) Polarizing optical microscope images for **P1** at 228 ^oC upon cooling and (c) **P3** at 300 ^oC upon cooling.

6.2.5 Thin film field effect transistors characterizations

Bottom-gate top contact organic field-effect transistors were fabricated to investigate the charge transport properties of the dithieno-naphthalimide-based polymers **P1** - **P3**. For the device fabrication, the polymers were deposited by spin coating 8 mg mL^{-1} solution in dichlorobenzene (DCB) or chloroform ($CHCl_3$) onto octadecyltrichlorosilane (ODTS) modified SiO_2/Si substrates. Then the polymer films were annealed at a selected temperature under N_2 or vacuum for 0.5 h. The devices were completed by patterning the source and drain Au electrodes. The FET devices were then characterized using a Keithley SCS-4200 probe station under ambient conditions in the dark. The field-effect mobility was calculated from the following equation in the saturation regime from the gate sweep: $I_{ds} = (W/2L)\mu C_i(V_{gs} - V_{th})^2$, where W and L are the channel width and length, respectively. C_i is the capacitance of the insulating SiO_2 layer per unit, V_{gs} and V_{th} are the gate voltage and the threshold voltage, respectively.

The transfer and output characteristics of polymers **P1** - **P3** are shown in Figure 6.4 and the device performance is summarized in Table 6.3. All the devices showed p-type characteristics, and reveal an average field-effect hole mobility of 0.15, 0.003 and 0.05 $cm^2\ V^{-1}\ s^{-1}$ for **P1**, **P2** and **P3**, respectively, after thermal annealing at 200 ^oC. The maximal charge carrier mobility could reach to 0.24, 0.005, and 0.06 $cm^2\ V^{-1}\ s^{-1}$ for **P1**, **P2** and **P3**, respectively. The small energy mismatch between the HOMO energy level of copolymers and

work-function of Au electrode reduces charge injection barrier. The **P1** exhibited the best performance up to 0.15 $cm^2 V^{-1} s^{-1}$ (on/off ratio of 10^7) after the optimization. While **P3** only showed a lower performance 0.05 $cm^2 V^{-1} s^{-1}$ (on/off ratio of 10^7) compared to **P1**, probably due to the 3-fold decrease in molecular weight. However, the mobility of **P3** is still high for short oligomeric chains with less repeating units, and it holds promise for further optimization if the molecular weight could be improved. **P2** also exhibited lower charge carrier mobility around 0.003 $cm^2 V^{-1} s^{-1}$ (on/off ratio of 10^5) compared to **P1** which may be ascribed to the distorted structure (*vide infra*). As can be seen from Table 6.3, a significant increase in charge carrier mobility was observed after thermal annealing at 200 ^oC, which could be explained by that the thermal annealing could remove the solvent residue and promote polymer chain reorganization to give an efficient solid state packing.

Table 6.3 The electrical properties of the field effect transistors based on polymers **P1 - P3**.

	solvents	Annealing temperature	μ_{max}[cm^2/Vs]	μ_{ave}[cm^2/Vs]	V_T[V]	I_{on}/I_{off}	S[V/decade]
P1	DCB	Pristine	0.01	0.007±0.002	-22 to -26	2×10^6	0.85
		200 ℃	0.24	0.15±0.01	-12 to -17	3×10^7	0.8
P2	$CHCl_3$	Pristine	8.8×10^{-4}	(4.3±0.4) $\times10^{-4}$	-28 to -32	1×10^5	1.5
		200 ℃	0.005	0.003±0.001	-6 to -12	5×10^5	1.2
P3	$CHCl_3$	Pristine	0.013	0.01±0.003	-32 to -37	2×10^6	1.4
		200 ℃	0.06	0.05±0.006	-9 to -14	1×10^7	0.6

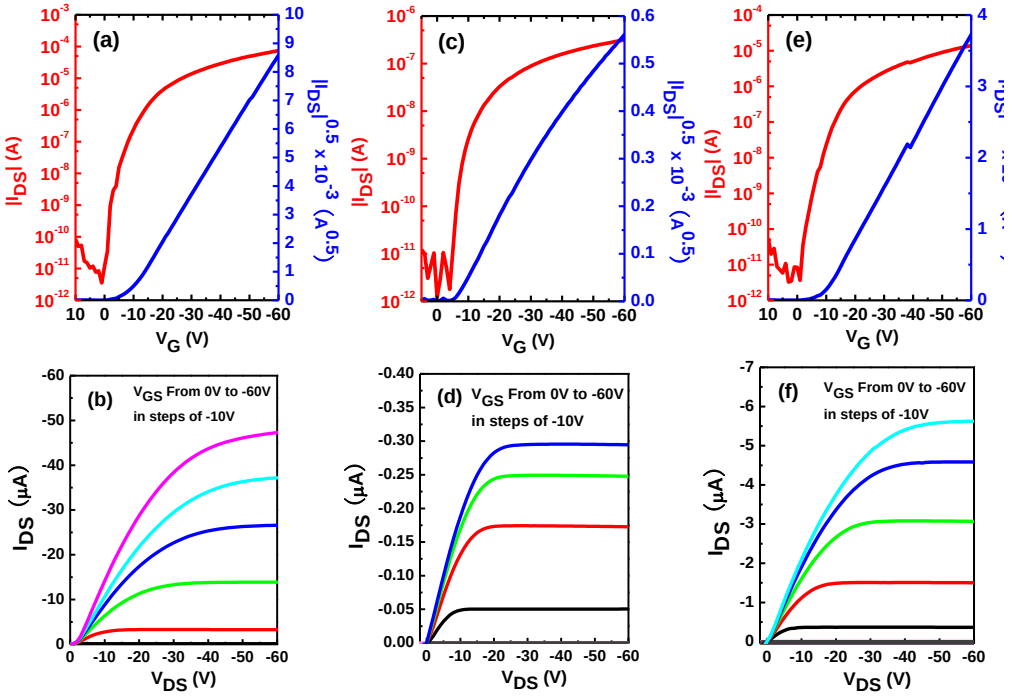

Figure 6.4 Transfer and output characteristic of the OFET devices of **P1** (a, b), **P2** (c, d), and **P3** (e, f) annealed at 200 ℃ on ODTS modified SiO_2/Si substrate.

Table 6.4 The performance change of the polymer devices after one month in ambient conditions.

Polymer	Initial			After storage		
	μ_{sat}[cm^2/Vs]	I_{on}/I_{off}	V_T[V]	μ_{sat}[cm^2/Vs]	I_{on}/I_{off}	V_T[V]
P1	0.15	3×10^7	-12 to -17	0.08	8×10^6	-15 to -20
P2	0.003	5×10^5	-6 to -12	0.001	1×10^5	-8 to -12
P3	0.05	1×10^7	-9 to -14	0.018	3×10^6	-10 to -15

6.2.6 Thin film morphology and microstructure

In order to understand the effect of the polymer structure and thermal annealing on the electrical performance of the present copolymers, the thin film microstructure and surface morphology were studied by X-ray diffraction (XRD) and tapping-mode atomic force microscopy (AFM). Figure 6.5 shows

the AFM images of the polymer thin film before and after thermal annealing. All the polymer thin films are uniform and display microcrystalline structure. Polymer **P1** showed largest grain size, while only smaller grains were observed for **P2** and **P3**. After thermal annealing, the rms surface roughness increased from 1.2 nm to 1.9 nm for **P1**, from 0.4 nm to 0.55 nm for **P2**, and from 0.36 nm to 0.5 nm for **P3**. Figure 6.6 shows thin film XRD patterns of **P1** - **P3** and a single family of Bragg reflections was found for all the polymers. For polymers **P1** and **P3**, up to third order diffraction peaks was observed. The peak intensity for **P1** is higher than **P3**, indicating its higher molecular order. The primary peak with a 2θ angle of 2.98° and 2.82° was determiend for **P1** and **P3**, respectively, which are correlated to the d-spacing values of 29.6 Å and 31.3 Å. A lamellar layered structure can be figured out for this two copolymers. While for **P2** only a week first order peak (2θ = 2.98 degree, d = 33.1 Å) was observed indicating its amorphous structure which results in a lower charge carrier mobility. The observed more ordered microstructure in **P1** is in accord with its higher OFET mobility versus the other polymers.

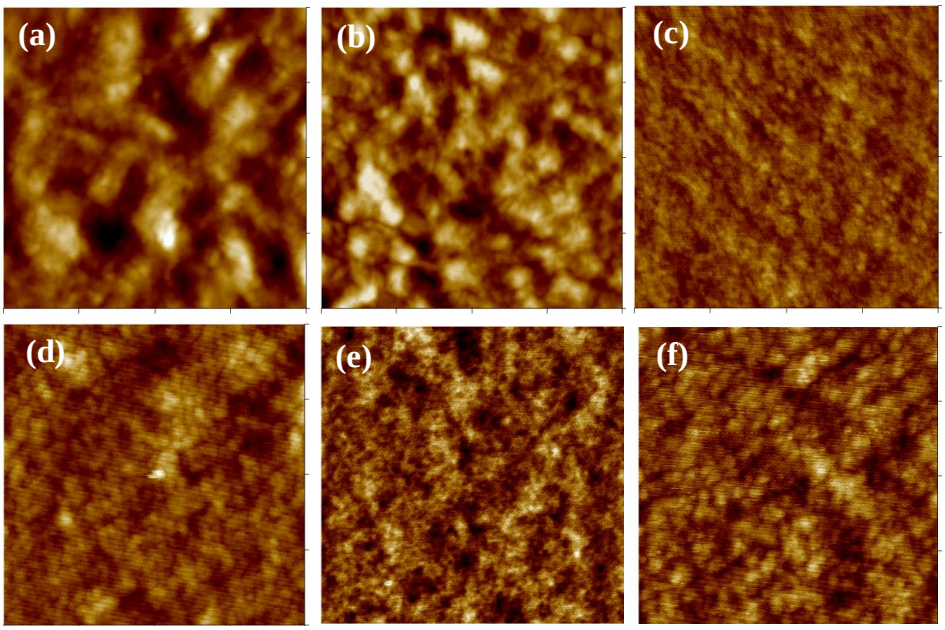

Figure 6.5 Tapping mode AFM images (1 um × 1 um) of pristine (left) and thermal annealed (right) thin films of **P1** (a, b), **P2** (c, d), and **P3** (e, f) spin-coated from DCB or $CHCl_3$ solution on ODTS modified SiO_2/Si substrate.

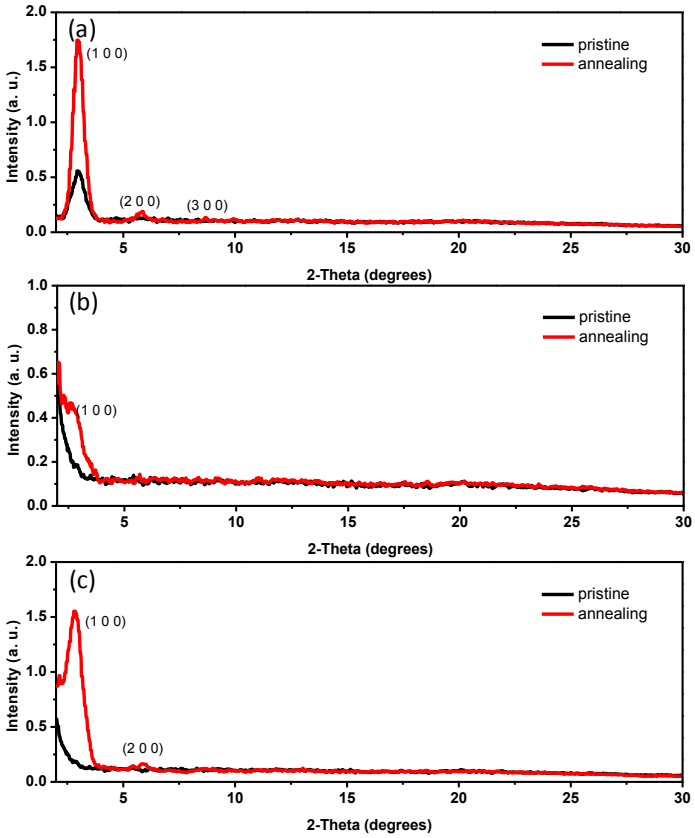

Figure 6.6 The thin film XRD patterns of **P1** (a), **P2** (b) and **P3** (c).

6.3 Summary

In this chapter, we have designed and synthesized a new thiophene-fused naphthalimide and prepared three conjugated copolymers with different thiophene units. The new polymers have good solubility in common organic solvents and exhibit good thermal stability. The **P1** exhibited the highest average hole mobility up to 0.15 cm^2 V^{-1} s^{-1} (on/off ratio of 10^7) after optimization. The similar structure dithiopheneimide based copolymers [4a,4b] exhibited a hole mobility of ~0.1 cm^2 V^{-1} s^{-1}. Another similar structure dithienophthalimide based copolymers[4c] exhibited a hole mobility of 10^{-6} cm^2 V^{-1} s^{-1} and PCE of 0.3%. The device performance can be correlated to their different polymer structure and microstructure in thin film. All the polymers showed relatively good environmental stability after storing in air. Synthesis and applications of new polymers based on the new building block **6-4** will be studied in future work.

6.4 Experiment section

6.4.1 General characterization method

^1H and ^{13}C NMR spectra were recorded using Advance 500 MHz Bruker spectrometer in $CDCl_3$ with tetramethylsilane (TMS) as the internal standard. The chemical shift was recorded in ppm and the following abbreviations were used to explain the multiplicities: s = singlet, d = doublet, t = triplet, m = multiplet, br = broad. Column chromatography was performed on silica gel 60 (Merck 40-60 nm, 230-400 mesh). EI mass spectra were recorded on Agilent

5975C DIP/MS mass spectrometer. Elemental analyses (C, H, and N) were performed on a Vario EL Elementar (Elementar Analyzen-systeme, Hanau, Germany). UV-vis absorption and fluorescence spectra were recorded on a Shimadzu UV-1700 spectrophotometer and a RF- 5301 fluorometer, respectively. Cyclic voltammetry and differential pulse voltammetry measurements were performed in HPLC grade chlorobenzene on a CHI 620C electrochemical analyzer with a three-electrode cell, using 0.1 M Bu_4NPF_6 as supporting electrolyte, AgCl/Ag as reference electrode, gold disk as working electrode, Pt wire as counter electrode, and scan rate at 50 mV s^{-1}. The potential was externally calibrated against the ferrocene/ferrocenium couple. Thermogravimetric analysis (TGA) was carried out on a TA instrument 2960 at a heating rate of 10 ℃ min^{-1} under nitrogen flow. Differential scanning calorimetry (DSC) was performed on a TA instrument 2920 at a heating/cooling rate of 10 ℃ min^{-1} under nitrogen flow. GPC were performed on a Waters 410 differential refractometer with two columns connected in series with a THF (the mobile phase) flowing rate of 0.3 mL min^{-1}. Tapping-mode Atomic Force Microscopy (TM-AFM) was performed on a Nanoscope V microscope (Veeco Inc.). X-ray diffraction (XRD) patterns of the thin film were measured on a Bruker-AXS D8 DISCOVER with GADDS X-ray diffractometer. Copper Kα line was used as a radiation source with λ = 1.5418 Å.

6.4.2 Synthesis

All reagents were purchased from commercial sources without further purification. Anhydrous dichloromethane (DCM), *N*, *N*-dimethylformaldehyde (DMF) was distilled from CaH_2. Toluene and THF were distilled from sodium-benzophenone immediately prior to use. 4,5-dibromophthalic acid (**6-1**)[5], tributyl(thiophen-3-yl)stannane, 2-decyltetradecan-1-amine, (4,4'-didodecyl-[2,2'-bithiophene]-5,5'-diyl)bis(trimethylstannane) (**6-6**)[8], (4,8-bis(dodecyloxy)benzo[1,2-b:4,5-b']dithiophene-2,6-diyl)bis(trimethylstannane) (**6-7**)[9], (3,6-didodecylthieno[3,2-b]thiophene-2,5-diyl)bis-(trimethylstannane) (**6-8**)[10] were prepared by following literature procedures.

Compound **6-2 5,6-dibromo-2-(2-decyltetradecyl)isoindoline-1,3-dione**

To a suspension of dibromo-phathalic acid **6-1** (1.51 g, 4.7 mmol) and DMF (3 drops) in toluene (35 mL) was added dropwise the oxalyl chloride (1.7 mL, 19.8 mmol). The mixture was heated to 80 ^{o}C for 1 h under argon, and then cooled to room temperature. The solvent was removed in vacuum. The amine $C_{24}H_{49}NH_2$ (1.60 g, 4.5 mmol) and anhydrous acetic acid (30 mL) were added and the mixture was heated to 145 ^{o}C for 1.5 h under argon. The mixture was cooled to room temperature and extracted with EtOAc (50 mL ×2). The combined organic phase was washed with brine (100 mL ×3) and saturated $NaHCO_3$ (100 mL) and dried over anhydrous Na_2SO_4. The organic solvent was removed under reduced pressure and the residue was purified by column chromatography (silica gel, EtOAc/Hexane = 1:30) to afford compound **6-2**

(1.16 g) in 40% yield. ^{1}H NMR (500 MHz, $CDCl_3$, ppm): δ = 8.07 (s, 2H), 3.55 (d, *J* = 7.0 Hz, 2H), 1.84 (br, 1H), 1.33-1.23 (m, 40H), 0.88 (t, *J* = 6.9 Hz, 6H); ^{13}C NMR (125 MHz, $CDCl_3$, ppm): δ = 166.71, 131.79, 131.22, 128.33, 42.75, 36.92, 31.91, 31.44, 29.91, 29.67, 29.64, 29.61, 29.55, 29.34, 29.32, 26.22, 22.68, 14.09. High resolution (HR) MS (EI): calcd for $C_{32}H_{51}Br_2NO_2$ (M^+), 641.2266; found, 641.2250 (error: -2.45 ppm).

Compound **6-3 2-(2-decyltetradecyl)-5,6-di(thiophen-3-yl)isoindoline-1,3-dione**

A mixture of compound **6-2** (1.610 g, 2.5 mmol), 3-tributylstannylthiophene (2.100 g, 5.6 mmol) and catalyst $Pd(PPh_3)_2Cl_2$ (177 mg, 5%) in anhydrous DMF (3 mL) and toluene (25 mL) was degassed by three freeze-pupm-thaw cycles. The mixture was heated at 90 ^{o}C under argon for overnight. The mixture was cooled to room temperature and extracted with EtOAc (30 mL ×2). The combined organic phase was washed with $NaHCO_3$ (50 mL ×2) and brine (50 mL ×1). The organic phase was dried over anhydrous Na_2SO_4 and organic solvent was removed under reduced pressure. The crude product was purified by column chromatography (EtOAc/Hexane = 1:30) to afford compound **6-3** (1.50 g) in 90% yield. ^{1}H NMR (500 MHz, $CDCl_3$, ppm): δ = 7.90 (s, 2H), 7.24-7.23 (m, 2H), 7.19-7.18 (m, 2H), 6.80-6.79 (dd, ^{3}J =4.4 Hz, ^{4}J = 1.3 Hz, 2H), 3.59 (d, *J* = 7.6 Hz, 2H), 1.91 (br, 1H), 1.39-1.25 (m, 40H), 0.94-0.86 (m, 6H) ; ^{13}C NMR (125 MHz, $CDCl_3$, ppm): δ = 168.45, 141.04, 140.42, 130.89, 128.28, 125.65, 124.94, 124.46, 42.48, 37.05, 31.91, 31.54,

29.98, 29.66, 29.64, 29.59, 29.34, 26.32, 22.67, 14.08. HRMS (EI): calcd for $C_{40}H_{57}NO_2S_2$ (M^+), 647.3831; found, 647.3822 (error: -1.39 ppm).

Compound **6-4 9-(2-decyltetradecyl)-8*H*-dithieno-[3',2':3,4;2'',3'':5,6]-benzo[1,2-f]isoindole-8,10(9*H*)-dione**

A solution of compound **6-3** (0.20 g, 0.3 mmol) in anhydrous DCM (200 mL) was sparged with argon for 30 minute. The solution of $FeCl_3$ (0.20 g, 1.2 mmol) in CH_3NO_2 (2 mL) was added dropwise to the reaction mixture via syringe at room temperature. After 20 minute stirring at room temperature, the reaction was quenched by 5 mL MeOH. (Caution: during the reaction, keep stirring and sparging with argon). The mixture was washed with $NaHCO_3$ (100 mL ×1) and brine (100 mL ×2). The organic phase was dried over anhydrous Na_2SO_4 and organic solvent was removed under reduced pressure. The crude product was purified by column chromatography ($CHCl_3$/Hexane = 1:10) to afford compound **6-4** (0.12 g) in 60% yield. ^{1}H NMR (500 MHz, $CDCl_3$, ppm): δ = 8.64 (s, 2H), 7.96 (d, *J* = 5.1 Hz, 2H), 7.58 (d, *J* = 5.1 Hz, 2H), 3.67 (d, *J* = 7.6 Hz, 2H), 1.96 (br, 1H), 1.45-1.15 (m, 40H), 0.88-0.83 (m, 6H); ^{13}C NMR (125 MHz, $CDCl_3$, ppm): δ = 168.61, 134.71, 134.61, 130.00, 127.73, 125.32, 122.93, 120.11, 42.61, 37.08, 31.89, 31.57, 30.00, 29.67, 29.65, 29.63, 29.61, 29.33, 26.33, 22.67, 22.65, 14.10, 14.08. HRMS (EI): calcd for $C_{40}H_{55}NO_2S_2$ (M^+), 645.3674; found, 645.3674 (error: -0.11 ppm).

Compound **6-5 2,5-dibromo-9-(2-decyltetradecyl)-8*H*-dithieno-[3',2':3,4;2'',3'':5,6]benzo[1,2-f]isoindole-8,10(9*H*)-dione**

To a solution of compound **6-4** (1.50 g, 2.3 mmol) in $CHCl_3$ (60mL) was added dropwise Br_2 (0.27 mL, 5.2 mmol) at 0 ^oC. After stirring at room temperature for overnight, the reaction was quenched by 50 mL saturated $NaHCO_3$ solution. The mixture was washed with $NaHCO_3$ (100 mL ×1) and brine (100 mL ×2). The organic phase was dried over anhydrous Na_2SO_4 and organic solvent was removed under reduced pressure. The crude product was purified by column chromatography ($CHCl_3$/Hexane = 1:10) to afford compound **6-5** (1.59 g) in 85% yield. ^1H NMR (500 MHz, $CDCl_3$, ppm): δ = 8.40 (s, 2H), 7.78 (s, 2H), 3.67 (d, *J* = 7.6 Hz, 2H), 1.95 (br, 1H), 1.40-1.22 (m, 40H), 0.88-0.84 (m, 6H); ^{13}C NMR (125 MHz, $CDCl_3$, ppm): δ = 168.01, 134.54, 134.22, 128.65, 128.31, 125.55, 119.84, 114.63, 42.82, 37.10, 31.90, 31.65, 29.99, 29.67, 29.64, 29.59, 29.33, 26.36, 22.65, 14.05. HRMS (EI): calcd for $C_{40}H_{53}Br_2NO_2S_2$ (M^+), 803.1864; found, 803.1872 (error: 1.05 ppm).

Copolymer **P1**

A mixture of monomer compound **6-5** (161 mg, 0.2 mmol), monomer 4,4'-didocecyl-5,5' -trimethylstannyl-2,2'-bithiophene (**6-6**) (166 mg, 0.2 mmol), and catalyst $Pd(PPh_3)_4$ (5 mg, 2 mol%) in anhydrous toluene (5 mL) and DMF (1 mL) was heated to 95 ^oC for 48 h under argon. After cooling to room temperature, the polymer was precipitated in acetone/methanol (1:1) solvent and filtered. Then the polymer was dissolved in $CHCl_3$, precipitated in methanol/THF (4:1) and filtered. This procedure was repeated for five times to give the pure copolymer **P1** as a dark red solid (142 mg) in 62% yield. GPC

(THF at 33 ^{o}C): M_n = 23,586 g mol^{-1}, M_w = 47,176 g mol^{-1}, and PDI = 2.00 (against PS standard). ^{1}H NMR (500 MHz, $CDCl_3$, ppm) 8.19 (br, 2H), 7.58 (br, 2H), 6.94 (br, 2H), 3.69 (br, 2H), 2.91 (br, 4H), 2.10-1.10 (m, 81H), 0.88 (m, 12H). Elemental Analysis: calculated for $(C_{72}H_{105}NO_2S_4)_n$: C, 75.53; H, 9.24; N, 1.22. Found: C, 75.34; H, 9.12; N, 1.18.

Copolymer **P2**

A mixture of monomer compound **6-5** (300 mg, 0.37 mmol), monomer (4,8-bis(dodecyloxy)benzo[1,2-b:4,5-b']dithiophene-2,6-diyl)bis(trimethylstan nane) (**6-7**) (330 mg, 0.37 mmol), and catalyst $Pd(PPh_3)_4$ (8.6 mg, 2mol%) in anhydrous toluene (10 mL) and DMF (2 mL) was heated to 95 ^{o}C for 48 h under argon. After cooling to room temperature, the polymer was precipitated in acetone/ methanol (1:1) solvent and filtered. The polymer was fractionated by Soxhlet extraction using MeOH, acetone, hexane, and $CHCl_3$, respectively. And then the polymer was dissolved in $CHCl_3$, precipitated in methanol/THF (3:1) and filtered. This procedure was repeated for five times to give the pure copolymer **P2** as a dark red solid (320 mg) in 71% yield. GPC (THF at 33 ^{o}C): M_n = 28,862 g mol^{-1}, M_w = 59,564 g mol^{-1}, and PDI = 2.06 (against PS standard). ^{1}H NMR (500 MHz, $C_2D_2Cl_4$, ppm) 8.60-6.80 (m, 6H), 4.45 (br, 4H), 3.74 (m, 2H), 2.60-1.10 (br, 81H) 0.93 (m, 12H). Elemental Analysis: calculated for $(C_{74}H_{105}NO_4S_4)_n$: C, 74.01; H, 8.81; N, 1.17. Found: C, 74.18; H, 8.89; N, 1.12.

Copolymer **P3**

A mixture of monomer compound **6-5** (300 mg, 0.37 mmol), monomer (3,6-didodecylthieno[3,2-b]thiophene-2,5-diyl)bis(trimethylstannane) (**6-8**) (300 mg, 0.37 mmol), and catalyst $Pd(PPh_3)_4$ (8.6 mg, 2mol%) in anhydrous toluene (10 mL) and DMF (2 mL) was heated to 95 ^oC for 4 days under argon. After cooling to room temperature, the polymer was precipitated in acetone/methanol (1:1) solvent and filtered. The polymer was fractionated by Soxhlet extraction using MeOH, acetone, hexane, respectively (the copolymer **P3** has limited solubility in hot hexane). And then the polymer was dissolved in $CHCl_3$, precipitated in methanol/THF (5:1) and filtered. This procedure was repeated for five times to give the copolymer **P3** as a red solid (390 mg) in 94% yield. GPC (THF at 33 ^oC): M_n = 9,739 g mol^{-1}, M_w = 14,131 g mol^{-1}, and PDI = 1.45 (against PS standard). ^1H NMR (500 MHz, $CDCl_3$, ppm) 8.32 (br, 2H), 7.72 (br, 2H), 3.67 (br, 2H), 3.12 (br, 4H), 2.10-1.10 (m, 81H), 0.88 (m, 12H). Elemental Analysis: calculated for $(C_{70}H_{103}NO_2S_4)_n$: C, 75.15; H, 9.28; N, 1.25. Found: C, 75.28; H, 9.35; N, 1.21.

References

[1] (a) Forrest, S. R. *Nature* **2004**, 428, 911; (b) Mayer, A. C.; Scully, S. R.; Hardin, B. E.; Rowell, M. W.; McGehee, M. D. *Mater. Today* **2007**, 10, 28; (c) Günes, S.; Neugebauer, H.; Sariciftci, N. S. *Chem. Rev.* **2007**, 107, 1324; (d) Arias, A. C.; Rivnay, J. D. I.; McCulloch, J.; Salleo, A. *Chem. Rev.* **2010**, 110, 3; (e) Dimitrakopoulos, C. D.; Malenfant, P. R. L. *Adv. Mater.* **2002**, 14, 99; (f) Wen, Y.; Liu, Y. *Adv. Mater.* **2010**, 22, 1331.

[2] (a) Allard, S.; Forster, M.; Souharce, B.; Thiem, H.; Scherf, U. *Angew. Chem., Int. Ed.* **2008**, 47, 4070; (b) Katz, H. E.; Bao, Z.; Gilat, S. L. *Acc. Chem. Res.* **2001**, 34, 359; (c) Osaka, I.; Zhang, R.; Sauve, G.; Smilgies, D.-M.; Kowalewski, T.; McCullough, R. D. *J. Am. Chem. Soc.* **2009**, 131, 2521; (d) Zhang, M.; Tsao, H. N.; Pisula, W.; Yang, C.; Mishra, A. K.; Müllen, K. *J. Am. Chem. Soc.* **2007**, 129, 3472; (e) Tsao, H. N.; Cho, D.; Andreasen, J. W.; Rouhanipour, A.; Breiby, D. W.; Pisula, W.; Müllen, K. *Adv. Mater.* **2009**, 21, 209.

[3] (a) McCullough, R. D. *Adv. Mater.* **1998**, 10, 93; (b) Sirringhaus, H.; Tessler, N.; Friend, R. H. *Science* **1998**, 280, 1741; (c) Sirringhaus, H.; Brown, P. J.; Friend, R. H.; Nielsen, M. M.; Bechgaard, K.; Langeveld-Voss, B. M. W.; Spiering, A. J. H.; Janssen, R. A. J.; Meijer, E. W.; Herwig, P.; Leeuw, D. M. d. *Nature* **1999**, 401, 685; (d) Ong, B. S.; Wu, Y.; Liu, P.; Gardner, S. *J. Am. Chem. Soc.* **2004**, 126, 3378; (e) Li, Y.; Wu, Y.; Liu, P.; Birau, M.; Pan, H.; Ong, B. S. *Adv. Mater.* **2006**, 18, 3029.

[4] (a) Letizia, J. A.; Salata, M.; Tribout, C. M.; Facchetti, A.; Ratner, M. A.; Marks, T. J. *J. Am. Chem. Soc.* **2008**, 130, 9679; (b) Guo, X.; Ortiz, R. P.; Zheng, Y.; Hu, Y.; Noh, Y.; Baeg, K.; Facchetti, A.; Marks, T. J. *J. Am. Chem. Soc.* **2011**, 133, 1405; (c) Wang, H.; Shi, Q.; Lin, Y.; Fan, H.; Cheng, P.; Zhan, X.; Li, Y.; Zhu, D. *Macromolecules* **2011**, 44, 4213.

[5] (a) Ashton, P. R.; Girreser, U.; Giuffrida, D.; Kohnke, F. H.; Mathias, J. P.; Raymo, F. M.; Slawin, A. M. Z.; Stoddart, J. F.; Williams, D. J. *J. Am.*

Chem. Soc. **1993**, 115, 5422; (b) Opris, D. M.; Nüesch, F.; Löwe, C.; Molberg, M.; Nagel, M. *Chem. Mater.* **2008**, 20, 6889.

[6] Zhang, Q. T.; Tour, J. M. *J. Am. Chem. Soc.* **1997**, 119, 5065.

[7] (a) Wu, J.; Watson, M. D.; Zhang, L.; Wang, Z.; Müllen, K. *J. Am. Chem. Soc.* **2004**, 126, 177; (b) Luo, J.; Zhao, B.; Shao, J.; Lim, K. A.; Chan, H. S. O.; Chi, C. *J. Mater. Chem.* **2009**, 19, 8327.

[8] (a) Usta, H.; Risko, C.; Wang, Z.; Huang, H.; Deliomeroglu, M. K.; Zhukhovitskiy, A.; Facchetti, A.; Marks, T. J. *J. Am. Chem. Soc.* **2009**, 131, 5586; (b) Zagbrska, M.; Krische, B. *Polymer* **1990**, 31, 1379.

[9] (a) Hou, J.; Park, M.-H.; Zhang, S.; Yao, Y.; Chen, L.-M.; Li, J.-H.; Yang, Y. *Macromolecules* **2008**, 41, 6012; (b) Zhang, Y.; Hau, S. K.; Yip, H.-L.; Sun, Y.; Acton, O.; Jen, A. K.-Y. *Chem. Mater.* **2010**, 22, 2696.

[10] (a) Heeney, M.; Wagner, R.; McCulloch, I.; Tierney, S. *Patent* WO2005111045, **2005**; (b) Lee, E. K.; Lee, B. L.; Han, K. M.; Lee, S. Y.; Jeong, E. J. *Patent* EP1993105, **2008**; (c) He, Y.; Wu, W.; Zhao, G.; Liu, Y.; Li, Y. *Macromolecules* **2008**, 41, 9760; (d) He, M.; Zhang, F. *J. Org. Chem.* **2007**, 72, 442.

[11] (a) Pommerehne, J.; Vestweber, H.; Guss, W.; Mahrt, R. F.; Bassler, H.; Porsch, M.; Daub, J. *Adv. Mater.* **1995**, 7, 551; (b) Chi, C.; Wegner, G. *Macromol. Rapid Commun.* **2005**, 26, 1532; (c) Chi, C.; Im, C.; Enkelmann, V.; Ziegler, A.; Lieser, G.; Wegner, G. *Chem. Eur. J.* **2005**, 11, 6833.

Appendix

NMR spectra of target molecules

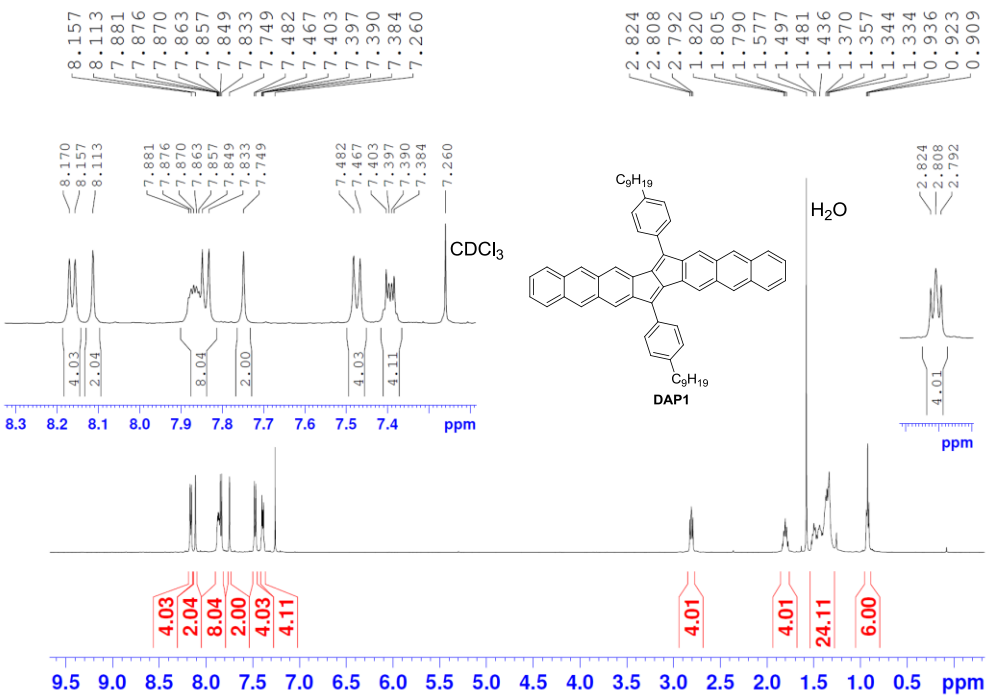

^{1}H NMR (500 MHz) spectrum of compound **DAP1** in $CDCl_3$

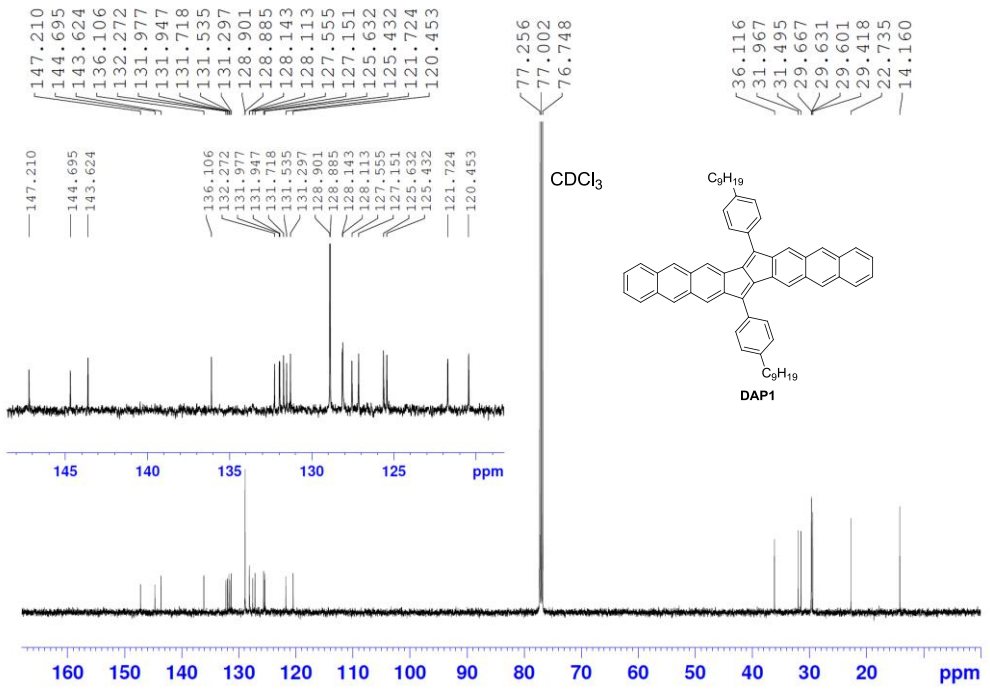

^{13}C NMR (125 MHz) spectrum of compound **DAP1** in $CDCl_3$

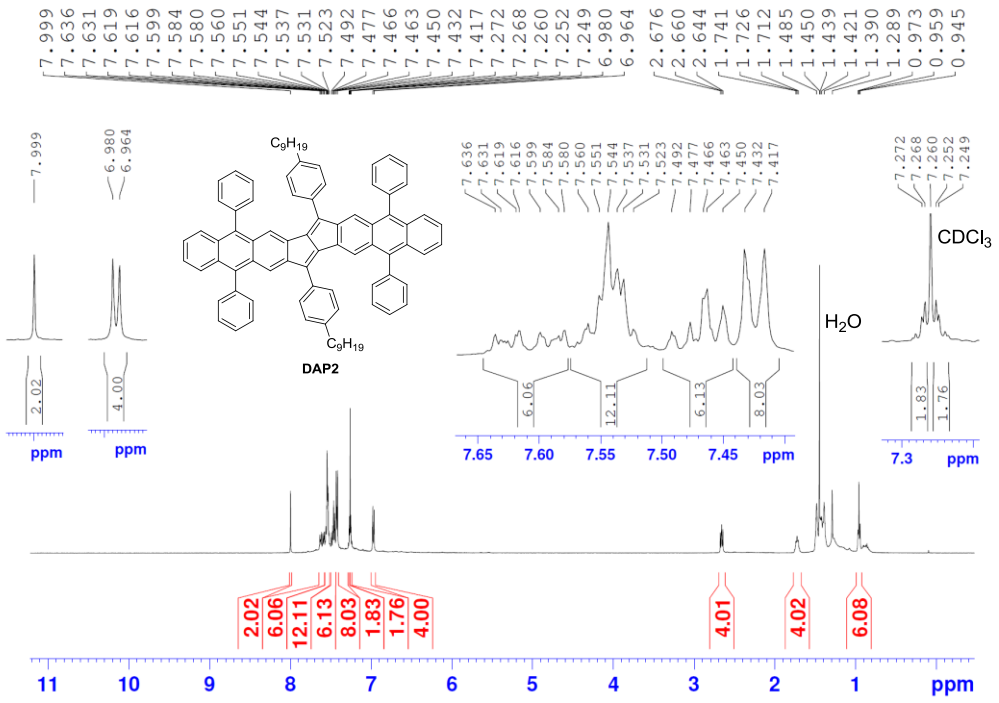

^{1}H NMR (500 MHz) spectrum of compound **DAP2** in $CDCl_3$

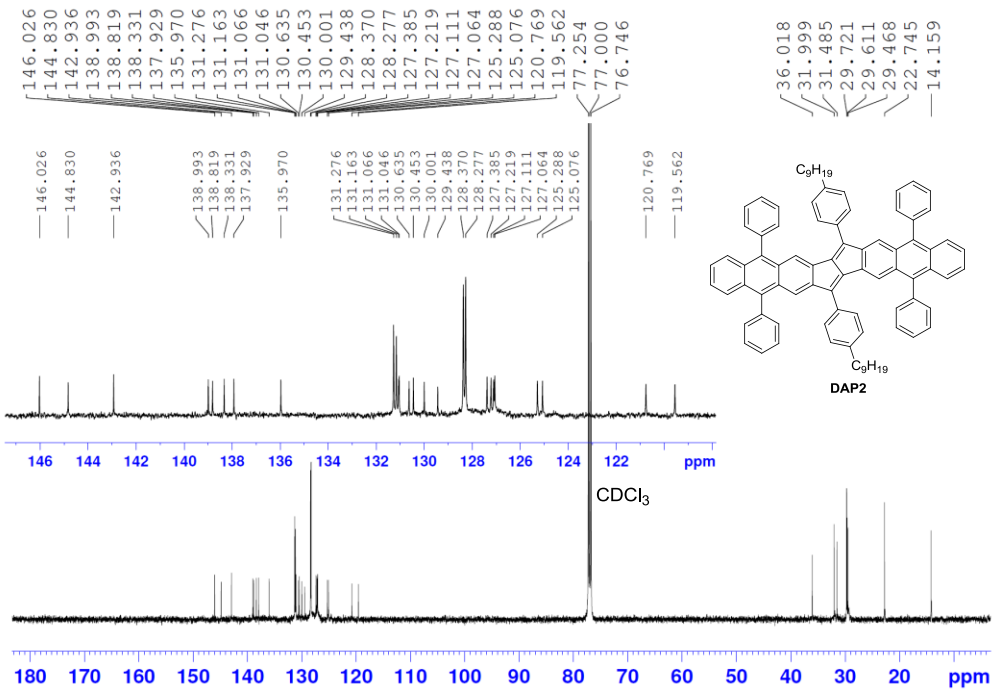

^{13}C NMR (125 MHz) spectrum of compound **DAP2** in $CDCl_3$

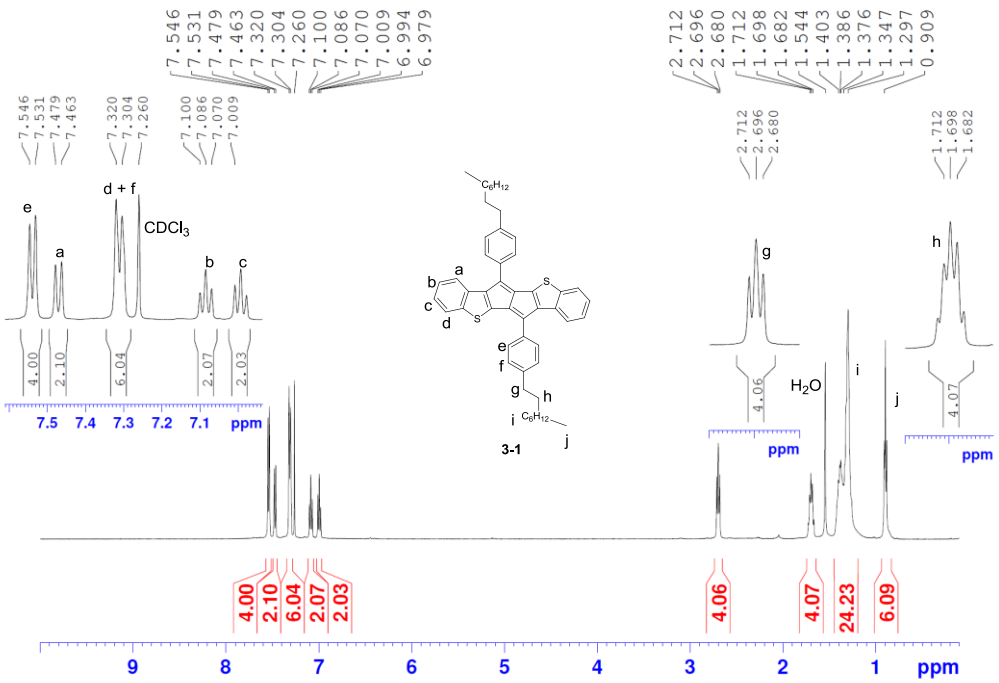

^{1}H NMR (500 MHz) spectrum of compound **3-1** in $CDCl_3$

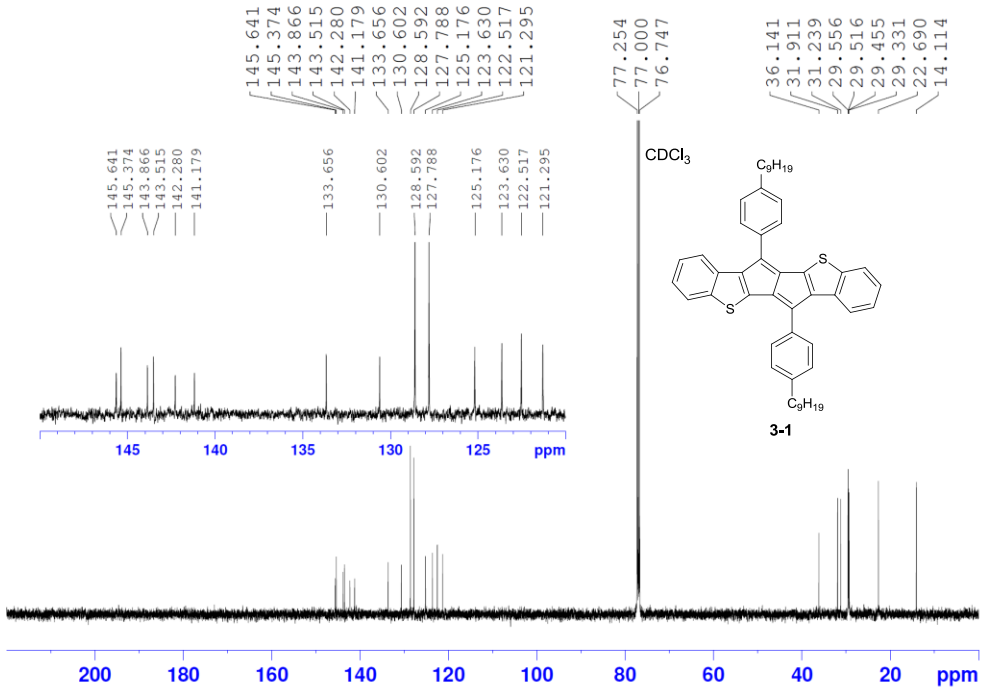

^{13}C NMR (125 MHz) spectrum of compound **3-1** in $CDCl_3$

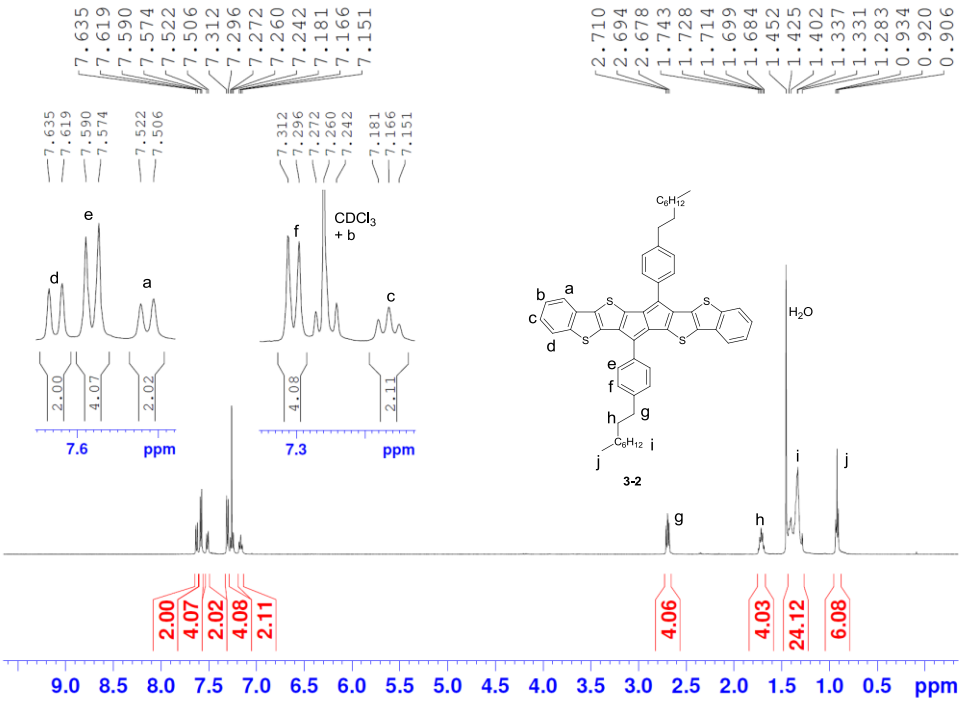

^{1}H NMR (500 MHz) spectrum of compound **3-2** in $CDCl_3$

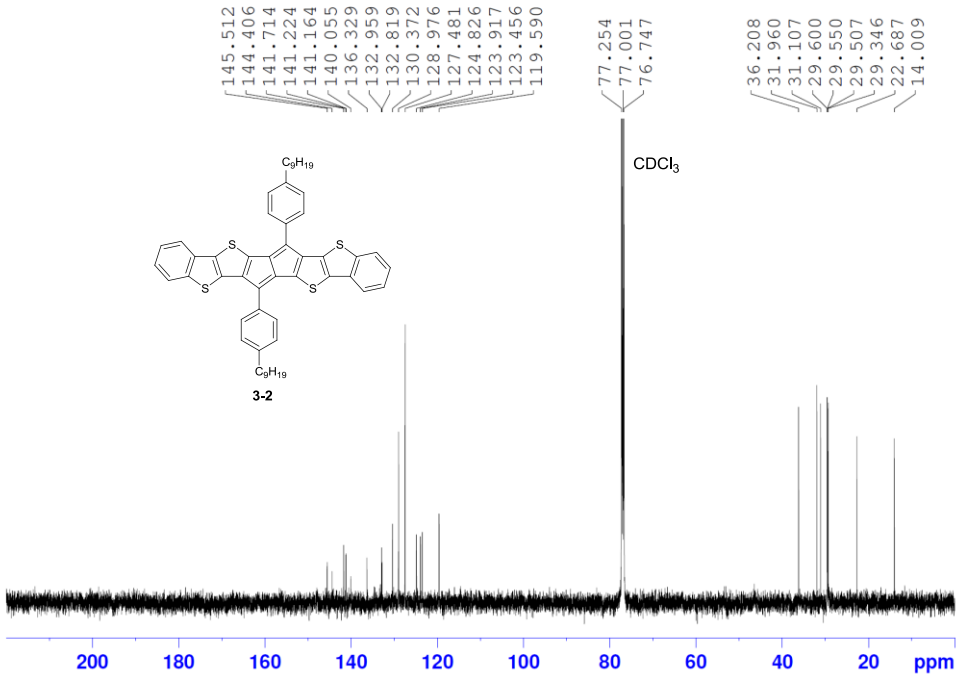

^{13}C NMR (125 MHz) spectrum of compound **3-2** in $CDCl_3$

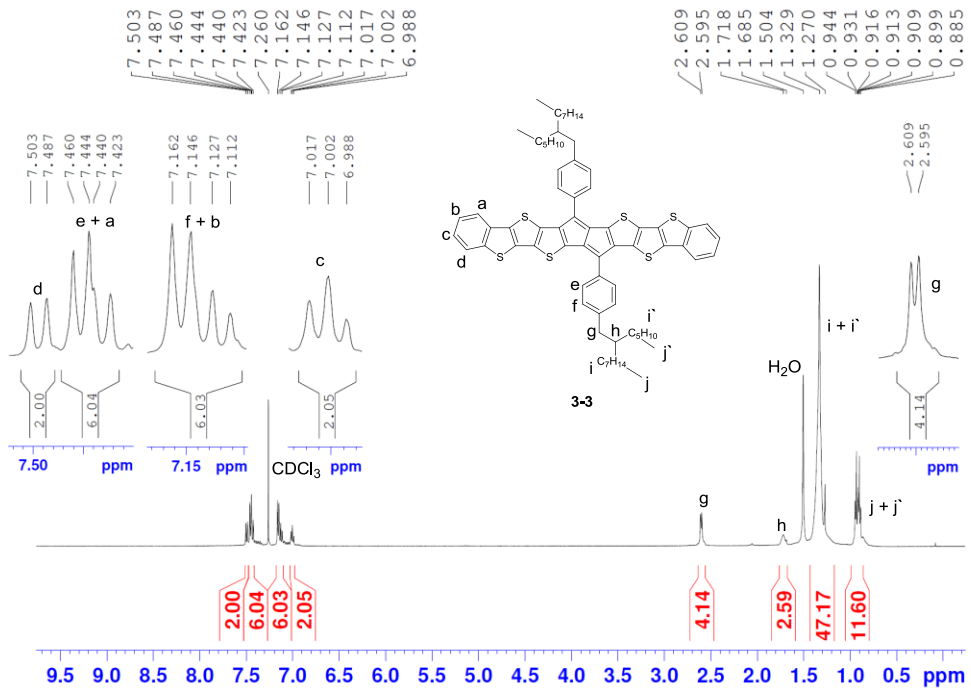

^{1}H NMR (500 MHz) spectrum of compound **3-3** in $CDCl_3$

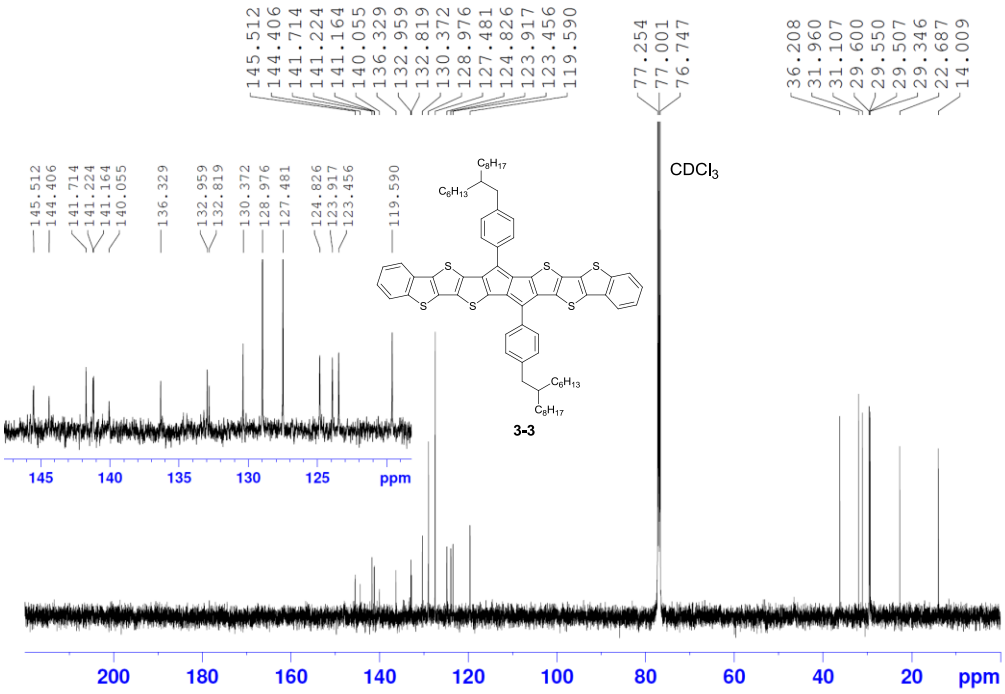

^{13}C NMR (125 MHz) spectrum of compound **3-3** in $CDCl_3$

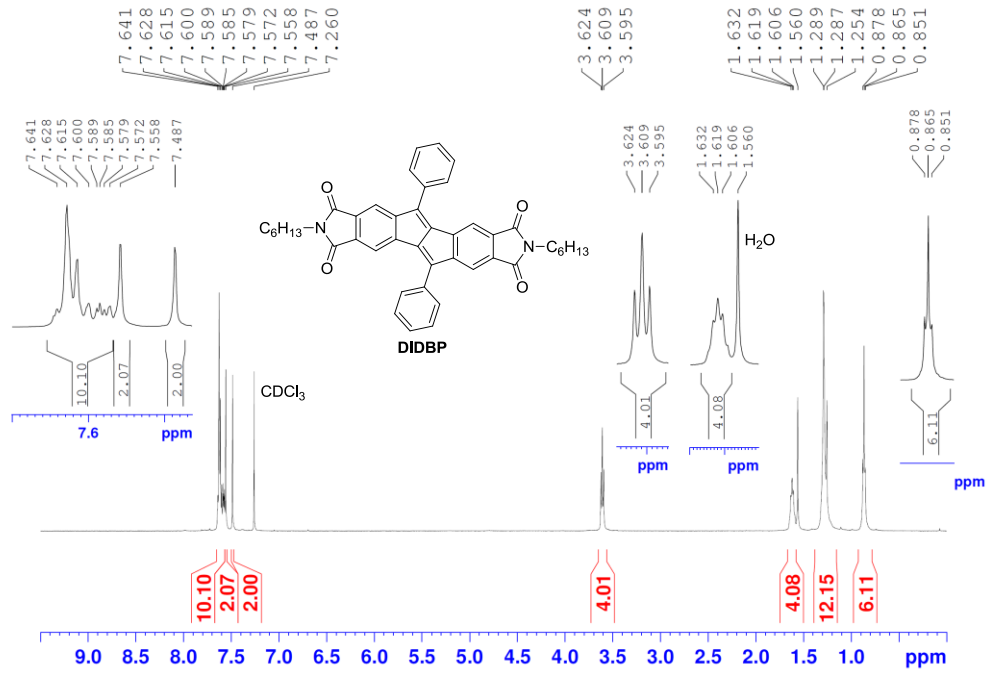

^{1}H NMR (500 MHz) spectrum of compound **DBPDI** in $CDCl_3$

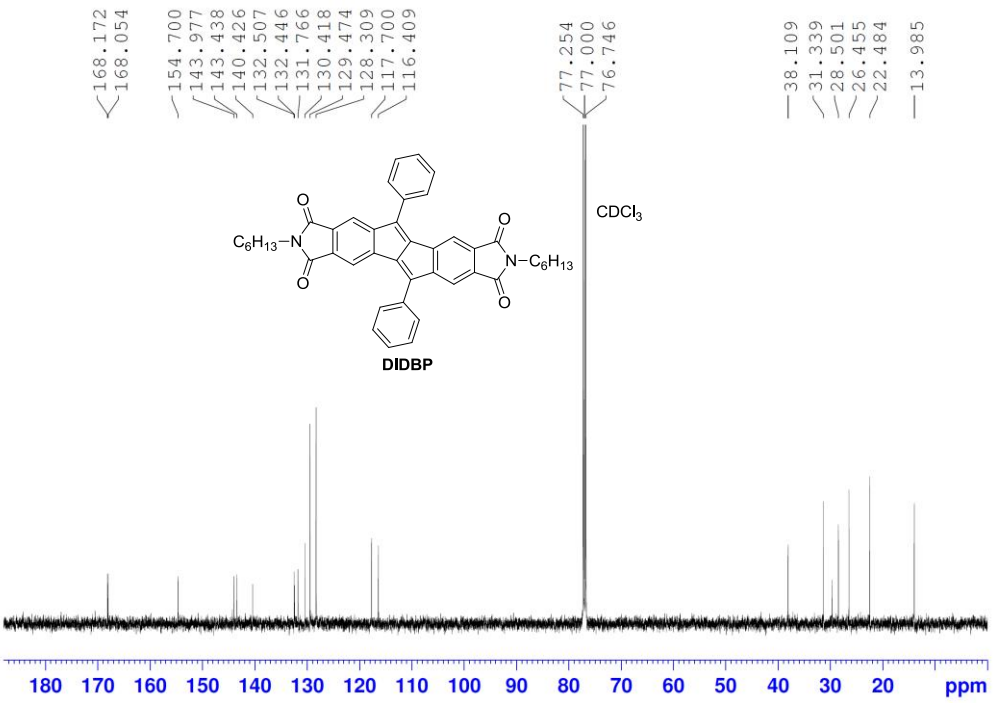

^{13}C NMR (125 MHz) spectrum of compound **DBPDI** in $CDCl_3$

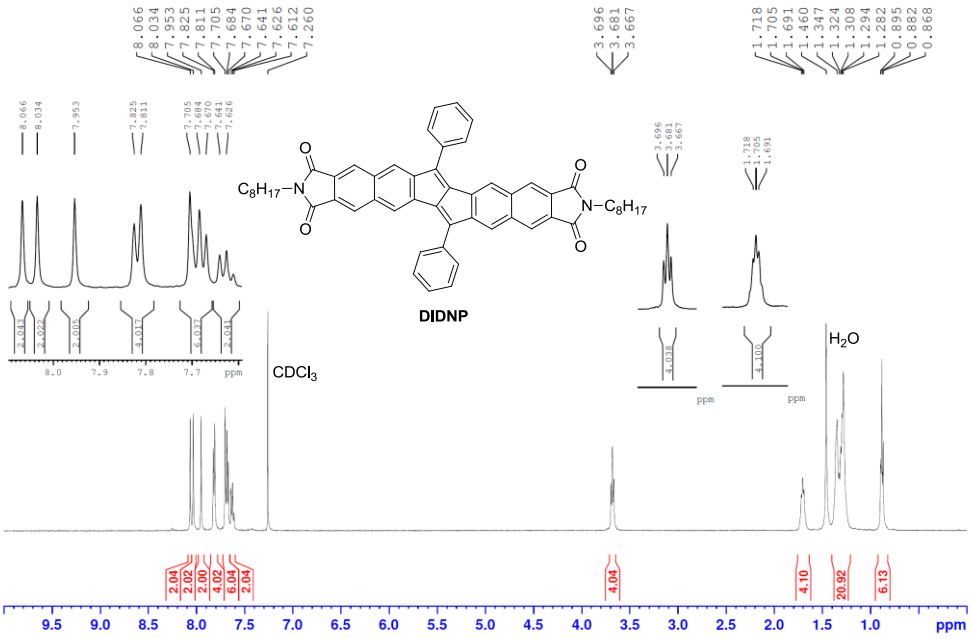

^{1}H NMR (500 MHz) spectrum of compound **DNPDI** in $CDCl_3$

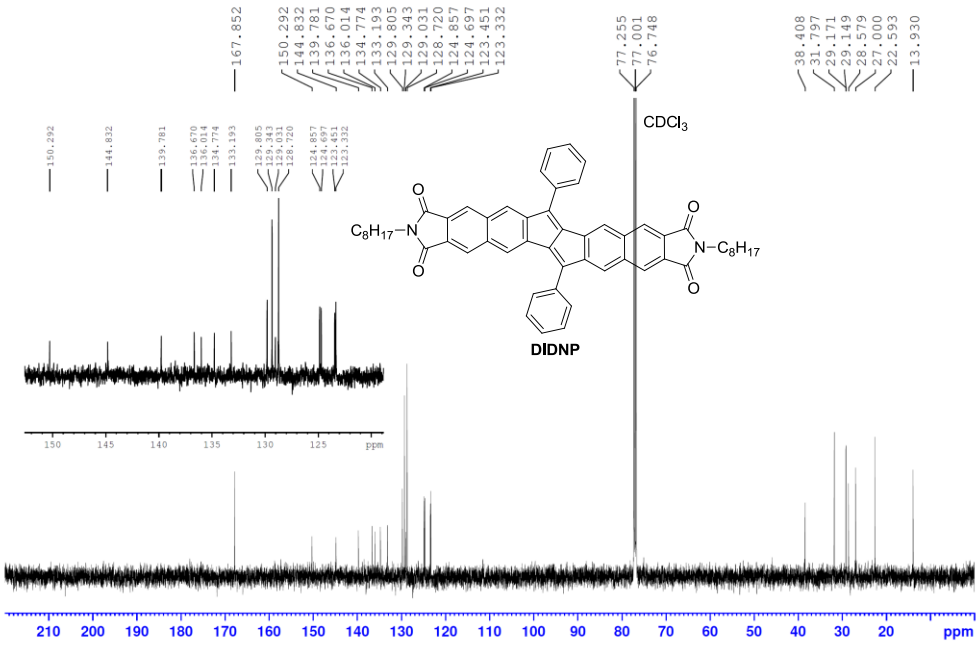

^{13}C NMR (125 MHz) spectrum of compound **DNPDI** in $CDCl_3$

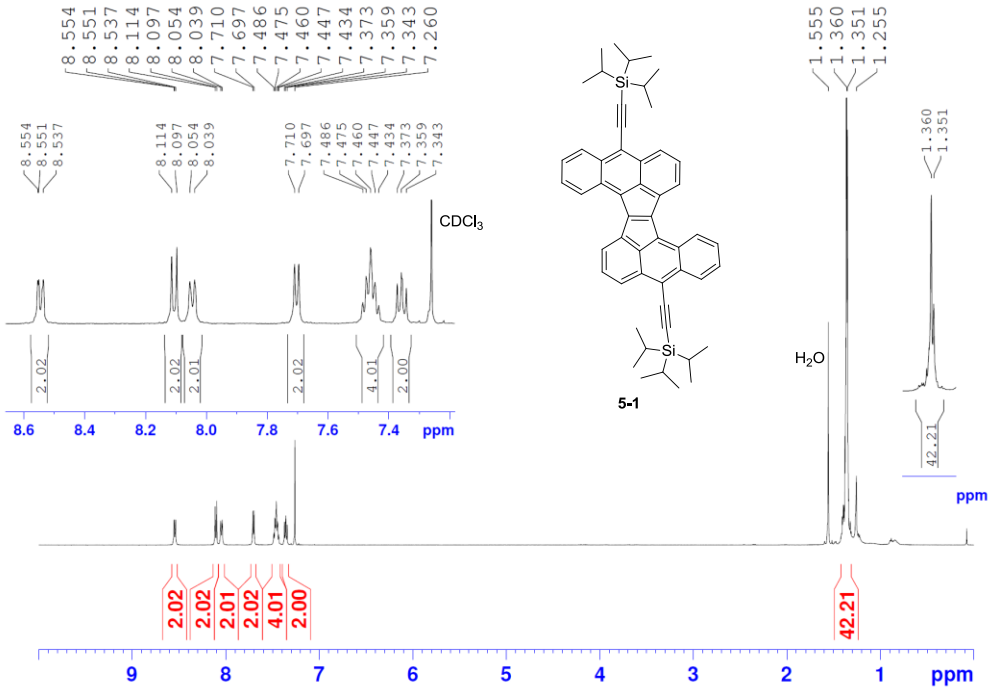

^{1}H NMR (500 MHz) spectrum of compound **5-1** in $CDCl_3$

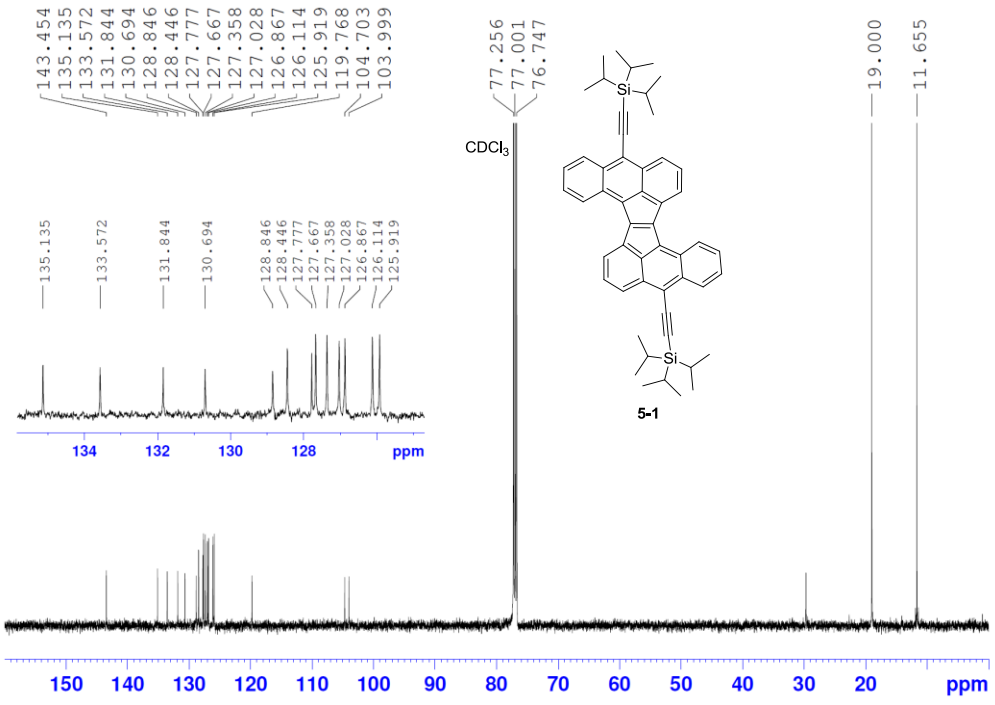

^{13}C NMR (125 MHz) spectrum of compound **5-1** in $CDCl_3$

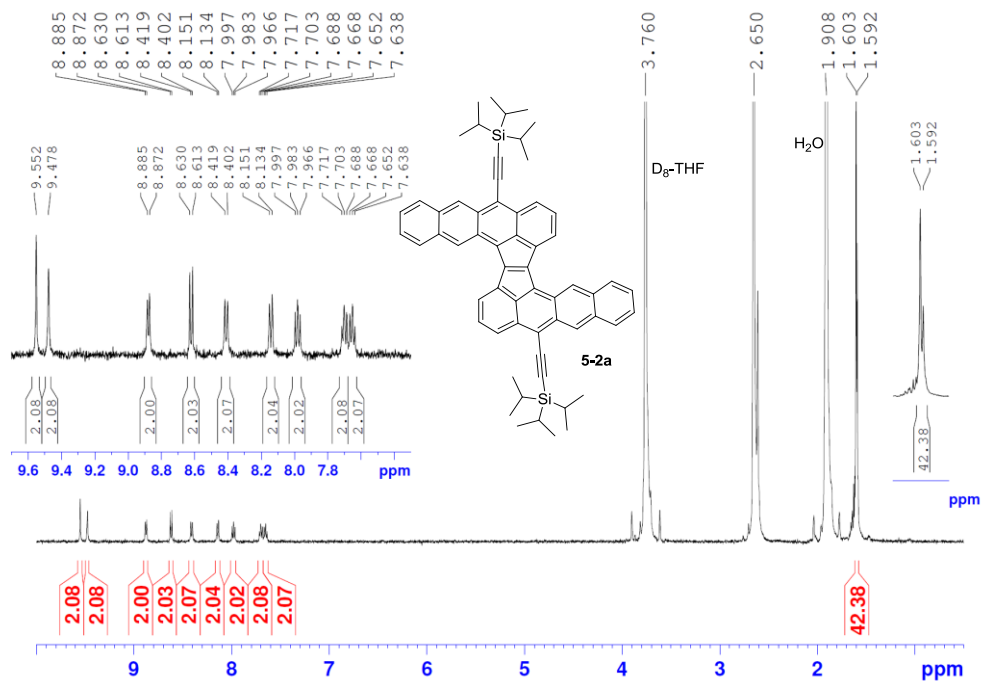

^{1}H NMR (500 MHz) spectrum of compound **5-2a** in D_8-THF

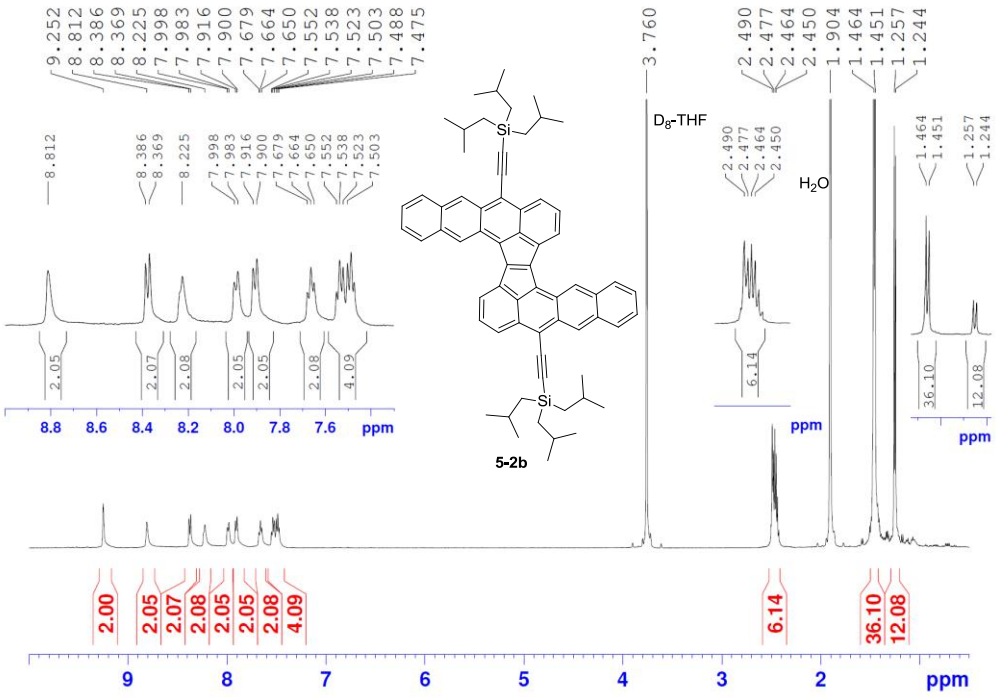

^{1}H NMR (500 MHz) spectrum of compound **5-2b** in D_8-THF

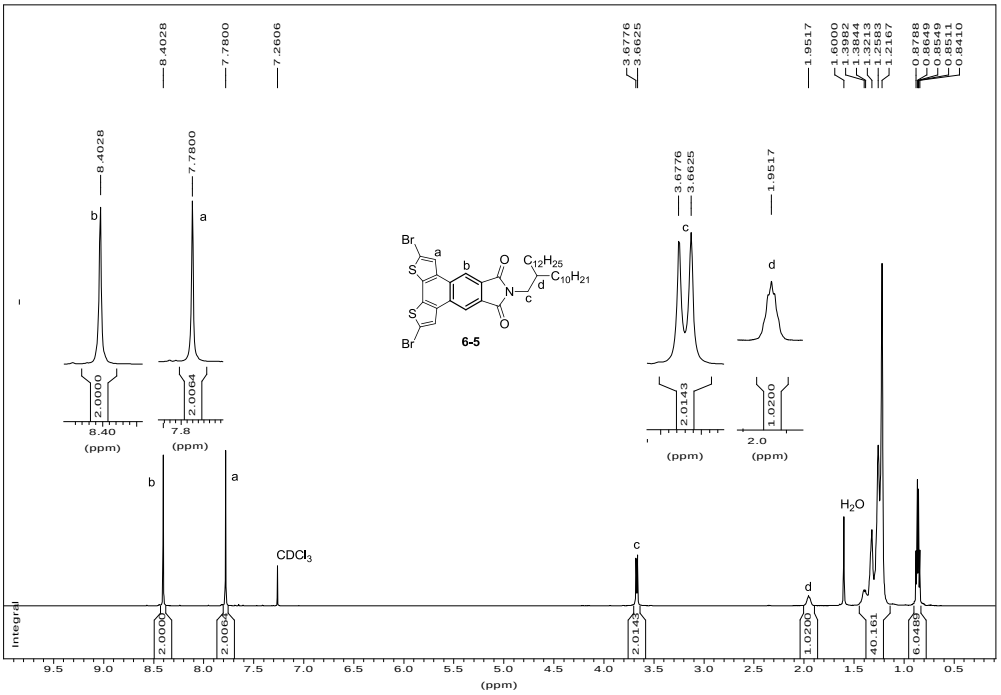

^{1}H NMR (500 MHz) spectrum of compound **6-5** in $CDCl_3$

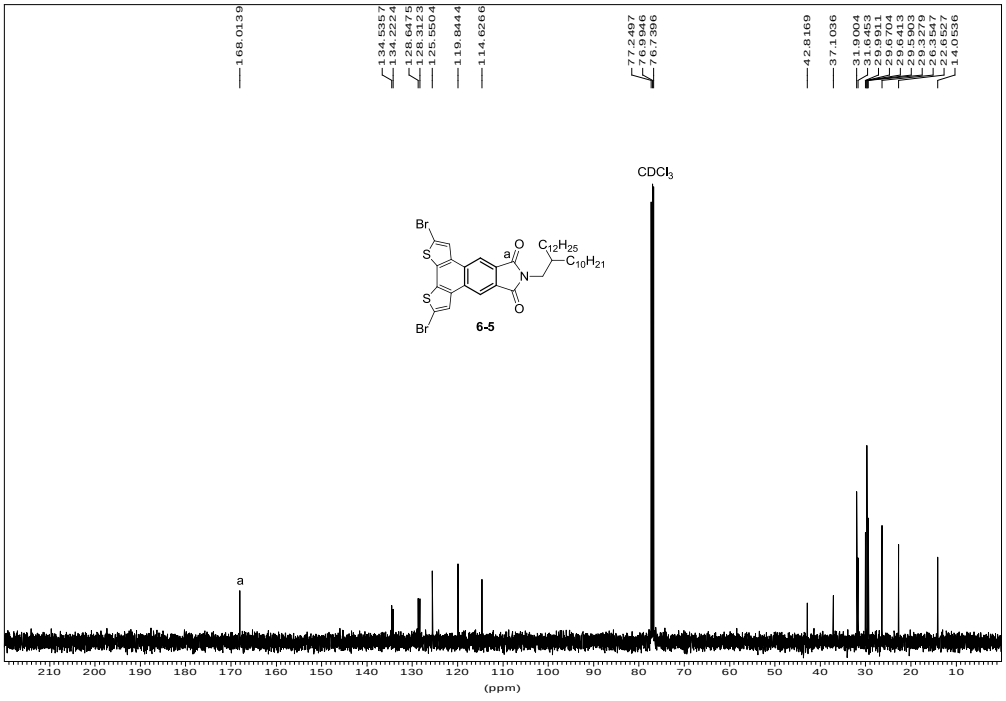

^{13}C NMR (125 MHz) spectrum of compound **6-5** in $CDCl_3$